UNIVERSITY OF SOUTHAMPTON

FACULTY OF MEDICINE

Human Development and Health

Simultaneous, Non-invasive Measurements of Skin Blood Flow and Oxygenation in Healthy Humans

by

Katarzyna Zofia Kuliga

Thesis for the degree of Doctor of Philosophy

February 2016

UNIVERSITY OF SOUTHAMPTON

ABSTRACT

FACULTY OF MEDICINE

Biomedical Engineering

Thesis for the degree of Doctor of Philosophy

SIMULTANEOUS, NON-INVASIVE MEASUREMENTS OF SKIN BLOOD FLOW AND OXYGENATION IN HEALTHY HUMANS

by Katarzyna Zofia Kuliga

Adequate blood flow within microcirculation and sufficient tissue oxygenation are essential for tissue health. However, the quantitative understanding of dynamics between the microvascular blood flow and oxygenation remains limited. The aim of this study was to explore and interpret simultaneous measurements of skin blood flux (BF) and oxygenation parameters (OXY) recorded from healthy skin.

Measurements were recorded using a recently developed (Moor Instruments Ltd, UK) combined Laser Doppler Flowmetry (LDF) and White Light Spectroscopy (WLS) technique, which offer an easy to perform assessment of skin microcirculation and skin oxygenation. In this thesis, two open studies have been conducted in cohorts of healthy volunteers to evaluate combined LDF-WLS measurements and to study the relationship between skin BF and OXY.

The engineering challenge of this thesis was to apply signal processing methods to analyse BF and OXY parameters and to extract information that reflect the physiological characteristics of the tissue. Signal processing methods such filtering, convolution, Fourier transform and others served as tools to identify different properties of the signals and subsequently describe the biological systems.

The measurements acquired across wide range of values led to mathematical description of the relationship between skin BF and oxygenation and revealed different oscillatory characteristics in BF and OXY signals. The analysis showed resting BF and OXY signals have the highest coherence across low frequency bands. Furthermore, OXY signals are delayed in respect to BF signals. Signal obtained during thermally induced vasodilation showed a shift in signal power to the cardiac frequency band.

In conclusion, simultaneous measurements of skin BF and OXY signals in combination with signal processing techniques offer an extended assessment of microvascular function, which may complement clinical assessment of tissue status. Further work is now required to combine presented in this thesis BF and OXY characteristics with other available analysis into clinically useful assessment.

Contents

List of Tables

List of Figures

DECLARATION OF AUTHORSHIP

I, KATARZYNA ZOFIA KULIGA

declare that the thesis entitled

Simultaneous, Non-invasive Measurements of Skin Blood Flow and Oxygenation in Healthy Humans

and the work presented in the thesis are both my own, and have been generated by me as the result of my own original research. I confirm that:

- this work was done wholly or mainly while in candidature for a research degree at this University;
- where any part of this thesis has previously been submitted for a degree or any other qualification at this University or any other institution, this has been clearly stated;
- where I have consulted the published work of others, this is always clearly attributed;
- where I have quoted from the work of others, the source is always given. With the exception of such quotations, this thesis is entirely my own work;
- I have acknowledged all main sources of help;
- where the thesis is based on work done by myself jointly with others, I have made clear exactly what was done by others and what I have contributed myself;
- parts of this work have been published as journal paper and conference presentations.

Signed: ……..

Date:……

Acknowledgements

First and foremost, enormous gratitude to Prof Geraldine Clough and Dr Andrew Chipperfield who were my main supervisors during the PhD journey. Thank you for your continuous support, inspiration and encouragement during this time. These four years were the best time of my life and a great learning experience covering not only the technical knowledge but also shaping personality and finding out the important values in life. Many thanks and appreciation are also due to Dr Rodney Gush who was my industrial supervisor and always smiled during our meetings.

I would like to acknowledge The UK Engineering and Physical Sciences Research Council and Moor Instruments for funding my research. I would like to thank Clive Higgs from Moor Instruments for technical support.

Thank you to all volunteers who unselfishly participated in measurements. Thank you to admin and clinical staff from Wellcome Trust Clinical Research Facility in Southampton General Hospital for their help in completing this research.

My sincere thanks also go to Prof Charles Michel for discussions and expert advice on parts of this thesis.

PhD was a great and unique adventure. It required a lot of effort and determination and would not be successful without a number of people who were supporting me to complete this work. I would like to thank my beloved husband Adam who always believes in me and supports me during good times and during not so good moments. His love, patience and ability to turn difficult situations into small simple steps are priceless. Thanks to my friends and office mates Berit, Vika, Gabriela, Stefania, Jim, Jahnabi and Vanessa for all great moments spent together. I also want to thank my friends back home Żaneta and Patrycja who always cheered me up.

Katarzyna Zofia Kuliga
Southampton, UK
February 2016

To my beloved husband Adam, who is the sense of my life.

Definitions and Abbreviations

ABP	Arterial Blood Pressure
ACh	Acetylcholine Chloride
AU	Arbitrary Unit
AUC	Area Under the Curve
AV shunts	Arterio-Venous Anastomosis
BF	Blood Flux
BMI	Body Mass Index
BZ	Biological Zero
CV	Correlation of Variation
DCS	Diffuse Correlation Spectroscopy
DRS	Diffuse Reflectance Spectroscopy
deoxyHb	Deoxygenated Haemoglobin
FC	Frequency Coherence
FFT	Fast Fourier Transform
FT	Fourier Transform
HF	High Frequencies
IBH	Inspiratory Breath-Holds
ICC	Intraclass Correlation
IQR	Interquartile Range
LDF	Laser Doppler Flowmetry
LF	Low Frequencies
MF	Maximum Level during PORH

NIRS	Near-infrared Spectroscopy
NO	Nitric Oxide
O2C	Oxygen2see®
oxyHb	Oxygenated Haemoglobin
PORH	Post-Occlusive Reactive Hyperaemia
PSD	Power Spectral Density
PU	Laser Doppler Perfusion Unit
RF	Resting Level
SD	Standard Deviation
SDF	Side-stream Dark Field
SO_2	Tissue Oxygenation (%)
$tcpO_2$	Transcutaneous Oxygen Pressure (mmHg)
totalHb	Total Haemoglobin
VSL	Visible Light Spectroscopy
WLS	White Light Spectroscopy
WT	Wavelet Transform

Chapter 1

Introduction

Medical technology has seen many useful advances over past 50 years including medical imaging, non-invasive diagnostic tools and telemedicine. Medical devices are nowadays often a major source of information about health or disease. They have a significant impact on modern health assessment – they help to improve and accelerate the diagnosis made by health professionals. The understanding and correct interpretation of information delivered by novel medical technologies is fundamental for successful transfer of these technologies into clinical setting.

This Chapter introduces the concept of non-invasive devices used to conduct the research presented in this thesis, presents the motivation and aims of this thesis, gives an overview of the structure of the thesis and ends with a list of publications resulting from the work carried out within this thesis.

1.1 Biomedical Signals

Computer processing of biomedical signals is an indispensable part of the current generation of medicine. The driving force behind many recent advances is the non-invasiveness and the improved accuracy of measurements. Also, new applications of existing techniques or new analysis methods and interpretation of already known signals provide new insights and knowledge which help to explore and understand health and disease.

Non-invasive technologies are highly desired in current medicine as routine tools to investigate biological systems. Whenever possible, it is advised to avoid invasive procedures as they carry a risk of complication and possible infection. The non-invasive optical techniques are used to measure blood flow and oxygenation in human tissues. Laser Doppler Flowmetry (LDF) is used as a research tool to investigate the physiology and pathology of skin blood flow. The research conducted on optical properties of human tissues has led to the development of near-infrared spectroscopy (NIRS) that non-invasively assesses the oxygenation of tissues such as brain or skeletal muscle. White Light Spectroscopy (WLS), based on a similar principle as NIRS, was developed to investigate oxygenation in human skin. Currently, the combined LDF and WLS techniques allow for simultaneous investigation of blood flux (BF) and oxygenation parameters

(OXY). These techniques may become reliable, clinical tools providing a measure of the microvascular status and helping to inform and assess the efficacy of treatments in clinical setting, only if the detailed understanding of these measurements is provided. Currently, there is very little known about the relationships between BF and OXY signals obtained from these techniques, and the usefulness and understanding of these combined measurements still need to be confirmed.

BF and OXY signals are usually recorded as continuous signals. The time and frequency domains are the most used modes in which these signals are analysed. Time-domain analysis supplies information about the changes happening over time, such as a change in blood flux and tissue oxygenation measured in arbitrary perfusion units (PU) and % respectively. Frequency-domain analysis reveals information about the oscillatory behaviour of the measurement e.g. heartbeat. Analysis in the time domain combined with analysis in the frequency domain may provide a comprehensive insight into the dynamics of the recorded signals. Blood flow and oxygenation are closely depended on each other, e.g. higher blood flow increases the oxygen delivery to the tissue. Therefore, it is important to study these two signals simultaneously.

1.2 Motivation for Research

The importance of reliable assessment of the microvascular health and the need for non-invasive tools drive the development of new technologies and their translation into clinical setting. Novel, combined LDF-WLS devices have a potential to provide a non-invasive assessment of microcirculatory BF and OXY parameters. A better understanding of BF and OXY signals will help to explore the dynamics of microcirculatory BF and tissue oxygenation (SO_2) and will help to assess its clinical value. In this thesis, data recorded from healthy volunteers have been used to establish a benchmark for normal microvascular function and normal responses to physiological perturbations measured with the combined LDF-WLS technique. The relationships between time-domain characteristics of BF and SO_2 signals and between the frequency components of those signals have been investigated. The identification of these relationships will help in the future to investigate and understand the pathological conditions associated with microvascular dysfunction.

1.3 Aims of the Thesis

The overall objective of this research was to investigate the properties of a combined LDF-OXY signals providing a simultaneous measure of tissue blood flux and oxygenation at the same body site. The aims of the studies described in this thesis are therefore:

- To determine the range and reproducibility of the combined measurements
- To identify the blood flux-oxygenation relationship in healthy volunteers
- To investigate time and frequency domains characteristics of blood flux and oxygenation signals at rest and during physiological perturbations such as short arterial occlusion and local skin warming
- To interpret the dynamic changes in blood flux and oxygenation following perturbations
- To apply signal processing methods to identify the characteristics of blood flux and oxygenation signals

1.4 Structure of the Thesis

Chapter 2 summarises the physiology of skin and evaluates the current literature in the field of microcirculatory blood flow and oxygenation. Chapter 3 describes the design and methodology used to perform two studies presented in this thesis. Chapter 4 presents and discusses results from Study 1 conducted in fifty healthy volunteers. This leads onto Chapter 5 which aims to address the measurements' issues identified in Chapter 4 i.e. heterogeneous study cohort and the influence of skin temperature on measurements. Chapter 5 presents results from the Study 2 conducted in carefully selected fifteen healthy volunteers. Finally, Chapter 6 aims to extend the understanding of signals from Chapter 5 by investigating the relationship between blood flux and oxygenation signals in time and frequency domains.

1.5 Contributions to the Body of Knowledge

The multidisciplinary nature of this thesis, combining the elements of engineering and medical approaches, extends the current understanding of the combined measurements of skin blood flux and oxygenation. The analysis of the measurements obtained during this PhD study enable the following contributions to the body of knowledge:

- The critical assessment of combined measurements identifying the reproducibility of the combined sensor (LDF-OXY)
- Mathematical description of the relationship between skin blood flux and oxygenation over a wide range of values based on experimental data

- Identification of time and frequency characteristics of blood flux and oxygenation signals at rest and during thermally induced vasodilation
- Utilisation of signal processing methods to describe the relationship between spontaneous oscillations in blood flux and oxygenation signals
- Identification and quantification of time delay observed between blood flux and oxygenation signals

1.6 List of Assimilations

The following publications, presentations and prizes were derived from the research presented in this thesis.

Journal articles:

- Kuliga KZ, McDonald EF, Gush R, Michel CC, Chipperfield AJ & Clough GF (2014). *Dynamics of microvascular blood flow and oxygenation measured simultaneously in human skin*. Microcirculation 21, 562-573.

Poster presentations:

- *Simultaneous measurement of microvascular blood flux and oxygenation in human skin using a combined laser Doppler fluximetry and white light reflectance spectroscopy probe.*
  62nd Annual Conference of the British Microcirculation Society and the Microcirculatory Society, Oxford, UK, 4-6 July 2012

- *Coherence between tissue blood flux and oxygenation measured using a novel combined laser Doppler flowmetry and white light spectroscopy probe.*
  British Microcirculatory Society Early Career Symposium Warwick, UK, 13 April 2013

- *A novel clinical tool for the non-invasive measurement of skin blood flow and tissue oxygenation.*
  Faculty of Medicine Research Conference 2013, 12 June 2013

- *Delay Estimation between Simultaneously Recorded Blood Flux and Oxygenation Signals from Healthy Human Skin.*
  36th Annual International Conference of the IEEE Engineering in Medicine and Biology Society, Chicago, US, 26-30 August 2014

Prizes:

- Terence Ryan Clinical Poster Prize,
  British Microcirculation Society Early Career Symposium Warwick 2013, 13 April 2013

Oral presentations:

- *Spectral analysis of non-invasive measurements of blood flow and oxygen level in a living tissue.*
  1st Postgraduate Conference of Engineering Sciences 2012, University of Southampton

- *Flow motion dynamics of blood flow and oxygenation*.
  10th World Congress for Microcirculation, Kyoto, Japan, 25-27 September 2015 (delivered by G.F. Clough)

Chapter 2

Research Background and Literature Review

Research background and literature review includes a short overview of anatomy and physiology of the microvasculature, focusing in particular on skin microcirculation and its importance as an accessible vascular bed in human body in which to study microvascular dysfunction. The current non-invasive techniques used to measure skin blood flow and tissue oxygenation are described and compared. The literature review summarises the scientific research performed to date in the field of non-invasive assessment of skin microcirculation and its clinical application.

2.1 Clinical Importance of Microcirculation

Adequate delivery of oxygen to the tissue is essential for the tissue health. The transport of oxygen within the body is facilitated by the cardiorespiratory system and it aims to supply the oxygen to every cell of the body to satisfy the metabolic demand of the tissue. The delivery of oxygen to cells takes place at the final level of the cardiorespiratory system called microcirculation. This refers to the circulation of blood in the network of the smallest blood vessels including arterioles, capillaries and venules (approx. <150μm in diameter). Nevertheless, all components of the cardiorespiratory system interact with each other and form complex regulatory mechanisms, which serve to meet the perfusion and oxygenation demands of all tissues. Understanding the interactions in the healthy system is the first step towards understanding the interactions in the pathological state.

An insufficient tissue oxygenation is a serious problem. The consequences of inadequate perfusion are retinopathy, ulcers, difficult to heal wounds, neuropathy, tissue hypoxia leading to cell death and amputations (Mathieu & Mani, 2007; De Backer et al., 2012). These are an increasing burden on the National Health Service (NHS) as these conditions become more and more prevalent. For example, cardiovascular disease leads to more than 88,000 deaths a year in the UK alone (NHS, 2012).

The skin microcirculation has been studied in healthy cohorts as well as in various pathological conditions including diabetes, hypertension, dyslipidaemia, insulin resistance, rheumatoid arthritis, scleroderma and also in diseases of the macrocirculation such as peripheral arterial

occlusive disease (Forst et al., 2008). An early detection of the abnormal changes may help to avoid serious complications by applying intervention at an early stage of the disease. For example, obesity is related to a reduced capillary density and endothelial dysfunction (De Boer et al., 2012). Understanding and quantifying the abnormal changes in an individual early on help to determine the best treatment and can thus help to improve the health outcomes. Similarly, people with diabetes very often suffer from foot problems, such as neuropathy and ulcerations (Sun et al., 2013), which are also associated with microvascular dysfunction.

Another relevant application of microvascular monitoring is the assessment of tissue flaps. The surgical procedures of tissue transfers are common practice to reconstruct tissue defects resulting from trauma or surgical operations. The success of tissue transfer depends on adequate microvascular perfusion after transplantation. The flap salvage or failure depends closely on vascular status of the flap following surgery (Mirzabeigi et al., 2012; Selber et al., 2012; Yang et al., 2014). LDF has a potential to inform about complications and flap failures by continuous assessment of skin perfusion. Furthermore, the combined measurements of BF and OXY parameters serve as a tool to study flap tissue (Henton et al., 2015) and may help to reduce flap failure by early detection of vascular and hypoxic inadequacies (Mucke et al., 2014).

The accurate and early identification of microvascular dysfunction may help to avoid these serious conditions. The development of reliable measurement techniques and screening tests helping to assess the state of microcirculation is a necessary step to detect early changes and begin treatment sooner compared to current practice.

2.1.1 Cardiovascular System and Microcirculation

The human vascular system can be considered as a network of large and small blood vessels including arteries, arterioles, capillaries, venules and veins. The term macrocirculation describes the blood flow within the large conduit and resistance arteries and veins. The microcirculation can be described as a circulation in the heterogeneous network of vessels smaller than 150μm in diameter (De Boer et al., 2012). The human vascular system has two main functions: (1) mass transport of blood and oxygen from the heart to the organs; and (2) buffering blood pressure changes originating from the heartbeat (Feihl et al., 2009).

Figure 2.1 shows a simple diagram of the human cardiovascular system. There are two circuits of circulation: the respiratory circuit and the body circuit. The heart, as the central organ,

pumps the blood into the macrocirculation. As the oxygenated blood travels into smaller vessels it enters the microcirculation and the gas exchange between the blood vessels and cells take place. The deoxygenated blood within capillaries returns back to the heart by venules and veins. The blood is then pumped again by the heart, but this time it travels to the lungs where at the level of the microcirculation oxygen is attached to red blood cells (RBC). Oxygenated blood returns to the heart and completes the cellular circulation. Macro- and microcirculation are directly linked and the interactions on one level affect the functions on the other level. The dynamics of the functions on the higher level, such as heartbeat and respiration, can be observed at the microcirculatory level. Many diseases affect both the macro- and microcirculation, but often the changes in macro- and microcirculation do not happen simultaneously but are modulated in time. The early detection of changes at the microcirculatory level may yield information about potential problems or complications at the macrocirculatory level and vice versa.

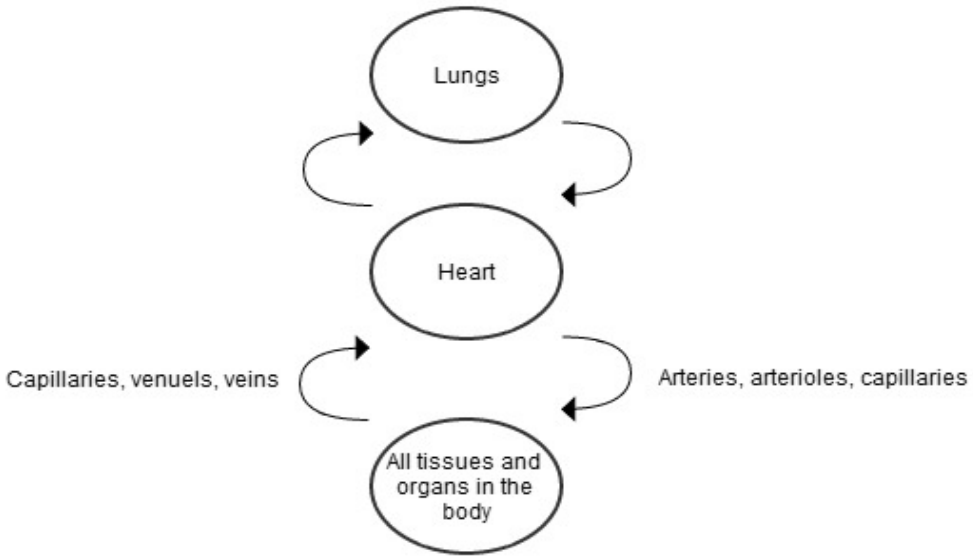

Figure 2.1 The macro- and microcirculation in the human cardiovascular system. The heart, arteries and veins are macrocirculation vessels and are directly linked to arterioles, capillaries and venules which comprise the microcirculation.

In the microcirculation, the delivery of oxygen is adjusted to meet local demand of the tissue (Pittman, 2005; De Boer et al., 2012) and in skin the delivery of oxygen exceeds the physiological need. A physiological stimuli, for example exercise, changes the global and local demands for oxygen in tissue. Resting muscle oxygen extraction varies between 20% and 40%,

whilst during a heavy exercise it increases to 70-80% (Korthuis, 2011). At the same time the skin circulation is increased to remove the heat resulting from the work done by muscles. The transport of oxygen from the vessels to the cells occurs by diffusion and is described by Fick's law (Equation 2.1.),

$$J_s = -DA\frac{\Delta C}{\Delta x} \qquad (2.1)$$

where J_s is a mass of solute transferred by diffusion per unit time, D is the diffusion coefficient, A is the surface area, ΔC is the concentration difference between vessels and cells, and Δx is the membrane thickness. Diffusion is only effective over short distances of about 100 µm (Secomb & Pries, 2011). Hence, the effective delivery of the oxygen to the tissue also depends on the capillary density and their perfusion state. Not all the capillaries are perfused continuously; they are 'recruited' depending on the oxygen demand in the tissue.

An important function of microcirculation is controlling the peripheral vascular resistance and subsequently the blood pressure. The vascular resistance is a difference in blood pressure across a vascular bed divided by the cardiac output. The main resistance vessels are terminal arteries and arterioles. Vasoconstriction and vasodilation change the lumen of the blood vessels and consequently change the vascular resistance. Vasodilation results in a fall in vascular resistance and the increase in blood flow while vasoconstriction induces the opposite effect.

2.1.2 Skin Microcirculation

The basic structure of the human skin is shown in Figure 2.2. There are three basic layers: epidermis, dermis and subdermis. The epidermis is the most outer layer of the skin (about 0.2 mm thick) and consists mostly of keratinocytes. These cells provide a barrier from the external environment. There are no blood vessels or nerve fibres in the epidermis.

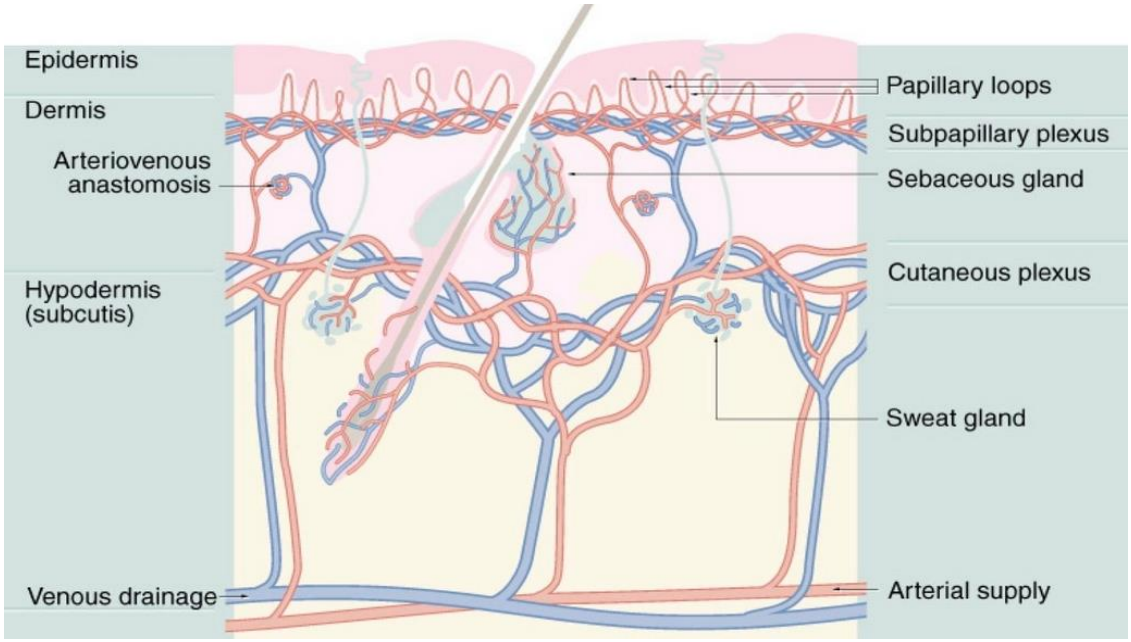

Figure 2.2 The structure of skin and placement of microcirculatory blood vessels within the skin. Adapted from studyblue.com.

The dermis is the layer of the skin beneath the epidermal layer. It is about 1-4 mm thick and consists mostly of collagen and elastin fibres. The dermis includes the nerve fibres and microcirculatory blood vessels. As shown in Figure 2.2, there are papillary loops (also considered to be the nutritive vessels) on the border between the epidermis and dermis. The slightly larger vessels are arterioles and venules. In some skin sites the arterio-venous (AV) anastomosis (AV shunts) are also present. They allow for faster blood flow directly from arterioles to venules without passing through the capillaries. AV shunts are present mainly in the skin of fingers tips and toes and serve as the thermoregulatory structures (Allen et al., 2002). They are under control of the sympathetic nervous system and facilitate thermoregulation by shunting the blood towards or away from the surface of the skin. Smooth muscles are only present around the vessels of diameter greater than 15 µm – the capillaries are not surrounded by muscles. The spontaneous vasomotion originating from these muscle cells plays a role in the blood flow control (Aalkjaer et al., 2011). This is described in more details later in this chapter (Section 2.5). In skin the majority of blood vessels are capillaries, however the greatest volume of blood resides in venules, hence the majority of RBC within skin microcirculation are also found in venules (Braverman, 1997).

The epidermis mostly consists of keratinocytes which synthesize protective protein keratin and dendritic cells. It comprises of four layers: the basal cell layer, the squamous cell layer, the

granular cell layer and the cornified cell layer. The basal cells of the epidermis proliferate continuously creating new layers of cells whilst the outer layer of the epidermis is considered as dead cells and it is replaced over time by the lower layers (Kolarsick et al., 2009).

The interface between the epidermis and dermis comprise the porous basement membrane zone that allows the exchange of cells and fluid between these two layers. This zone contains the epidermal-dermal junctions which provide mechanical support for the epidermis, a barrier to the exchange of cells and some large molecules between the layers and the adequate adherence between epidermis and dermis (Kolarsick et al., 2009).

The dermis is a complex fibrous connective tissue that includes nerve and vascular networks. The dermis contains large amount of collagen and elastic fibres which provide the pliability, elasticity and tensile strength of the skin. The dermal vasculature consists of two plexuses: the superficial and the lower plexus. The superficial plexus include capillaries, arterioles and venules whilst the lower plexus contain larger blood vessels (Kolarsick et al., 2009). Lymph vessels generally accompany blood vessels, however in skin the lymphatic vessels are located more distant from the epidermis than blood vessel and they do not form anastomosis (Skobe & Detmar, 2000).

The sweat glands are embedded in the lower dermis. They form small tubular structures and create the duct that carries the sweat through the dermis and epidermis to the top surface of the skin. The sweat glands are involved in the regulation of body temperature (Kolarsick et al., 2009).

The main function of skin microcirculation is the thermoregulation. During the exposure to cold ambient temperature the skin blood vessels constrict to keep the warm blood in deeper tissues and to minimise the heat loss through the skin. In a hot environment the blood vessels dilate and the blood flow increases in order to dissipate the excess of heat (Lenasi, 2011). The adjustments of skin circulation are the greatest in the extremities, especially where the AV shunts are present (Cracowski et al., 2006). The constriction and the dilation of AV shunts are regulated by the autonomic nervous system (de Mul et al., 2009).

Glabrous skin contains noradrenergic vasoconstrictor nerve fibres whilst nonglabrous skin also contains the cholinergic vasodilator nerves. The glabrous skin in response to heat reduces the activity of sympathetic nervous system and therefore induces passive vasodilation. The skin sites rich in AV shunts have the ability to cause large changes in blood flow by opening and closing the shunts. The nonglabrous skin in addition to passive vasodilation exhibits an active

vasodilation mechanism. The release of acetylcholine from sympathetic cholinergic nerves increases the vasodilation. Another mechanism of heat dissipation is sweating. The heat dissipation is mediated by activation of sympathetic cholinergic nerves (Tansey & Johnson, 2015).

The blood flow exhibits rhythmic oscillations which can be observed also in the microcirculation. There are several distinct mechanisms which contribute to the overall blood flowmotion. The heartbeat is the highest frequency oscillation observed in blood flowmotion. Next lower are respiration induced Mayer waves. They occur in phase with respiration and originate from the oscillation in sympathetic tone and the baroreceptor reflex. There are also other cyclic changes in diameter of blood vessels including myogenic, neurogenic and endothelial. The flowmotion is described in more detail in section 2.5.

The microvascular function is a general term describing complex interaction happening in microcirculation. Endothelial function is one of the microvascular mechanisms. The endothelial cells, which line the internal surface of blood vessels, play an important role in controlling blood flow. They release the vasoconstricting and the vasodilating factors controlling the behaviour of the vessels (Kvernmo et al., 2003; Cracowski et al., 2006; Humeau-Heurtier et al., 2013). The endothelial dysfunction, i.e. altered secretion of constricting and dilating factors, is associated with the vascular diseases such as coronary heart disease, ischemic stroke and peripheral artery disease. It is also a precursor to atherosclerosis (Hansell et al., 2004). The assessment of endothelial function derived from the measurements of microcirculation function may help to improve the management of these diseases.

The human skin can be easily and noninvasively accessed which makes it a convenient site for a number of non-invasive measurements. The microcirculation measurements taken from the skin can reflect the state of the microcirculation in deeper tissues, hence the skin microcirculation can be considered as surrogate of the microvascular function in deeper tissues (Humeau-Heurtier et al., 2013). Due to the complexity of human physiology, it is challenging to treat the skin as a model for other vascular beds. However, the microcirculation changes resulting from disease are often present in the skin as well as in other tissues (De Boer et al., 2012). There are many examples of research linking microvascular function to macrovascular function or internal microvascular function to peripheral microvascular function (Sax et al., 1987; Chang et al., 1997; Roustit & Cracowski, 2012), therefore skin can be considered as a source of information about deeper tissues.

Changes in skin microcirculation have been shown to precede changes in the macrocirculation (review: (Fromy et al., 2002; Wiernsperger et al., 2007; Forst et al., 2008; Czernichow et al., 2010; Strain et al., 2012)). Analysis of blood flow signals from patients with complex regional pain syndrome helped to distinguish the presence or absence of the regional sympathetic vasoconstriction, which was beneficial to clinical treatment (Roustit et al., 2011). The study of skin microcirculation helped to explore the mechanisms of the vascular function in natural aging (Schroeter et al., 2004; Holowatz et al., 2008; Minson, 2010; Roustit & Cracowski, 2012) and in various diseases including systemic sclerosis and Raynaud's phenomenon (Boignard et al., 2005), the heart failure (Andersson et al., 2005; Green et al., 2006), peripheral arterial disease (Rossi & Carpi, 2004), type I and type II diabetes (Eberl et al., 2005; Jaffer et al., 2008; Prazny et al., 2009; Sun et al., 2012; Sun et al., 2013), renal disease (Coulon et al., 2012) and sepsis (De Backer et al., 2011).

2.2 Techniques for Measuring Skin Blood Flow

The assessment of the microvascular function is important for understanding and diagnosing multiple diseases. In this section, the methods for measuring the microvascular blood flow are reviewed and in the subsequent section (Section 2.3) the methods for measuring the microvascular oxygenation are summarised. Only non-invasive techniques are considered as they are most relevant to this research.

2.2.1 Current Techniques for Measuring Skin Blood Flow

Microcirculatory blood flow can be non-invasively investigated using venous displacement plethysmography, laser Doppler flowmetry, LD imaging, diffuse correlation spectroscopy (DCS), side-stream dark field (SDF) and orthogonal polarisation spectral cameras, nailfold capillaroscopy and optical coherence tomography. The main characteristics of these methods are summarised in Table 2.1. The principles and output measures are presented in the first two columns followed by the reproducibility, advantages, limitations and current applications. The references to relevant research work and reviews are also included in Table 2.1.

Table 2.1 A summary of non-invasive methods for measuring microcirculatory blood flow.

Technique	Principle	Output measure	Reproducibility	Advantages	Limitations	Applications
Volume Displacement Plethysmography	Changes in limb volume due to blood flow, measured by a strain gauge placed around the limb	Changes in limb volume correspond to the arterial blood flow, blood flow is expressed in the absolute units (ml per minute per 100ml of forearm) or relative units as change from baseline	Within subject ~13-39% (Walker et al., 2001; Thijssen et al., 2005; Kooijman et al., 2007) Intra-subject: 19%-39% (Petrie et al., 1998) CV[1] of relative measurements: 6-9% (Thijssen et al., 2005)	Simple design	Whole limb blood flow (combined muscle and skin tissues) Limited accuracy and movement sensitive	Measurement of blood flow to the whole limb (Wilkinson & Webb, 2001) Measuring the vascular resistance and capillary hydraulic permeability
Laser Doppler Flowmetry	Doppler effect in laser light induced by moving RBC	Blood flux (RBC concentration x velocity), expressed in arbitrary perfusion units. Signal comes from arterioles, capillaries and venules contained in $1mm^3$ of sampled tissue	High CV[1] for baseline measurements; CV[1] of response to the physiological perturbations: 9-25% (Agarwal et al., 2010); 5-22% (Yvonne-Tee et al., 2005); 21% (Binggeli et al., 2003)	Continuous measurement (ability to record dynamic changes) High sampling rate	Small sampling volume; Temporal and spatial variability; Only stationary measurements (patient movement induces artefacts)	Assessment of microvascular function; (Cracowski et al., 2006) (Humeau et al., 2007)
Diffuse correlation spectroscopy (DCS)	Fluctuations in reflected near-infrared light caused by motion of RBC	Blood flow index in deeper tissue, expressed in cm^2/s	Peak blood flow after arterial occlusion: 8% variation (Yu et al., 2007)	Continuous measurement Easy to use	Temporal and spatial variability; Relative measurement	Cerebral blood flow (Durduran et al.; Mesquita et al., 2011)

[1] Coefficient of Variation (explained in detail in section 3.5.4)

Technique	Principle	Output measure	Reproducibility	Advantages	Limitations	Applications
Side-stream dark field and orthogonal polarisation spectral cameras	Visualisation of microvascular vessels by illuminating tissue with light absorbed by haemoglobin	Images of capillaries and venules, vascular density, diameter and perfusion (microcirculatory flow index) is assessed by semi-quantitative image processing,	Good reproducibility of automatic methods of image analysis: less than 4% difference in total vessel density (Bezemer et al., 2011)	In vivo visualisation, ability to look at individual vessels and microcirculation heterogeneity	Taking good quality images is difficult and require training and practice; Images are limited to mucosal surfaces and very thin skin (neonates) Image processing is time consuming and require experienced investigator; Movement and pressure artefacts	Intensive care and sepsis (Sakr et al., 2004; Trzeciak et al., 2007; De Backer et al., 2010), exposure to hypoxia (Martin et al., 2010)
Nailfold capillaroscopy	Transillumination of a nailfold of finger or a toe under microscope	Capillary morphology of the nailfold (diameter, density, loop size, tortuosity, angiogenesis)	Excellent inter and intra observer agreement for some but not all parameters (ICC[2] 0.94-1.0 (Sekiyama et al., 2013)) Weighted kappa statistics[3] (0.4-0.9 depending on the analysed parameter (Ingegnoli et al., 2009))	Good resolution and magnification Direct in vivo observation	No quantitative measure, poor reproducibility for some parameters, require specialised training	Systemic sclerosis, Raynaud's phenomenon (Vasdev et al., 2011; Cutolo & Smith, 2013)

[2] Intra Class Correlation (explained in detail in section 3.5.4)
[3] Kappa statistics refer to inter-rater agreement

Technique	Principle	Output measure	Reproducibility	Advantages	Limitations	Applications
Optical coherence tomography	Difference in dynamic scattering between moving RBC and static scattering of surrounding tissue	3D tomographic images, deep-resolved blood perfusion maps, skin morphology	Varies depending on OCT mode and post processing; excellent intra observer reproducibility (ICC<0.966) and intra visit and inter visit repeatability (CV 3.7 and 5.2 respectively)(Chen et al., 2016)	High resolution	Sensitive to movement artefacts, extensive post processing;	Number of different skin conditions (for review on application see (Gambichler et al., 2015)), wound healing ((Kuck et al., 2014)),

Each of the methods presented in the Table 2.1 offers a different measurement modality including the quantitative and the qualitative measurements. The origins of these measurements differ and hence the applications also differ. The only methods that allow for continuous measurement of blood flow in the microcirculation are LDF and DCS. Furthermore, LDF provides a measure of skin microcirculation whilst DCS samples the deeper tissues such as muscle or brain (Durduran 2004). Thus, LDF is currently the most suitable method for continuous monitoring of skin microcirculation. LDF has already been applied to study a wide range of physiological and pathological conditions. The principles and operation of LDF are described in the next section.

2.2.2 Laser Doppler Flowmetry

Laser Doppler Flowmetry (LDF) is based on the Doppler Effect, which was first described by Christian Doppler in 1842 and applied by Buys Ballot in 1845 to sound waves. The Doppler Effect states that a wave will change frequency when it is reflected from a moving object. As blood flows, both liquid plasma and RBC are moving along the microcirculation. In 1975 Stern (Stern, 1975) first applied spectral analysis to laser light scattered from skin. After 1975 many other researchers investigated the different aspects of blood flow using LDF and advancing the knowledge of the complexities of the blood flow physiology.

Figure 2.3 shows the principle of LDF as commonly applied. A source of coherent laser light is delivered via an optical fibre to an emitter placed on the surface of the skin. Some of the photons travelling through the tissue are scattered at different depths by cellular components and travel in random directions. Some photons are absorbed and some are reflected back towards the light source and the detector. The photons reflected back by moving RBC travel at a different frequency than the originally emitted photons. The Doppler shift is induced by the movement of RBC within arterioles, capillaries and venules (Nilsson et al., 1980; Bonner & Nossal, 1981). The observed Doppler shifts are linearly dependent on RBC velocity at low blood tissue concentration (Bonner & Nossal, 1981) observed in skin.

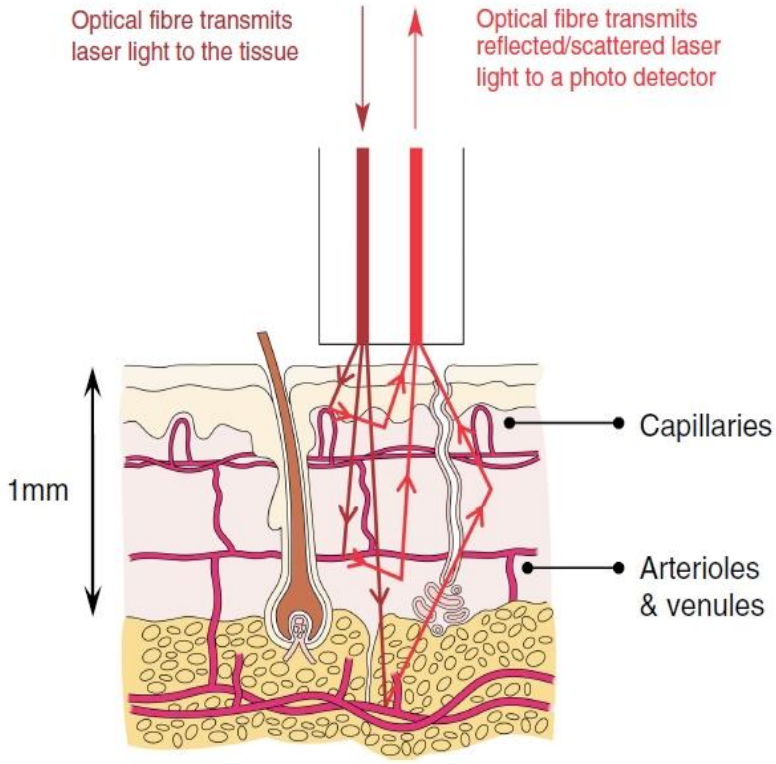

Figure 2.3 The principle of Laser Doppler flowmetry (adapted from Moor Instruments).

The information about blood flow is extracted from the broadening of the width of the frequency spectrum (the Doppler effect) between emitted and reflected photons (Gush et al., 1984). The Doppler frequency shift depends on blood velocity and orientation of moving RBC. For RBC moving perpendicularly to the illuminating beam of light the Doppler shift will be minimal. In the opposite scenario when RBC are moving parallel to the incoming photons, the Doppler shift will be maximal (Gush et al., 1984). The output signal is defined as blood flux (BF) and it is a product of RBC concentration and RBC velocity. The depth of tissue from which the LDF signal is derived depends on the laser power, wavelength and the separation of the emitting and collecting fibres (Gush et al., 1984; Jakobsson & Nilsson, 1993; Larsson et al., 2002; Morales et al., 2003; Clough et al., 2009).

The structure of the human skin differs throughout the body, hence the BF signals recorded at different skin sites also differ. The common sites for LDF measurements are at the foot, forearm and fingers, however other skin sites such as forehead, and chest are also commonly investigated. The important difference between forearm and fingers is the presence of AV anastomoses in the fingers. This is reflected in LDF signals as a higher baseline signal.

LDF usually records the blood flux signal at high sampling rate; therefore it is possible to observe rapid changes in mass flow such as the changes during the post-occlusive reactive hyperaemia as well as the cardiac pulse-wave and other blood flowmotions. The LDF system used for measurements in this thesis has a sampling rate of 40 Hz. Using a high frequency sampling rate yields more samples per second and may improve the accuracy of analysis of short segments of the signal.

An example of resting measurement (baseline) of forearm skin BF is illustrated in Figure 2.4. The signal was recorded during rest from the forearm of a healthy person over 5 minutes at a sampling rate of 40 Hz. It is worth noting that the signal is not constant over time and there are multiple oscillations present with higher frequencies superimposed on lower ones.

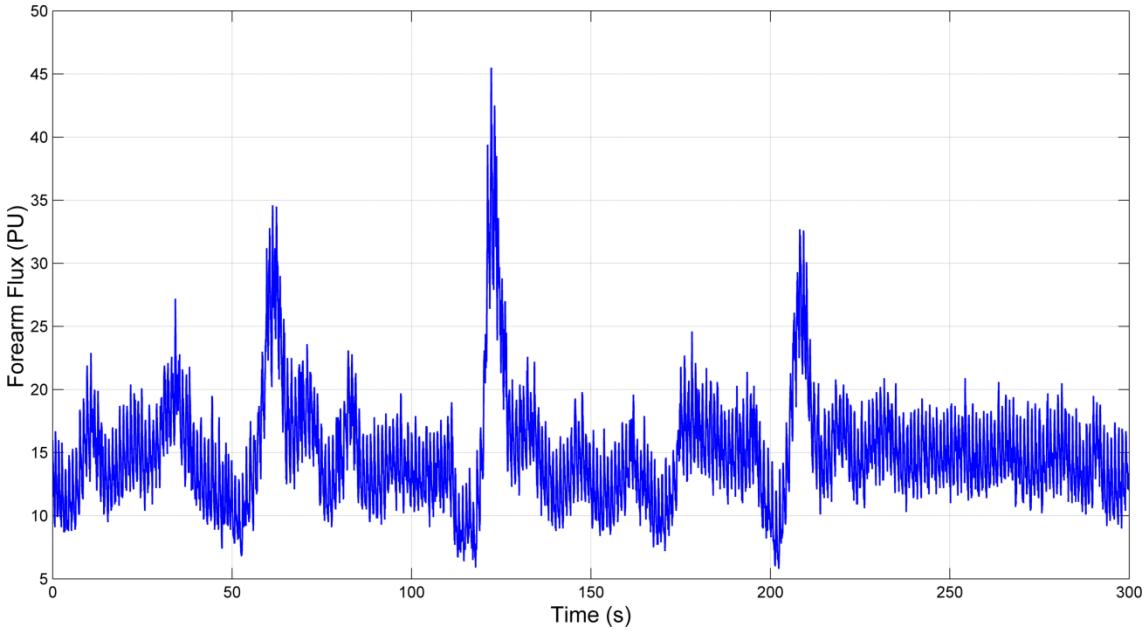

Figure 2.4 Forearm skin blood flux recorded during rest in a healthy volunteer.

LDF measure of blood flux is expressed in arbitrary units called Perfusion Units (PU), which cannot be converted to the absolute flow values. Due to the intra-site and intra-subject variability and the heterogeneity of the sampled tissue, the baseline measurements are usually compared to the measurements following a physiological perturbation of blood flow. The relative change to a challenge has been found to be more informative than the absolute value measured before and after the perturbation (Morales et al., 2005; Tikhonova et al., 2010; Agarwal et al., 2012; Humeau-Heurtier et al., 2013).

The system response to a challenge may be studied as a separate variable or it may be normalised to some reference value, for example the baseline measurement. Commonly used

challenges include post-occlusive reactive hyperaemia (PORH), inspiratory breath-holds (IBH), local warming, local cooling and iontophoresis of vasoactive compounds for example acetylcholine (Gooding et al., 2006; Hodges et al., 2006; Kruger et al., 2006; Clough et al., 2009; L'Esperance et al., 2013).

The response to PORH involves endothelial dependent and independent mechanism but it is often considered as a measure of microvascular and endothelial functions (Yvonne-Tee et al., 2005; Cracowski et al., 2006; Forst et al., 2008). PORH is used to test the ability of the microcirculation to recruit arterioles and capillaries after transient ischemia (De Backer et al., 2012). PORH is achieved by placing a cuff around the limb (arm, thigh or ankle) and inflating it above the systolic blood pressure to induce arterial occlusion. Figure 2.5 shows an example of a baseline recording followed by PORH, recorded from the forearm of a healthy individual. The upper plot is the cuff pressure and the lower trace is the blood flux. In the example shown in Figure 2.5 the pressure cuff was inflated to 180 mmHg after 60 s of baseline measurement. This resulted in a rapid fall in BF. However, the BF signal does not reach zero during supra systolic arterial occlusion. The level of BF reached during occlusion is known as biological zero (BZ) and it is thought to be caused by Brownian motion of RBC (Kernick et al., 1999). The occlusion was maintained for three minutes. In literature the time of occlusions vary, however three minutes is considered as standard occlusion time. After the cuff pressure is released a reactive hyperaemia occurs with about 10 fold increase in forearm BF. BF then returns to approximately baseline level. There are several measures that can be extracted from the PORH sequence. The most common are the resting value (baseline before occlusion; RF), biological zero (BZ), maximum value after release of occlusion (MF), area under the hyperaemia curve (AUC), time to peak, and time to half recovery after peak. Furthermore the ratio of the maximum flux and resting flux (MF/RF) is often reported as it is a normalised value describing the system's response to an applied stimulus (Morales et al., 2005; Roustit et al., 2010a). Some researchers express data as Cutaneous Vascular Conductance (CVC) (Roustit et al., 2008; Roustit et al., 2010a; Tew et al., 2011). It is calculated as BF divided by mean arterial blood pressure.

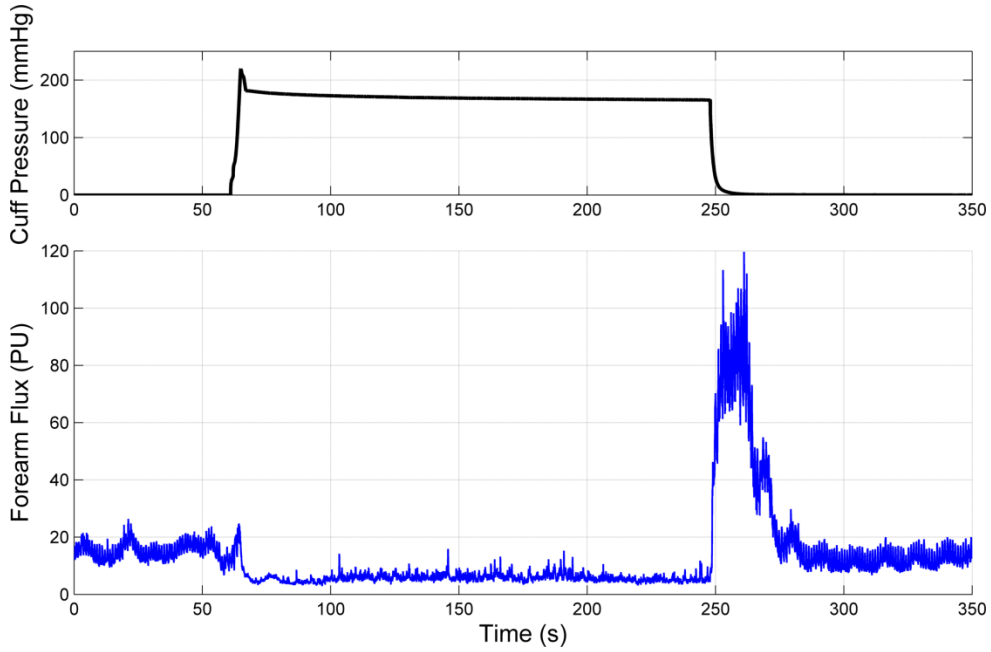

Figure 2.5 Post-occlusive reactive hyperaemia recorded from the forearm of healthy subject. The pressure cuff around the arm was automatically inflated to 180 mmHg for three minutes.

Microvascular function is altered in many diseases including cardiovascular disease, diabetes, Raynaud's phenomenon, systemic sclerosis, peripheral vascular disease and carpal tunnel syndrome (Mahé et al., 2012; Roustit & Cracowski, 2013). The results of PORH test serve as a marker of microvascular function (Cracowski et al., 2006; Roustit et al., 2010a), therefore it has been used to investigate the state of microvascular function in numerous conditions. In cardiovascular disease the maximal flow after occlusion is lower and time to peak is longer than in healthy subjects (Binggeli et al., 2003; de Mul et al., 2009; Strain et al., 2010). In patients with diabetes the shape of PORH has been found to be different from healthy subjects. The response recorded after cuff deflation is lower. Also the area under the PORH curve is smaller (Prazny et al., 2009; Yamamoto-Suganuma & Aso, 2009). In Raynaud's phenomenon and systemic sclerosis the time to recovery after occlusion was longer compared to healthy subjects (Roustit et al., 2008; Grattagliano et al., 2010). There are more examples in literature showing differences in PORH parameters between healthy and diseased states, however currently it is not possible to diagnose the disease from PORH analysis alone. The altered response to occlusion may indicate pathology, but does not specify the underlying cause.

Figure 2.6 presents the blood flux signal during the inspiratory breath-holds (IBH), which can be used in the assessment of autonomic sympathetic vasoconstrictor response (Feger & Braune, 2005; Young et al., 2006). The volunteer is asked to take a deep breath and hold it for

6 seconds. Breathing influences both the autonomic and sympathetic nervous systems causing local variation in skin blood flow and temperature (Allen et al., 2002). Figure 2.6 shows two inspiratory breath-holds starting at the points of arrows and lasting about 6 seconds. Holding the breath causes the drop in BF. Venous return to the heart evokes a sympathetic constrictor response and reduces peripheral blood flow. In the literature it has been shown that the change in BF induced by IBH also causes a fall in temperature indicating the activity of AV shunts (Allen et al., 2002; L'Esperance et al., 2013).

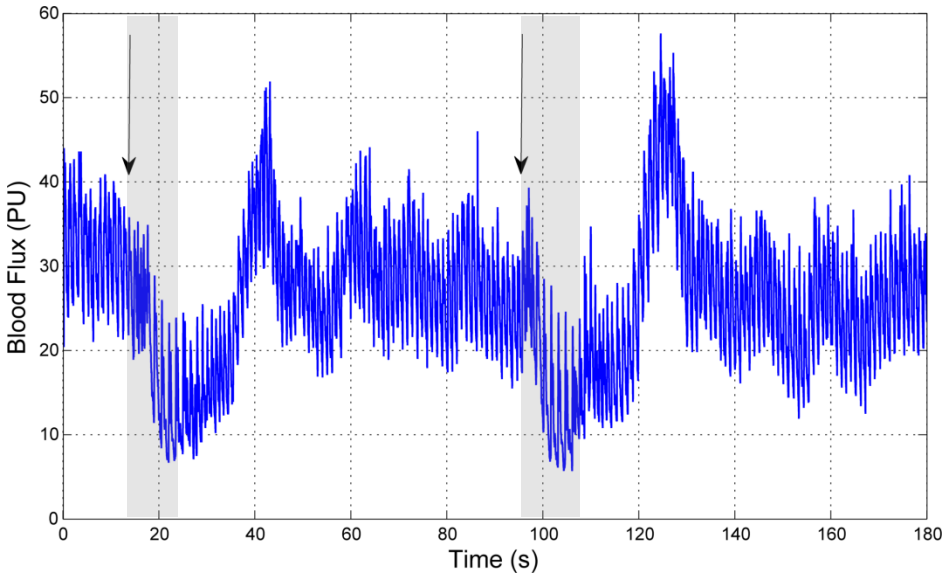

Figure 2.6 An example of inspiratory breath-holds. The arrows indicate the start of a breath-hold and the shaded areas the duration of breath-holds.

Blood flux during IBH has been studied in models of multiple system atrophy and pure autonomic failure. Both models showed the reduced response to IBH, which may correspond to reduced nerve density in these subject (Young et al., 2006). The drop in BF in response to IBH in children with sickle cell anaemia was larger than control subjects suggesting greater autonomic reactivity in children with sickle cell anaemia (L'Esperance et al., 2013). IBH has also been studied in diabetic neuropathy and showed reduced responses in subjects with painful diabetic neuropathy indicating that measuring BF during IBH can detect the impaired sympathetic activity (Quattrini et al., 2007). The studies of BF responses to IBH in healthy and unhealthy populations provide information about sympathetic nerve activity, however, at the current time, they do not quantify the extent of the impairment. Further studies are required to develop better understanding of observed responses and their importance in assessment of sympathetic nervous function.

Local warming from ambient temperature to 42-44°C, as shown in Figure 2.7, induces vasodilation. It is a simple test of the vasodilatory capacity of the cardiovascular system (Cracowski et al., 2006; Roustit et al., 2010a). The initial peak in blood flow is mediated by axon-reflex, whilst further sustained plateau is nitric oxide (NO)-dependent (Charkoudian, 2003; Boignard et al., 2005; Minson, 2010). Warming allows the investigation of the neural axon-reflex response and NO-dependent vasodilation (Minson, 2010).

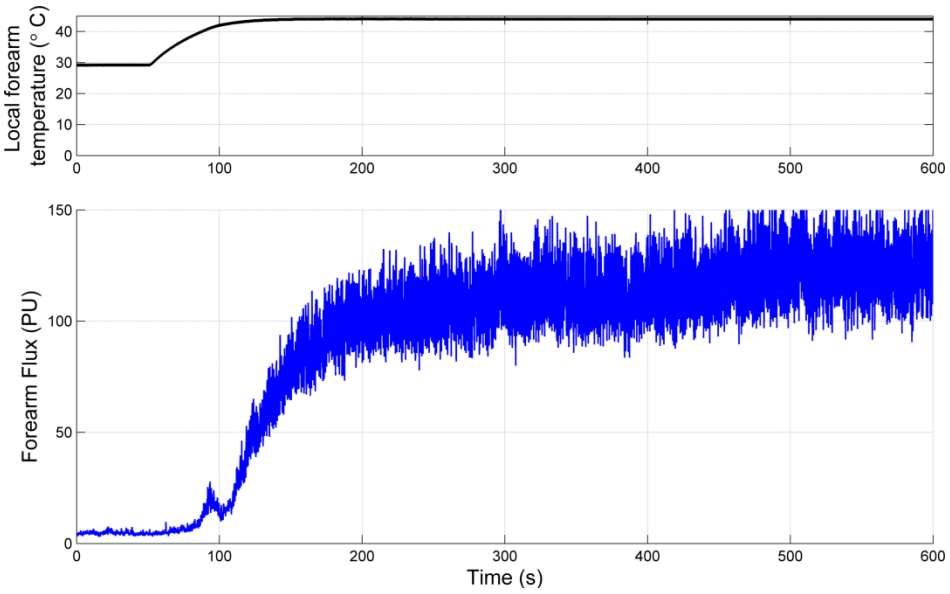

Figure 2.7 An example of local warming. The step change in temperature (top trace) from subject baseline temperature to 44°C results in vasodilation and multifold increase in blood flux (bottom trace).

The response to local warming involves multiple mechanisms, therefore it may be used as a model to study a number of abnormalities. The altered characteristics of the response to local heating have been reported to correlate with Framingham and Cardiorisk scores (Kruger et al., 2006). The shape and amplitude of response to thermal challenge was found different in patients with systemic sclerosis and Raynaud's phenomenon (Boignard et al., 2005; Gunawardena et al., 2007; Roustit et al., 2008). In smokers the area under the curve during warming was smaller compared to healthy volunteers (Avery et al., 2009). In diabetes the maximal flow during warming is smaller than in healthy subjects (Jan et al., 2013).

Response to cooling, similar to warming, is biphasic. The initial response of sensory nerves activates the sympathetic vasoconstriction. It is followed by a sustained vasoconstriction caused by endothelial response to reduced NO (Hodges et al., 2006; Kellogg, 2006; Sheppard et al., 2011). The response to cooling may be used as another test of the microvascular

function. It has been shown that subjects with Huntington's disease exhibit an augmented response to local cooling compared with controls (Melik et al., 2012). Another study found that vasoconstriction induced by prolonged cooling is increased in hypoxia (Simmons et al., 2011). All these studies provide some information about complex response to local cooling with emphasis on difference between healthy and unhealthy subjects. Currently, no methods can classify these differences and assign them to a particular physiological mechanism.

The dynamics of vasodilation and vasoconstriction are non-linear and depend on the temperature rate of change. Vuksanovi et al. (2008) showed that warming and cooling between 24-42°C with rate of change 1°C /min results in a hysteresis loop. Different response curves obtained for heating and cooling indicate the importance of the design of warming and cooling stimuli. The vasodilation achieved after warming to 42°C depends on the rate of warming. Fast warming results in higher BF compared to slow warming (Del Pozzi et al., 2016).

Iontophoresis is mostly used to enhance drug delivery. A low intensity current is applied to the skin to enhance the diffusion of ionic drugs to cross the epidermal barrier into the skin (Tyle, 1986). The most often applied agent in conjunction with skin BF measurements is acetylcholine chloride (ACh) as it induces endothelium-dependent vasodilation. ACh causes a short initial peak in BF, followed by long endothelium-dependent vasodilation. These responses are altered in a number of pathologies, thus iontophoresis in combination with vasoactive agents may serve as a test of specific microvascular mechanisms and endothelial function (Turner et al., 2008; Debbabi et al., 2010). However, a number of studies showed no difference in response to ACh between healthy women and women with a history of gestational diabetes (Hannemann et al., 2002) or in adolescents with essential hypertension (Monostori et al., 2010). The significant change in response to ACh has been found in systemic sclerosis and Raynaud's phenomenon (Khan & Belch, 1999; Anderson et al., 2004). Also women who had preeclamptic pregnancy (Blaauw et al., 2005) showed an abnormal response to ACh (measurements were performed between 3 and 11 months after childbirth). The endothelial function has been assessed by measuring skin BF response to ACh iontophoresis in adult subjects with type 2 diabetes. The endothelial function was found to improve after 14 months of progressive resistance training (Cohen et al., 2008).

Sampled Volume

The blood flux measured with LDF is the sum of fluxes from all vessels contained in the measured volume. It includes arterioles, capillaries and venules and it is not possible to distinguish the flux in a single vessel. Also, in LDF there is no information about the number and size of vessels (De Backer et al., 2012). It is important to have knowledge of the measurement volume as there are different microvascular beds at different depths. The microvasculature in different tissues is controlled by different mechanisms and therefore should be studied and interpreted separately.

The depth of LDF measurement depends on the fibre separation between emitter and detector, laser power, laser wavelength, optical properties of the tissue, skin pigmentation, blood volume and haemoglobin oxygenation (Nilsson et al., 1980; Jakobsson & Nilsson, 1993; Larsson et al., 2002; Sakr, 2010). The higher the power of the laser and the longer wavelength results in deeper light penetration through the tissue. Also, larger fibre separation results in deeper measurements (Clough et al., 2009; Rajan et al., 2009). Most of the currently used LDF systems have a penetration depth estimated to be 1 mm, with the tissue volume sampled being 1 mm^3 (Braverman, 2000; Humeau et al., 2007). It is not possible to exactly measure the sampling depth of LDF, as it is affected by multiple scattering events and will vary due to the heterogeneous structure of the tissue. The studies performed during the course of this PhD were conducted in human healthy skin. The measurements are considered to originate from skin microcirculation only.

The penetration depth can also be estimated using Monte Carlo modelling. In Monte Carlo simulations, photons are considered as particles on a 'random walk' through the structure of tissue. The results estimate the three-dimensional pathways of photons. Information about the penetration depth, sampling depth and total photon path length are estimated from these pathways. However, Monte Carlo modelling requires the absorption and scattering coefficients of the tissue to be known (Jakobsson & Nilsson, 1993). The absorption and scattering coefficients depend on the structure and content of the skin. It is difficult to determine these coefficients experimentally and the work done in this field does not provide a clear answer (Fredriksson et al., 2008). Nevertheless, in LDF the exact information about measurement depth is not necessary to assess the microvascular function. The assessment of microvascular function using LDF aims to detect systematic changes affecting microcirculation. Therefore the measurements registered at different depths within the skin will reflect the general state of

microcirculation. LDF is not suitable for assessment of heterogeneous conditions or changes affecting volume smaller than $1mm^3$.

Spatial and Temporal Variability

The heterogeneity of skin structure and microcirculation is reflected in LDF spatial and temporal variability (Braverman, 2000; Yvonne-Tee et al., 2005; Humeau et al., 2007) and has been a subject of several studies. The temporal variability is linked to the changes in tissue structure and is associated with tissues homeostasis. The tissue perfusion is controlled in a complex way and it changes continuously. The question arises how much does it vary under normal resting conditions? Is it possible to determine normal limits? The findings from studies performed in healthy and unhealthy subjects suggest there is a large overlap in baseline measurements taken from healthy and pathological conditions. However, the responses to physiological perturbations may help to distinguish between health and disease and to assess the mechanisms of disease (Kruger et al., 2006; Quattrini et al., 2007; Yamamoto-Suganuma & Aso, 2009; Agarwal et al., 2012). Therefore, the majority of research performed on skin BF involves measuring the response to physiological perturbations, as described above.

Movement Artefacts

The LDF technique is sensitive to movement of the probe relative to the skin and of the optical fibre lead (due to speckle illumination from a multimode fibre). Accidental movement of the probe or the optical fibre lead during LDF measurement results in spike in the recorded signal, as shown in Figure 2.8. For meaningful analysis, the regions with artefacts should not be selected for analysis.

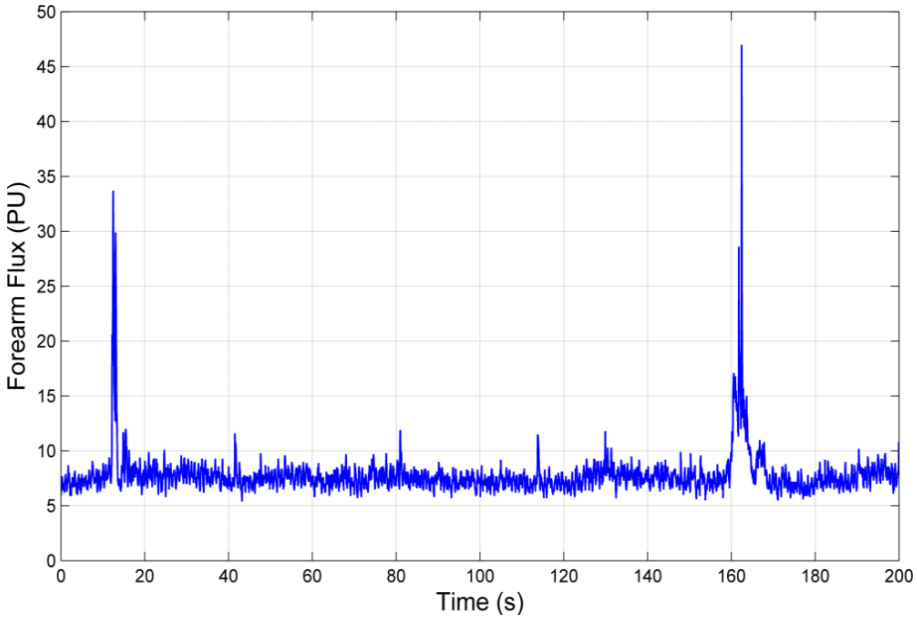

Figure 2.8 The accidental movement of optical fibres results in artefacts; i.e. spikes as shown at about 15 and 160 s here.

This is straightforward for time-domain analysis, when the user can manually select a region of interest and calculate perfusion parameters for an artefact-free region. However, for frequency-domain analysis, long recordings are required, in particular for analysis of low frequency oscillations. To avoid false results, the measurement signal has to be carefully checked if it contains obvious movement artefacts to ensure that frequency domain analysis is not compromised by a poor quality signal. Most movement artefacts appear as fast spikes with amplitude far higher than the average resting signal. Thus, they can be easily identified visually and also computationally using peak detecting algorithms. The influence of movement artefacts on frequency-domain analysis has been described by Wei Qi (Qi, 2011). He has shown that movement spikes significantly alter the frequency-domain analysis and may lead to inaccurate conclusions.

2.2.3 Summary

LDF is an easy to use, non-invasive technique for measuring microcirculatory blood flow. It is simple to set up and record the signal from the skin. In combination with physiological perturbation it provides a tool to investigate the microvascular function in health and disease. The previous reproducibility and variability studies showed an acceptable level of confidence when analysis included a response to physiological perturbations. The main disadvantages of LDF are the sensitivity to the movement artefacts, small measurement volume and the inability

to determine absolute blood flow. However, LDF has been validated in a number of research settings and is widely used for measurements of relative flow changes in skin microcirculation. Compared to other available techniques LDF is the only technique which offers the continuous measurement of skin microcirculation.

2.3 Tissue Oxygenation

The previous section showed the importance of microcirculatory blood flow and the technical methods used to assess skin perfusion. This section considers the measurement of tissue oxygenation, its clinical importance and applications.

2.3.1 Tissue Oxygenation throughout the Body

Adequate oxygenation throughout all tissues is necessary for survival. It is maintained by regulating oxygen delivery to meet oxygen demand. Oxygen delivery and consumption vary between tissues and depend on the functional state of the tissue. At rest the highest oxygen consumption occurs in brain cortex (0.08-0.1 ml/g/min), kidney cortex (0.09-0.1 ml/g/min) and heart (0.07-0.1 ml/g/min). However, during increased activity such as strenuous exercise the oxygen consumption in the heart can increase up to 0.4 ml/g/min. The oxygen consumption in skeletal muscle during physical exercise can increase by 20 to 50 fold. The oxygen consumption also depends on body temperature. The higher the body temperature the higher oxygen consumption. The microcirculation is vital in delivering oxygen to the tissue. The oxygen availability depends on the arterial oxygen concentration and blood flow rate. Blood flow rate varies between different tissues and in consequence the oxygen availability varies. At rest, skin oxygen delivery exceeds oxygen utilisation but a number of pathological conditions such as diabetes or foot ulcers are associated with poor microcirculation and inadequate tissue oxygenation (De Backer et al., 2012).

2.3.2 Current Techniques for Assessment of Tissue Oxygenation

The current techniques for non-invasive investigation of tissue oxygenation include pulse oximetry, white light reflectance spectroscopy (WLS) or visible light spectroscopy (VLS) or lightguide tissue spectrophotometry (O2C), near-infrared spectroscopy (NIRS), transcutaneous oxygen tension ($tcpO_2$) assessed by Clark electrode and flow mediated fluorescence. White light reflectance spectroscopy, lightguide tissue spectrophotometry and visible light spectroscopy are all essentially based on the same principle, described in detail in the next

section. The techniques for non-invasive measurements of tissue oxygenation are summarised in Table 2.2 in the same way as a summary of techniques for measuring blood flow (Section 2.2.1, Table 2.1). The technique, its principle and output measure are shown in first three columns, followed by the reproducibility of the technique, advantages, limitations, applications and the references to scientific research and reviews.

Table 2.2 The summary of non-invasive methods for measuring tissue oxygenation.

Technique	Principle	Output measure	Reproducibility	Advantages	Limitations	Applications
Pulse oximetry	Difference in light absorption by oxyHb and deoxyHb	Oxygen saturation of haemoglobin in arterial blood (SaO_2), expressed in %	Good reproducibility in high SaO_2 readings	Easy to use, instant reading; Approved as clinical diagnostic device	Movement artefacts, only approximate measure, sensitive to physiologic and environmental factors (arrhythmia, peripheral vasoconstriction, nail polish, bright ambient light, etc.)	Suspected tissue hypoxia(Elliott et al., 2006)
Near-infrared spectroscopy (NIRS)	Difference in light absorption by oxyHb and deoxyHb	The relative amount of oxygenated and deoxygenated haemoglobin in microcirculation, arbitrary units (AU) but can be converted to absolute units	Good reproducibility CV[4] 20-30% (Kragelj et al., 2000; Van Beekvelt et al., 2001)	Continuous measurements	Skin pigmentation may reduce the accuracy	Dynamics of oxygenation in deeper tissues(brain, muscle) (Blasi et al., 1993; Sakr, 2010; Ferrari et al., 2011; Pellicer & Bravo, 2011; Scheeren et al., 2012; Waltz et al., 2012)
White light reflectance spectroscopy (WLS), visible light spectroscopy (VLS) and lightguide tissue spectrophotometry (O2C)	Difference in light absorption by oxyHb and deoxyHb	The amount of oxygenated and deoxygenated haemoglobin in microcirculation, arbitrary units (AU)	Good reproducibility	Continuous measurements	Spatial variability	Dynamics of oxygenation in skin (Liu et al., 2005)

[4] Coefficient of Variation (explained in detail in section 3.5.4)

Technique	Principle	Output measure	Reproducibility	Advantages	Limitations	Applications
Transcutaneous oxygen tension ($TcpO_2$ or TCOM)	Oxygen diffusion to skin surface induced by local warming	Oxygen tension (mmHg)	Acceptable intra- and inter-subject reproducibility (Kragelj et al., 2000; Jorneskog et al., 2001; Gélis et al., 2009)	Approved as clinical diagnostic device	Measurements taken during thermal hyperaemia, low sampling rate, poor spatial and temporal resolution	Predicting wound healing, assessment of amputation level, (Boyko et al., 1996; Rich, 2001; Poredos et al., 2005; Iabichella et al., 2006)
Flow mediated fluorescence	Changes in florescence of reduced nicotinamide adenine dinucleotide (NADH) reflecting changes in oxygen supply	Relative amount of oxygen supply to skin	So far no data on reproducibility	Higher sensitivity compared to absorption spectroscopy; high spatial resolution	Up to date small number of studies confirming application of technique	Cardiovascular disease (Piotrowski et al., 2016)

Among the presented techniques, pulse oximetry is the most used technique for assessment of arterial haemoglobin oxygen saturation and pulse rate. It is used in numerous clinical setting on a daily basis. It is cheap and easy to use compared to other techniques; however it also has a number of limitations. In many conditions such as low perfusion, vasoconstriction or hypothermia the measurement might be inaccurate (Elliott et al., 2006). Pulse oximetry cannot be directly compared to the other techniques because it assesses arterial oxygen saturation rather than microvascular oxygenation.

Near-infrared spectroscopy allows for real-time, non-invasive and accurate measurements of oxygenated and deoxygenated haemoglobin in deeper tissues such as brain or muscle. The assessment of brain oxygenation is important in clinical management of critical care patients, therefore a non-invasive method such as NIRS is often employed (Kim et al., 2010; Boas & Franceschini, 2011). NIRS monitoring can also be employed during brain surgery to provide information about cerebral oxygenation. It is also increasingly used in psychology and psychiatry to assess the brain activity (Murkin & Arango, 2009; Fukuda, 2012). In muscles, NIRS allow for the assessment of haemodynamic variables, in particular the oxygen consumption during rest and exercise (Ferrari et al., 2011).

White light reflectance spectroscopy, diffuse correlation spectroscopy, lightguide tissue spectrophotometry and visible light spectroscopy can be considered as one technique with different names. It is most suitable for non-invasive, continuous measurement of skin oxygenation. The next section presents in detail white light reflectance spectroscopy and its application in studying dynamic changes in oxygen content in microcirculation.

2.3.3 White Light Spectroscopy

The chromophores are the light-absorbing compounds. In the human skin, melanin and haemoglobin are the most abundant chromophores. Melanin, found in the epidermis absorbs and scatters UV light protecting the skin from UV damage. Haemoglobin (Hb) is the main protein of red blood cells and it binds oxygen and transports it around the body. Haemoglobin mostly absorbs visible light and the absorption spectrum depends on the oxygen content bound to it.

Melanin is a natural pigment determining skin and hair colour. Higher melanin concentration in skin results in darker skin colour. Melanin is produced in lowest layer of epidermis and found throughout upper layers of epidermis. It protects cells from DNA damage from UV radiation by

high absorption of UV light (200-400nm). In consequence, most of UV light is not transmitted to deeper layers of the skin. For longer wavelengths (visible light) the transmission of light in skin is higher therefore light reaches deeper layers of skin. In those layers oxyHb and deoxyHb are important absorbers of light. The spectroscopic techniques are based on different absorption profiles for oxyHb and deoxyHb within spectrum of visible and infrared light. The absorption profiles of melanin, oxygenated and deoxygenated haemoglobin within visible light spectrum are shown in Figure 2.9. Melanin exhibits a broadband absorption, whilst oxyHb and deoxyHb have well defined absorbance peaks. The section of interest lies between 500 and 650 nm, where light is relatively highly absorbed by haemoglobin. Furthermore, oxyHb and deoxyHb have multiple isosbestic points (the wavelength at which the absorbance for oxyHb and deoxyHb is the same). For oxyHb and deoxyHb these points are 498, 525, 548, 568 and 585 nm (Jue & Masuda, 2013).

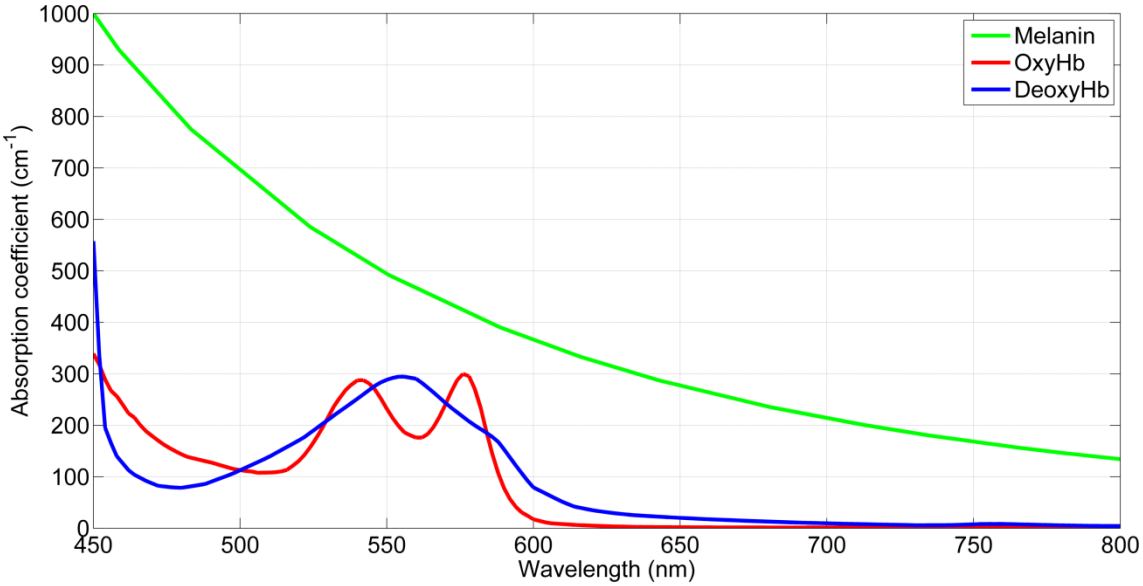

Figure 2.9 Light absorption coefficients for melanin, oxygenated (OxyHb) and deoxygenated (DeoxyHb) haemoglobin within light spectrum between 450 and 800 nm.

White light spectroscopy allows for the measurement of oxygen content in the blood. The principal of WLS is based on light absorption properties of the OxyHb and DeoxyHb (as shown above in Figure 2.9) – the spectroscopy is the study of interactions between electromagnetic radiation and matter. The modified Beer-Lambert Law (Equation 2.2) describes the optical interactions between photons and chromophores,

$$A(\lambda) = \varepsilon(\lambda) \times c \times I(\lambda, c) + G(\lambda) \quad (2.2)$$

where λ is the light wavelength, A is the attenuation, ε is the molar extinction coefficient of the chromophore, c is the molar concentration of the chromophore, I is the mean path length and G is the scattering loss. The attenuation A is defined as (Equation 2.3),

$$A(\lambda) = \log_{10}(\frac{I_0(\lambda)}{I(\lambda)}) \quad (2.3)$$

where I is the reflected light and I_0 is the incident light.

The source of white light is positioned on the skin such that the light source is as close to the surface as possible. The light contained within the spectrum between 500-650 nm penetrates the skin and is absorbed differently by oxyHb and deoxyHb in the RBC. The oxygenated haemoglobin induces a double-peak spectrum, whilst deoxygenated haemoglobin results in a single-peak spectrum (Figure 2.9).

The received spectrum is processed to calculate the percentage of RBC carrying oxygen. Spectral analysis of the scattered light reveals how much haemoglobin in the sampled volume carries oxygen and how much do not carry oxygen. The measure is indirect and it is expressed in the arbitrary units (AU). The parameter of oxygen saturation (SO_2) is calculated as (Equation 2.4),

$$SO_2 = \frac{oxyHb}{oxyHb + deoxyHb} \quad (2.4)$$

where $oxyHb$ denotes haemoglobin which carry oxygen and $deoxyHb$ the haemoglobin without oxygen.

The SO_2 parameter is a normalised measure and it is most often reported as the descriptor of tissue oxygenation. However, the sources of SO_2 measure are oxyHb and deoxyHb signals, which reflect the light absorption at different wavelengths. They provide separate information of changes in oxyHb and deoxyHb, therefore allow for more precise tracking of changes in amount of oxygen present in the microvasculature. The SO_2 measure is insensitive to same-direction changes i.e. the simultaneous increase or decrease in oxyHb and deoxyHb will not change the ratio. Thus, it is important to analyse oxyHb and deoxyHb signals in addition to the SO_2 signal.

Figure 2.10 shows a combined measurement of blood flux and tissue oxygenation recorded from the forearm of a healthy subject during rest. However, as with blood flux, the measurements of tissue oxygenation are often taken in conjunction with physiological perturbations in order to assess microvascular functionality. These have been reviewed in Section 2.2.2.

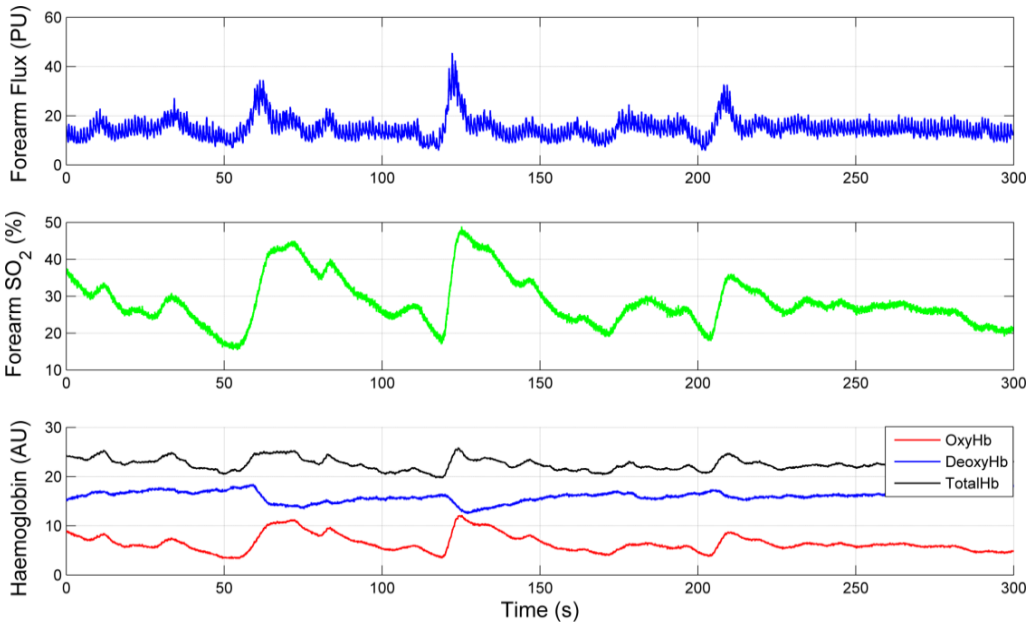

Figure 2.10 Blood flux (top trace), tissue oxygenation (middle trace) and haemoglobin concentrations (bottom trace) during rest. The fluctuations present in the signal are attributed to the spontaneous, physiological oscillations. Total haemoglobin is the arithmetic sum of OxyHb and DeoxyHb.

The techniques discussed above serve as tools for assessment of tissue oxygenation, which is a fundamental characteristic of tissue health. However, the measurements combining the assessment of tissue blood flow and oxygenation have an advantage over separate measurements of blood flow and/or tissue oxygenation by enabling simultaneous observation and studying the dynamics between these two measurements. The combined techniques are discussed in the next section (2.4).

2.4 Monitoring Blood Flux and Oxygenation Simultaneously

2.4.1 Importance of BF and SO_2 in Clinical Setting

Blood flow and tissue oxygenation are directly linked as the oxygen molecules are carried by RBC. Some diseases or acute conditions affecting blood flow result in poor delivery of oxygen

to the tissue (e.g. peripheral vascular disease, stroke). However, in other conditions such as anaemia, the perfusion is normal whereas the delivery of oxygen is reduced due to the haemoglobin deficiency. In the clinical setting, there is a recognised need to measure BF and SO_2 together in order to assess adequately the tissue status. In basic science the combination of BF and OXY measurements has the potential to provide complimentary information about tissue health status.

Some of the techniques described in the previous sections have been coupled into single systems to measure BF and SO_2 simultaneously. However, this is not yet routinely applied, as the combined techniques are not yet widely used and validated to provide useful clinical information (Benedik, 2014). Most LDF studies performed to date have focused on blood flow alone, as only recently the combined systems have been developed. The combined measurements create an opportunity to understand how the microcirculatory blood flow is controlled as well as how it is related to tissue oxygenation.

2.4.2 Combined Monitors for Assessment of Skin Blood Flux and Oxygenation

There are number of commercial LDF and WLS systems. The equipment used during the course of this thesis was developed by Moor Instruments Ltd, UK, and is described in more details later. The monitors are called moorVMS-LDF and moorVMS-OXY. Another developer of a combined system is LEA Medizintechnik. Their system is called O2C (oxygen to see). It is the combination of LDF and WLS. It illuminates the tissue with laser light (830nm 30mW) and white light (500-800nm, 20mW). The reflected light is detected and processed to give blood flux and oxygen saturation. This system has been used to study muscle perfusion and oxygenation in subjects with diabetes (Joshi et al., 2010). Forst et al. (2008) studied the reproducibility of the O2C system in healthy and diabetic subjects and reported skin BF coefficient of variation (CV; this relates to reproducibility of measurement and is explained in detail in section 3.5.4) of 50% and 34% for non-diabetic and diabetic subjects respectively, the muscle BF CV was 43% and 36%. Tissue oxygenation showed lower CV: in skin it was 17% and 18% (non-diabetic and diabetic), in muscle it was 25% and 10%. They also measured peak BF and SO_2 in PORH and found these measurements the most reproducible with CV values of 10% or less (Forst et al., 2008). Beckert et al. (2004) reported no significant differences in BF and SO_2 measurements taken in healthy volunteers on two consecutive days. However, most of the studies indicate that the combined measurements are reproducible.

Other examples of combined measurements are DCS and NIRS, which have been used to study blood flow and oxygenation in the deeper tissue, mostly brain, muscle or breast (Durand et al., 2004; Shang et al., 2009; Lin et al., 2012).

2.4.3 Spontaneous Oscillation and Coupling

The spontaneous oscillation in microcirculatory blood flow and oxygenation are well recognised across different tissues. They have been studied in the brain, muscle and skin (Bracic & Stefanovska, 1998; Li et al., 2010; Boas & Franceschini, 2011) but the majority of these studies investigated only one of the measures. It is clear that there is a coupling between blood flow and oxygenation e.g. brain autoregulation – the brain vasculature responds to the increased oxygen demand by vasodilation of the blood vessels; this results in increasing blood flow and delivering more oxygen. However, there are several questions that can be asked: What is the delay between these events? How closely the oscillations in one measure (blood flow) are reflected in another measure (tissue oxygenation)? Are there specific coupling mechanisms indicating direct interaction between blood flow and tissue oxygenation? Furthermore, these questions can be asked for different tissues. The main focus of this thesis is skin microcirculation, therefore the majority of the literature review relates to human skin.

2.4.4 Does Tissue Oxygenation Help to Assess Tissue Oxygen Consumption?

In the clinical setting tissue oxygenation is understood as the availability of oxygen for cells to consume. Another concept linked to tissue oxygenation dynamics is tissue oxygen consumption (VO_2), also called the oxygen utilisation. The rate of oxygen consumption varies in different tissues and depends on tissue activity. For normal tissue function, the oxygen delivery has to match or exceed the oxygen consumption. The brain receives approximately three times more oxygen than it uses and the exercising muscle has an oxygen delivery rate of about 1.5 times higher than the consumption rate (Wolff, 2013). The exercising muscle consumes up to 50 times more oxygen compared to the resting muscle (Boas & Franceschini, 2011). Poor blood and oxygen delivery, for example in peripheral arterial disease (PAD), can lead to ulcers, chronic wounds and gangrene (Mathieu & Mani, 2007). If oxygen delivery is lower than tissue requirements it may lead to organ failure (Ekbal et al., 2013). Thus, it is important to assess both: the oxygen delivery and the oxygen consumption (De Backer et al., 2012).

Oxygen delivery is usually measured by analysing both the oxyHb and deoxyHb spectra of the blood. Quantifying the oxygen consumption has been approached predominantly by analysing

oxyHb and deoxyHb during arterial occlusion. Blasi at al. (1993) used a NIRS probe placed on the forearm to record skeletal muscle oxygenation. They calculated the desaturation rate of oxyHb during arterial occlusion. To calculate oxygen consumption, the rate of change of oxyHb and deoxyHb was multiplied by the molecular ratio between haemoglobin and oxygen (1:4) and multiplied by the density of muscle tissue (1.33g/ml). The output of these calculation was oxygen consumption expressed in µmoll/l*100g. Boas & Franceschini (2011) reviewed a number of studies aiming to assess the oxygen consumption in skeletal muscle, brain and breast. They indicated that the arterial occlusion method is adequate for calculating muscle oxygen consumption as the arterial occlusion stops the inflow of 'new' oxygenated blood. However, in other tissues where it is not possible to induce a rapid change in blood flow the oxygen consumption measurements are cofounded by BF, hence BF and SO_2 have to be monitored together (Boas & Franceschini, 2011).

A different principle to estimate oxygen consumption was used by Binzoni et al. (2010). They conducted a study with NIRS measuring oxyHb and deoxyHb in exercising muscle. They derived the oxygen consumption from cyclic changes in oxyHb and deoxyHb during muscle contraction and relaxation. The oxygen consumption was calculated as the difference between oxygen accumulated during relaxation and oxygen leaving the muscle during contraction. This method proved to work for estimation of the oxygen consumption in muscle but it has not been applied to other tissues.

The assessment of the oxygen consumption in human skin remains challenging due to difficulty in changing the metabolic rate in skin. However, the arterial occlusion method reviewed above may provide an indication of resting skin oxygen consumption.

2.5 BF and OXY Signal Analysis

The LDF and WLS techniques record the physiological dynamics of skin BF and OXY parameters as digital signals. The acquired signals have to be processed to extract specific information. This section summarises the concepts of signal processing methods applied to BF and OXY signals.

Signal processing is an engineering methodology, which can be described as a set of operations performed on a signal that lead to the disclosure of embedded information. The processing of the signal may include various operations such as detection, transformation, filtering, recovery, enhancement, translation and decomposition. For BF and OXY signals the two

analytical approaches are time-domain and frequency-domain, which are reviewed below (section 2.5.1 and 2.5.2 respectively).

2.5.1 Time-Domain

Time-domain methods refer to extracting the average value of the measurement at particular states for example at rest, during occlusion, after occlusion, etc. Time-domain analysis is relatively easy to conduct and does not require such in-depth technical knowledge as frequency-domain methods. Time-domain analysis is most common as it aims to assess the changes in variables over time. Such analysis often includes calculating mean, minimum, maximum and other relevant statistics of the recorded data. These statistics can be measured at the particular time point or over the period of time. Time-domain analysis also includes detecting time constants, rates of change, curve fitting and finding the dynamic equations describing the system.

2.5.2 Frequency-Domain

The frequency-domain analysis refers to analysis performed on the frequency components of the signal. The time-domain signal is decomposed into a series of component signals which will have different time period, phase and amplitude. Frequency-domain analysis complements time-domain analysis. They help to investigate the oscillatory patterns in time series data and underlying processes associated with them. It is of great importance in studying BF and OXY signals together as there are spontaneous physiological oscillations presents in these signals.

In section 2.1.1 the central and local control of skin microcirculatory blood flow was described. These mechanisms are also reflected in resting BF signals as oscillatory patterns. To date, six distinct activities have been identified within the microvascular flowmotion. These mechanisms have different time constants and therefore have different characteristic frequencies (Bracic & Stefanovska, 1998; Sheppard et al., 2011). Table 2.3 summarises the oscillatory activities influencing microvascular blood flux. Time constants of oscillations are expressed in seconds and also in Hertz (Hz) as non-overlapping approximate ranges (Stefanovska et al., 1999; Kvandal et al., 2006).

Table 2.3 Time constants and origins of the periodic activities regulating microvascular blood flow.

Periodic activity	Time constant (s)	Frequency (Hz)	Origin
Endothelial nitric oxide independent	>105	<0.0095	Mechanisms other than NO, originating from endothelial cells, for example endothelial derived hyperpolarizing factor (EDHF)
Endothelial NO-dependent	48-105	0.0095-0.02	NO production by endothelial cells
Neurogenic	17-48	0.02-0.06	Sympathetic nervous system
Myogenic	7-17	0.06-0.15	Smooth muscle surrounding blood vessels
Respiratory	2.5-7	0.15-0.40	Breathing
Cardiac	0.6-2.5	0.40-1.60	Heartbeat

The alterations in a particular activity e.g. endothelial activity may be associated with pathological changes in microcirculation. Since Bracic & Stefanovska published the frequency-domain analysis of BF signals in 1998, there have been a growing number of studies about the spontaneous oscillations present in BF signals. The main frequency-domain methods used to study and compare healthy and unhealthy BF signals are the Fast Fourier Transform (FFT) and the Morlet Wavelet Transform (WT).

It is difficult to apply these methods to biomedical signals in the context of engineering. Biomedical signals represent complex systems, which vary greatly between different representations of the same system and they change over time in a difficult-to-predict manner. The dynamic interactions between intrinsic and extrinsic factors may be reflected in the studied signals but they are often difficult to extract from the data and to assign to physiological behaviour. It is therefore desired to apply known methods and optimise them for specific applications e.g. studying microcirculatory blood flow and oxygenation. The engineering approach to these biological signals may help to identify and quantitatively describe the characteristics originating from the physiology of the studied system such as skin microcirculation. These characteristics can later be used to assess the status of the system or help to predict future physiological events.

Fourier Transform

The Fourier Transform (FT) is the translation of a signal in the time-domain into one in the frequency-domain. Its primary use is to permit the analysis of a signal in terms of the frequency components of the original signal. FT decomposes the signal into an infinite sum of sine and cosine waves of different periodicity and amplitude such that its sum is equal to the original signal. The Fourier transform of a function $x(t)$ is defined as (Equation 2.5),

$$F[x(t)] = \int_{-\infty}^{\infty} x(t)e^{-j\omega t}dt = X(\omega) \qquad (2.5)$$

where ω is the frequency of oscillation and $X(\omega)$ is the frequency-domain representation of $x(t)$. The inverse Fourier Transform converts the frequency-domain representation back into the time-domain signal. The discrete Fourier Transform (DFT) is used to analyse digital signals, as those are not continuous functions but discrete representations of continuous functions. The Fast Fourier Transform (FFT) is a fast algorithm for computing the DFT. DFT requires the number of signal samples to be a power of two allowing for much faster calculations.

FT itself does not directly provide information about the time that events occur in a signal, but only estimates the power at a given frequency in the signal. Therefore it is not possible to analyse frequency components in time using FT. There are other methods such as wavelet analysis, which combine both: the time and frequency analysis.

Wavelet Transform

The Wavelet Transform (WT) allows for analysis of time and frequency contents of signals and was introduced in 1983 (Morlet et al., 1983). It has the advantage over the FT in providing information about changes in frequency and power of distinct oscillations over time. In the FT this information is lost as the frequency components are averaged over the length of a sampled signal.

Wavelet is a mathematical function with the characteristic shape and scale. The wavelet functions are diverse and the choice of wavelet depends on the nature of studied signals. The WT is widely used in analysis of biological signals (Addison et al., 2009). WT is simply a convolution of a wavelet function with the signal resulting in another representation of the same signal. The better the correlation between the wavelet and the signal, the larger the transform value obtained. There are a number of different wavelet functions available,

including Haar, Meyer, Gaussian and others, but here the discussion is restricted to the Morlet wavelet as it has been the most commonly used in BF and OXY signal processing.

One advantage of the Morlet WT is that it is useful for visualising the change of frequency components over time. For a perfectly periodical signal with only one frequency component the WT results in a straight line, however for more complex signals with multiple frequency components of varying magnitude over time, the WT returns a curved surface. Averaging the transform at the particular frequency over time results in an average scalogram, which is often reported in research papers.

In the time domain the continuous WT transform $\tilde{F}(s,t)$ of signal $f(u)$ is defined as (Equation 2.6),

$$\tilde{F}(s,t) = \int_{-\infty}^{\infty} \overline{\Psi}_{s,t}(u) f(u) du \qquad (2.6)$$

where $\overline{\Psi}_{s,t}$ is a family of basic function obtained by stretching or compressing the mother wavelet by factor s. In the time domain the Morlet wavelet is defined as (Equation 2.7),

$$\Psi(u) = \frac{1}{\sqrt[4]{\pi}} \left(e^{-i\omega_0 u} - e^{\frac{-\omega_0^2}{2}} \right) e^{\frac{-u^2}{2}} \qquad (2.7)$$

where ω_0 is the basic frequency.
In order to describe and compare signals, the quantitative measures are derived from FFT or WT. The analysis of the average energy density within a particular frequency range $\varepsilon_i(f_{i1}, f_{i2})$ is used to compare flowmotion between groups of subjects. The average energy density is defined as (Equation 2.8),

$$\varepsilon_i(f_{i1}, f_{i2}) = 1/t \int_0^t \int_{\frac{1}{f_{i2}}}^{\frac{1}{f_{i1}}} \frac{1}{s^2} \tilde{f}(s,t)^2 ds dt \qquad (2.8)$$

Furthermore, the relative energy contribution of each frequency interval is defined as a ratio of energy of the particular band and total energy within the studied range (Equation 2.9):

$$e_i(f_{i1}, f_{i2}) = \frac{\varepsilon_i(f_{i1}, f_{i2})}{\varepsilon_{total}} \qquad (2.9)$$

The computation of the energy density involves specifying a number of variables such as window function and span, number of FFT, sampling rate. The values of these parameters are

chosen by user and there is no universal consensus in the field of BF and OXY signals. It is not practical to directly compare frequency-domain results performed by different research teams as often they may have used different analysis parameters.

BF signals can be analysed by both FFT and WT to reveal frequency components. However, in most studies the average power in the particular frequency range is of most interest, hence it does not require time information. It does not make a significant difference which method has been used but FFT and WT cannot be directly compared as they are computed differently. The normalised outputs such as power spectral density contribution may allow for valid comparison.

Researchers often compare the power or amplitude in frequency bands of healthy and unhealthy subjects. It has been shown that lower endothelial and neurogenic oscillations are related to microvascular dysfunction (Jan et al., 2009; Liao & Jan, 2011). Bracic & Stefanovska analysed BF signals recorded from athletes and control groups using the Morlet WT. They showed significant differences in the energy and the average amplitude within the cardiac and endothelial frequency bands between athletes and the control group (Bracic & Stefanovska, 1998).

Spectral analysis helps to investigate physiological mechanisms in healthy subjects as well as differences between healthy and unhealthy groups. Sheppard et al. (2011) analysed oscillations in BF signal recorded at normal temperature, during cooling and heating. Cooling increased normalised spectral energy in the myogenic band and decreased the normalised spectral energy in the cardiac band. Alternatively, warming the hand caused a decrease in normalised spectral energy in the myogenic band and increase in the endothelial band (Sheppard et al., 2011).

Huang et al. (2011) analysed power spectral density of BF signals in healthy subjects, individuals with Carpal Tunnel Syndrome and individuals with diabetic neuropathy. They recorded BF from the finger when the wrist was in the neutral and maximally flexed positions. They found differences between groups in some frequency bands, however they were not consistent between the two positions (Huang et al., 2011). Possibly, the heterogeneity of BF at different sites, demographic factors (e.g. age, BMI) and small group sizes cofounded the results. The control and diabetic neuropathy sample sizes were only 11 and 12 subjects.

Frequency-domain analysis has also been applied to BF signals recorded from free flaps (skin inserted surgically from one body part to another) and intact skin showing differences in low

frequency oscillations (Soderstrom et al., 2003). The absolute spectral power was significantly higher in intact skin across all frequency bands, but the normalised power was significantly higher in the intact skin only in endothelial and neurogenic bands.

Spectral analysis of BF signals in diabetic feet with a presence and absence of sympathetic skin response and in a group with pre-ulcerative skin lesions (at-risk group), was performed by Sun et al. (2013). BF was recorded on the dorsum of a big toe. The amplitude of time-averaged wavelet transform was normalised in the same way as in the above study of free flaps and the intact skin. The study of diabetic feet by Sun et al. (2013) found significantly lower normalised amplitude in endothelial band in at-risk group.

Another application of frequency-domain methods to BF signals was presented by Humeau et al. (2000). They tested various types of wavelets to de-noise BF signals and assess peak flow and time to peak in PORH sequence (Humeau et al., 2000). They investigated different coefficient thresholds to remove oscillations and smooth the signal such that the peak flow and time to peak can be accurately assessed. This approach might be useful for some applications, however it removes important oscillations from the BF signal and changes the signal dynamics. Moreover, there are simpler methods for estimating the peak flow and time to peak such as identifying the peak and calculating the time to peak in the time domain.

2.5.3 Other Methods for Signal Processing

A number of other signal processing techniques have been applied to study BF and OXY signals. Researchers have used different entropy measures to investigate the complexity of skin BF signals (Humeau et al., 2008; Humeau et al., 2010; Figueiras et al., 2011). Other approaches included wavelet coherence analysis (Han et al., 2014; Tankanag et al., 2014), intrinsic mode functions (Humeau-Heurtier & Klonizakis, 2015) and Hilbert transform (Liao & Jan, 2012). These research attempts aimed to discover new and interesting features of BF signals. However, so far they have not managed to find clear and robust characteristics allowing for reliable and reproducible assessment of microvascular function.

2.6 Summary

Microvascular function is an important clinical marker of tissue health. There are a number of techniques that allow for measurement and analysis of skin blood flux and oxygenation. Some of the techniques have been adapted to clinical practice and are used as screening tools.

Dual systems, which measure skin BF and OXY simultaneously, are not yet being used routinely as these systems are relatively new. There is a lack of knowledge about the properties of combined measurements, the relationship between BF and SO_2 signals and their potential to inform about disease. Therefore, there is a need to explore the characteristics of the combined BF and OXY signals and subsequently to understand the physiology behind them.

The aims of this thesis address some of the above challenges, in particular the validation of the simultaneous combined measurement of skin blood flux and oxygenation, exploring the values and the interpretation of these measurements. This thesis also applies the signal processing techniques to identify the characteristics of blood flux and oxygenation signals and the relationship between these signals.

Chapter 3

Research Design and Methodology

This chapter describes the design and methods for the study of microvascular blood flux and oxygenation performed on healthy volunteers. One of the main aims of this thesis is to investigate skin blood flux and oxygenation measurements racorded with a combined laser Doppler flowmetry and white light spectroscopy technique. These techniques have been reviewed in Chapter 2. Here, the detailed descriptions of the specific protocols and signal analysis are described.

Two studies were performed during the course of this work. The first study was designed to identify the relationship between skin blood flux and oxygenation over a wide range of values. The second study was designed to investigate the properties of blood flux and oxygenation signals at controlled skin temperatures. The measurements were recorded at thermo-neutral skin temperature (33°C) and during thermally induced vasodilation (local skin warming to 43°C).

3.1 Ethics Approval

The studies were approved by Research Ethics Committee of University of Southampton and Southampton General Hospital (REC Number: SOMSEC091.10; RHMMED0992). The studies were performed in accordance with standards set by the Declaration of Helsinki. All participants gave written informed consent. A copy of the Participant Information Sheet and the Consent Form can be found in Appendices 1 and 2.

3.2 Instrumentation

Skin blood flux, oxygenation parameters and skin temperature were measured using combined laser Doppler and white light reflectance spectroscopy probes. The measurements collected during the first study were obtained using moorCP1T-1000 probe with an LDF fibre separation of 0.5 mm and WLS separation of 1 mm, using a single point 785 nm, 1 mW low power near infrared laser light source (moorVMS-LDF2, Moor Instruments Ltd, UK) and a 400-700 nm, <6 mW white light source (moorVMS-OXY, Moor Instruments Ltd, UK). The second study was performed using the moor CP7-1000 blunt needle probe with the same LDF fibre separation and WLS separation as the Moor CP1T-1000 probe. During the second study the skin

temperature was controlled using a Moor VHP1 skin heating block with moorVMS-HEAT skin heater to warm the skin between 20-45°C with a precision of ±0.1°C and resolution of 0.1°C. All signals were recorded at a sampling rate of 40 Hz. In Study 1, transcutaneous oxygen pressure was recorded using a TCM4 series, Radiometer UK Ltd, Crawley UK. Figure 3.1 illustrates moorVMS-OXY, moorVMS-LDF and TCM4 used during this work. The combined probes and fibres' configuration is shown in Figure 3.2.

Figure 3.1 Combined blood flux and oxygenation monitors (left) and transcutaneous oxygen pressure monitor (right) used to collect data from healthy volunteers.

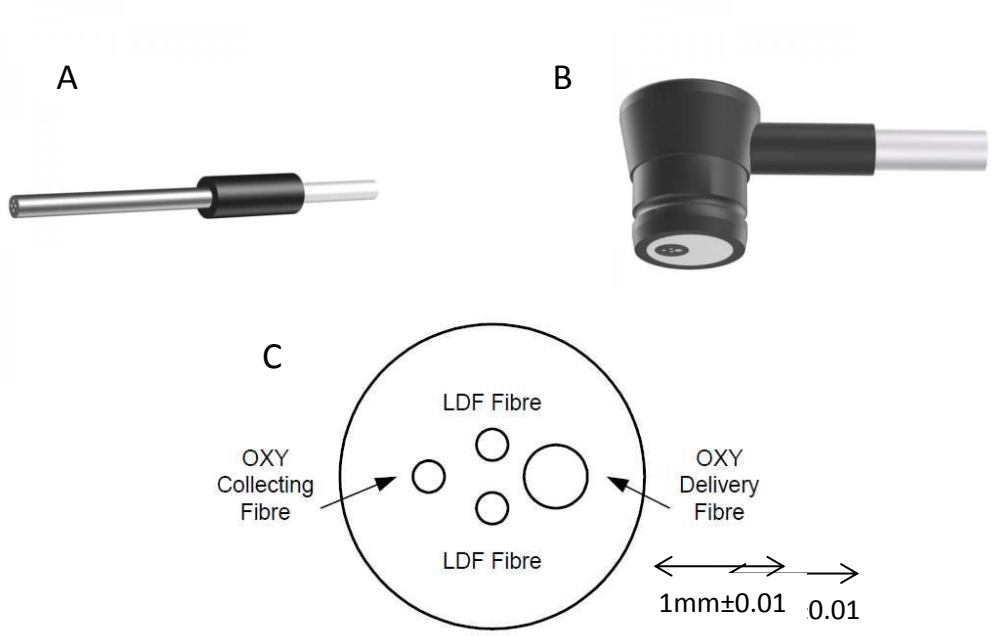

Figure 3.2 The combined probes (A) CP7-1000 and (B) CP1T-1000. The drawing (C) illustrate fibres configuration.

For measurements on the forearm the combined probe was placed on the volar part of the forearm using a double-sided sticky O-ring, approximately 10 cm from the wrist and avoiding

visible veins. The $tcpO_2$ probe was placed about 5 cm distal to the combined probe, as shown in Figure 3.3.

Figure 3.3 Placement of combined BF and SO_2 probe (left) and $tcpO_2$ probe (right) on the forearm of healthy volunteer.

3.2.1 Calibration

LDF has been calibrated every month or every ten volunteers using a motility standard provided by Moor Instruments. Motility standard is a suspension of polystyrene microspheres in water. The Brownian motion of the motility standard provides a repeatable Doppler power spectrum which serves as calibration principle for LDF. The Doppler shift generated by the particles in Brownian motion was used to calibrate the system's overall integrity for a comparison of measurements at different time intervals.

The calibration of OXY module was performed using a calibration probe supplied by Moor Instruments at the same time as LDF calibration. These calibration tests ensured the measurements were acquired according to intended use and manufacturer recommendations.

3.3 Study Protocol

The studies were open, non-randomised, non-interventional investigations on healthy people. Most participants were required to attend only one session with the exception of those participating in reproducibility tests which were performed over two consecutive days.

All subjects were asked to refrain from caffeine containing drinks and large meals at least 2 hours prior to measurements and to not exercise on the day of the measurements.

Before the volunteers were recruited into the study, the aims and design of the study were explained and a printed copy of the participant information sheet was given to each volunteer.

Each volunteer was asked to read this carefully and sign a consent form. The volunteer was then given an identification number and all measurements taken were saved with this reference anonymising all personal data.

3.3.1 Environmental Conditions

Measurements were taken in a temperature-controlled room in the Wellcome Trust Clinical Research Facility, Southampton General Hospital or within University of Southampton premises. The subject was sitting comfortably with the arm at heart level. The time taken to explain the study and sign the consent form served as acclimatisation of the subject to the environmental conditions of the room. The acclimatisation time was at least 20 min. Room temperature was recorded on the data collection sheet.

All subjects were asked to sit still and avoid talking during recordings to limit movement artefacts that might compromise the quality of acquired data.

3.3.2 Data Collection Sheet

Before measurement began, the volunteer's height and weight were recorded on the Data Collection Sheet. In addition, questions about drinking coffee, exercising and taking medication on the day of measurement were asked. The room temperature was measured by an LCD room temperature meter and also recorded on the Data Collection Sheet (Appendix 3). Completed Data Collection Sheets were stored in the study folder and could be accessed only by researchers involved in the study.

3.3.3 Measured Variables

The recorded variables included: BF, RBC concentration, SO_2, oxyHb, deoxyHb, totalHb, skin temperature and cuff pressure (if arterial occlusion was performed). Blood flux was recorded in arbitrary perfusion units (PU), oxyHb, deoxyHb and totalHb in arbitrary units (AU), SO_2 as percentage, temperature in °C and the cuff pressure in mmHg.

In a subset of volunteers the transcutaneous oxygen tension ($tcpO_2$) was measured in addition to blood flux and oxygenation. $TcpO_2$ technique was reviewed in Chapter 2 in Table 2.2. $TcpO_2$ was expressed in mmHg.

Body mass index (BMI) was calculated according to the standard formula originally developed by Adolphe Quetelet in 19th century (Equation 3.1),

$$BMI = \frac{bodymass(kg)}{height(m)^2} \quad (3.1)$$

3.3.4 Perturbations of Blood Flow

BF and OXY signals were recorded at rest and during physiological perturbations of blood flow. The subject had one or more perturbations applied including post-occlusive reactive hyperaemia (PORH), inspiratory breath-holds (IBH) and local skin warming. Study 1 involved following perturbations: PORH, IBH and local skin warming. Study 2 involved only local skin warming.

For the arterial occlusion and hyperaemic response protocol (PORH), the automatic pressure cuff was placed around the arm above the elbow. The automatic pressure cuff was connected to moorPRES monitor and programmed according to PORH protocol. PORH included 10 min baseline recordings (no pressure in the cuff) followed by 3 min arterial occlusion (pressure cuff inflated to 180 mmHg) and at least 5 minutes of post-occlusion recordings.

The sympathetic vasoconstriction response to breath-holds was obtained by asking the subject to take a deep breath and hold it for 6 seconds. This was repeated three times. The average minimum value across three breath-holds was reported as IBH minimum value. The percentage change (IBHmin %) was calculated as the ratio of baseline signal directly before the breath-hold and the minimum during breath-hold.

Local warming in Study 1 was induced by the $tcpO_2$ probe whilst for Study 2 by a heating disc developed by Moor Instruments in conjunction with the combine LDF-OXY probe. In the warming protocol signals were recorded before, during and after warming. The warmed value was defined as the mean value over 1-2 minutes determined after 20 minutes of warming. The mean value was extracted from artefact free region within last five minutes of warming.

In Study 2 the measurements were taken on a reclining infusion chair with the arm at heart level. The volunteer sat in a comfortable position and stayed still and relaxed during the course of measurements. Figure 3.4 shows the measurement probe and the heating disc (left), and the probe attached to the forearm (right). The site for measurements was chosen on the volar forearm avoiding superficial vessels. The heating disc with combined LDF-OXY probe was

attached using double-sided sticky O-ring. The optical leads were secured with the micropore tape to minimise movement artefacts.

All measurements were taken during the morning in the same experimental room with the ambient temperature controlled between 23.0-23.5°C.

The first five volunteers had measurements taken from dry skin as normally recommended by the supplier. However, the response to warming showed a different response than expected. The initial vasodilatory peak resulting from axon-reflex was absent in the measurements. To improve the heating regime, ultrasonic gel was applied on the surface of the heating disc to increase heat transfer. Ten volunteers were measured using the gel.

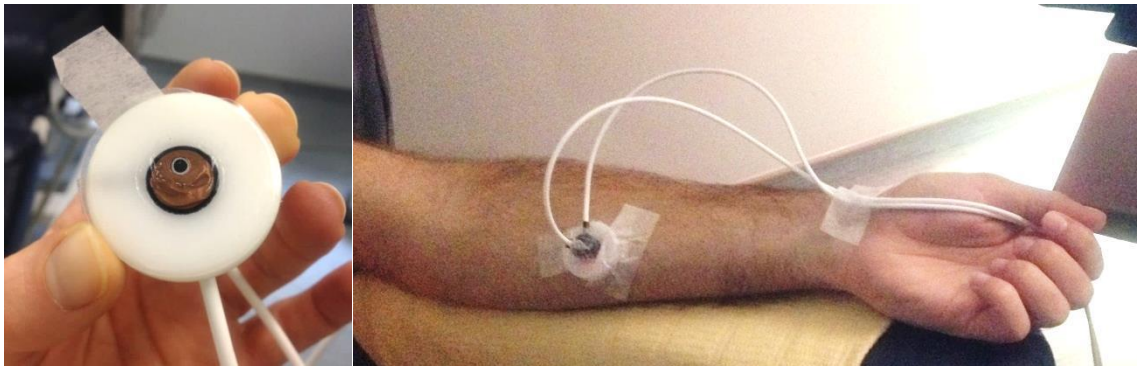

Figure 3.4 The combined LDF and WLS probe inserted into a heating disc (left) and attached to the skin (right).

The measurement protocol for local skin warming consisted of three step changes in temperatures. There were no breaks between the stages and the temperature was controlled by the moorVMS-HEAT monitor.

- Stage 1: *resting skin temperature* – the measurements were recorded for 20 min at volunteer's physiological skin temperature
- Stage 2: *33°C* – the temperature of the heating disc was increased to 33°C and measurements were recorded for 20 min
- Stage 3: *43°C* – vasodilation, the temperature of the heating disc was increased to 43°C and measurements were recorded for 25 min

Figure 3.5 illustrates an example of raw data recorded using Moor Instruments equipment and moorVMS-PC software. The traces from the top are: blood flux, SO_2, oxyHb, deoxyHb, totalHb and temperature. The vertical lines show where the subsequent stages occurred. This protocol was used in the same configuration for all volunteers.

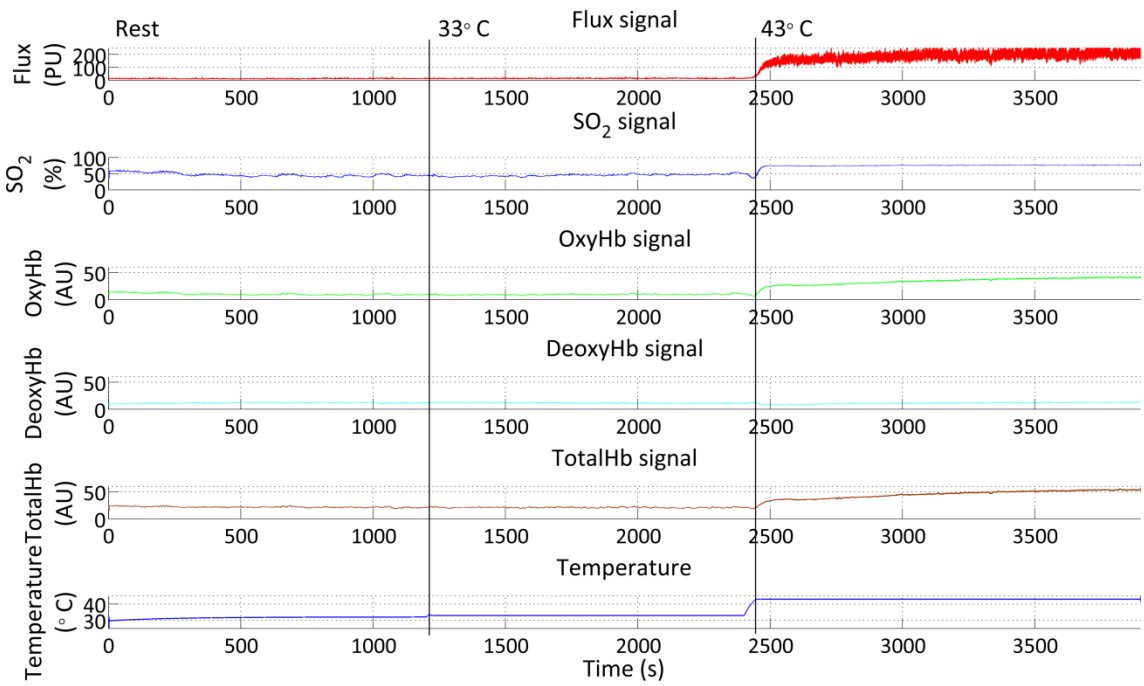

Figure 3.5 An illustrative example of measurements acquired during Study 2.

3.3.5 Transcutaneous Oxygen Pressure in Study 1

$TcpO_2$ is a widely accepted technique for assessment of tissue oxygenation. The principle of operation was described earlier in Chapter 2. Both $tcpO_2$ and SO_2 are measurements of tissue oxygenation. However, they are based on different operation modes and thus measure different variables. $TcpO_2$ was used here to investigate whether $tcpO_2$ measurements correlate with SO_2 measurements. The measurements were taken in the same skin area by first taking resting BF and OXY measurements, then removing the combined probe and attaching $tcpO_2$ probe to the same skin area. After 20 min when $tcpO_2$ measurement was stable, the reading was recorded and the probe was removed. The site was blotted dry with a paper towel and the BF-OXY probe was re-attached to measure BF and OXY at the warmed site.

3.3.6 Reproducibility – Study 1

To test the reproducibility of the measurements of BF and OXY using the combined probe, the repeated measurements were made in a sub-set of 10 participants from Study 1 at two sites and at the same site on two consecutive days. The sites from the first day were marked with a waterproof pen and on the second day probes were carefully attached to the marked sites in the same orientation as indicated in Figure 3.6.

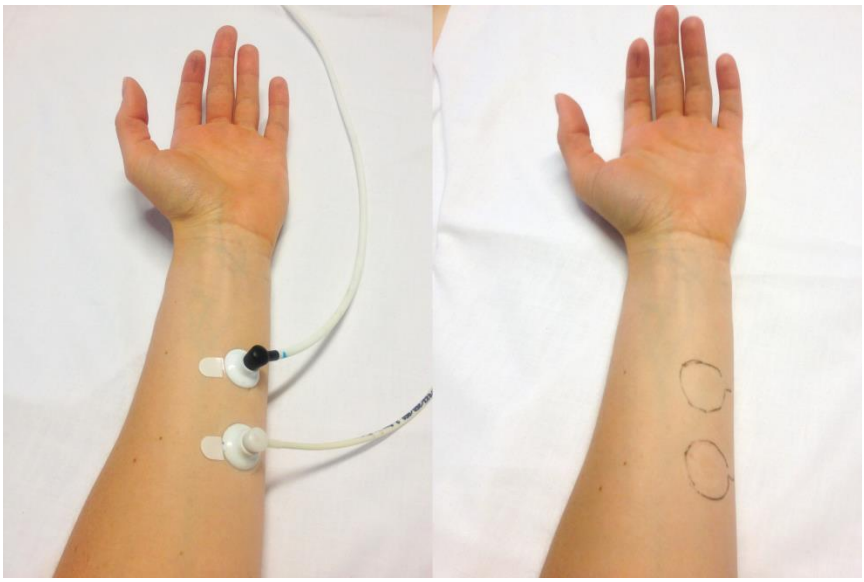

Figure 3.6 Probes attached to the forearm during reproducibility study (left). The waterproof marks (right) were drawn around the probes in order to attach the probe to the same site on the following day.

3.4 Subject Recruitment

The study was performed on a cohort of healthy subjects. The exclusion criteria included history of cardiovascular disease, smoking, diabetes, on-going pregnancy and taking medication that could affect blood flow. To satisfy the study ethics, individuals recruited to the study had to be registered with the UK NHS.

3.4.1 Study Subsets

Study 1 presented in Chapter 4 was designed to investigate the relationship between BF and SO_2 over a wide range of values (BF: 2-352PU, SO_2: 0-93%). In order to obtain both low and high values of BF and SO_2, different physiological challenges were applied to different subsets of volunteers. It was not possible to perform all the challenges in all volunteers due to time taken to perform the measurements. In some volunteers more than one challenge was applied. Overall, 50 healthy volunteers (24 males) were recruited to Study 1. Fourteen volunteers were recruited by Erin McDonald, ten by Geraldine Clough. The rest of volunteers were recruited by the author of this thesis. Mean age, BMI and ambient skin temperature are summarised in Table 3.1.

Table 3.1 Study 1 demographic data (n=50).

Age, y; mean (SD)	29.2 (8.1)
BMI, kg/m^2; mean (SD)	24.3 (3.2)
Skin temperature, °C; mean (SD)	29.1 (2.0)

There were four analysis subsets obtained from the different challenges. Figure 3.7 presents study subsets in Study 1. PORH was measured in 35 subjects, inspiratory breath-holds in 19 subjects, $tcpO_2$ and local warming measurements were conducted in 21 subjects and the reproducibility measurements were performed in 10 subjects.

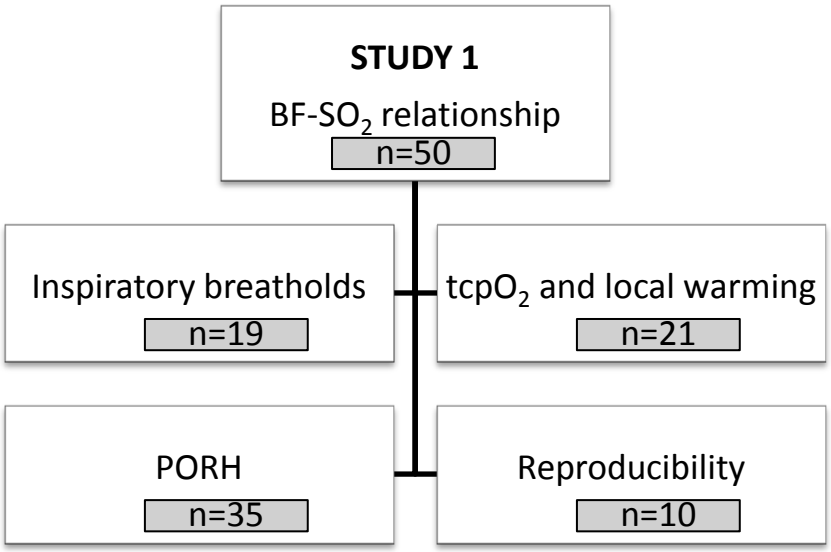

Figure 3.7 Study subsets within the Study 1.

Study 2, described and presented in Chapter 5 and Chapter 6 was performed on fifteen young, healthy men. The exclusion criteria were as for the Study 1. Additionally, the aim of this study was to recruit a homogeneous group of subjects, therefore only men in the age between 20-30 y were recruited. The subjects were asked to comply with the same directions as Study 1, i.e. to refrain from caffeine at least 2 hours before the measurements and to refrain from exercise for 24 hours prior to the measurements. Figure 3.8 presents the structure of Study 2 conducted during this PhD. Mean age, BMI and skin temperature are shown in Table 3.2.

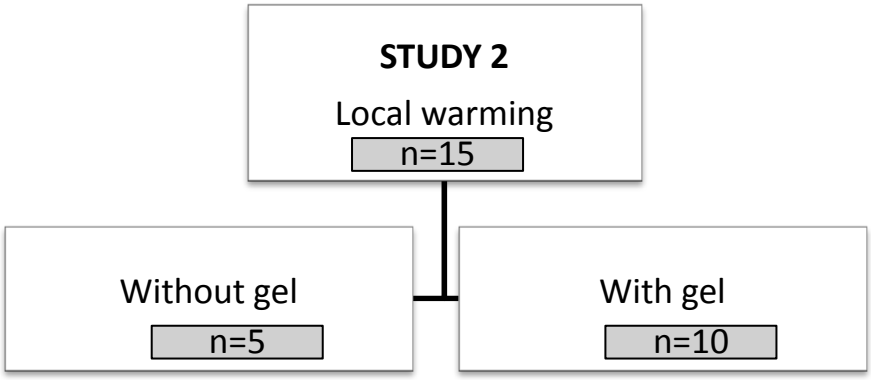

Figure 3.8 Study subsets within the Study 2.

Table 3.2 Study 2 demographic data (n=15).

Age, y; mean (SD)	24.3 (2.4)
BMI, kg/m^2; mean (SD)	23.7 (2.8)
Skin temperature, °C; mean (SD)	31.2 (1.0)

3.5 Analysis Methods

3.5.1 Time-Domain Analysis

Time-domain analysis was performed in moorVMS-PC software using automatic analysis for PORH and manual analysis for IBH and local warming. To analyse IBH, regions of interest were chosen just before the deep breath (baseline) and over the last 3 seconds of the breath-hold. The statistics (mean, SD) of regions of interest were generated using moorVMS-PC and were exported to excel for further analysis.

In Study 1 the effect of local warming was assessed by choosing regions of interest in the raw data files at baseline (unwarmed) and after 20 min of warming. Statistics generated for all selected regions were saved and exported to Microsoft Excel 2010 (Microsoft Corporation, US) for further analysis.

Analysis of decrease in SO_2 and oxyHb, and increase in deoxyHb and totalHb during arterial occlusion were performed on the first 60 seconds of occlusion. Linear equations $y = ax + b$ were fitted to the experimental data. Coefficients are reported together with goodness of fit to a linear line expressed as an r^2 value.

In Study 2, the mean value of each signal was extracted as the mean over 5 min at the end of each stage: resting temperature, at 33°C and at 43°C.

3.5.2 Statistics

Statistical analysis was performed using GraphPad Prism (Prism 6, GraphPad Software, Inc., USA), IBM SPSS Statistics 19 (IBM United Kingdom Limited, UK) and Microsoft Excel 2010 (Microsoft Corporation, US). Results were considered significant if $p < 0.05$. Data were tested for the normal distribution using D'Agostino & Pearson omnibus normality test. Data are presented as either mean ± standard deviation (SD) for normally distributed data or median with interquartile range for non-normally distributed data. Normally distributed data were compared using the Student *t*-test and non-normally distributed data using a Mann-Whitney test. Differences were deemed to be significant if $p < 0.05$.

3.5.3 Linear Regression Modelling

Linear regression modelling was conducted in SPSS. First, the bivariate correlations between BF, SO_2, oxyHb, deoxyHb, totalHb, forearm temperature, sex and BMI were calculated and the significant correlations were considered for further regression analysis.

A number of assumptions were made about the data in order to use multiple regression modelling. These assumptions were that variables were continuous, there was a linear relationship between variables, there were no significant outliers, the observations were independent, the variance along the line of best fit remained similar and data were normally distributed.

Tissue oxygenation was entered as an independent variable. Blood flux, forearm temperature, sex and BMI were entered as predictor variables. The model was computed using the Enter method, which does not take into account the order of importance of predictor variables, but assumes that all of the predictor variables are equally important. All independent variables are entered into the equation in one step. The goodness of the model was assessed with an R^2 value defined as the variance explained in SO_2 by entered dependent variables.

3.5.4 Reproducibility

The reproducibility measurement determines the range of the results of the same measurement which may be registered in different subjects belonging to the same group e.g.

healthy volunteers. The reproducibility can also be determined for different measurements in the same volunteer, i.e. measurements in two separate skin sites within the same area of the body. These are important characteristics of the measurement as they indicate how the measurements vary regardless of the external factors such as physiological stimuli or health changes. In particular, for the assessment of microcirculation using a single point light source, the reproducibility range defines the natural variability and the device uncertainty.

The repeatability of the measurement is another important characteristic as it provides information on how close are the measurements taken on two different occasions.

For the purpose of the study conducted in this thesis, the reproducibility and repeatability were determined for resting measurements registered in the subset of 10 volunteers who attended two sessions.

The reproducibility was reported as the coefficient of variation (CV) calculated as the standard deviation of paired differences (σ) divided by square root of 2 divided by the overall mean μ (Equation 3.2 (Svalestad et al., 2010)),

$$CV = \frac{\sigma}{\sqrt{2}\mu} \quad (3.2)$$

The repeatability of the measurements was expressed by the intraclass correlation coefficient (ICC). ICC describes the relative extent to which two measurements on different occasions are related. An ICC value of 1 means two measurements are identical, and ICC is defined as (Equation 3.3),

$$ICC = \frac{\sigma_b^2}{\sigma_b^2 + \sigma_w^2} \quad (3.3)$$

Where σ_b^2 is variance between subjects and σ_w^2 is variance within a subject. ICC is influenced by the composition of the sample, the greater the variability within a population the higher the ICC value.

3.5.5 Signal Variance

The statistical variance expresses the variation of the studied variable such as resting blood flux. The larger the variance, the larger the variations in the amplitude of the signal. For a given vector X, variance V, is calculated as (Equation 3.4),

$$V(X) = \frac{1}{N-1}\sum_{i=1}^{N}|X_i - \mu|^2 \quad (3.4)$$

where μ is the mean of X and N is a number of data points.

The standard deviation is the square root of the variance.

3.5.6 Absolute Power

The power is proportional to the amplitude squared. For a signal x, the power P is defined as (Equation 3.5),

$$P_x = |x(n)|^2 \quad (3.5)$$

When comparing different frequency components of the signal, the power vs. frequency plots make it easier to find the most significant frequencies contributing to the overall signal.

3.5.7 Frequency-Domain Analysis

The digital signals were recorded with a sampling rate of 40 Hz. According to the Nyquist-Shannon sampling theorem, the sampling rate of the digital signal has to be at least twice the highest frequency of interest in order to capture the desired frequency components. The highest frequency of interest in LDF signals is the heartbeat (0.4 to 1.6 Hz). In order to reconstruct this frequency and all lower frequencies, the sampling rate needs to be at least 3.2 Hz. The data recorded in moorVMS-PC were exported to Matlab (R2014a, MathWorks, UK). Prior to spectral analysis, all traces were visually assessed for the presence of movement artefacts and poor quality recordings were excluded. The frequency analysis was only performed on 600 s long, artefact-free signals recorded during rest. Signals were filtered using a zero-phase low-pass filter with cut-off frequency of 2 Hz, resampled to 10 Hz and detrended using a moving average with a 200 second window to remove frequency content below 0.005 Hz. 600 s long, artefact-free segments for each stage (resting temperature, 33°C and 43°C) were selected. The flowchart presented in Figure 3.9 illustrates a process of frequency-domain analysis leading to PSD profiles. Frequency coherence and delay estimation analyses were performed in analogues way.

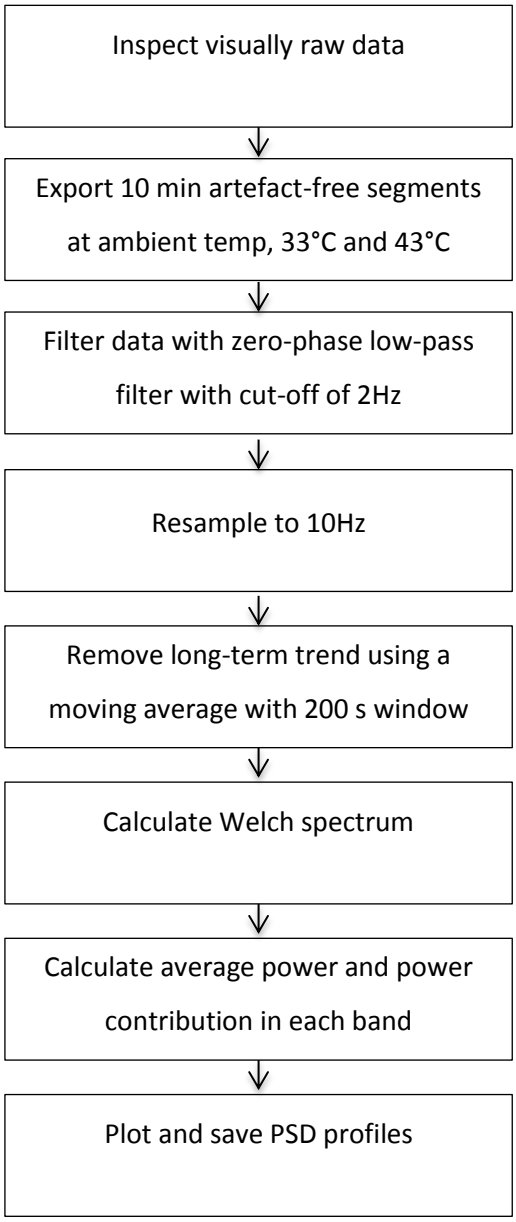

Figure 3.9 Flowchart illustrating the frequency domain analysis.

An example of data selected for frequency analysis in Study 2 is shown in Figure 3.10. 600 s long segments are marked in pink.

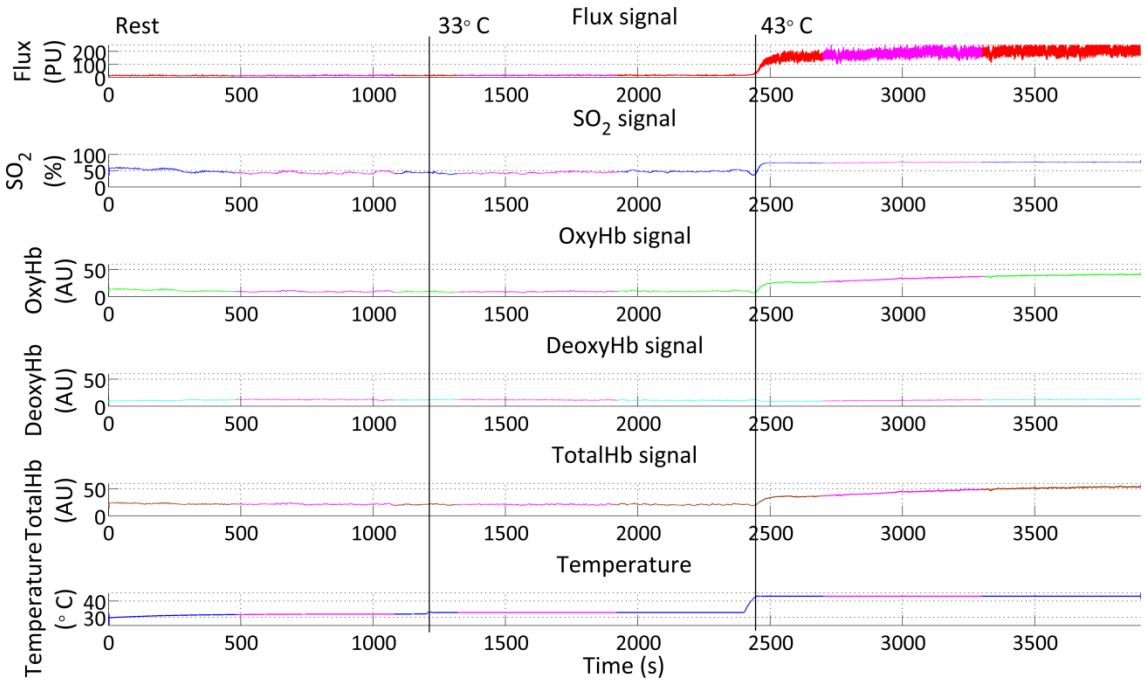

Figure 3.10 The selection of 600 s long data segments for frequency analysis is marked in pink. The segments were selected avoiding movement artefacts.

Morlet Wavelet Transform

To visualise and to compare the distribution of oscillations in BF and SO_2 signals Morlet WT was performed. This was done using the 3-dimensional plots computed in Matlab using the Morlet WT. The basic Morlet wavelet is illustrated in Figure 3.11.

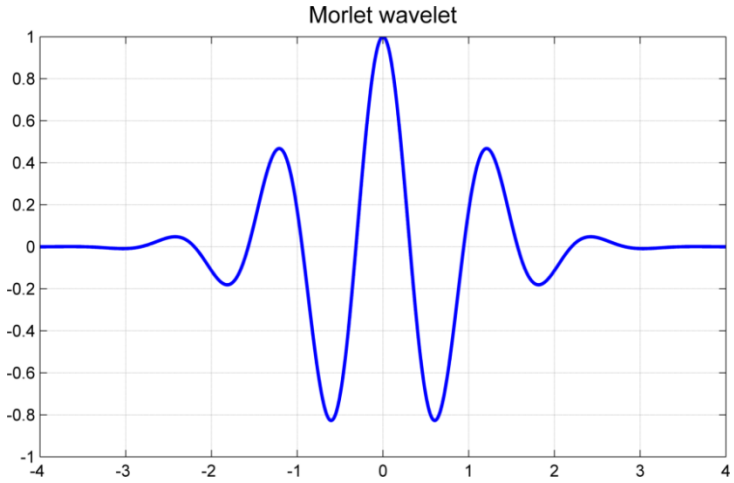

Figure 3.11 The basic Morlet wavelet which was used to create a family of Morlet wavelets that were used in wavelet transform.

This basic wavelet was scaled and translated resulting in the family of wavelets. WT for both signals was calculated for the frequency range 0.0095 – 1.6 Hz. This frequency range was previously studied in BF signals by numerous research groups (Stefanovska et al., 1999; Kvandal et al., 2003; Rossi et al., 2005a; Sun et al., 2013). Morlet wavelets accentuate low frequencies which are of particular interest in BF and SO_2 signals and correspond to endothelial activity. The low frequencies require a longer period of measurement time to capture the dynamics of the processes. The lowest frequency of interested is 0.0095Hz, which equals to period of 105 s. In order to analyse the processes occurring at certain frequency, a number of full cycles are required (if the process is periodic 2 full cycles are sufficient to describe the frequency content of the signal. However, BF and OXY signals are not fully periodic. In order to increase the confidence of frequency analysis a higher number of cycles is used to estimate the frequency content). 600 s long recordings cover five full cycles of the lowest frequency and this length is considered sufficient to describe the frequency content of BF and OXY signals.

Power Spectral Density

Welch's method of Fourier transform with Hanning window size of 200 s and 50% overlap between windows was applied. Power spectral density was calculated as the area under the square of the magnitude of Fourier transform $|F[x(t)]|^2$, where $x(t)$ was the analysed signal and $F[x(t)]$ was its Fourier transform. The power spectral density was calculated as an integral of the magnitude of the Fourier transform. The normalised power spectral density was calculated as the contribution of a particular frequency band to the total spectral power. The power in the frequency band from f_1 to f_2 was calculated as (Equation 3.6):

$$\int_{f_1}^{f_2} |F[x(t)]|^2 df \qquad (3.6)$$

The PSD contribution was evaluated within the frequency range (0.0095–1.6 Hz) divided into frequency intervals corresponding to endothelial activity (0.0095–0.02 Hz), sympathetic activity (0.02–0.06 Hz), myogenic activity in the vessel wall (0.06–0.15 Hz), respiration (0.15–0.4 Hz), and heartbeat (0.4–1.6 Hz). PSD contribution was calculated as a ratio of signal power in a particular frequency band and total signal power across all five bands (0.0095-1.6Hz).

Frequency Coherence

The frequency coherence function describes how well one signal correspond to another signal at a certain frequency. BF and OXY signals originate from the same source and share a number of characteristics in time domain. Thus, it can be expected that these signals also share some characteristics in frequency domain. Frequency coherence was calculated by finding the relation between power spectral densities and cross power spectral density according to 3.7:

$$C_{xy}(f) = \frac{\left|P_{xy}(f)\right|^2}{P_{xx}(f)P_{yy}(f)} \quad (3.7)$$

Where $C_{xy}(f)$ is the coherence between the input signals x and y, $\left|P_{xy}(f)\right|^2$ is the cross power spectral density at the certain frequency, $P_{xx}(f)$ and $P_{yy}(f)$ are the power spectral densities of signals x and y at the chosen frequency (Pereda et al., 2005).

The frequency coherence within 5 spectral bands between BF and OXY signals was estimated by magnitude squared coherence across previously described frequency bands. The results presented in Chapter 4 relate only to the frequency coherence between BF and SO_2 signals.

In Chapter 6 the coherence has been calculated for following signals pairs:

- Flux-SO_2
- Flux-oxyHb
- Flux-deoxyHb
- Flux-totalHb

The calculations have been performed separately for forearm at 33°C and at 43°C.

3.5.8 Delay Estimation

The true cross-covariance sequence of two jointly stationary random processes, x_n and y_n, is the cross-correlation of mean-removed sequences ((3.8),

$$cov_{xy} = E[(X - \mu_x)\big(Y - \mu_y\big)'] \quad (3.8)$$

Figure 3.12 illustrates an example of cross-covariance between BF-OXY signals at rest depending on the time shift. It works by 'sliding' in time one signal against the other and calculating the cross-correlation at each time point. The better the signals are overlapping on top of each other, the higher the value of cross-correlation. The top panel is the control panel

showing the cross-correlation of the same signal. In this case it was a resting forearm BF signal from one of the subjects. The cross-correlation is at its maximum at time-point 0 and decreases rapidly towards the sides. At time point 0 two identical signals are superimposed, such that they are in the perfect alignment and the value of cross-correlation is in its maximum=1. The bottom panel illustrates cross-covariance for BF and OXY signals. Here, the cross-covariance takes its maximum at different time-points indicating the time delay between signals. Figure 3.13 is a magnification around t=0 of the plots in Figure 3.12 and it shows the delay in OXY signals in respect to BF. The calculations have been normalised to express the delay in seconds (the time lag on the *x*-axis is expressed in seconds). In this example the delay between BF and OXY signals is between -1 and -5 seconds.

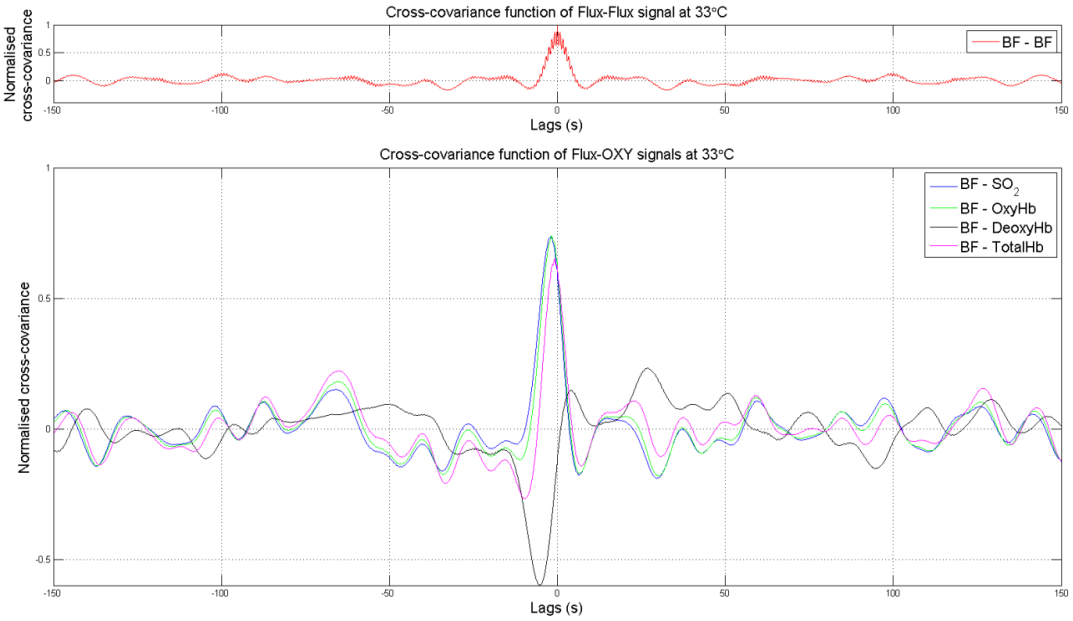

Figure 3.12 The overal cross-covariance functions between (top) Flux-Flux and (bottom) Flux-OXY signals at 33°C.

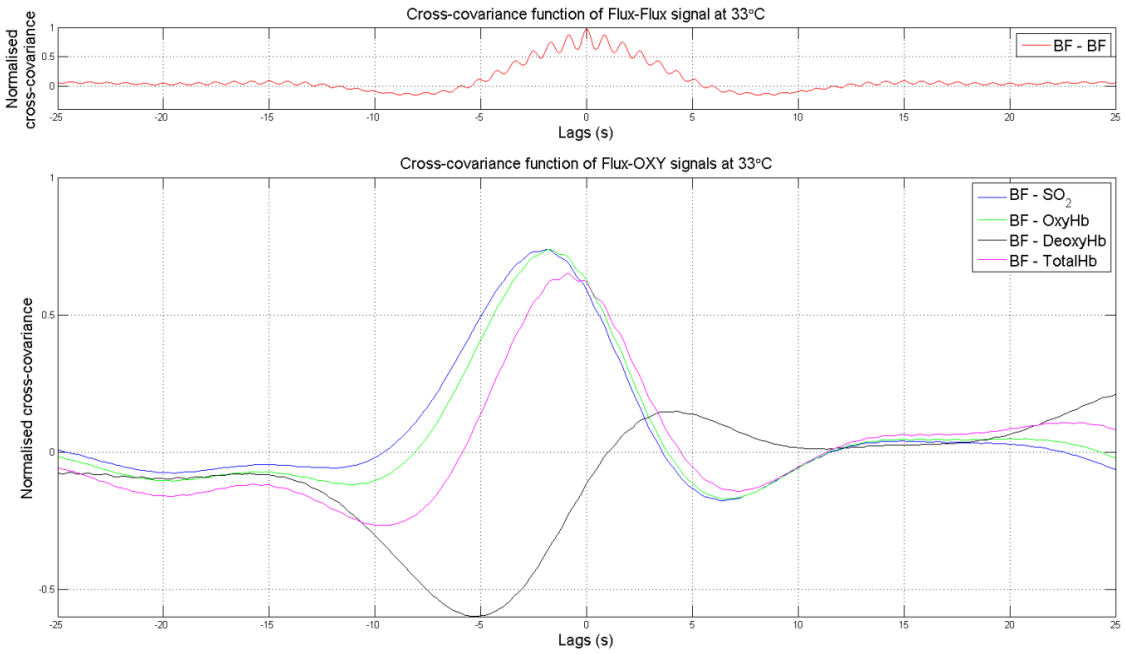

Figure 3.13 The maximum of the cross-covariance function between (top) Flux-Flux and (bottom) Flux-OXY signals at 33°C. The cross-covariance of Flux-Flux has maximum of 1 at lag 0 s – two identical signals have perfect alignment at lag 0. Flux-OXY signals have maximum cross-covariance <1 and at lags different from 0.

The valid alignment was considered for cross-covariance higher than >0.3 and delay lower than 10 s. The threshold of 0.3 was chosen to exclude signals that were poorly correlated and thus not suitable for delay analysis. The delay less than 10 s was chosen to exclude the misaligned signals that met the correlation threshold. The minimum value of correlation threshold and maximum delay was chosen based on the nature of the signals and by the visual assessment of signals' alignment. Higher value of cross-covariance indicates that compared signals share similar characteristics and the confidence of alignment is high.

3.6 Summary

In this Chapter, the methods used in the open, non-randomised, and uncontrolled (non-interventional) studies reported in this thesis, have been described. The following chapters present and discuss the experimental results. Continuous BF and OXY signals are analysed in time- and frequency- domains to identify the characteristics of these signals and interpret them in regards to physiology of studied system.

Chapter 4

Time- and Frequency- Domain Analysis of Flux and OXY Signals Measured in Healthy Human Skin

In this chapter the properties of the combined LDF-OXY measurements are investigated. Study 1 presented here was conducted to investigate measurements and signal properties in different physiological states in order to establish the relationship between BF and SO_2 measured at the same site. The advantage of the combined measurements is the simultaneous assessment of the microcirculatory blood flux and oxygenation in the same site. The main contribution presented in this chapter is the identification of the relationship between BF and SO_2 over a wide range of values (BF between 2-352 PU and SO_2 between 0-93%). This relationship, described in the time-domain, is further accompanied by frequency-domain analysis providing an insight into oscillatory characteristics of both BF and SO_2 signals. Some of the data presented in this chapter has been published in *Microcirculation* (Kuliga et al., 2014).

4.1 Results

BF and OXY signals have been recorded from skin of fifty healthy volunteers (male and female) at rest, during PORH, IBH, and local skin warming induced by $tcpO_2$ measurements. The measurements have been analysed using methods presented in Chapter 3.

4.1.1 Reproducibility

The inter-individual coefficient of variation (CV) for resting BF and SO_2 measured using the combined probe was 0.15 and 0.09, respectively (n=10). The intra-individual CV for BF and SO_2 measured at the same site on two consecutive days was 0.20 and 0.07, respectively. The inter-individual CVs for oxyHb, deoxyHb and totalHb were 0.19, 0.09 and 0.10, respectively.

The intraclass correlation coefficient (ICC) for resting BF and SO_2 measured using the combined probe was 0.85 and 0.68, respectively (n=10).

4.1.2 Response to Perturbations

BF, SO_2 and oxyHb were greatest during warming indicating substantial vasodilation. The lowest readings of BF, SO_2 and oxyHb were expected and obtained towards the end of arterial occlusion. DeoxyHb was the highest at the end of arterial occlusion indicating an accumulation of deoxygenated blood in the sampled tissue volume. The lowest deoxyHb was measured during the peak of PORH – this corresponds to the mechanical washout of deoxyHb with fresh oxygenated blood. The baseline and perturbed values of BF, SO_2, oxyHb and deoxyHb are summarised in Table 4.1. The response to inspiratory breath-holds recorded in the subset of 19 volunteers is presented separately in Table 4.2. The statistically significant decrease is indicated with * (resting and minimum values tested with Student t-test). A significant decrease was observed in BF during IBH – it dropped from 14.3 (6.4) PU at baseline to 8.6 (3.2) PU at the minimum ($p = 0.0013$). SO_2, oxyHb and deoxyHb did not change significantly during IBH.

Table 4.1 Mean (SD) blood flux, oxygenation, oxygenated and deoxygenated haemoglobin during rest and blood flow perturbations.

	Blood Flux (PU) mean (SD)	**SO_2 (%) mean (SD)**	**oxyHb (AU) mean (SD)**	**deoxyHb (AU) mean (SD)**
Resting	11.7 (6.2)	44.3 (12.5)	6.8 (3.3)	8.6 (3.4)
Occluded	3.2 (0.7)	2.0 (3.5)	0.4 (0.6)	20.9 (7.6)
Peak PORH	71.2 (28.4)	80.7 (5.7)	24.1 (6.6)	5.9 (2.5)
Warmed	183.0 (77.3)	83.1 (4.1)	33.3 (8.5)	7.1 (3.1)

Table 4.2 Mean (SD) blood flux, oxygenation, oxygenated and deoxygenated haemoglobin during rest and during the drop induced by inspiratory breath-holds. * indicates $p < 0.05$ (resting and minimum values tested with Student t-test)

	Blood Flux (PU) mean (SD)	**SO_2 (%) mean (SD)**	**oxyHb (AU) mean (SD)**	**deoxyHb (AU) mean (SD)**
Resting	14.3 (6.4)*	49.5 (13.3)	8.4 (4.0)	9.1 (4.6)
Minimum IBH	8.6 (3.2)	41.8 (13.8)	7.4 (4.7)	10.0 (4.5)
p value	0.0013	0.0885	0.45	0.56

4.1.3 Forearm Blood Flux and Oxygenation Relationship

The relationship between simultaneously recorded BF and SO_2 measured at rest and during perturbations of skin blood flux is shown in Figure 4.1 where the different symbols correspond to different perturbations. The resting data (●) show the highest spread across BF and SO_2 compared to perturbed data. During warming (▼), SO_2 was consistent across volunteers but the maximal BF resulting from local warming varied. The BF-SO_2 relationship is best described by a one-phase association curve (4.1),

$$SO_2 = -18.07 + 99.2 \times (1 - e^{-0.096 \times flux}) \quad (4.1)$$

This equation is based on 164 measurements taken from 50 volunteers. The goodness of the fit was $R^2 = 0.88$. The SO_2 asymptote had value of 79-84%. Interestingly, at low flux values (<40 PU), SO_2 increases linearly. Figure 4.2 shows BF-SO_2 relationship for BF values below 40 PU. The slope of this relationship was 2.6. Thus for each 1 PU increase in BF there is expected 2.6 % increase in SO_2 (note % is treated here as the unit of SO_2).

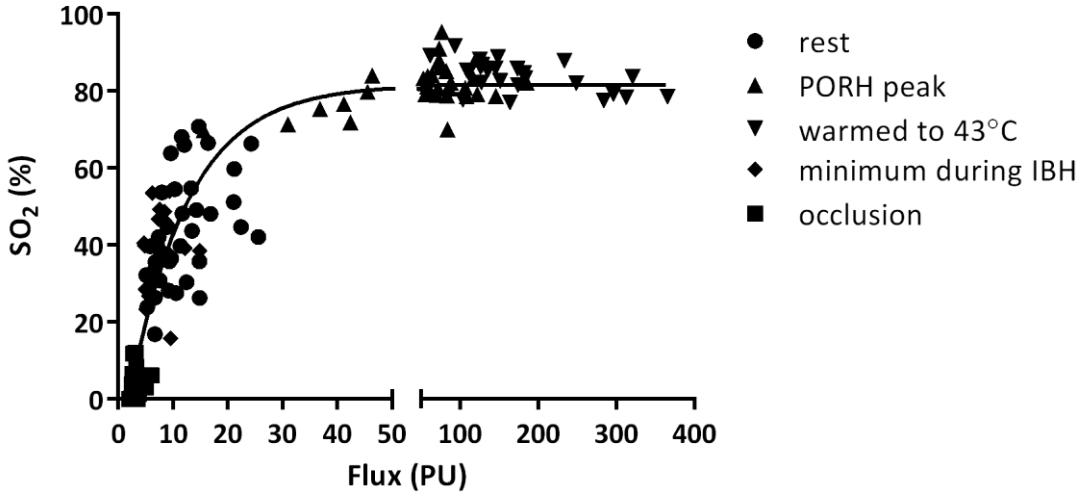

Figure 4.1 Relationship between forearm blood flux (BF) and tissue oxygenation (SO_2) for simultaneously recorded values of BF and SO_2 at rest (●) and during arterial occlusion (180 mmHg 3 min) (■); peak post occlusive reactive hyperaemia (▲); local thermal warming (43°C 20 min) (▼); and during the vasoconstrictor response to deep inspiratory breath-hold (♦). Data are from n=50 healthy individuals.

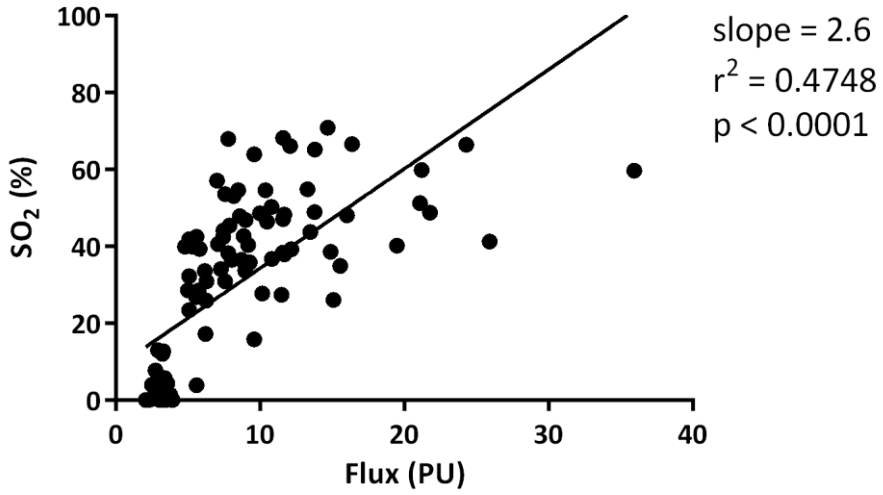

Figure 4.2 The linear relationship between Flux and SO_2 at blood flux values <40PU.

4.1.4 The Influence of Skin Temperature on Resting Blood Flux and Oxygenation

Skin BF is a significant determinant of the skin temperature as reviewed in Chapter 2. In order to quantify the relationship between skin temperature and BF and SO_2 measurements for this group of healthy volunteers, resting skin temperature was plotted against resting BF and SO_2 measurements. Resting blood flux and tissue oxygenation were both positively correlated with skin temperature (blood flux r^2=0.123, p=0.014; SO_2 r^2=0.275, p=0.0001) as shown in Figure 4.3 illustrating both relationships. A difference in resting skin temperature of 1°C between subjects results in a difference in BF of 0.8 PU. For SO_2 a difference in skin temperature of 1°C results in change in SO_2 of 3.2 % (note % is treated here as the unit of SO_2). The implications of these findings are discussed later in this chapter.

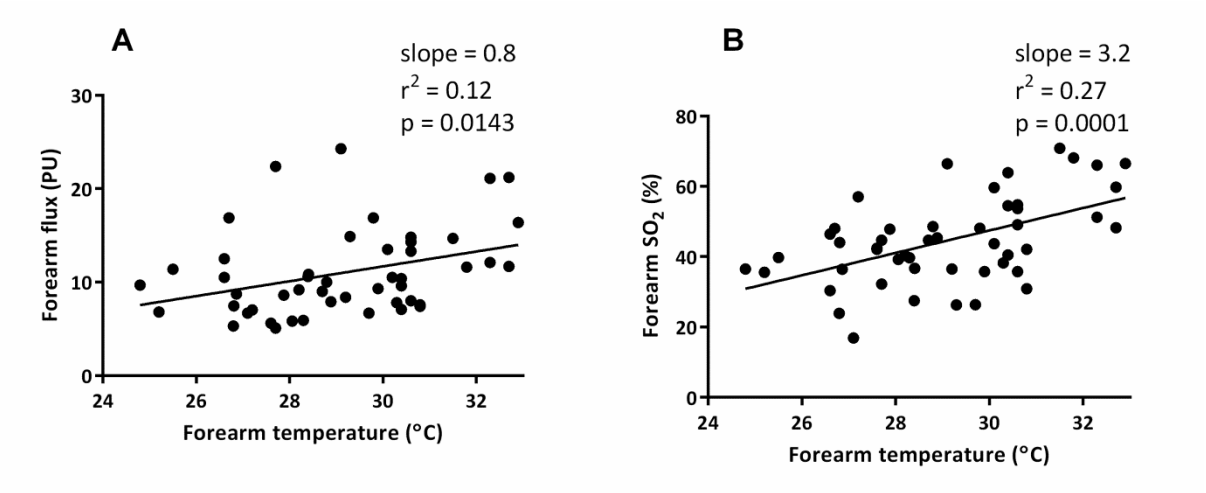

Figure 4.3 Positive correlations between forearm temperature and (A) resting forearm blood flux and (B) resting forearm oxygenation.

4.1.5 Regression Modelling of Blood Flux and Oxygenation

In order to find the significant contributors explaining the variability of resting BF and SO_2, bivariate analysis has been undertaken. The correlations between BF, SO_2, age, forearm temp, BMI and sex are summarised in Table 4.3. Forearm BF and SO_2 correlated with forearm temperature (r=0.365, p=0.009 and r=0.387, p=0.006 respectively). SO_2 correlated with BMI (r=0.344, p=0.016). There was no significant correlation between resting BF or SO_2 and age and sex.

Table 4.3 Bivariate correlations between forearm BF, forearm SO_2, forearm temperature, age, BMI and sex. The significant correlations are shown in bold.

		SO_2	Temp	Age	BMI	Sex
BF	Pearson Corr.	**.427**	**.365**	-.215	.070	-.094
	p	**.002**	**.009**	.134	.629	.527
SO_2	Pearson Corr.		**.387**	-.198	**.344**	.009
	p		**.006**	.172	**.016**	.955
Temp	Pearson Corr.			.018	.035	.081
	p			.899	.811	.583
Age	Pearson Corr.				-.089	-.012
	p				.538	.938
BMI	Pearson Corr.					**-.341**
	p					**.018**

The correlation between BF or SO_2 and age did not reach the significance level of $p<0.05$. However, in the studied cohort the majority of subjects were of similar age thus it was unlikely to see these correlations. Similarly, there was no significant correlation between resting BF or SO_2 and gender in the studied cohort.

Partial correlations between BF and SO_2 controlling for forearm temperature, BMI and sex was 0.388 ($p=0.009$) confirming the association between BF and SO_2 was independent of forearm temperature, BMI and sex.

Linear regression modelling serves as a tool helping to identify and to describe the relationship between multiple factors. The aim of the regression modelling was to determine whether resting SO_2 was associated with BF independently, regardless the correlations found from bivariate analysis. The model that included BF, forearm skin temperature and BMI accounted for 58% of the variance in SO_2. SO_2 signal was the dependent variable and BF, forearm skin temperature and BMI were independent variables (predictors).

Beta coefficients describe the estimates of multiple regression in the normalised manner. The analysis of the independent variables are standardised so their variances are equal to 1. Beta coefficients indicate separately the influence of BF, age, BMI and forearm temperature on SO_2. The value of an unstandardized beta coefficient indicates the amount of increase (positive beta coefficients) or decrease (negative beta coefficients) in SO_2 caused by a 1-unit increase in particular variable. An increase in BF of 1 PU will result in an increase in SO_2 of 0.6%. Forearm temperature and BMI increase SO_2 by 1.4% and 1.1% respectively. These coefficients are useful when considering which parameters influence the variability of the signal and thus when designing an experiment which parameters should be controlled most to avoid the inherent variability. The t statistic is the sample regression coefficient divided by its standard error.

Table 4.4 The beta coefficients of multiple linear regression modelling with forearm oxygenation set as independent variable and forearm blood flux, forearm temperature, age and BMI set as predictors.

	Unstandardized Coefficients		Standardized Coefficients		
	B	Std. Error	Beta	t	Sig.
(Constant)	-28.750	22.282		-1.290	.204
BF	.594	.250	.310	2.377	.022
Temp	1.430	.715	.260	1.999	.052
BMI	1.088	.424	.312	2.568	.014

4.1.6 Measurements of SO_2 and $tcpO_2$ at the Same Skin Area

SO_2 and $tcpO_2$ were measured at the same skin site at rest and during warming resulted from $tcpO_2$ measurement. The mean (SD) SO_2 value before warming was 40 (13) %. The mean (SD) SO_2 value measured at the site warmed by $tcpO_2$ was 83 (3.7) %. The mean (SD) $tcpO_2$ value after 20 min warming was 89 (14) mmHg.

There was no significant correlation between SO_2 measured at the site warmed by $tcpO_2$ and $tcpO_2$ value (**Error! Reference source not found.**) or SO_2 value measured on an adjacent, nwarmed site and $tcpO_2$ value (**Error! Reference source not found.**). Note, in **Error! Reference source not found.** the values of $tcpO_2$ vary greatly between subjects, although these values were recorded at the same skin temperature – $tcpO_2$ measurements in principle require warming to 43°C. At warming, SO_2 shows less variation between subjects compared to measurements at rest (SD of SO_2 measurements during warming and rest were 4% and 9% respectively). These results imply, SO_2 and $tcpO_2$ are measuring two different phenomena and cannot be directly compared or used interchangeably. This issue is further discussed in section 4.2.5.

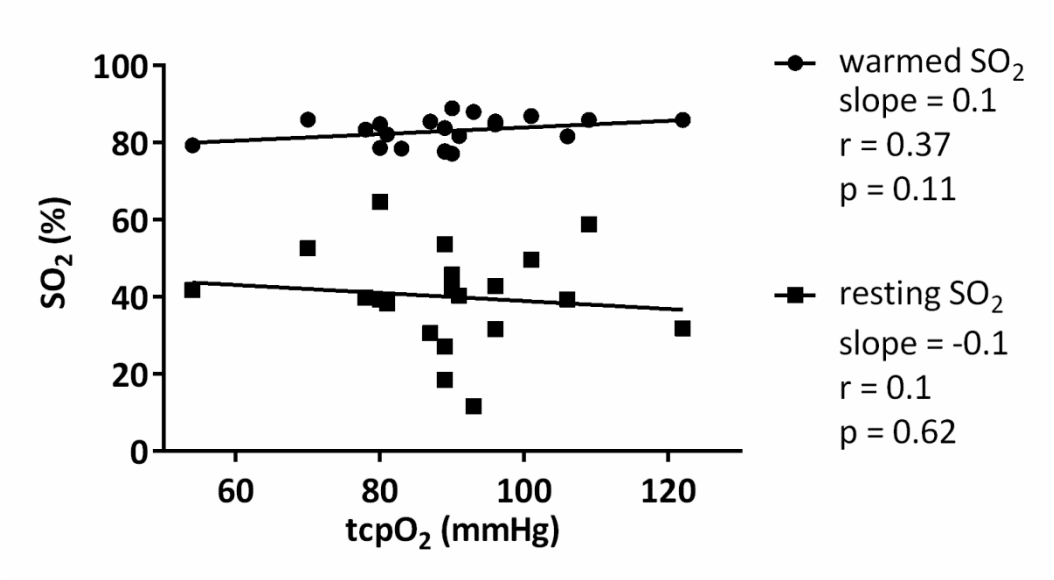

Figure 4.4 The relations between SO_2 and $tcpO_2$ measurements during local warming by $tcpO_2$ and between SO_2 at rest (■) and warmed $tcpO_2$ (●). $TcpO_2$ and SO_2 do not correlate at neither the warmed site nor the unwarmed site.

4.1.7 Coefficient of Oxygen Consumption during Arterial Occlusion

Arterial occlusion has been widely used to study various parameters of BF and can also be used to study the oxygen consumption. The work presented here introduces a parameter linked to oxygen consumption in skin. This parameter is called the coefficient of oxygen consumption. In this research, data collected from the forearm skin during the arterial occlusion protocol were used to analyse the rate of oxygen consumption in skin. The protocol included three minutes of arterial occlusion. The analysis showed that the decrease in oxyHb and increase in deoxyHb over the whole time of the occlusion were not linear but decayed exponentially. Hence, the coefficient of oxygen consumption decreased over time. Figure 4.5 illustrates an example of signals recorded 60 s before occlusion and during full 180 s of the arterial occlusion. The nonlinearity of the signals during the whole course of occlusion is attributed to complex physiological mechanisms resulting from accumulating metabolites within the tissue. However, oxyHb and deoxyHb signals can be considered as linearly decreasing and increasing respectively during the first 60 s of occlusion.

The rate of oxygen consumption was calculated over the first 60 s of the occlusion to simplify the estimation to a linear equation and to limit interpretation to the initial rate of oxygen consumption prior to any effects of the sustained arterial occlusion. At the start of the

occlusion indicated by the arrow, a linear decrease in SO_2 and oxyHb was observed whilst deoxyHb exhibited a linear increase. TotalHb remained almost unchanged. There was an immediate, sustained drop in BF confirming that arterial inflow had been cut off by the cuff. The linear decrease in SO_2 can be taken to represent the rate of oxygen removal/consumption by the tissue in the absence of inflow of arterial blood. The coefficients of linear increase/decrease were calculated from the linear regression fitted to the first 60 s of arterial occlusion.

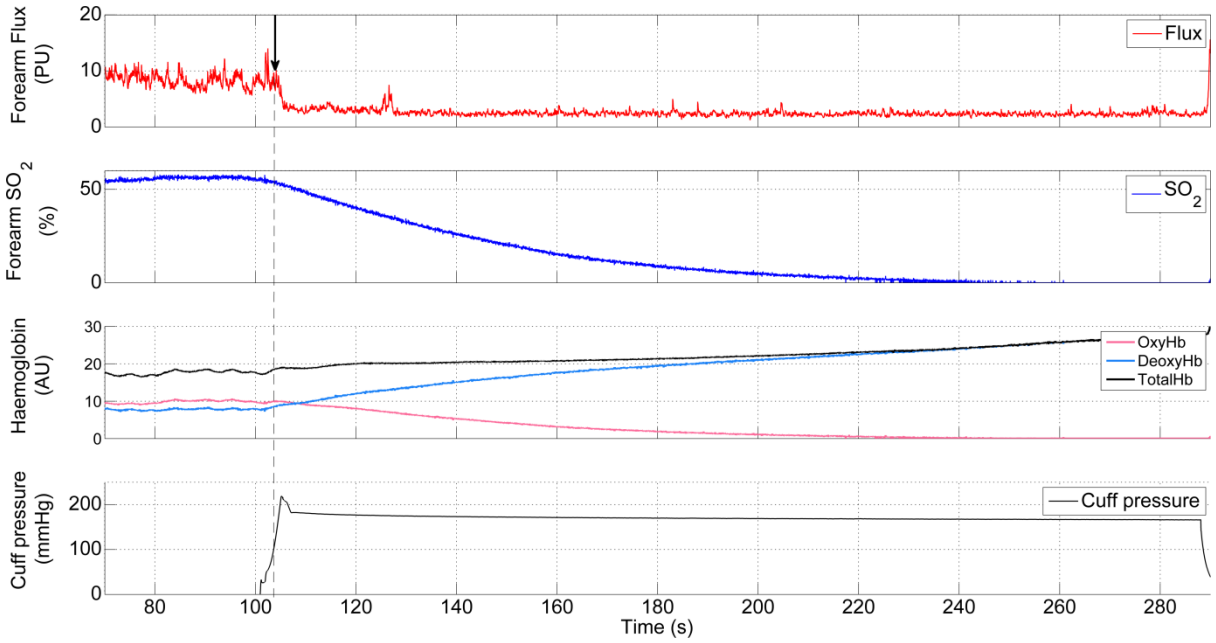

Figure 4.5 Changes in skin blood flux (top), oxygenation (middle) and heamoglobin parameters 30 seconds before arterial occlusion and during three minutes of arterial occlusion. The black line indicate the start of arterial occlusion.

The coefficients were calculated as the rate of change per second. The SO_2 signal decreased on average 0.46 % per s and the OxyHb 0.07 AU per s. DeoxyHb and TotalHb increased on average 0.13 AU per s and 0.06 AU per s respectively. The summary of the coefficients and the goodness of the linear fit are presented in Table 4.5.

Table 4.5 The rate of linear decrease/increase for forearm oxygenation, oxygenated, deoxygenated and total haemoglobin during the first 60 seconds of arterial occlusion. r^2 is a measure of goodness of linear fit. n = 34.

	a coefficient, mean (SD)	r^2 of linear fit, mean (SD)
SO_2	-0.46 (0.17)	0.92 (0.23)
OxyHb	-0.07 (0.05)	0.87 (0.24)
DeoxyHb	0.13 (0.06)	0.94 (0.23)
TotalHb	0.06 (0.04)	0.75 (0.23)

4.1.8 Differences in Oscillatory Components of Blood Flux and Oxygenation Signals

Figure 4.6 illustrates an example of the absolute wavelet transform of the BF and SO_2 signals plotted against time and frequency (top plots) and the average scalograms of these transforms (bottom plots). Higher frequencies are absent in the SO_2 signal (higher frequencies refer here to frequencies > 0.2 Hz). The frequency components between 0.2 and 2Hz correspond to respiration and heartbeat. These oscillations appear absent in the SO_2 signal.

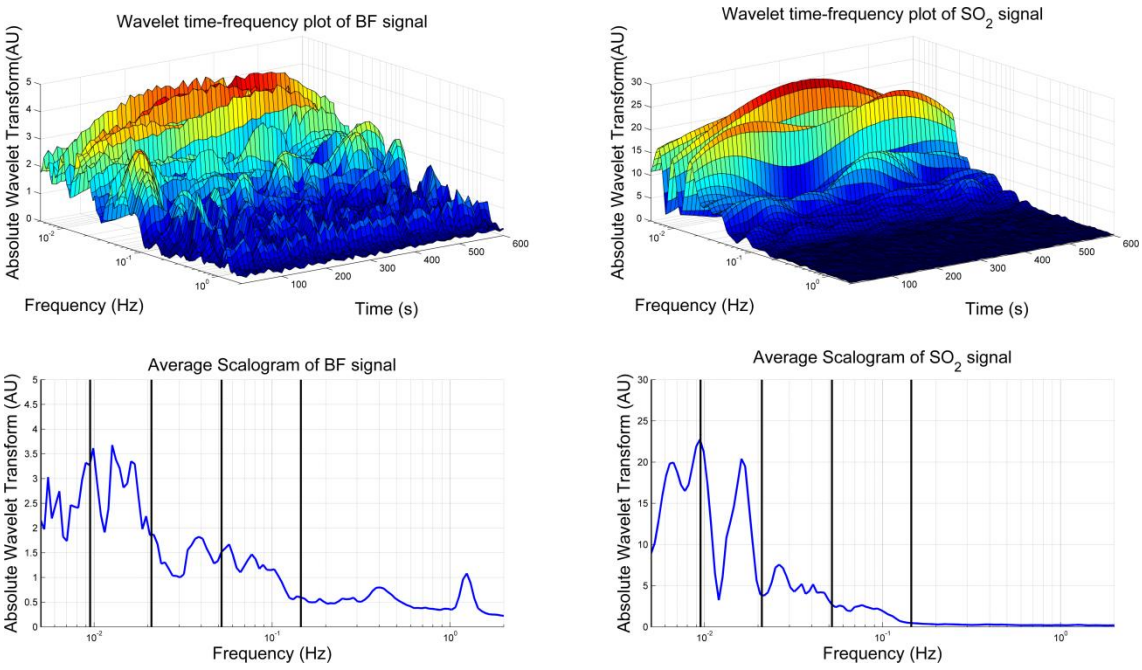

Figure 4.6 Differences in oscillatory components of BF and SO_2 signals illustrated with Morlet wavelet transform (top plots) and average scalograms (bottom plots). Note the scales are different. SO_2 signal has higher value of the transform in lower frequencies but it is flat for higher frequencies. The plots represent data from one individual.

4.1.9 Power Spectral Density Analysis of Blood Flux and Oxygenation

A raw plot of blood flux and oxygenation signals and their power spectral density is shown in Figure 4.7. The signals were 600 s long segments of the resting signals and the PSD profiles were estimated in the frequency range 0.0095 – 1.6 Hz. The frequency bands associated with physiological processes (Stefanovska et al., 1999) are labelled and marked with black vertical lines. The PSD profile in the endothelial, neurogenic and myogenic bands of the SO_2 signal had greater power than in the BF signal. However, the SO_2 signal exhibited a large drop in power in the respiratory band and low power in cardiac band. On the other hand, BF signal exhibited a pronounced peak in power in the cardiac band – this indicates a greater contribution of heart

rate to the overall power of the BF signal. The analysis of PSD contribution showed that the resting BF signal contains a substantial power in the cardiac band whilst the oscillations within respiratory and cardiac bands of SO_2 were negligible.

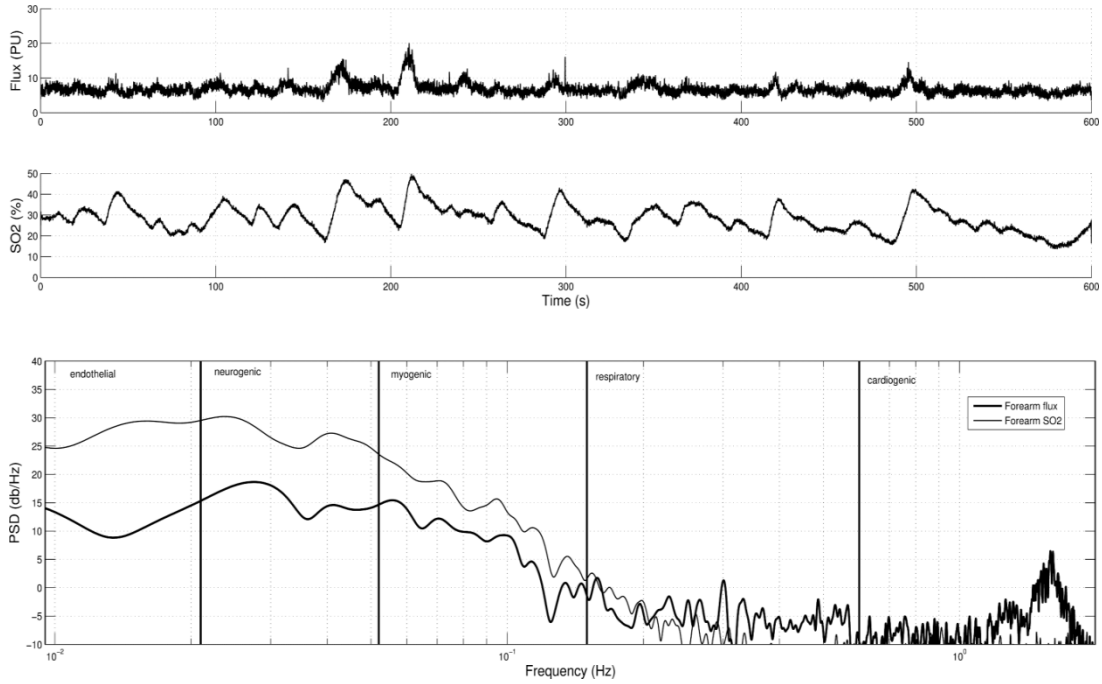

Figure 4.7 An example of raw resting forearm blood flux and oxygenation signals and their power spectral densities from a single individual.

The total spectral power of the BF was lower than the total spectral power of the SO_2 signal. Furthermore, the distribution of the absolute power across five frequency bands (0.0095 – 1.6 Hz) differed between BF and SO_2 signals. In particular, the spectral power of SO_2 signal in respiratory and cardiac bands was very low. Table 4.6 summaries the absolute power of BF and SO_2 signals across five frequency bands.

Table 4.6 Absolute power of forearm blood flux and SO_2 signals across frequency bands (0.0095 – 1.6 Hz).

Frequency band	BF (PU^2), median (IQR)	SO_2 (AU^2), median (IQR)
Endothelial	0.38 (0.14-1.01)	5.65 (2.53-13.56)*
Neurogenic	0.88 (0.54-1.70)	6.61 (4.07-13.47)*
Myogenic	0.56 (0.27-0.98)	0.87 (0.33-1.51)
Respiratory	0.40 (0.15-0.74)	0.04 (0.02-0.05)*
Cardiac	0.74 (0.36-1.69)	0.06 (0.05-0.10)*
Total	3.16 (1.84-5.86)	13.95 (8.85-27.06)*
* $p<0.05$, tested with Mann-Whitney test		

The contribution of particular frequency bands to the total power spectral density was initially calculated for the frequency range 0.0095 – 1.6 Hz. However, as the SO_2 signal appeared to contain very little power in higher frequency bands (0.15 – 1.6 Hz). Calculations were repeated to include only the three low frequency bands (0.0095 – 0.15 Hz). The results are presented in Figure 4.8. The PSD contribution in the endothelial band was lower for BF (mean BF PSD: 0.20 vs SO_2 PSD: 0.44; $p<0.0001$). In the neurogenic bands PSD contributions did not differ (mean BF PSD: 0.46 vs SO_2 PSD: 0.48; $p=0.52$). Finally, in the myogenic band the PSD contribution was higher in BF compared to SO_2 (mean BF PSD: 0.34 vs SO_2 PSD: 0.08; $p<0.0001$).

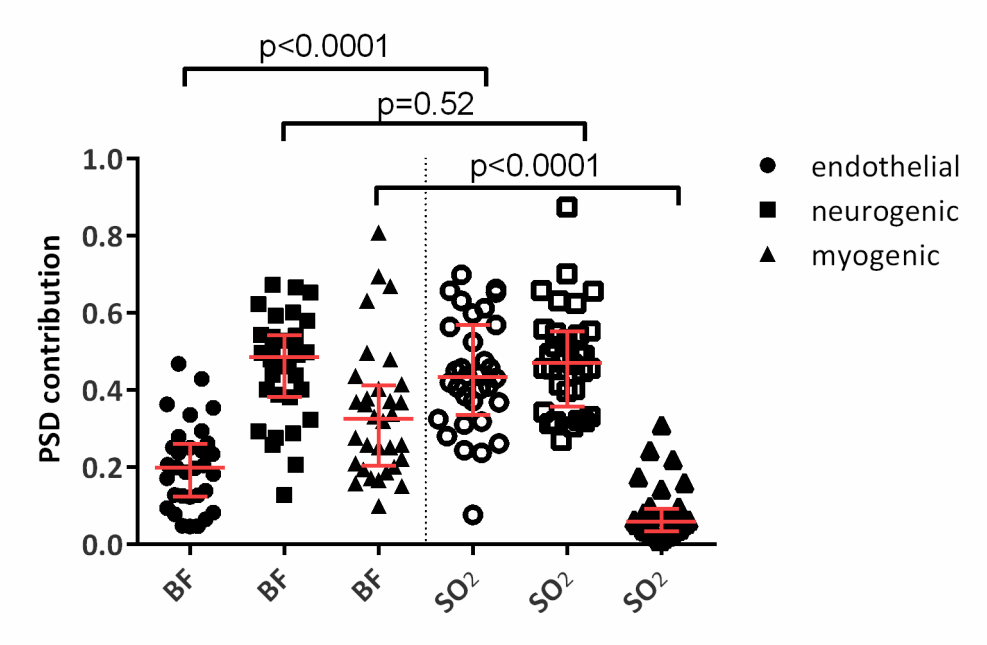

Figure 4.8 Power spectral density (PSD) contribution across three frequency bands (endothelial 0.0095-0.02 Hz, neurogenic 0.02-0.06 Hz, myogenic 0.06-0.15 Hz) expressed relative to total power spectral density in the frequency range 0.0095-0.15 Hz in simultaneously recorded BF and SO_2 signals measured at the same skin site. Results were spread over wide range and are presented as scatter plots with median (IQR). The PSD contribution in each band was compared between BF and SO_2 using the unpaired t-test (n = 32). The significant differences between means were found in endothelial and myogenic bands.

PSD contributions of blood flux and oxygenation signals were positively correlated within the low frequency bands (endothelial, neurogenic, myogenic). Figure 4.9 depicts the slopes of these correlations. The SO_2 signal had the lowest PSD contribution from the myogenic band, however it showed the strongest correlation with the myogenic PSD contribution in BF signal.

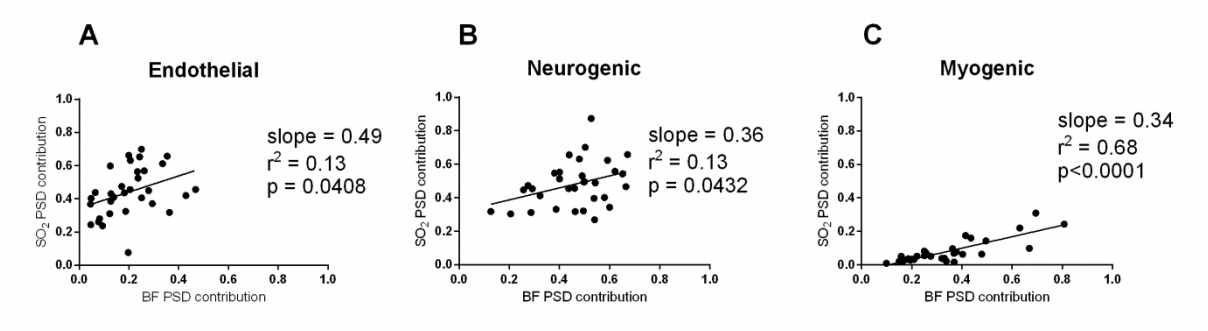

Figure 4.9 Linear regression of BF and SO_2 power spectral density (PSD) contributions measured simultaneously at the same skin site at rest in 32 healthy volunteers for (A) endothelial (0.0095-0.02 Hz), (B) neurogenic (0.02-0.06 Hz), (C) myogenic (0.06-0.15 Hz) activity.

4.1.10 Frequency Coherence between Blood Flux and Oxygenation

The frequency coherence was estimated for the three lowest frequency bands: endothelial (0.0095-0.02 Hz), neurogenic (0.02-0.06 Hz), and myogenic (0.06-0.15 Hz). Mean (SD) coherence was 0.57(0.20), 0.56 (0.15) and 0.25 (0.12) for endothelial, neurogenic and myogenic bands, respectively. These results are presented in Figure 4.10.

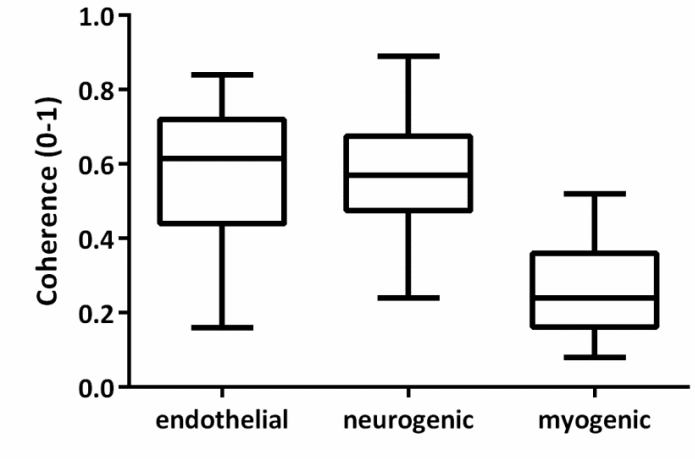

Figure 4.10 Frequency coherence between resting forearm blood flux and oxygenation measured at rest in 32 volunteers calculated within endothelial (0.0095-0.02 Hz), neurogenic (0.02-0.06 Hz) and myogenic (0.06-0.15 Hz) bands.

4.2 Discussion

The objective of this part of the research was to investigate the relationship in time- and frequency-domains between simultaneously recorded skin blood flux and oxygenation using a novel, combined laser Doppler flowmetry and white light spectroscopy probe. A key finding from the frequency analysis showed different PSD contributions to total PSD power of BF and SO_2 signal in endothelial and myogenic frequency bands. Another important finding presented in this chapter is the strong influence of skin temperature on measurements of microcirculatory activity. Skin temperature has been found to be a significant contributor to resting blood flux and OXY measurements. The discussion presented below, provides consideration of various aspect of this relationship in both the time- and frequency- domains. The final section discusses the skin oxygen desaturation rates obtained during arterial occlusion. The frequency domain analysis presents the relationship between the oscillatory components of blood flux and oxygenation signals. The characteristics of the power spectral density and frequency coherence of BF and SO_2 signals present important similarities and differences between these signals.

4.2.1 Reproducibility

The reproducibility of measurements of BF using LDF has been questioned widely in literature and differs depending on reported parameters (Braverman, 1997; Roustit et al., 2010b; Klonizakis et al., 2011). The overall reproducibility is often expressed by stating CV and ICC. Svalestad et al. (2010) reported inter-individual CV for resting facial skin BF in the range of 33% to 72%. Warming reduced the CV from 85% to 33% (Svalestad et al., 2010). The ICC for intra-individual intraday variation was poor (-0.09 and 0.31 respectively).

The reproducibility of baseline BF measurements is often worse than that from warmed or PORH measurements. Roustit et al. (2010a) investigated inter-week reproducibility of PORH and warming measured on a forearm and on a finger. They considered a CV<35% as acceptable and ICC values of <0.4 as poor, 0.40-0.75 as fair to good and >0.75 as excellent. They reported good reproducibility of finger PORH peak amplitude (CV=25%, ICC=0.56). However, CV of the forearm PORH peak amplitude was higher (CV=45%, ICC=0.26). Warming to 44°C gave better reproducibility than PORH (finger CV=24%, ICC=0.60; forearm CV=41%, ICC=0.62) (Roustit et al., 2010a). Svalestad et al. (2010) reported an inter-week within-subject CV of 58%.

The CV of BF measurements presented in this work was lower than in the studies mentioned above. These CV metrics ensured the BF measurements presented in this work are reproducible. Furthermore, the ICC metrics were excellent, confirming the repeatability of measurements. The reproducibility measurements performed in this work were acquired over two different days and are considered is an approximation of reproducibility over longer periods of time. The reproducibility measured on three or more different occasions could define reproducibility with more accuracy. However, more measurements introduce greater opportunity for errors related to different placement of the probe, ambient temperature, humidity and physiological and mental state of the subject. These factors are difficult to control with high accuracy and therefore not practical.

The reproducibility of SO_2 reported here is comparable to results obtained with combined lightguide spectrophotometry (Beckert et al., 2004; Forst et al., 2008; Thorn et al., 2011; Wollina et al., 2011) (Beckert et. al reported measurements at two different days as 'not significantly different'; Forst et al reported SO_2 CV of 16.9±4.6%). Furthermore, the reproducibility data of BF and SO_2 also agree with reproducibility of the oxygen saturation and blood flux measured in deeper tissues such as muscle (Joshi et al., 2010; Gurley et al., 2012). The agreement between reproducibility of the combined Moor LDF-OXY and other combined techniques confirm that this combined technique provides as reliable information about dynamics of BF and SO_2.

Some researchers express the LDF data as Cutaneous Vascular Conductance (CVC) (Roustit et al., 2008; Roustit et al., 2010a; Tew et al., 2011). It is calculated as BF divided by mean arterial blood pressure. Tew et al. (2011) reported poor reproducibility of baseline BF expressed as CVC and good reproducibility of the warming plateau expressed as CVC normalised to maximal BF measured during warming to 44°C.

There are no clearly agreed limits of good reproducibility and various studies have reported a wide range of reproducibility characteristics (Morris & Shore, 1996; Binggeli et al., 2003; Yvonne-Tee et al., 2005). However, the perturbation tests such as PORH or warming improve the reproducibility (Yvonne-Tee et al., 2005; Agarwal et al., 2010; Roustit et al., 2010b; Svalestad et al., 2010). Also, careful site selection and site localisation for repeated measurements improves CV (Yvonne-Tee et al., 2005; Cracowski & Roustit, 2012). There are also other factors which may influence the measurements such as room temperature, humidity or time of the day when the measurement is taken. The variation of these factors

should be kept to a minimum by performing repeated measurements under the same conditions.

4.2.2 Baseline and Perturbed Skin Blood Flux and Oxygenation

Studies reported in the literature have investigated the responses to physiological perturbations but only for BF – the combined sensors are relatively new. Many studies have investigated BF responses to challenges in healthy and unhealthy cohorts to assess overall microvascular function (Minson, 2010; Roustit & Cracowski, 2012; Stiefel et al., 2012) but only a few studies have investigated SO_2 responses to perturbations. To date, it is not clear whether the response to different perturbation observed in SO_2 and OXY signals follow the pattern identified in BF. The range of values for SO_2 reported here (measured using the combined BF and SO_2 sensor) is comparable with those determined in skin at rest using combined light guide spectrophotometry (Beckert et al., 2004; Forst et al., 2008; Thorn et al., 2011; Wollina et al., 2011) and those measured in skeletal muscle during sub-maximal exercise (Joshi et al., 2010) and fatiguing exercise and muscle ischaemia (Gurley et al., 2012).

The inspiratory breath-holds induced a transient sympathetically mediated drop in blood flux. SO_2 showed a trend towards decrease, however it was not substantial. Perhaps such a short duration of physiological challenge (holding the breath) is too short to induce a significant change in tissue oxygenation. It has been observed previously in skin blood flux (Allen et al., 2002; Feger & Braune, 2005; L'Esperance et al., 2013), muscle oxygenation (Kume et al., 2013) and cerebral oxygenation (Liu et al., 2002). The observations from the work presented in this thesis suggest the SO_2 signal is sensitive to inspiratory breath-holds in similar way as BF.

The mathematical relationship between simultaneously recorded skin blood flux and oxygenation has not been previously reported. It has been published for the first time in the research paper resulting from this work (Kuliga et al., 2014). The relationship between blood flux and oxygenation has been a subject of numerous studies, performed mainly in brain and muscle (Buxton & Frank, 1997; Mintun et al., 2001; Yu et al., 2005; Shang et al., 2012) but not many studies investigated this relationship in skin. Recently Ikawa & Karita (2015) investigated BF and OXY parameters recorded simultaneously from the finger and forearm during rest, mental challenge and venous occlusion. They reported values of BF and OXY from finger (tip and middle phalanx), ventral palm and ventral forearm. At rest they reported higher BF and SO_2 from the finger compared to forearm, however totalHb did not differ between these sites. They observed a simultaneous decrease in BF and SO_2 during mental task at the finger but not

in the forearm. However, 4 out of 21 volunteers did not exhibit changes during mental task. Venous occlusion resulted in increase in deoxyHb and consequently a decrease in SO_2. The results presented in this thesis relate to the finding of Ikawa & Karita (2015) and extend the analysis of forearm BF-SO_2 dynamics by more detailed analysis of different parameters describing BF and OXY dynamics during rest and PORH.

The equilibrium of 84% indicates that during increased perfusion (during PORH and local warming), the obtained oxygenation signal has its limit at 84% (in healthy population). This indicates the SO_2 measurements originate from mixed arterial and venous pool. The component of deoxyHb resulting from tissue metabolism is present within the sampled volume at rest and during vasodilation. It is important to understand that skin SO_2 measurements registered with WLS should not be compared to arterial blood gas measurements obtained with pulse oximeter or direct arterial blood gas analysis (from arterial blood sample). Pulse oximeter signals and arterial blood samples originate from arteries which transport the oxygenated blood to arterioles and capillaries where tissue gas exchange takes place. The SO_2 signal originates from arterioles, capillaries and venules, therefore it combines the oxygenated and deoxygenated blood. In healthy skin the value of ~84% has been identified as maximum oxygenation induced by local skin warming. It is the advantage of the WLS technique to measure SO_2 as a characteristic of actual tissue status which includes both arterial and venous flows and therefore reflect tissue metabolism. The SO_2 asymptote identified from experimental data may be considered as a new characteristic of microcirculation; it may contribute to assessment of microvascular function. Considering the inherent variability of BF and SO_2 measurements, the goodness of the fit of the estimated equation to experimental data (0.88) can be considered high. It confirms a good match between the experimental data and the identified equation.

4.2.3 Oxygen Mass Balance Analysis

The skin oxygenation was calculated as a fraction of oxygenated haemoglobin and total haemoglobin. The theoretical relationship between blood flux and oxygenation can be expressed using Fick's principle for mass balance of oxygen in the tissue. The oxygen consumption (OC) in the tissue is the product of blood flux and the difference between the arterial oxygen saturation (SO_{2_a}) and the venous oxygen saturation (SO_{2_v}) (Pittman, 2005; Pittman, 2012). As the oxygen amount depends on the total haemoglobin, it has to be included in the calculations as shown below in the equation 4.2 (Prof C. Charles Michel),

$$OC = BF \times [totalHb] \times (SO_{2_a} - SO_{2_v}) \quad (4.2)$$

This relationship indicates that tissue oxygenation is linearly related to blood flux and total haemoglobin. Figure 4.11 presents the experimental data as the relationship between the reciprocal of blood flux corrected by the total haemoglobin, and the tissue oxygenation.

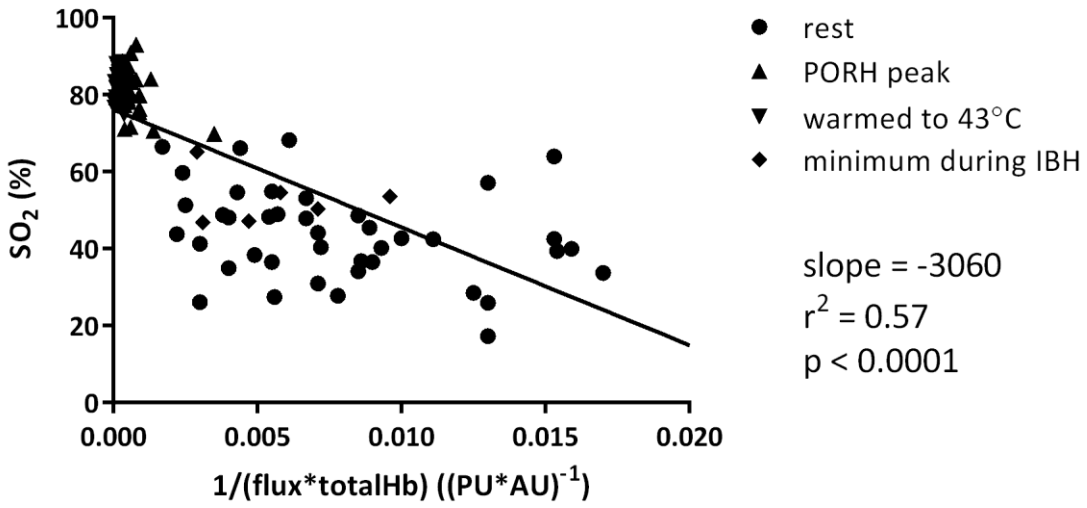

Figure 4.11 Graph showing the relationship between the reciprocal of forearm blood flux (BF) corrected for totalHb, and tissue oxygenation (SO_2) for the simultaneously recorded values of BF and SO_2 in healthy volunteers for BF>5 PU. BF and SO_2 were measured at rest (●) and during peak post occlusive reactive hyperaemia (▲), local thermal warming (43°C 20 min) (▼) and during the vasoconstrictor response to deep inspiratory breath-hold (♦). (n= 50 volunteers) (r^2 = 0.57, p < 0.0001).

The SO_2 intercept in Figure 4.11 corresponds to the SO_2 plateau in Figure 4.1 and is related to the maximal capacity of the system to vasodilate. In a compromised system, this value is expected to be altered due to the microvascular dysfunction or other pathology related to the vascular system. Currently it is not possible to identify and quantify the specific pathologies based on this value – more research is needed to determine how the pathological behaviours are reflected in BF-SO_2 relationship.

4.2.4 The Positive Relationship between Skin Temperature and Resting Blood Flux and Oxygenation

Simultaneously recorded BF and SO_2 measured at rest showed a significant correlation with skin temperature (Figure 4.3). It has been shown previously that BF is positively correlated with skin temperature (Boyko et al., 2001; Green et al., 2006; Avery et al., 2009; Gregson et al., 2011). Resting skin oxygenation has not been widely studied, therefore the correlation between resting skin oxygenation and skin temperature is not known. Kelechi & Michel (2007) investigated skin temperature, tissue perfusion and tissue oxygenation and reported no correlation between skin temperature and tissue oxygenation. However, they have measured tissue oxygenation using $tcpO_2$, which measures oxygen pressure in the skin warmed to 44°C. Study by Kelechi & Michel (2007) was not answering the question about the relationship between resting skin oxygenation and temperature as they have not measured skin oxygenation under resting temperature but at 44°C. They studied the correlation between skin oxygenation at 44°C and resting skin temperatures which were between 31.6-33.3°C. Study 1 described in this chapter reported a novel finding that resting skin oxygenation is positively associated with resting skin temperature in a healthy population. It is important, as resting temperatures vary substantially between individuals. The measurements were taken in a temperature controlled room to limit the effect of environmental temperature on skin temperature. Despite the standardised ambient temperature, there was a large variation in individual resting skin temperatures and in consequence large variation in resting measurements. It is an important finding as large variability limits the usefulness of these measurements and differential assessment. The measurement could instead be acquired at a standardised resting temperature in order to characterise resting blood flux and oxygenation. In the case of patient groups with altered microcirculation, measurements at standardised resting temperature may be different enough to overcome the natural variability.

4.2.5 Blood Flux and Oxygenation Regression Modelling

The multiple regression model that included BF, age, BMI and skin temperature showed these variables account for 58% of the variance in SO_2. This confirms that BF and SO_2 are influenced by physiological factors i.e. age, BMI and skin temperature. It is therefore important to consider carefully these characteristic during assessment and comparisons of BF and/or SO_2. Resting measurements in Study 1 were recorded at controlled environmental temperature and at subject's skin temperature. The results showed the temperature explains a high degree of the variability of resting measurements. It is natural that everyone has a different skin temperature and therefore different resting BF and OXY measurements. In order to reduce the influence of skin temperature on the measurements, a standardised skin temperature can be introduced. Controlling skin temperature can be achieved by local warming or cooling. The measurements taken at the same skin temperature which can be considered physiologically neutral temperature (33°C) i.e. temperature which does not perturb skin blood flow, may offer lower variability of measurements in the studied cohort. Consequently, reducing the variability within healthy subject may offer a higher sensitivity of this test when compared to measurements from subjects suffering from microcirculation problems.

Regression modelling also helps to adjust the measurements to the basic demographic data of participants. Results from Study 1, showed that the age did not have influence on resting BF and SO_2. However, subjects with higher BMI had higher resting SO_2. The studied cohort included healthy subjects with majority of subject within the healthy BMI range (<25). The results suggest that, even within the healthy population there is a relationship between SO_2 and BMI.

4.2.6 Tissue Oxygenation vs. Transcutaneous Oxygen Pressure

SO_2 and haemoglobin parameters were expected to be related with $tcpO_2$ as described by the oxygen dissociation curve. However, the experimental data did not fit the oxygen dissociation curve. Furthermore there was no correlation between $tcpO_2$ and SO_2. The possible reasons for the lack of the agreement with dissociation curve are different blood vessels systems contributing to each signal and working principles of the $tcpO_2$ and SO_2 techniques. $TcpO_2$ signal relies on the chemical reaction between the electrode placed on the skin and the oxygen available on the surface of the skin. In case of SO_2 measurements, the signal originates only from the microcirculatory blood vessels. As the principle is different for SO_2 and $tcpO_2$, it is likely that the signal comes from different vascular compartments and therefore SO_2 and $tcpO_2$

measurements reflect different variables. Therefore, these measurements should be interpreted separately – $tcpO_2$ as a measure of oxygen diffusing to the surface of the skin under maximal dilated condition to 'arterialise' the blood and SO_2 as the ratio (expressed in %) of light absorption of oxyHb and deoxyHb. The major limitation of $tcpO_2$ measurements is the sampling rate. $TcpO_2$ measurements were taken with a sampling rate of 0.1 Hz compared to 40 Hz for SO_2 measurements. Due to this slow sampling rate of $tcpO_2$ measurements, it is impossible to monitor the rapid changes in tissue oxygenation using $tcpO_2$.

In the literature, there are a few studies investigating $tcpO_2$ and BF (Mars et al., 1998; Svalestad et al., 2010) but there is little literature reporting simultaneous measurements of $tcpO_2$ and SO_2 under the same conditions. In the studies comparing $tcpO_2$ and BF Mars et al. (1998) investigated $tcpO_2$ and heated and unheated BF in patients with peripheral vascular disease before amputation (Mars et al., 1998). They measured $tcpO_2$ and BF on the chest and on the limb and calculated the $tcpO_2$ and BF indexes as the ratio of these two sites. They found a strong, positive correlation between $tcpO_2$ and heated BF, $tcpO_2$ index and heated BF, $tcpO_2$ index and BF index. They also found a positive but weak correlation between $tcpO_2$ and unheated BF. Figoni et al. (2006) found no correlation in healthy subjects between $tcpO_2$ and BF measured with laser Doppler Imaging. This is in agreement with findings from this thesis. Nevertheless, Figoni et al. (2006) found significant but weak correlation in the ischemic patients. This may be explained by a reduced blood flux in ischemic patients resulting in reduced oxygen content within the tissue. In healthy subjects the local blood flow is high enough, so it does not limit the $tcpO_2$ measurement. It may be difficult to observe the relationship between BF and $tcpO_2$ in healthy subject as their skin is adequately perfused all they time and the oxygenation is high.

4.2.7 Sampled Volume

The principles applied to calculate the volume of tissue sampled by the probe are similar for LDF and WLS. Barun et al. (2007) described the relationship between penetration depth into a three-layer model of skin and the wavelength of light projected into the skin. According to the authors, the white light penetrates the skin to a depth of ~1 mm. They found the depth of penetration by analysing the absorption coefficients of the skin for various light wavelengths. For both LDF and WLS the depth of penetration also depends on the separation between the source and detector (Forst et al., 2008). It is widely accepted that the sampled volume for combined LDF and WLS is within the same vascular compartment and it is estimated to be 1 mm^3 (Fredriksson et al., 2007; Sampoalesi, 2012). The simultaneous measurements of BF and

SO_2 are considered to reflect the changes occurring in the similar volume of tissue. However, the lack of direct evidence for the penetration depth for LDF and WLS may be considered as one of the limitations of the combined measurements.

4.2.8 Coefficient of Oxygen Consumption

In healthy population the amount of oxygen available across the tissues is greater than the demand. The oxygen consumption varies in different tissues and it depends on the intensity of the activity occurring in that tissue. The measurement of oxygen consumption is used not only in sports medicine but also in clinical setting as diagnostic and prognostic information about cardiovascular fitness.

The approach presented in this work proposes a simple measure of the coefficient of oxygen consumption. The linear decrease in oxygenation during first 60 s of arterial occlusion may serve as surrogate of tissue oxygen consumption. Arterial occlusion rapidly restricts the blood flow to the tissue and consequently the delivery of oxygen. The tissue can only consume oxygen that has been delivered before the occlusion. The rate of decrease in SO_2 can be considered as a coefficient of oxygen consumption. However, SO_2 and Hb signals are expressed in arbitrary units, therefore they do not provide information about the absolute oxygen consumption, and currently cannot be converted to absolute units. Nevertheless, it is not always necessary to express the measurement in the absolute units. The measurement indicating a change expressed in relative units is as important as measurements expressed in absolute units.

A different approach to investigate skin oxygen consumption was taken by Thorn et al. (2011). They observed spontaneous anti-phase swings in oxyHb and deoxyHb in human skin during rest using white light spectroscopy. They linked them to vasomotion related endothelial activity. However, these swings did not have regular time constant and were not observed in all subjects. The mechanism for these swings remains unclear and needs to be better understood before this approach can be used as an indication of the oxygen consumption. Perhaps, if combined with other assessments of oxygen consumption, such as PORH, these swings may provide a valid measure of oxygen consumption. It is an interesting approach, but requires more specific description and wider validation.

Coefficient of oxygen consumption presented here may be altered in people with circulation problems. Further studies may look at the coefficient of oxygen consumption in subjects with poor circulation to assess whether microvascular dysfunction is reflected in skin oxygenation

and whether the skin coefficient of oxygen consumption and subsequently metabolism is altered by reduced blood flow.

4.2.9 OxyHb and DeoxyHb as More Informative Variables Compared to SO_2

SO_2 is derived from oxyHb and totalHb (oxyHb + deoxyHb) and is therefore insensitive to the same-direction, same-magnitude changes in the component variables e.g. the increase in oxyHb by 10 AU with simultaneous increase in deoxyHb by 10 AU will not affect the ratio i.e. SO_2. OxyHb and deoxyHb measurements are the component variables of SO_2 and provide information about the relative amount of oxygenated and deoxygenated Hb present in the tissue. They can inform about abnormal behaviour of each components separately rather than SO_2 ratio, which does not supply information about changes in oxyHb and deoxyHb. It was observed in the data that behind the same SO_2 value (across different volunteers), there can be different oxyHb and deoxyHb values. For example two different volunteers had baseline SO_2 of 54.8% and 55.0%, whilst their oxyHb levels were 7.5AU and 18.5AU, and deoxyHb levels 6.1AU and 12.5AU. Whilst SO_2 is a useful ratio illustrating the fraction of oxygenated haemoglobin to total haemoglobin, it is recommended to analyse oxyHb and deoxyHb primarily or with combination with SO_2.

4.2.10 Power Spectral Density Profiles

The surface plots and scalograms presented in Figure 4.6 illustrate major differences between the dominant frequency components in BF and SO_2 signals. Studies investigating SO_2 oscillations in muscles and brain showed similar results (Li et al., 2010; Li et al., 2013; Yano et al., 2013). The possible explanation of the absence of higher frequency oscillation in SO_2 signal may be based on longer physiological time constant driving tissue oxygenation. The mechanisms regulating oxygen delivery to the tissue might not be related to individual heartbeats. Another explanation may refer to signal registration technique. Although it is estimated that SO_2 signal comes from the tissue up to 1 mm deep, the penetration depth cannot be exactly determined. If the signal originates only from capillaries excluding arterioles and venules, the heartbeat oscillation in these vessels might be almost fully attenuated by the peripheral vascular resistance.

The values of relative PSD in BF signal reported in this thesis are different from those reported previously (Kvernmo et al., 2003; Soderstrom et al., 2003; Clough et al., 2009). Kvernmo et al. (2003) reported the highest relative amplitude for endothelial band, followed in decreasing

order by neurogenic, myogenic and respiratory bands. The cardiac band had relative amplitude similar to respiratory band. Soderstrom et al. (2003) showed the opposite pattern reporting the highest normalised power for heartbeat, followed by lower normalised power for respiratory and myogenic bands (similar values) and the lowest normalised power was found in the neurogenic and endothelial bands. Clough et al. (2009) reported similar trend in relative spectral power to the trend in relative spectral amplitude reported by Kvernmo et al. (2003). Nevertheless, these results cannot be directly compared as they refer to different variables. There are more examples of different frequency characteristic reported in the literature, which were obtained using different devices; hence they are not always comparable. Huang et al. (2011) reported data as absolute power and power ratio computed with S-transform. Humeau et al. (2008) expressed results as relative energy of the scalogram. Other groups reported relative amplitude or power spectral density (Rossi et al., 2011; Fedorovich, 2012). Due to the above it is not possible to directly compare results. There is no consensus for spectral analysis and all methods may have advantages and disadvantages. For example FFT provide information about the frequency components of the entire signal, whilst WT focuses on local features. FFT decomposes signal into sine and cosine waves whilst WT convert the signal into scaled mother wavelets. Both approaches are valid and provide different information.

Averaging of individual scalograms across the volunteers may obscure some of the time-varying frequencies and PSD over time, particularly as the higher frequency activities are present in one data set (BF) and not the other (SO_2). Similarly, averaging the coherence from the group may obscure the variability present in the individuals. These issues will need to be addressed in future studies if the consequences of changes in rhythmical flowmotion on tissue perfusion and oxygenation under pathophysiological conditions are to be investigated.

4.2.11 Frequency Coherence

Frequency coherence relates to the similarity in periodic fluctuations between signals. Low frequency coherence indicates that signals contain distinct frequency components. In terms of BF and SO_2, high frequency coherence across some frequency bands confirms the link between BF and SO_2. It also indicates that they may be regulated by the same or closely related mechanisms acting within the same frequencies.

Good frequency coherence in endothelial and neurogenic bands suggests that BF and SO_2 signals are similarly influenced by endothelial and neurogenic functions. Good frequency coherence in the neurogenic band may indicate that sympathetic nerves responding to

decrease or increase in oxygen trigger the vasodilation or vasoconstriction and thus regulate blood flow.

Frequency coherence has been used to study various biological signals. Some examples include the coherence between the ECG signals (Clayton & Murray, 1999; Pachauri & Mishra, 2012) and neurophysiological signals such as EEG, magnetoencephalogram (MEG), cerebral blood flow (Miranda de Sá et al., 2002; Pereda et al., 2005; Simpson et al., 2005; Tan et al., 2016). The studies investigating the frequency coherence aimed to determine the oscillatory coupling between two or more signals. The coupling between BF and SO_2 has been reported to some extent. The frequency coherence can be computed for all frequency components in the signals or particular frequency bands. The study comparing standard and high power LDF probes by Clough et al. (2009) found the best coherence in the lowest frequency bands (endothelial and neurogenic) and reduced coherence in higher frequency bands (myogenic, respiratory and cardiac). The measurements by Clough et al. were taken on the forearm. The results presented in this thesis agree with these findings; however they refer to different signals. Clough et al. (2009) investigated two BF signals registered with standard and high-power probes. The work presented here investigated BF and SO_2 signals.

The frequency coherence estimation does not provide information about synchronicity of the signals. From these estimations it is not possible to extract information on how the oscillation in the signals behave in time, how are they modulated and shifted in time. These issues should be addressed in future studies as they might hold valuable information about interaction between BF and SO_2. Further discussion on this topic is presented in Chapter 5 and Chapter 6.

Thorn et al. (2009) investigated the spontaneous oscillations in SO_2 in relation to Hb signals (oxyHb, deoxyHb and totalHb) recorded from healthy human skin. They identified two types of swings: a type I swing when change in SO_2 resulted from change in oxyHb and totalHb with no change in deoxyHb, and type II swing which resulted in antiphase changes in oxyHb and deoxyHb with no change in totalHb. Thorn et al. (2009) proposed that these swings reflect constant metabolic demand and oxygen usage (type I swing) and oxygen extraction due to change in oxygen demand or cutaneous blood flux (type II swing). However, Thorn et al. (2009) did not measure blood flux but assessed changes in blood volume from the totalHb signal. It would be interesting to explore the BF signal on top of these signals presented by Thorn et al. (2009) and this has been addressed in the next paper from research group lead by C. Thorn. They published a study in which they investigated the role of vasomotion on oxygen extraction (Thorn et al., 2011). In addition to previously studied signals (oxyHb, deoxyHb and totalHb)

they also measured skin blood flux using LDF. They have demonstrated that oscillation in SO_2 can be a consequence of endothelial activity. Nevertheless, these findings were reported as individual analysis of 24 subjects with only 19 subjects exhibiting the spontaneous oscillations. These studies investigated the dynamics between BF and SO_2 but focused only on low frequency oscillations rather than PSD profiles and complete frequency content of BF and SO_2.

4.2.12 Limitations

There are a number of unknowns that may have had an influence on my results and their interpretation. BF and OXY signals were based on the optical measurements. However, to date it is not possible to measure the exact optical properties of the tissue non-invasively. The modelling studies mentioned in this thesis presented the estimated values for optical properties of skin.

Another limitation of the study was the definition of a healthy volunteer. Subjects were asked a question whether they were 'healthy' and whether they suffered from any medical condition. Only subjects who answered that were healthy and do not suffer from any disease were included. However, it could be the case that there were underlying medical conditions that subjects were unaware of.

Another fundamental limitation is the body site from which the measurements were acquired. The signals of BF and OXY were registered purely from skin, which is considered as a surrogate of microcirculation in other tissue. However, this is not entirely true. Some conditions that affect microvascular function may not be reflected in skin microcirculation. It is difficult to draw the border of when the changes could be detected in skin, but it should be always discussed whether the health condition of the person may have an effect on the skin microcirculation.

The recorded BF and OXY signals were assumed to represent the entire process (consisting of multiple independent and dependent mechanisms) generating the signal. This is not the exact case when analysing biological signals. Furthermore, the lowest frequencies analysed in BF and SO_2 signals were ~0.0095 Hz which means 1 cycle happed over 105 s. The analysed signals were 600 s long, therefore the slowest activity had only a few cycles present in the recorded signal. Biological signals are not perfectly regular so the oscillations are not identical in each cycle. Higher numbers of cycles of interest in an analysed signal increases the accuracy of the analysis. In this research 600 s was assumed to be long enough for the frequency analysis. Considering the lowest frequency of interest had a period time of 105 s, there were 5 full

cycles in the sampled period. This is adequate to identify and describe this periodic activity. However, it is recognised that the accuracy of low frequency analysis may be improved by recording and analysing longer traces.

4.3 General Considerations

LDF was developed over 30 years ago and since then many papers have been published related to LDF. A simple search in PubMed using '((laser) AND doppler) AND flowmetry' performed on 19th June 2015 returned 10132 results. When narrowed to include 'skin' (((laser) AND doppler) AND flowmetry) it only returned 2980 results. It is clear that there is a large amount of data, however the technique has not been translated into clinical setting. The main application of LDF is to study microvascular function. Although a number of studies have reported the changes attributed to the microvascular dysfunction being reflected in LDF signals, these findings have never made their way into a standardised assessment.

To date, the blood flux and oxygenation measurements show physiological responses but fail to distinguish physiological states well enough in order to apply these to the general population. Measurements vary greatly and there is no standardisation between different research groups on what is the correct way of recording the measurement, analysing and interpreting it (Cracowski et al., 2006; Roustit & Cracowski, 2012; Cracowski & Roustit, 2015).

What about negative results?

In general, there are fewer studies reporting negative results. Null or negative results are often unconsciously considered less interesting and unimportant. Furthermore, it is more difficult to publish negative results from a study as they may be considered as not having enough scientific contribution. As a result it is not known how much research has been already done outside the reported studies. Perhaps other research groups have already asked similar research questions and performed the investigation but did not publish their work. The integrity of knowledge is an important aspect of research, but unfortunately it is sometimes missing due to various reasons such as conflict of interest, lack of funding, time constrains, etc.

Another consideration regarding similar, unpublished studies relates to simple statistics. The more similar studies are performed, the higher the probability of statistically significant findings (Ioannidis, 2005). Once the significant finding is obtained, it is more likely to be published. Consequently, other researchers have access to these findings but not to the

unpublished findings. They may not realise that majority of studies resulted in different conclusions.

Importance of *n* numbers

The studies conducted in human cohorts aim to describe the whole population or the population with a particular physiological state such as disease, based on the data from subjects recruited to the study. The higher the number of subjects (n) under investigation the higher the power of the study, and subsequently the trust in the reported findings. However, the question remains what is the minimal n number we can trust?

It is also the case for research in BF. One of the first studies reporting frequency analysis of BF signals was based on only nine control subject and nine athletes (Bracic & Stefanovska, 1998). A year later they published another research paper based on nine athlete subject, most probably the same nine subjects (Stefanovska et al., 1999). The evidence for this are the same characteristic of average and total energy reported in both papers. These two studies have later become a 'gold standard' for BF frequency analysis and frequency band definitions. According to Google Scholar these papers have been cited 159 times and 359 times ((Bracic & Stefanovska, 1998) and (Stefanovska et al., 1999) respectively), (checked on 22/06/2015). Interestingly, the frequency bands definitions based on nine subjects only, have been used since then. The following study published by the same group was based on 17 subjects (Bracic et al., 2000)). Another study published by the same groups was based on 32 subjects; however the focus of this study was on respiration and heartbeat, rather than lower frequency components (Lotrič Bračič & Stefanovska, 2000)).

The sample size remains a problem in a number of other studies. Other examples are studies published by the research team lead by Rossi. They aim to assess the differences in spectral components in different physiological and pathological conditions. They studied how the power in the frequency bands change in response to insulin in 20 healthy subjects (Rossi et al., 2005b). They have shown an increase in spectral density across all frequency bands. It was an expected result as the BF increased. Unfortunately, they have only reported mean spectral density which does not express the contribution from the band to the overall flowmotion. Thus, it is not possible to assess from these results how insulin affects flowmotion.

Another study aimed to assess flowmotion in healthy subjects and subjects with peripheral arterial obstructive disease (PAOD) (Rossi et al., 2005a). Each group consisted of 20 subjects. They showed higher peak powers in endothelial, neurogenic and myogenic bands in subjects

with PAOD compared to healthy controls. However, the SDs of the measurements were large, indicating a high variability in both cohorts. In some cases the SDs even exceeded the reported value. It is highly possible that these results could be false. Furthermore, these results were based on only 20 subjects. In the study published in 2006 they compared subjects with essential arterial hypertension and healthy subjects. The groups consisted of 20 and 30 subjects respectively.

4.4 Summary and Contributions to the Body of Knowledge

The research presented in this chapter was designed to validate and test the combined BF-OXY measurements. The relationship in healthy skin between BF and SO_2 over wide range of values was identified. The novel combined BF-OXY probe was evaluated under multiple physiological tests. The inter-individual and intra-individual reproducibility were determined for BF, SO_2, oxyHb, deoxyHb and totalHb. The BF and SO_2 signals were analysed using multiple time and frequency methods.

The key contributions to the body of knowledge resulting from this chapter are the analysis of SO_2 measurements in addition to previously known BF measurements. The simultaneous measurement of BF and SO_2 provide extended information about tissue state. The BF-SO_2 relationship determined for healthy subjects (Equation (4.1)) may serve as a reference for other studies. For example, in diabetes the BF-SO_2 relationship may have lower asymptote and lower rate of linear increase at low flux values.

The results showed the resting BF and SO_2 are related to skin temperature which can vary greatly between healthy subjects. In order to standardise the measurements and reduce the influence of variable skin temperature, the measurements should be taken at the same skin temperature for all subjects. This idea leads to the next set of measurements conducted at the standardised temperature. This idea is further developed in Chapter 5.

The results also showed marked differences between BF and SO_2 in the frequency domain, in particular in the respiratory and cardiac frequency bands. However, the frequency analysis was only performed on resting signals. The frequency characteristics may change under physiological challenge – it remains unclear how the spontaneous oscillations adapt to different physiological state such as sustained vasoconstriction or vasodilation.

Chapter 5

Further Investigations of Time and Frequency Components of BF and OXY Signals Measured in Healthy Skin

The measurements from the study presented in Chapter 4 showed that the skin temperature was the main contributor to the variability of resting BF and SO_2 signals. This variability limits the translation of these measurements into a useful clinical test. The question arises as to whether the BF and SO_2 measurements carried out at the standardised skin temperature will result in a consistent and less variable assessment of microvascular function. In this Chapter the combined measurements taken at the same but physiologically-neutral skin temperature (33°C) and during local thermal hyperaemia (43°C) across the cohort of healthy subjects are explored in time- and frequency- domains.

The analysis presented in Chapter 4 showed the differences in the spontaneous oscillatory activity embedded in resting BF and SO_2 signals. The frequency characteristics were only explored at rest due to limitations placed by the need to acquire artefact free, steady state signals of 10 min duration. The frequency characteristics at rest provided only limited information about the microvascular system. To extend the assessment and the knowledge about the frequency characteristics of the microvascular function, the analysis presented in this chapter have been studied at rest and under physiological stress. Local warming has been applied as the physiological challenge, to measure the capacity of the microvascular system to vasodilate. A steady state vasodilation was achieved by local skin warming to 43°C for 20 min. The spontaneous oscillations of BF and OXY signals were explored using extensive frequency-domain analysis.

BF and OXY signals were recorded from skin of fifteen healthy men at ambient temperature and at 33°C and at 43°C during local warming using a combined LDF and WLS probe from Moor Instruments. The measurements at ambient skin temperature and at 33°C were recorded continuously for 15 min each. Warming to 33°C and 43°C was achieved with moorVMS-HEAT device which was programmed to increase the temperature of the metal disk placed on the skin. The measurement probes were mounted within the heating disc according to the

manufacturer's design. The measurements at 33°C were followed by immediate warming of the heating disc to 43°C and BF and OXY signals were recorded for 25 min. Data for time-domain analysis were extracted as the mean over a 1-2 min period within the last five minutes of recording at each stage. Data for frequency-domain analysis were selected as 10 min long artefact-free segments from recordings at ambient skin temperature, at 33°C and at 43°C. The signals were filtered to remove frequencies >2Hz which are outside the range of interest and detrended to remove long-term drifts. A figure representing raw output from Study 2 was shown in Chapter 3 (Figure 3.5 (p.53)) and the analysis methods were described in Chapter 3, section 3.5 (p.56).

5.1 Results

Mean forearm skin temperature during the last five min at resting skin temperature was 31.2±1.0 °C. Data obtained during warming the skin to 33°C and 43°C showed that some variables (SO_2 and oxyHb) were non-normally distributed. Normally distributed data presented below are shown as mean (SD) and non-normally distributed data are shown as median and interquartile range taken over 1-2 min period within the last 5 min of warming to either 33°C or 43°C.

5.1.1 Characteristics of BF and OXY Signals in Time-Domain

The recordings from the first five volunteers were taken with the probes applied directly to the dry skin. However, it was observed that warming of the skin failed to induce the expected axon-reflex response (described in short in 2.2.2 and discussed later in this Chapter). This was taken to be indicative of poor thermal contact between the skin and the heating probe. It was therefore decided to use a small amount of ultrasonic gel (as a thin film on the heating disc) to improve the heat transfer between the heating disc and the skin. The results showed the gel had no influence over the absolute value of measurements. Mean (SD) values of BF and OXY parameters for measurements without and with gel are summarised in Table 5.1. There were no statistically significant differences in any of the signals taken without and with the gel at 33°C or at 43°C (p-values of student t-tests can be found in Appendix 4). The use of ultrasonic gel did not influence the presence of axon-reflex (it was absent in measurements without and with the gel). The gel had no influence on measurements taken, therefore, data from all fifteen participants have been considered together during analysis.

Table 5.1 Mean (SD) values of BF and OXY signals for measurements with and without gel at 33°C and 43°C.

	Without gel at 33°C n=5	With gel at 33°C n=10	Without gel at 43°C n=5	With gel at 43°C n=10
BF (PU)	12(2)	14(6)	218(71)	214(66)
SO_2 (%)	45(11)	41(12)	74(2)	73(3)
oxyHb (AU)	6(2)	6(3)	35(13)	32(10)
deoxyHb (AU)	8(3)	9(5)	12(3)	12(3)
totalHb (AU)	14(3)	15(8)	47(16)	44(13)

Measurements at ambient skin temperature, at 33°C and 43°C

The mean (SD) values of BF, SO_2, oxyHb, deoxyHb and totalHb at resting skin temperature, at 33°C and at 43°C are summarised in Table 5.2.

Table 5.2 Mean (SD) values of BF and OXY signals at ambient temperature, at 33°C and at the end of 25 min skin warming to 43°C. p-values of student t-test comparing measurements at ambient skin temperature and at 33°C. n = 15.

	Ambient skin temperature (31.2±1.0 °C)	33°C	43°C	p-value
BF (PU)	11(5)	13(5)	215(65)	0.25
SO_2 (%)	37(9)	42(11)	73(3)	0.26
oxyHb (AU)	5.2(1.9)	6.2(2.9)	33.3(10.9)	0.25
deoxyHb (AU)	8.9(3.7)	8.6(4.3)	11.8(2.7)	0.84
totalHb (AU)	14.1(4.9)	14.8(6.3)	45.1(13.5)	0.73

Comparisons of Measurements at ambient skin temperature and at 33°C

Temperature strongly influences BF as shown in previous chapter. To limit the influence of resting skin temperature in Study 2, the local warming to 33°C was used. Measurements at ambient temperature and 33°C were compared using student t-test. There were no significant

differences in any signal measured at physiological skin temperature (mean 31.2°C) and at 33°C. Mean (SD) measurements were presented in Table 5.2 above and p-values of the comparisons between measurements at ambient skin temperature and the measurements taken at 33°C. These results confirm that warming the skin to 33°C does not induce a physiological reaction influencing BF and/or OXY signals and therefore it can be used as a standardised measurement temperature for assessment of a resting microvascular function.

Effect of warming to 43°C on BF and OXY signals

Median (IQR) change in BF and OXY signals from 33°C at the end of the 25 min warming on the forearm has been calculated as the normalised difference and expressed as a fold change (Equation 5.1):

$$Change_{43} = \frac{value_{43} - value_{33}}{value_{33}} \quad (5.1)$$

Table 5.3 presents the fold increase in the signal measured at 33°C compared to 43°C. The highest increase occurred in BF – it increased 15.6 (10.3-22.8) times. OxyHb increased 4.8 (3.5-5.9) times. The increase in SO_2 was 0.6 (0.5-1.3) times.

Table 5.3 Median (IQR) of the change from 33°C at the end of warming to 43°C. The change is expressed as a fold change.

	Fold change from 33°C at 43°C, median (IQR)
BF (PU)	15.6 (10.3-22.8)
SO_2 (%)	0.6 (0.5-1.3)
oxyHb (AU)	4.8 (3.5-5.9)
deoxyHb (AU)	0.6 (0.1-1.1)
totalHb (AU)	2.3 (1.5-3.1)

All signals exhibited an increase towards the end of measurements at 43°C compared to an initial response to warming. Figure 5.1 shows median (IQR) of signals at the beginning of warming (maximal value within first three minutes) at 43°C and after 25 min of warming. The increase in the BF and Hb signals (oxyHb, deoxyHb and totalHb) was statistically significant

(tested by Mann-Whitney test). On the other hand, the SO_2 signal was steady and did not show any changes.

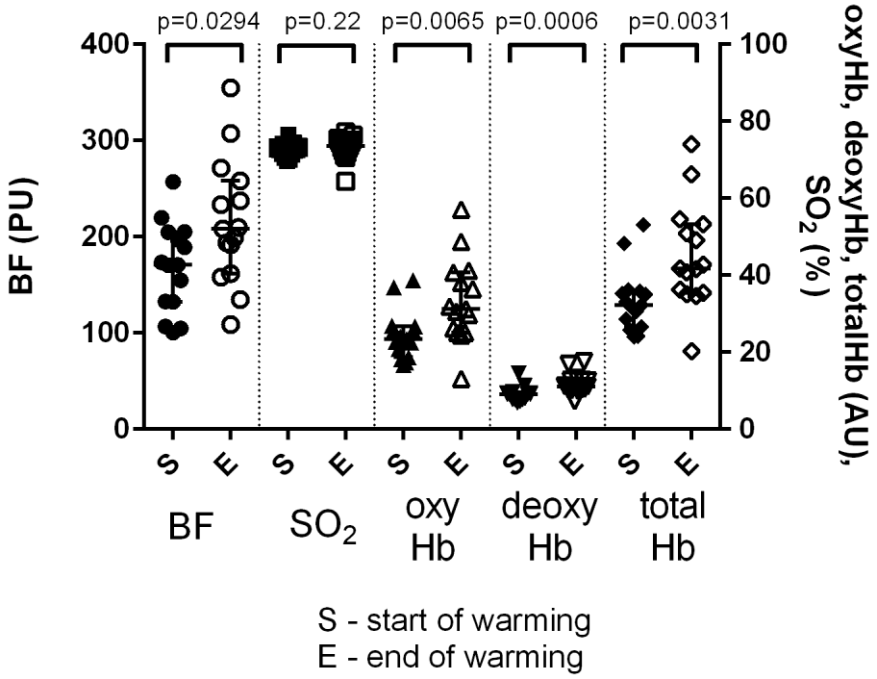

Figure 5.1 Median (IQR) of BF and OXY signals at maximum value within the first three minutes of warming (S – start of warming) and over the period of 1-2 minutes within the last five minutes of warming (E – end of warming). An increase in all signals except SO_2 was significant (see p-values on the top of the figure). n = 15.

Variance of BF and OXY signals

Table 5.4 summarises the variance in BF and OXY signals at 33°C and 43°C across the cohort of young, healthy men (n=15). Not all the datasets were normally distributed, therefore the results are presented as median (IQR). BF and SO_2 signals showed a large but opposite change in variance of the signal during warming. The variance of BF signal increased, whilst the variance of SO_2 signal decreased. The variance of deoxyHb dropped much less compared to SO_2 signal. There was no significant difference between the variance at 33°C and 43°C of oxyHb and totalHb signals.

Table 5.4 Median (IQR) variance of BF and OXY signals at 33°C and 43°C. Variance at 33°C was compared against variance at 43°C using the Mann-Whitney test.

	Variance at 33°C, median (IQR)	Variance at 43°C, median (IQR)	p value
Flux	4.36 (2.08 - 6.80)	317.0 (172.6 - 490.2)	<0.0001
SO_2	8.15 (3.50 – 20.77)	0.19 (0.12 – 0.23)	<0.0001
OxyHb	0.32 (0.29 – 0.56)	0.43 (0.31 – 0.71)	0.2147
DeoxyHb	0.06 (0.04 – 0.26)	0.04 (0.03 – 0.05)	0.0208
TotalHb	0.45 (0.41 – 0.95)	0.64 (0.45 – 1.09)	0.1358

5.1.2 Correlations of BF and OXY Signals in Time-Domain

Figure 5.2 illustrates the correlations between BF and SO_2 at 33°C and 43°C. The higher the blood flux, the higher SO_2. It has been shown in the previous chapter that BF and SO_2 are positively associated with resting skin temperature. Here, even though the skin temperature was set at 33°C and 43°C for all volunteers, there is a positive correlation between BF and SO_2. Interestingly, this correlation holds not only for measurements recorded at 33°C but also for the steady state vasodilation (measurements recorded at 43°C). There is a significant positive correlation between BF and SO_2 at 33°C (slope=1.331, r^2=0.32, p=0.0276) and at 43°C (slope=0.0329, r^2=0.48, p=0.0041). These results are further discussed in section 5.2.3. Furthermore, partial correlation between BF and SO_2 controlling for BMI was 0.607(p=0.021) confirming the association was independent of BMI.

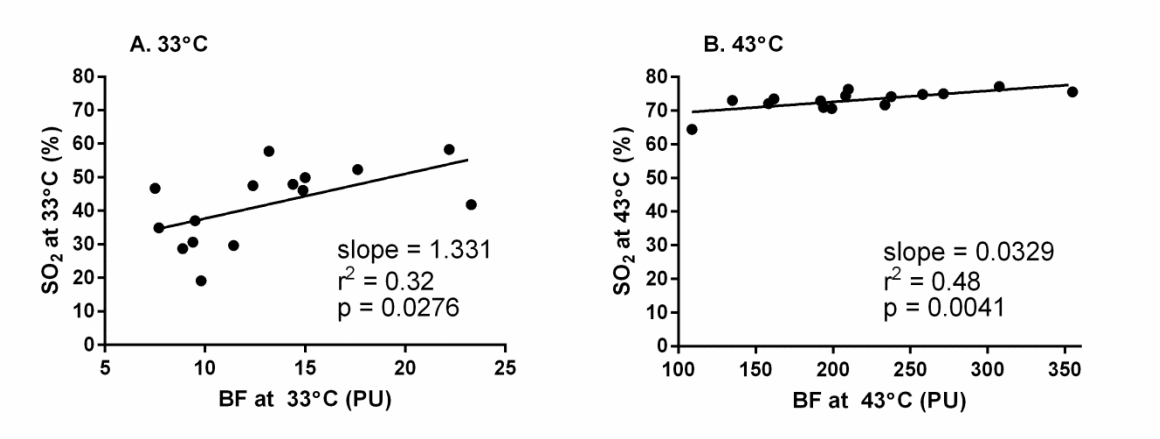

Figure 5.2 The correlations between BF and SO_2 at (A) 33°C and (B) 43°C, n=15.

SO_2 is mathematically derived from oxy- and deoxyHb signals. It might be anticipated that SO_2 will correlate with its component variables: oxyHb, deoxyHb and totalHb. However, as shown in Figure 5.3, these correlations are not all significant. There was a significant, positive correlation between SO_2 and oxyHb at 33°C (slope=0.1387, r^2=0.31, p=0.0302), but deoxyHb and totalHb did not correlate with SO_2 at 33°C (p=0.2367 and p=0.9072 respectively). At 43°C all Hb parameters showed a significant positive correlation with SO_2 at 43°C (oxyHb: slope=2.922, r^2=0.69, p=0.0001; deoxyHb: slope=0.6054, r^2=0.48, p=0.004; totalHb: slope=3.528, r^2=0.65, p=0.0003).

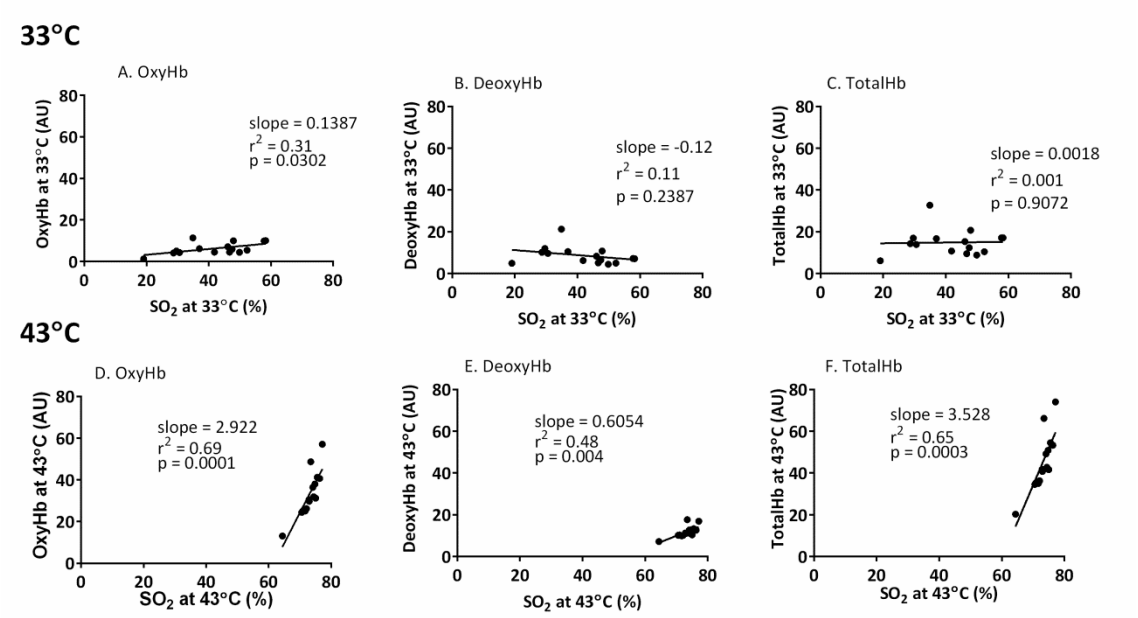

Figure 5.3 The correlations between Hb signals and SO_2 signal (A, B, C) at 33°C and (D, E, F) 43°C. At 33°C only oxyHb is positively correlated with SO_2. At 43°C all Hb signals correlate with SO_2 signal. Notice the slope for oxyHb changes from 0.14 at 33°C to 2.92 at 43°C.

Figure 5.4 illustrates positive correlations between oxyHb vs deoxyHb, oxyHb vs totalHb and deoxyHb vs totalHb at 33°C. Resting oxyHb weakly but significantly correlated with deoxyHb (r^2=0.30, p=0.0351). Stronger correlations occurred between oxyHb and totalHb (r^2=0.68, p=0.0002). Furthermore, the strongest correlation was between deoxyHb and totalHb (r^2=0.86, p<0.0001).

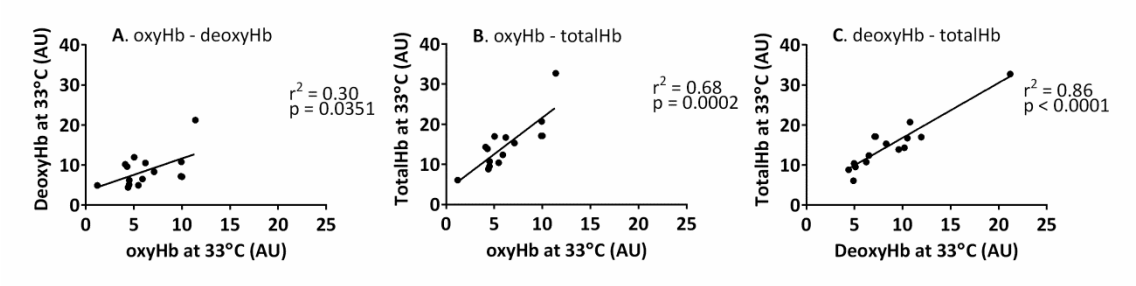

Figure 5.4 The correlations between (A) oxyHb vs deoxyHb, (B) oxyHb vs totalHb and (C) deoxyHb vs totalHb at 33°C.

5.1.3 Characteristics of BF and OXY Signals in the Frequency-Domain

Figure 5.5 illustrates an example of detrended BF and OXY signals collected at 33°C and 43°C for 10 min. The top panel depicts 600 s long signals, while the bottom panel shows 100 s long segment of the top panel (between 100-200 s) to illustrate more details. All signals exhibited multiple oscillatory components. The heartbeat is clearly visible in BF signals at 33°C and 43°C. In OXY signals at 33°C the heartbeat is weakly visible; however during warming it becomes more pronounced. At 33°C, SO_2 signal exhibits higher variance compared to BF signal, however at 43°C the opposite holds: SO_2 signal is smooth with lower variance compared to 43°C, whilst BF signal shows an increased variance of high frequencies.

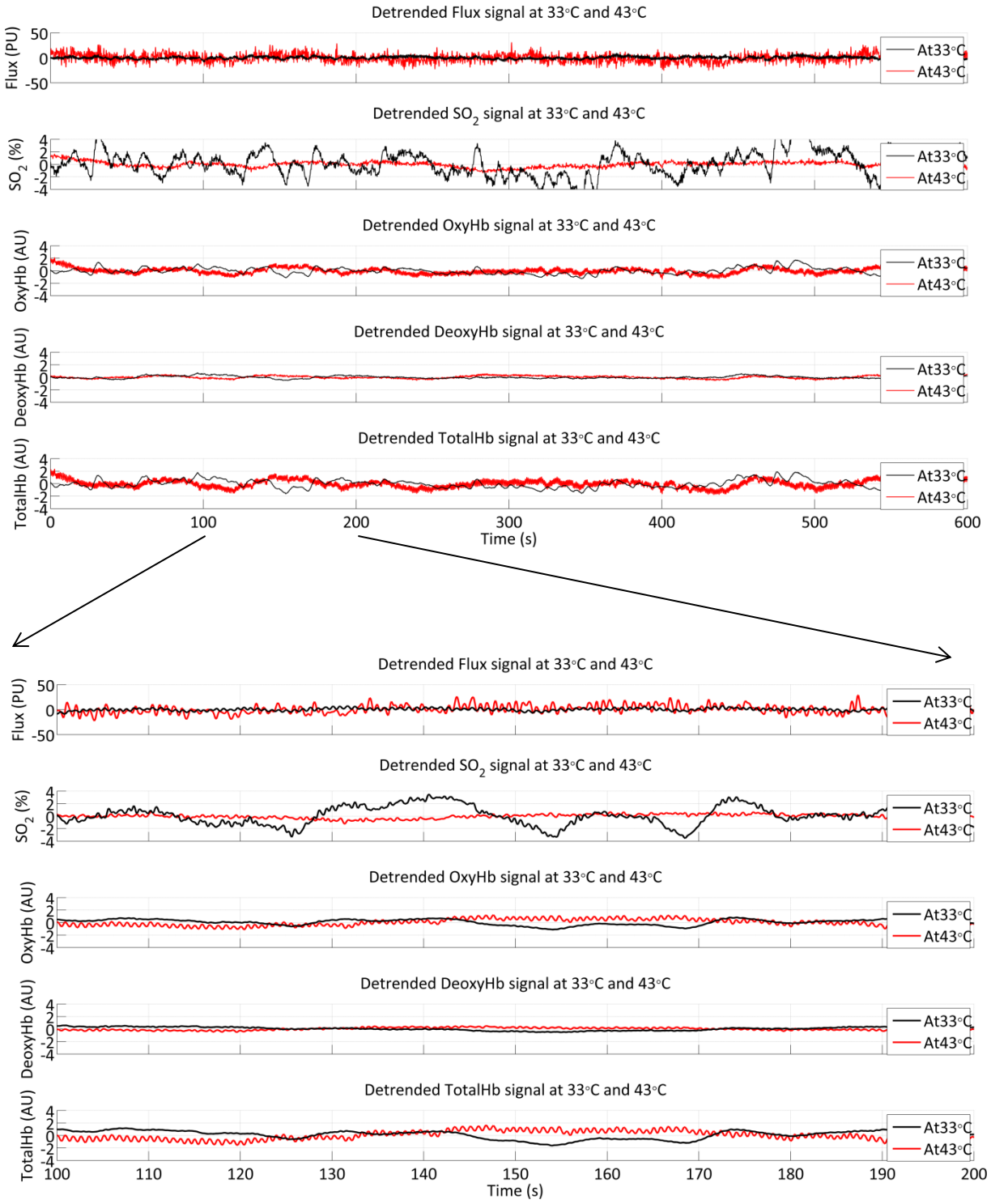

Figure 5.5 An illustrative example of (top) 600 s long and (bottom) 100 s long detrended signals at 33°C (black) and 43°C (red). At 33°C, the heartbeat is clearly visible only in BF signal, however at 43°C the heartbeat is pronounced in all signals.

5.1.4 Absolute Power of BF and OXY Signals at 33°C and 43°C

The absolute power is a mean squared value and it can be used to quantify the overall oscillations in the signal. It reflects the amount of the amplitude oscillations present in the signal across all frequencies. Figure 5.6 presents a median (IQR) absolute power of BF and OXY signals at 33°C and 43°C. The power of the BF signal greatly increased at 43°C, whilst the absolute power of the SO_2 signal decreased. The smaller power of the SO_2 signals at the warmed state indicates, there are fewer oscillations in this signal – this can be observed in Figure 5.5 (the SO_2 signal at 43°C is smoother than the SO_2 signal at 33°C). The power of deoxyHb signal dropped at 43°C compared to 33°C. The power of oxyHb and totalHb signals remained unchanged at 43°C.

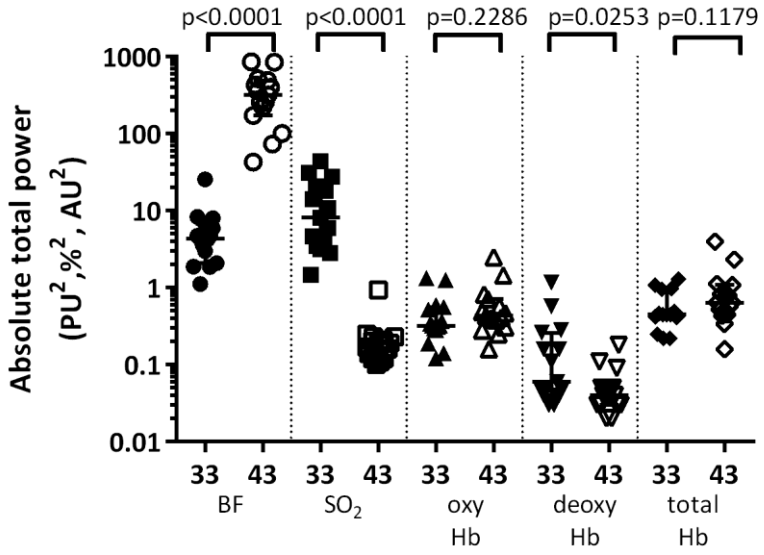

Figure 5.6 The comparision of absolute total signal power at 33°C and 43°C. Warming to 43°C induced a substantial increase in BF signal power ($p < 0.0001$) and a substantial decrease in SO_2 signal power ($p < 0.0001$). The power of deoxyHb signal dropped ($p = 0.0253$). The power of oxyHb and totalHb remained unchanged ($p > 0.05$).

Another interesting aspect of analysis of absolute power is to ask whether there is an association between the absolute power of the signal at 33°C and the absolute power of the signal at 43°C. The correlation analysis showed there were no significant correlations in any signal between absolute power at 33°C and absolute power at 43°C as illustrated in Figure 5.7.

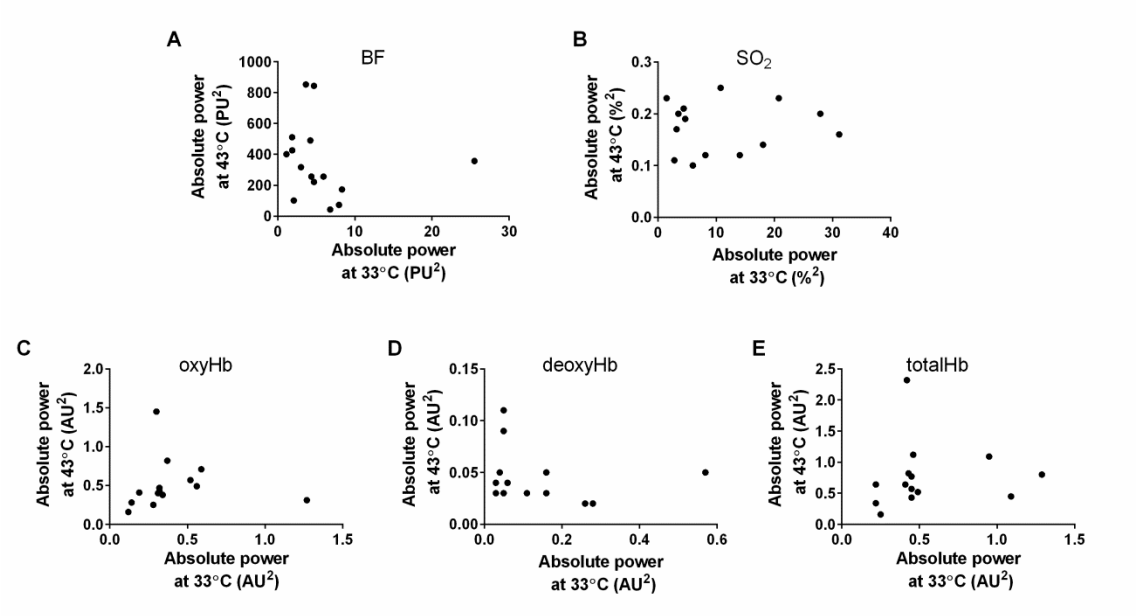

Figure 5.7 Plots of absolute power at 33°C vs absolute power at 43°C for (A) BF, (B) SO_2, (C) oxyHb, (D) deoxyHb and (E) totalHb. The absolute power of the signals at rest and during warming to 43°C did not correlate for any of the BF and OXY signals. n=15.

5.1.5 PSD Profiles

The plots below (Figure 5.8 and Figure 5.9) illustrate PSD spectra for BF, SO_2 and Hb signals at 33°C and 43°C. The graphs include PSD profiles from all individuals (n=15) at 33°C (thin blue lines) and the mean across the cohort (black line). Respectively, at 43°C the individual PSD profiles are marked by thin green lines and the mean with a red line. The borders of the frequency bands associated with the physiological activities (endothelial, neurogenic, myogenic, respiratory and cardiac) are marked with black vertical lines. PSD profiles are expressed in 'unit'^{2}/Hz. Note the x-axis is logarithmic. The power-frequency profiles were lacking in visible peaks in the lower frequency bands indicating the oscillations happening in these bands did not exhibit dominant frequencies in each band. They were either composed of multiple frequency components or the principal frequency component in particular band

varies in time. Conversely, the cardiac band exhibited a clear peak around 1Hz – this indicates that the principal activity of this band (heartbeat) has the frequency of ~1Hz.

BF and SO_2 profiles at 33°C and at 43°C did not overlap, but were located at different power levels (Figure 5.8). BF had higher power at 43°C whilst SO_2 had higher power at 33°C as shown above in Figure 5.6. BF profiles exhibited a large contribution from the cardiac band. There was a clear peak representing heartbeat at about 1Hz at both temperatures, but the contribution from the cardiac band was larger at 43°C. The PSD of the BF signal across all five bands was higher at 43°C compared to 33°C, but the shape of both spectra was similar. It confirms the overall oscillatory activity of BF signal increased during warming.

The PSD profiles of SO_2 signal showed the opposite behaviour to BF profiles. During warming the PSD was lower across all frequency bands compared to 33°C. The cardiac peak was lower and less prominent indicating low power within the cardiac frequency band. Similarly as in BF PSD profile, there was a large drop in power within the respiratory band and the lowest PSD occured in the respiratory band. SO_2 had large contribution from LF components and little contribution from HF bands. These results imply the oxygenation in the tissue does not oscillate with each heartbeat but are mostly controlled by low frequency processes (endothelial, neurogenic and myogenic).

PSD profiles of oxyHb, deoxyHb and totalHb had a number of similarities. At LF, the PSD profiles at 33°C and at 43°C were in partial overlap. The mean PSD at 33°C was only slightly higher than at 43°C. Another common characteristic was a larger drop in PSD in high frequency (HF) bands at 33°C compared to 43°C. It can be observed, there is a crossover between the spectra at 33°C and 43°C within the respiratory band. Interestingly, the Hb signals had a low power in HF at 33°C with heartbeat peak barely distinguishable in oxyHb and totalHb, furthermore the heartbeat peak was absent in deoxyHb signal. However, during steady state vasodilation at 43°C, the Hb signals gained power within the cardiac band and the heartbeat became clearly visible.

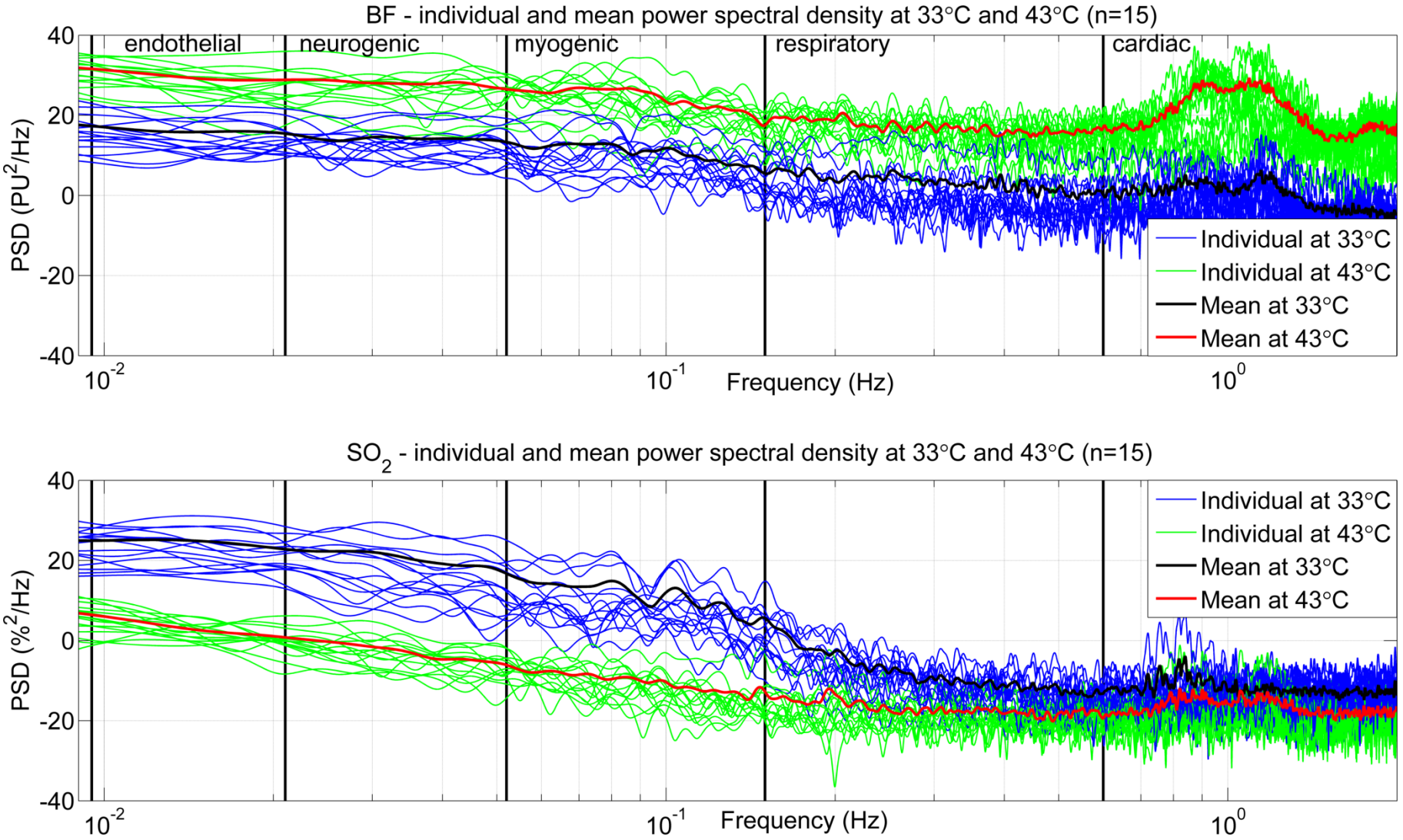

Figure 5.8 Individual and mean PSD spectra of Blood Flux and SO_2 signals at 33°C (individual spectra - blue lines, mean - black) and 43°C (individual spectra - green lines, mean - red), n=15. The borders of the frequency bands associated with the physiological activities (endothelial, neurogenic, myogenic, respiratory and cardiac) are marked with black vertical lines.

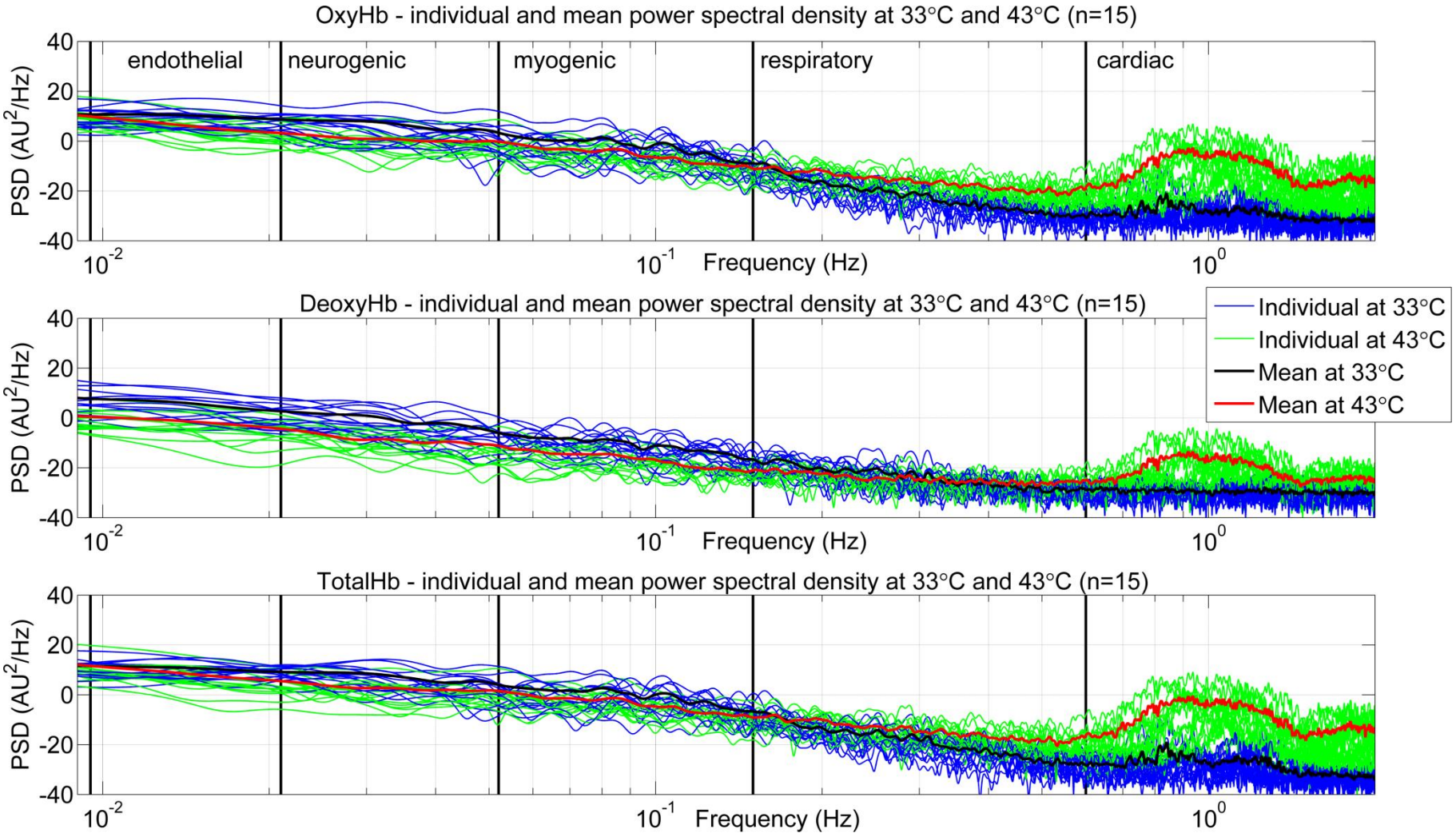

Figure 5.9 Individual and mean PSD spectra of OxyHb, DeoxyHb and TotalHb signals at 33°C (individual spectra - blue lines, mean - black) and 43°C (individual spectra - green lines, mean - red), n=15. The borders of the frequency bands associated with the physiological activities (endothelial, neurogenic, myogenic, respiratory and cardiac) are marked with black vertical lines.

5.1.6 PSD Contributions

The analysis of PSD contribution presented below was conducted using the 5 frequency bands described in section 2.5.2 (p. 40). The contributions were calculated as a ratio of the power in the particular band to the total power over the 5 frequency bands (0.0095 Hz – 1.6 Hz). The contribution is expressed as a fraction between 0-1 and the sum of all contributions equals 1.

Figure 5.10 summaries the PSD contribution in BF signal at 33°C and 43°C. At 33°C BF contained 37% of the power coming from the cardiac band. It was the highest contribution to the overall power of the signal. The second and third highest contributions were from neurogenic and myogenic bands respectively. These contributions were around 20%, and the lowest contributions were found for the endothelial and respiratory bands. At 43°C the contribution from cardiac band increased from 37% to 76% dominating all the other processes.

It can be observed in Figure 5.8 and Figure 5.9 that PSD peak within the cardiac band during warming had higher amplitude compared to PSD peak at 33°C. This indicates that during local vasodilation, small blood vessels (source of BF and OXY signals) exhibit more prominent pulsation originating from the heartbeat.

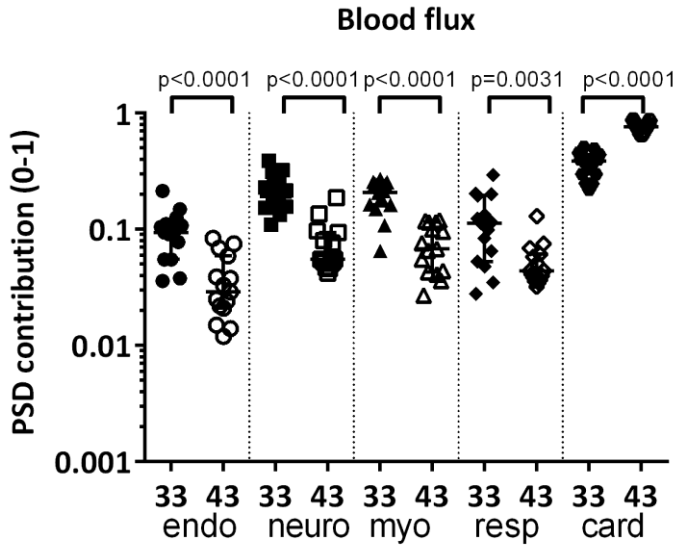

Figure 5.10 PSD contributions in BF signal across five frequency bands at 33°C and 43°C. Temperature-induced vasodilation caused a significant change in all contributions. The greatest change was the increase in contribution from the cardiac band (0.37 at 33°C vs 0.76 at 43°C). All other frequency bands showed a decrease. n=15.

SO_2 showed a different pattern in PSD contribution when compared to BF. Figure 5.11 shows there was a higher contribution at 33°C from endothelial and neurogenic bands and lower contribution from higher frequency bands. At 43°C the cardiac band gained more relative power at the expense of all other bands. The pattern of other bands contributions was sustained; there was no clear shift from one particular band to the other.

The PSD profiles shown in the previous section illustrated that total power of the SO_2 signal was reduced during warming at 43°C, compared to 33°C. Furthermore, the absolute power in respiratory and cardiac bands was negligible. However, the PSD contribution showed the increase in cardiac and respiratory bands during warming. The PSD contribution is a ratio and it does not account for the absolute power. The sum of PSD contributions across all frequency bands always equals one. The increase of PSD contribution from the cardiac band indicates that despite the overall reduction in spectral power, the intensity of cardiac activity in relation to other activities increased.

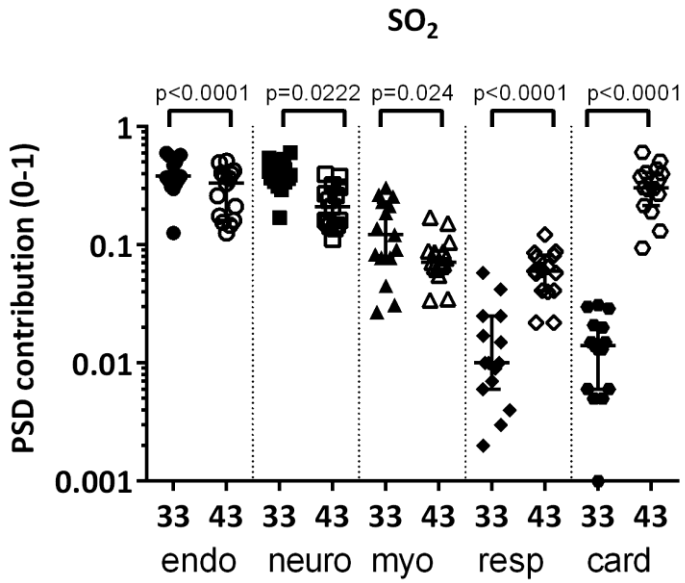

Figure 5.11 PSD contributions in SO_2 signal across five frequency bands at 33°C and 43°C. At 33°C the contributions from respiratory and cardiac bands were negligible. Temperature-induced vasodilation caused a significant increase in contribution from the cardiac band (0.01 at 33°C vs 0.33 at 43°C). There was also an increase in respiratory band (0.02 at 33°C vs 0.06 at 43°C) and the decrease in endothelial, neurogenic and myogenic bands. n=15.

Similarly to the SO_2 signal, the Hb signals contained most power in the endothelial and neurogenic bands at 33°C (OxyHb – 80%, DeoxyHb – 81%, TotalHb – 78%), and little power in the respiratory and cardiac bands as depicted in Figure 5.12. At 43°C, there was a shift in frequency contribution to the cardiac band. During warming the cardiac activity became a dominant activity in relation to endothelial, neurogenic, myogenic and respiratory activities.

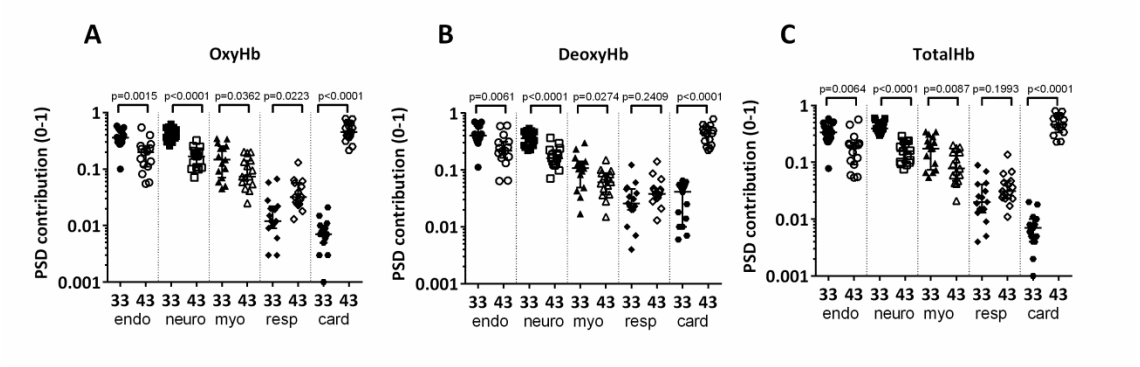

Figure 5.12 PSD contribution in (A) OxyHb, (B) DeoxyHb, (C) TotalHb across five frequency bands at 33°C and 43°C. At 33°C the contributions from respiratory and cardiac bands were negligible. Temperature-induced vasodilation caused a significant increase in contribution from the cardiac band. n=15.

5.2 Discussion

The aim of this study was to determine whether the characteristics of OXY parameters are related to the characteristics of BF at a standardised resting skin temperature of 33°C and during steady state vasodilation induced by local skin warming to 43°C which has been previously shown to increase both BF and SO_2 signals in the time- and frequency- domains. The main findings were related to the significant differences between PSD profiles of BF and OXY signals. The results highlighted that warming to 43°C changed the relative contributions of five physiological activities embedded in BF and OXY signals in similar way for BF and OXY signals. All signals showed an increase in the cardiac PSD accompanied by the reduced contribution from LF bands (endothelial, neurogenic and myogenic). However, the analysis of the absolute total power showed dissociation between BF and OXY signals during warming to 43°C. In the engineering context, the changes in the absolute signal power indicate changes in the oscillatory components of the signals. These oscillatory components attributed to physiological activities serve as a tool in studying biological mechanisms involved in regulation of blood flow and oxygenation during rest and thermally-induced vasodilation.

The discussion of the findings focuses on available literature that relates to the response of BF and OXY signals to local warming, time- and frequency-domain analysis and their meaning and importance for clinical assessment.

5.2.1 The Gap in the Body of Knowledge in Simultaneously Measured BF and OXY Signals

The measurements of tissue oxygenation (in various tissues) create a rapidly growing field with over 200 papers published a year. NIRS combined with DCS can provide information on cerebral blood flow and oxygenation. In 2014 Boas et al. (2014) published a review on NIRS as a tool to study brain haemodynamics. Another review published by Ferrari et al. (2011) explored NIRS as a tool to study oxygenation in muscle tissue. Overall, there is an increasing interest in using NIRS to study oxygenation dynamics in deeper tissues. Although these studies extend the knowledge of the physiology of brain and muscle, they do not apply directly to skin tissue. It may be beneficial to learn from studies performed with NIRS but the dynamics between BF and SO_2 in skin will differ from those in brain or muscle.

To date, research groups conducting simultaneous BF and OXY measurements in skin, focused mostly on analysis of resting BF and OXY signals (Thorn et al., 2011; Dunaev et al., 2014). Thorn et al. (2011) investigated skin blood flow and oxygenation during rest, whilst Dunaev et al. (2014) studied BF and SO_2 at rest and in response to adaptive changes such as exercise. The study by Messere & Roatta (2013) looked at the influence of skin microcirculation on muscle microcirculation measurements using NIRS. They observed a gradual increase in totalHb in response to local warming resulting from increased microcirculation in skin and muscles. However, they did not observe an increase in total oxygenation index (in this thesis called tissue oxygenation or SO_2). The main focus of their work was the influence of cutaneous circulation on NIRS measurements and the above findings were only secondary observations. They did not explore skin oxygenation further (Messere & Roatta, 2013).

In essence, there is a gap in the body of knowledge in regards to simultaneous measurements of BF and OXY signals in skin, in particular in response to perturbations such as local skin warming. There are no studies reporting and comparing frequency components of BF and OXY signals at rest and during thermally induced vasodilation. The findings from Study 2 discussed below provide an exciting starting point for further research.

5.2.2 Response to Local Skin Warming

In response to local warming BF and OXY signals increased multifold. It was expected as the response of skin BF to warming challenge has been extensively studied in the time-domain. Single step warming to 42-44°C is characterised by biphasic response with the early peak

occurring shortly after warming (within a few minutes) followed by a sustained rising plateau after approx. 15min (Kellogg, 2006; Minson, 2010; Vionnet et al., 2014). The thermally-induced vasodilation results in the multifold increase from resting value. Del Pozzi & Hodges (2014) reported the increase in forearm BF from 11 PU at baseline to 219 PU after warming to 42°C for 35min. The results presented in this work agree with work by Del Pozzi & Hodges (2014) and extend the findings by presenting the response of OXY signals in addition to BF signals.

The large increase in BF induced by local warming caused an increase in OXY parameters. The simultaneous substantial increase in oxyHb indicated the maximum amount of oxyHb that can be delivered with increased BF. The increase in oxyHb was not accompanied by a corresponding increase in deoxyHb. DeoxyHb showed only a small increase resulting from more vessels being recruited (perfused) during warmed measurements. At rest, skin maintains constant oxygen consumption (deoxyHb is constant) and it is perfused with excess of oxygen (the metabolic rate of skin is low compared to other tissues and the main function of skin is thermoregulation which does not require high oxygen consumption). During vasodilation the oxygen consumption may increase due to increased activity of smooth muscles around blood vessels, but this increase is not substantial.

From an engineering perspective, the measurements of oxyHb and deoxyHb reflect the amount of light absorbed by the molecules of oxygenated and deoxygenated haemoglobin. The increase in oxyHb and deoxyHb signals results from a higher number of these molecules present in the sampled volume. As a result of the thermally induces vasodilation, more blood vessels were perfused and therefore the overall amount of haemoglobin was higher and the absorption of light increased. The optical measurements of oxyHb and deoxyHb inform about the relative amount of these components in the tissue, which in combination with measurement of BF provide assessment of tissue perfusion, available oxygen (oxyHb) and tissue metabolism (deoxyHb).

5.2.3 Correlations in Time-Domain

Resting and maximal BF and SO_2 were found to be positively correlated. It was an expected result and it is in agreement with Study 1 which has been already published (Kuliga et al., 2014). However, the previously published measurements were recorded at subjects' physiological temperatures which varied between 24.7-32.9°C. The purpose of setting the temperature to 33°C in Study 2, was to reduce the effect of individual resting skin temperature and the inter-subject variability. A temperature of 33°C has been shown to be a neutral

temperature and not to perturb the physiological blood flow. The positive correlation at 33°C between BF and SO_2 confirmed that, in healthy population BF and SO_2 are linearly related. This implies that the resting level of BF and SO_2 measured at 33°C is an individual characteristic for every person. Further results also indicated the linear relationship between BF and SO_2 during warming to 43°C. The SO_2 measurements at 43°C were expected to be within the flat part of the BF-SO_2 relationship presented in Chapter 4 (Figure 4.1, p.69) and it was expected that at 43°C SO_2 measurements will not correlate with BF measurements. Interestingly, the linear relationship between BF and SO_2 was stronger at 43°C compared to 33°C). However, in Study 1 the measurements were collected from the diverse group of healthy subjects (male and female, age range: 21-60) and warming protocol was different. The results from Study 2 come from a carefully selected, uniform group of healthy men and can be considered a stronger evidence of linear relationship between BF and SO_2 during local warming to 43°C than warming measurements from Study 1.

The correlations between SO_2 and Hb parameters showed a strong link between maximum SO_2 and maximum oxyHb, deoxyHb and totalHb. This implies, the higher the amount of oxyHb, deoxyHb or both, the higher maximal SO_2. However, at neutral temperature of 33°C only oxyHb was significantly correlated with resting SO_2. It may be that the totalHb would be a better predictor of SO_2, assuming the higher haemoglobin status provides higher tissue oxygenation.

An interesting finding was the resting oxyHb correlated with deoxyHb (r^2=0.30, p=0.0351). These two reflect the delivery of oxygen (oxyHb) and the tissue oxygen utilisation (deoxyHb). The oxygen consumption and, resulting from it, deoxyHb does not depend on the amount of available oxyHb but on tissue metabolism. Therefore, it may be that resting oxyHb and deoxyHb are characteristic for each person and relate to the individual metabolism and continuous homeostasis.

5.2.4 Lack of Correlations between Absolute Signal Power at 33°C and at 43°C

There were no significant correlations in any signal between absolute power at 33°C and absolute power at 43°C. These findings indicate that the power of the spontaneous oscillations at 43°C does not reflect the power of the oscillations at 33°C. Resting and thermally induced vasodilation are two distinct physiological states and the change in spontaneous oscillation in response to warming is not directly related to the spontaneous oscillations at rest. The relative contributions from endothelial, neurogenic, myogenic, respiratory and cardiac bands show

different patterns at resting and warming as discussed earlier in this chapter. The lack of correlation between the absolute power at 33°C and 43°C implies that some of the resting markers of microvascular function such as the absolute power of the signal cannot approximate the signal characteristics at 43°C.

The absolute power of the BF and SO_2 signals at rest from Study 1 reported in Chapter 4 did not differ from the absolute power of the BF and SO_2 signals obtained from Study 2 presented in this chapter. Median (IQR) absolute powers are presented in Table 5.5. The differences between studies were tested with the Mann-Whitney test. The results from both studies were consistent.

Table 5.5 Median (IQR) total power of BF and SO_2 signals in Study 1 and Study 2.

	Study 1	Study 2
Total power of BF signal (PU^2), median (IQR)	3.16 (1.84-5.86)	4.4 (2.1-6.8)
Total power of SO_2 signal (AU^2), median (IQR)	13.95 (8.85-27.06)	8.2 (3.5–21)

5.2.5 Differences in Frequency Content of BF and OXY Signals at 33°C and during Warming to 43°C

Study 1 presented in Chapter 4 has shown that at rest at ambient skin temperature, there is less power in the higher frequencies in OXY signals compared to lower frequencies. Thus, the analysis was focused on LF bands only. However, the PSD profiles of warmed signals in Study 2 revealed an increase in PSD in cardiac frequency band, which represents a HF.

This research is the first to discuss the low frequency oscillations in simultaneously recorded BF and OXY parameters during a temperature-neutral state and temperature induced vasodilation in skin. The characteristics of BF signals have been studied extensively by other research groups (Stefanovska et al., 1999; Kvandal et al., 2006) reporting a number of different signal characteristics. Two of the relevant characteristics are total power of the signal and relative power contribution from endothelial, neurogenic and myogenic bands. However, there are no studies reporting spectral analysis of simultaneously recorded BF and OXY signals during rest and warming to 43°C.

Study 2 presented in this Chapter reported the increase in BF signal power during maximal vasodilation. It is in agreement with other studies investigating thermally induced vasodilation and reporting increased signal power during vasodilatation (Stefanovska et al., 1999; Kvandal et al., 2003; Geyer et al., 2004; Kvandal et al., 2006; Sheppard et al., 2011). Recently, Dunaev et al. (2014) has undertaken spectral analysis of BF and oxygenation signals. They reported synchronisation between vasomotion in BF and SO_2 only within the myogenic band during rest. The study by Dunaev et al. (2014) sheds some light on the dynamics between BF and OXY signals at rest, but its main focus was on oxygen consumption during adaptive changes (sport, PORH). They did not measure these signals under thermal vasodilation challenge. Furthermore, they did not analyse Hb signals separately. They only reported on BF and SO_2 signals (Dunaev et al., 2014). On the other hand, the work conducted in this thesis investigates the oscillations in OXY parameters within the frequency bands known for BF oscillations and how these oscillations change during thermally induced vasodilation.

The total power for BF and SO_2 signals did not differ at 33°C, but oxyHb, deoxyHb and totalHb exhibited lower total signal power compared to BF and SO_2. DeoxyHb signal showed the lowest total power indicating the oscillations within the deoxyHb signal have the lowest amplitude. The oscillations in Hb signals are related to oscillations in BF (Thorn et al., 2009; Thorn et al., 2011; Dunaev et al., 2014) but the exact mechanisms linking these oscillations are not yet understood. The increased power of the BF signal during warming denotes increased fluctuations in BF signal. The increased fluctuations can be interpreted as intensified physiological activities related to these oscillations. Alternatively, the reduction in SO_2 signal power during warming indicates weaker oscillation in the SO_2 signal. Interestingly, the power of Hb signals does not change during warming, confirming the oscillations in OXY signals do not disappear but change their dynamics. By definition, the SO_2 signal is the ratio between oxyHb and totalHb (oxyHb + deoxyHb) therefore if oxyHb and deoxyHb increases at the same time by the same amount, SO_2 will not change. At maximal vasodilation SO_2 signal is at a maximum value of ~80% and the oscillations are greatly attenuated as reflected in reduced SO_2 signal power.

Power spectral density plots illustrated the individual and mean spectra for fifteen healthy men obtained from 600 s long measurements at 33°C and 600 s long measurements during thermally induced vasodilation at 43°C. None of the spectra exhibited clear, single peaks within assumed frequency bands except the cardiac band. The overall shape was smooth indicating the measured signals were complex and comprised multiple component frequencies or that

these component frequencies were continuously changing. PSD spectra of BF showed an increase in all frequency bands during vasodilation. The peak within the cardiac band became more pronounced, indicating the measurements were detecting a stronger heartbeat signal. SO_2 signal showed an opposite behaviour – maximal vasodilation caused a substantial reduction in power across all frequency bands. As previously reported, the power in higher frequency bands (respiratory and cardiac) at rest was low (Kuliga et al., 2014) indicating the SO_2 signal was weakly modulated by respiration and heartbeat. Vasodilation reduced the modulation by respiration and heartbeat further. Although the borders of frequency bands associated with physiological frequencies have been widely used, they should be considered as approximate borders. These bands may vary between individuals, but in order to maintain consistent analysis they have been assumed to be the same across healthy volunteers.

PSD spectra of Hb signals disclosed interesting dynamics. The power in low frequencies at maximal vasodilation remained unchanged compared to the power at 33°C. Interestingly, the peak in cardiac frequency was intensified at the vasodilation. Despite the heartbeat being weak in resting Hb signals, it became visible during warming. In particular, the cardiac peak was absent in the deoxyHb signal at rest, but during vasodilation it was clearly pronounced. This implies the thermally induced vasodilation enhances the conductance of the heartbeat wave further down the system of circulation and microcirculation, so that it is also pronounced in venous compartment of the vasculature. The healthy blood vessels are flexible and able to distend with high fidelity in response to mechanical force from the heart. In response to local warming, the vessels dilate and allow more blood to pass through the microvasculature. It may be that stiff, calcified vessels during vasodilation do not exhibit the heartbeat peak due to the loss of flexibility caused by vascular calcification. If that is the case, the analysis of PSD spectra of deoxyHb signal during vasodilation may be an early indicator of vascular stiffness. Further studies exploring this idea need to be conducted to confirm or reject this hypothesis. By examining whether the power of the cardiac band in deoxyHb signal during vasodilation correlates with vessel stiffness, a new characteristic may be identified and perhaps a simple test can be developed to assess the vessel stiffness based on the microvascular response to local warming.

5.2.6 PSD Contributions as Signal Characteristics

Results presented in this Chapter extend the analysis of spontaneous oscillations presented in Chapter 4 which were performed only for resting signals. The low power of the warmed SO_2

signal may reflect the physiological state of tissue saturation with oxygen. During warming, skin perfusion increases to dissipate the heat but at the same time it delivers more oxygen, which is not required by the tissue. Therefore the fluctuations in tissue oxygenation are diminished.

The results presented in this thesis showed a decrease in relative power in endothelial, neurogenic and myogenic bands during warming compared to relative power at rest. At the same time, during warming there was a higher contribution from the cardiac band. These are contradictory findings to research published by Geyer et al. (2004). They reported an increase in the normalised power of BF signal of the endothelial and neurogenic bands and the decrease in the normalised power of the myogenic band in healthy subjects (Geyer et al., 2004). However, the findings presented by Geyer et al. (2004) cannot be directly compared to the findings reported here as they used a different heating procedure with 3 min at 35°C followed by increase in temperature 1°C/min and final period of 3 min at 45°C. They did not collect data during a sustained vasodilation. Different heating regimes induce different responses of physiological activities reflected in BF signal (Del Pozzi et al., 2016) and should not be directly compared. Further research is needed to explain the differences in these findings.

de Jongh et al. (2008) have reported altered power contribution from the endothelial and neurogenic band and reduced total energy density in obese women compared to lean women. Their findings implied that the differences in microvascular blood flow control can be related to obesity and subsequently to the increased risk of microvascular dysfunction. Perhaps the differences in microvascular blood flow control induced by obesity can manifest the presence of microvascular dysfunction at an early stage. However, de Jongh et al. (2008) did not normalise the reported findings and therefore those findings are difficult to interpret and could lead to incorrect conclusions. Another study by Vinet et al. (2015) investigating subjects with the metabolic syndrome, found the overall reduction in the flowmotion compared to controls. Rossi et al. (2005b) showed an insulin induced increase in power density in the myogenic band, but Vinet et al. (2015) reported contradictory findings related to insulin-induced change in power density of the myogenic component. To date, there is not enough evidence to confirm how the PSD contributions from different bands are affected by the microvascular dysfunction or other related condition. Larger studies in well-defined subject groups are required to establish the link between different flowmotion patterns and the dysfunction status or disease symptoms.

In the study presented in this thesis, there were no significant differences in the distribution of PSD contribution at 33°C and 43°C in endothelial, neurogenic and myogenic bands when looking at the whole study cohort. This means that in response to warming challenge, healthy tissue is able to maintain the same ratio of the oscillatory processes within endothelial, neurogenic and myogenic bands. The physiological response to local warming involves complex mechanisms including sympathetic responses and multiple signalling pathways releasing number of molecules acting on different receptors. Despite high complexity at the molecular level, PSD contributions from endothelial, neurogenic and myogenic bands stayed the same at rest and during warming.

5.2.7 Variability in Responses and Individual Changes in Oscillations Induced by Warming to 43°C

The differences in PSD contributions across low frequency bands exhibited wide variation between individuals. The vasodilation enhanced blood flux oscillations and attenuated SO_2 oscillations. The increase in variance indicated an increase in deviations of components of the signal from its mean value. However, the variance is an overall measure of the amplitude changes in the signal and it does not provide information about oscillations at different frequencies which are associated with the physiological activities such as endothelial, neurogenic, etc. During local warming the number of the perfused vessels in the same volume of tissue is larger. It is not clear whether the fluctuations across individual vessels are in phase or antiphase as the BF-OXY probe cannot resolve the signal from separate vessels. However, if the fluctuations had opposite phases, they would cancel out each other and result in lower output.

The variability is a common problem in studies investigating LDF responses in both time- and frequency-domains. In the time-domain, often the absolute values do not show differences between controls and the cohorts with microvascular dysfunction, indicating that natural variability is high and each person may have individual borders of healthy BF. To overcome this challenge, researchers look at relative changes for example the difference between maximal BF during hyperaemia and the resting BF. Similarly, in the frequency-domain, the PSD analysis exhibited wide variability in the healthy population. It is therefore less probable to find differences and it is not clear how to interpret the findings. The possible solution can be to analyse the change in PSD contributions in response to the stimulus.

Analysing the change in PSD induced by warming at the individual level may reveal some patterns. Figure 5.13 illustrates individual changes in PSD in endothelial, neurogenic and myogenic bands for BF signals induced by warming. The PSD at 33°C is marked as a starting circle and the arrow depict the direction (increase or decrease) and the magnitude of a change. Each colour corresponds to different subject. The smallest change was observed in neurogenic band with almost all individuals exhibiting a change of less than 0.05 implying that the neurogenic component of microvascular control remained the same at 33°C and at 43°C. The changes in endothelial and myogenic bands were more apparent, however they went in both directions: some individuals exhibited an increase and others a decrease in PSD contribution during warming. The lack of uniform behaviour or clear trends in this demographically uniform group of young and healthy men suggests the human microvascular control is a complex process and the PSD analysis alone cannot sufficiently describe it. The multiple biological processes driving the thermoregulation interact and influence each other aiming to preserve the balance in overall control. Based on PSD contribution analysis, the microvascular response to local warming promotes endothelial, neurogenic and myogenic activities with similar strength. In healthy skin these activities are modulated and result in sustained contribution from each band. Perhaps, the microcirculation with abnormalities will promote a particular frequency band to compensate for the dysfunction within other bands.

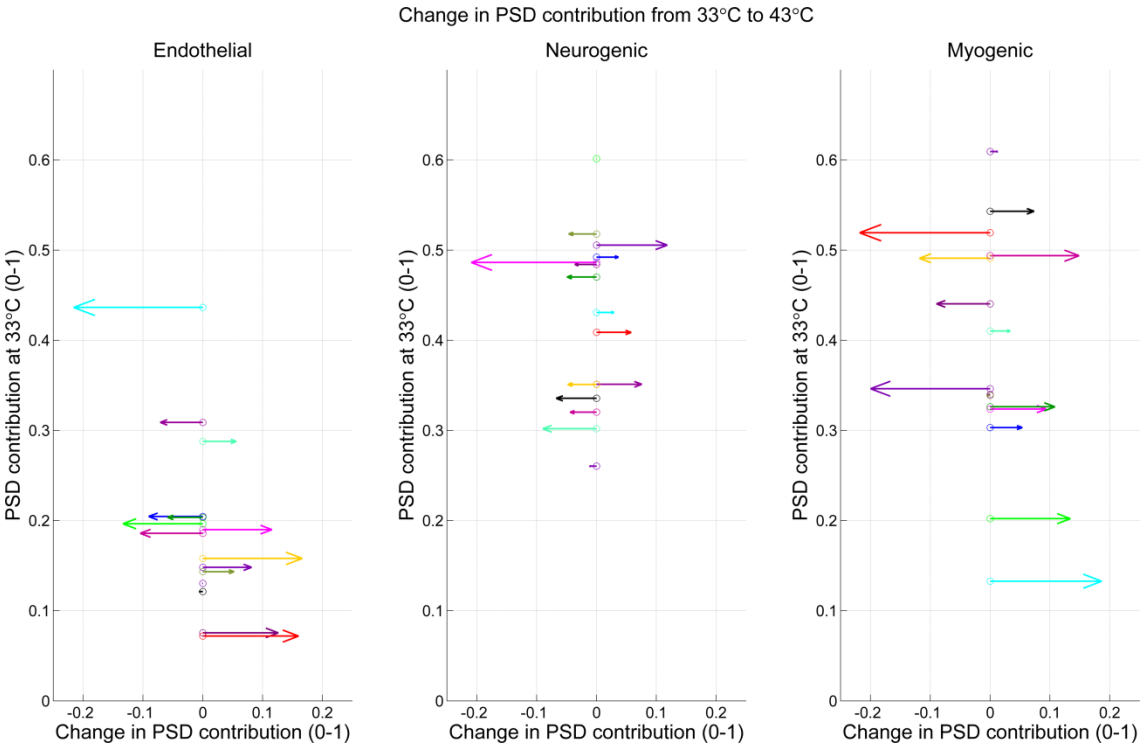

Figure 5.13 Individual changes in BF PSD contributions between 33°C and 43°C across endothelilal, neurogenic and myogenic bands (n=15).

Time-domain and frequency-domain analysis of BF and OXY signals presented in this Chapter showed weaknesses of LDF-WLS measurements. The main limitation is the variability of measurements observed in healthy population. Furthermore, the signal processing methods used to extract specific information about the signals such as PSD across different frequency bands, did not find consistent pattern across the data. Thus, without further understanding or improvement in LDF-OXY data acquisition and analysis the information provided by these measurements is limited and unclear. The individual changes in PSD contributions shown in Figure 5.13 illustrate the variability in responses in carefully selected healthy population. It was expected to find a similar pattern across volunteers showing how does the PSD contribution change in response to local warming. However, the results showed the PSD contributions across LF bands change in both directions, without any clustering. Consequently, no conclusions can be drawn from these analyses. There are some characteristics of LDF-OXY measurements, which have been demonstrated to show different responses associated with multiple risk factors e.g. smoking or diabetes (e.g. PORH test) however the findings are contradictory (Fredriksson 2010) and not clearly indicative of specific disease.

Another constrain of frequency analysis are the definitions of frequency bands as presented in table 2.3. They have their origin in studies performed over 15 years ago by Stefanovska et al. (1999). Since then these bands have been freely accepted by other research groups and quoted in research associated with blood flowmotion, assuming the limits of frequency bands are precise and correct, and can be applied to any population. These frequency bands shall be considered as approximation rather than precise ranges; further studies should aim to investigate the variability in frequency bands and to establish the methodology for identifying the accurate borders of frequency bands. Possibly, these borders can be an individual characteristic for each person and should be incorporated into frequency-domain analysis.

LDF and WLS have a great advantage of providing a non-invasive assessment of microcirculation. However, these techniques have some disadvantages too. They provide relative measurements, which at the moment cannot be converted into absolute units. Furthermore, the individual optical properties of the tissue are not assessed during measurements – the algorithm for conversion of the optical signal into digital signal assumes certain optical properties based on experimental and modelling data, however the individual optical properties of measured skin tissue are not known. The measurements are susceptible to movements' artefacts; therefore they can only be performed in stationery settings. The measurement volume is approx. $1mm^3$ which may be inadequate to account for the heterogeneity of the skin. The reproducibility measurements presented here were performed on two different days paying much attention to record measurement from the same site, however practically it is an inconvenient requirement. Moreover, the resting measurements vary substantially between subjects; consequently large n numbers are needed to perform adequately powered studies.

5.2.8 An Increasing Trend in absolute value of BF and OXY during Local Skin Warming

Study 2 showed BF and OXY signals were continuously increasing towards the end of 25 min of warming to 43°C suggesting the increasing trend may continue. The increase in Hb parameters resulted from the increase in BF so the total volume of blood in the sampled volume also increased. The studies reporting BF during warming normally use 30-40 min of warming (Jan et al., 2013; Esen et al., 2014; Hodges & Del Pozzi, 2014; Stanhewicz et al., 2014), but they did not bring attention to the constant increase towards the end. They have not reported it but it can be seen e.g. in the raw data presented in the paper by Jan et al. (2013). During sustained warming NO is released continuously. It may be that, the accumulation of NO is an ongoing

process slowly acting on the vessels' walls. After 30 min the limit/maximal concentration of NO production is not reached and it is reflected in the continuous increase in BF and Hb parameters.

The steady increase in BF and Hb parameters indicate that even after 25 min of continuous warming, the perfusion of the tissue and subsequently the amount of Hb are still increasing. Thus, when discussing different studies, it is important to note how long the site has been warmed before taking the measurement. The steady increase in BF and Hb signals observed in Study 2 is important in comparison of time-domain results with other studies, but it has no influence on the frequency analysis as all signals were detrended during pre-processing so that, the increasing trend was removed.

5.3 Summary and Contributions to the Body of Knowledge

The study presented in this chapter extended the findings discussed in the previous chapter. It aimed to explore how the physiological oscillation present in the BF and OXY signals responded to thermally induced vasodilation. The analysis presented in this chapter identified the differences in frequency components in BF and OXY signals at 33°C and during local skin warming to 43°C. The warming did not induce changes in PSD contributions across low frequency bands suggesting the microvascular control during thermally-induced vasodilation in healthy skin is sustained by complex interaction between component activities. In response to the thermally induced vasodilation, the overall BF oscillations expressed as absolute power of the signal increased, but SO_2 oscillations decreased. The absolute power of the oxyHb and totalHb signals did not change but the power of the deoxyHb signals decreased.

The relative contributions across cardiac frequency band changed in response to thermally induced vasodilation – all signals exhibited an increased contribution from cardiac band at the cost of low frequency bands (endothelial, neurogenic and myogenic). This means, that the oscillations in microcirculatory blood flux, originating from the heartbeat, has higher intensity during warming. Therefore, the microcirculatory perfusion during warming depends in the higher degree on the heartbeat compared to microcirculatory perfusion at rest which is controlled by more equally by low frequency bands. Consequently, it may be possible to use local warming as a test of interaction between micro- and macro- circulations.

The cardiac wave was absent in OXY signals at rest but became visible during steady state vasodilation. This can perhaps be utilised to develop a new, non-invasive technique for assessment of the calcified blood vessels.

The analysis undertaken in this chapter investigated multiple frequency characteristics of the BF and OXY signals, but focused on each signal separately. The next step will be to investigate further the relationship between BF and OXY signals in time- and frequency- domains in order to better understand the dynamics of microvascular BF and oxygenation. Chapter 6 presents and discusses the frequency coherence and the delay between BF and OXY signals.

Chapter 6

Towards Understanding Dynamics between LDF and OXY Signals

Chapter 5 investigated the effect of local warming on physiological oscillation embedded in BF and OXY signals. The results revealed the changes in the absolute power and the relative contribution from endothelial, neurogenic, myogenic, respiratory and cardiac bands in response to local warming. These characteristics and changes induced by local warming were analysed separately for each signal. This chapter aims to investigate the link between BF and OXY signal.

Figure 6.1 illustrates the simplified system investigated in this thesis. The changes in the tissue oxygenation are influenced by multiple factors but they also depend on the microcirculatory blood flux. The overall tissue homeostasis is the result of numerous control and signalling mechanisms occurring continuously at different levels of microcirculation, e.g. tissue hypoxia triggers vasodilation and subsequently increases blood flux. The analysis presented in this Chapter is focused on the frequency coherence and delay estimation. It aims to answer the question, what is the frequency coherence and the delay between BF and OXY signals in healthy skin and how should they be interpreted?

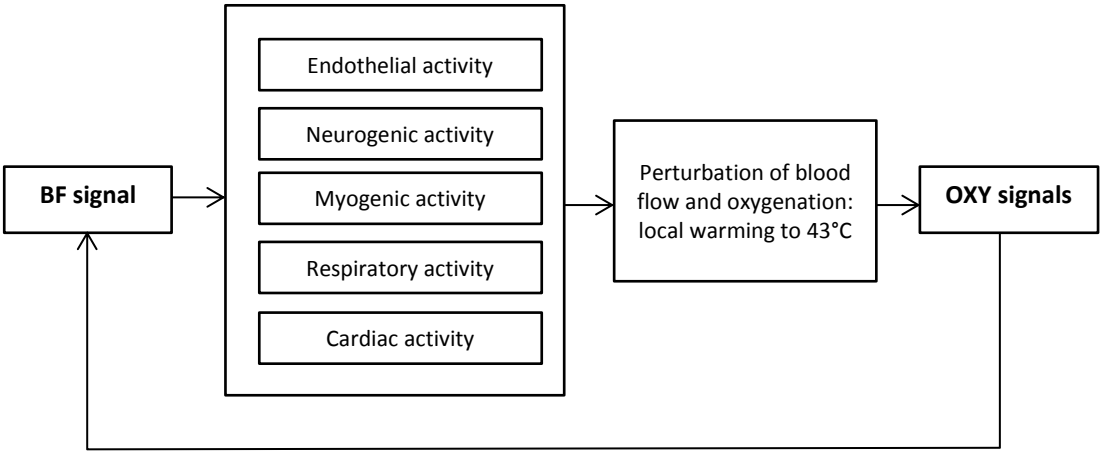

Figure 6.1 Simplified block diagram of relationship between BF and OXY signals. Changes in BF signal in response to the physiological control mechanisms and/or external perturbations induce changes in OXY signals. Changes in OXY signals influence BF signal and create and continuous feedback loop. This also happen in the reverse direction where OXY signals in response to the physiological control mechanisms and/or external perturbations induce changes in BF signals.

Frequency coherence (FC) is a measure of similarity between the oscillatory content of the signals at a given frequency. It has often been used to study various biomedical signals (Ropella et al., 1989; Clayton & Murray, 1999). Some examples include studies focusing on the coherence between the ECG signals (Clayton & Murray, 1999; Pachauri & Mishra, 2012) and neurophysiological signals (Miranda de Sá et al., 2002; Pereda et al., 2005; Simpson et al., 2005) showing some synchronicity between the signals. Knowledge about the synchronicity, or lack of it, helps to understand physiological phenomena driving these signals. The studies investigating the frequency coherence aim to determine the oscillatory coupling between two or more signals. The frequency coherence can be computed for all frequency components in the signals or for particular frequency bands. BF and OXY signals exhibit oscillatory behaviour as described in Chapter 4 and Chapter 5. The power density spectra of these signals have a similar shape indicating a significant agreement in the oscillatory components. However, these similarities or coupling have not yet been quantified and described. The work presented below is an important step towards understanding these couplings in the skin microcirculation by extending current analysis techniques to include the analysis of frequency coherence and time delay between signals.

The frequency coherence between resting BF SO_2 signal has been briefly discussed in Chapter 4. Nevertheless, the analysis was only conducted for resting BF and SO_2. This chapter extends

the analysis to other signal pairs such as BF-oxyHb, BF-deoxyHb and BF-totalHb. Furthermore, the analysis is performed on resting and warmed signals obtained from the well-defined group of subjects as described in Chapter 5. The analysis will help to identify how the coherence and delay between BF and OXY signals are influenced by thermally induced vasodilation.

6.1 Results

The results presented below explore the frequency coherence and time delay between BF and OXY signals acquired from the cohort of 15 healthy male subject described as Study 2 in detail in Chapter 5. The principles of coherence and delay estimation have been described in Chapter 3.

6.1.1 Frequency Coherence

The full summary of results (mean and SD) at 33°C for all signals pairs (BF-SO2, BF-oxyHb, BF-deoxyHb, and BF-totalHb) is shown in Table 6.1. Frequency coherence values at 33°C and at 43°C are summarised in

Table 6.3, Table 6.4 and

Table 6.5.The values in bold indicate the highest frequency coherence between different pairs of signals.

Table 6.1 Frequency coherence between different signals pairs at 33°C.

	Endothelial		Neurogenic		Myogenic		Respiratory		cardiac	
	mean	SD	mean	SD	mean	SD	mean	SD	mean	SD
BF-SO_2	**0.82**	0.07	**0.54**	0.16	**0.44**	0.20	0.13	0.04	0.15	0.04
BF-oxyHb	0.79	0.06	0.50	0.19	0.42	0.20	0.17	0.09	0.19	0.06
BF-deoxyHb	0.78	0.07	0.35	0.18	0.28	0.13	0.17	0.11	0.13	0.03
BF-totalHb	0.76	0.08	0.41	0.20	0.38	0.20	**0.18**	0.12	**0.21**	0.05

At 33°C, BF-SO_2 showed the highest coherence within endothelial, neurogenic and myogenic bands compared to other signals pairs (BF-oxyHb, BF-deoxyHb and BF-totalHb).

During warming to 43°C the coherence between BF-SO_2 dropped compared to the coherence between BF-SO_2 at 33°C. It became the highest for BF-totalHb in endothelial 0.79(0.07) and neurogenic bands 0.52(0.19), whilst BF-oxyHb exhibited highest coherence in myogenic band 0.46(0.11) compared to other signals pairs. The respiratory band showed the lowest coherence. Interestingly, the coherence in cardiac band at 43°C increased compared to 33°C. The summary of results at forearm warming to 43°C for all signals pairs (BF-oxyHb, BF-deoxyHb, and BF-totalHb) is shown in Table 6.2.

Table 6.2 Frequency coherence between different signals pairs at 43°C.

	Endothelial		Neurogenic		Myogenic		Respiratory		Cardiac	
	mean	SD	mean	SD	mean	SD	mean	SD	mean	SD
BF-SO_2	0.72	0.06	0.38	0.10	0.28	0.09	0.14	0.04	0.21	0.06
BF-oxyHb	0.78	0.07	0.51	0.19	**0.46**	0.11	**0.22**	0.05	0.46	0.09
BF-deoxyHb	0.75	0.07	0.42	0.17	0.31	0.15	0.16	0.05	0.35	0.08
BF-totalHb	**0.79**	0.07	**0.52**	0.19	0.44	0.11	**0.22**	0.05	**0.47**	0.09

Table 6.3 Frequency coherence between forearm SO_2-oxyHb at 33°C and 43°C.

	Endothelial		Neurogenic		Myogenic		Respiratory		Cardiac	
	mean	SD	mean	SD	mean	SD	mean	SD	mean	SD
at 33°C	**0.97**	0.02	**0.91**	0.05	**0.93**	0.04	**0.73**	0.11	**0.77**	0.08
at 43°C	0.82	0.08	0.67	0.13	0.52	0.16	0.39	0.15	0.42	0.11

Table 6.4 Frequency coherence between forearm SO_2-deoxyHb at 33°C and 43°C.

	Endothelial		Neurogenic		Myogenic		Respiratory		Cardiac	
	mean	SD	mean	SD	mean	SD	mean	SD	mean	SD
at 33°C	0.75	0.11	0.37	0.18	**0.34**	0.19	0.19	0.06	**0.58**	0.10
at 43°C	**0.77**	0.10	**0.56**	0.10	0.25	0.09	**0.32**	0.13	0.47	0.09

Table 6.5 Frequency coherence between forearm SO_2-totalHb at 33°C and 43°C.

	Endothelial		Neurogenic		Myogenic		Respiratory		Cardiac	
	mean	SD	mean	SD	mean	SD	mean	SD	mean	SD
at 33°C	**0.85**	0.09	**0.73**	0.14	**0.77**	0.12	**0.34**	0.09	0.16	0.04
at 43°C	0.77	0.08	0.62	0.14	0.44	0.17	0.23	0.13	**0.23**	0.08

The comparison of frequency coherence between OXY signal pairs: SO_2-oxyHb, SO_2-deoxyHb and SO_2-totalHb identified that oxyHb exhibited the highest coherence with SO_2, suggesting the measure of SO_2 is mostly driven by oxyHb. This is discussed in more detail in section 6.2.

6.1.2 Delay Estimation

Sensitivity analysis was performed to determine the robustness of the cross-covariance threshold value used for delay estimation. From the available data, a threshold value of 0.3 was the most suitable determinant of the number of correctly classified delays (<10s) with respect for number of cases qualified for analysis (satisfying the threshold value). The incorrect alignment of signals results in artificially high delays, therefore the delays >10 s were considered incorrect and excluded from analysis. The total number of volunteers (cases) was 15. Table 6.6 shows for each signal pair (BF-SO_2, BF-oxyHb and BF-deoxyHb) the number of cases meeting the threshold value and number of cases which met the threshold value but should be excluded from analysis due to delay value >10 s. At the lowest threshold value of 0.1 all cases met the condition of threshold, however 9 cases were incorrect due delay >10 s. At threshold value 0.2, 38 cases met threshold and 4 cases were incorrectly classified. Threshold of 0.3 showed that 31 cases met threshold and only one case was incorrect. Higher values of threshold (0.4 and 0.5) resulted in lower number of cases meeting the threshold value and therefore reducing the power of analysis. In conclusion, the threshold value of 0.3 was found

most pragmatic for the datasets considered here to maximise number of cases included in delay analysis.

Table 6.6 Influence of min cross-covariance threshold on number of cases included in delay analysis.

	BF-SO_2		BF-oxyHb		BF-totalHb	
Min cross-covariance threshold	No. of cases meeting threshold	Excluded by too high delay >10s	No. of cases meeting threshold	Excluded by too high delay >10s	No. of cases meeting threshold	Excluded by too high delay >10s
0.1	15	3	15	2	15	4
0.2	14	2	12	0	12	2
0.3	12	0	10	0	9	1
0.4	9	0	9	0	5	0
0.5	5	0	4	0	2	0

For the BF-SO_2 pair, three subjects did not meet the cross-covariance criteria for alignment. For BF-oxyHb, four subjects were below the 0.3 threshold and for BF-totalHb five. DeoxyHb exhibited the lowest oscillations and these oscillations were mostly antiphase. Therefore, the alignment of BF-deoxyHb was poor with only two subjects meeting the threshold of 0.3. BF-deoxyHb delay analysis was deemed inappropriate and they were not taken into further consideration.

Table 6.7 presents the cross-covariance values and the time delay (s) estimated for all signal pairs recorded at 33°C. The values marked in red indicate the cross-covariance below the threshold level of 0.3. Negative values of delay indicate that the second signal is delayed in respect to the first signal. From the results, it is clear that OXY signals are delayed in respect to BF signals. For BF-totalHb one more subject was identified as misaligned due to a delay of 44.6 s. Such a large delay is unlikely to be a true result therefore it has been excluded from analysis. Data presented in red in Table 6.7 indicate the values that did not meet the threshold and therefore were excluded from further analysis. The cross-covariance between flux and deoxyHb was below the threshold for 13 out of 15 subjects.

Table 6.7 Individual maximum cross-covariance and time delay for different signals pairs from the forearm across all subjects.

	Forearm at 33°C							
	BF-SO_2		BF-oxyHb		BF-deoxyHb		BF-totalHb	
id	max cov*	Delay (s)	max cov*	Delay (s)	max cov*	Delay (s)	max cov*	Delay (s)
1	0.56	-0.1	0.58	-0.1	0.26	0	0.56	-0.1
2	0.4	-2.4	0.17	-2.4	0.14	110.3	0.17	293.3
3	0.74	-1.3	0.65	-1.2	0.32	70.4	0.31	44.6
4	0.42	-0.9	0.48	-0.9	0.24	1	0.47	-0.1
5	0.43	-4.8	0.46	-2.5	0.3	1	0.48	-1.3
6	0.38	-5.8	0.42	-3.6	0.22	-261.4	0.28	-2.4
7	0.15	-300.3	0.17	-300.2	0.1	-82.4	0.17	-300.2
8	0.34	-3.1	0.27	-2	0.23	-201.9	0.22	302.1
9	0.44	-2	0.45	-1.9	0.19	-314.1	0.41	-1.1
10	0.58	-1.1	0.61	-1	0.13	-202.2	0.57	-0.1
11	0.52	-0.9	0.42	-0.9	0.22	301.2	0.32	-0.9
12	0.74	-1.8	0.74	-1.7	0.23	26.9	0.65	-0.9
13	0.26	-11.6	0.24	0.9	0.12	-210	0.21	0.9
14	0.39	-1.3	0.38	-1.2	0.16	11.3	0.33	0.4
15	0.22	160.7	0.19	160.7	0.2	-117.8	0.19	-118.2
*Maximum cross-covariance value								

Mean (SD) cross-covariance and delay (expressed in seconds) for data meeting the threshold are shown in Table 6.8. The highest cross-covariance was achieved for BF-oxyHb, however the highest number of datasets that met the threshold criteria was for BF-SO_2. This pair also showed the longest delay compared to BF-oxyHb and BF-totalHb. BF-totalHb exhibited the lowest delay, however the alignment criteria were met by only 8 out 15 datasets.

Table 6.8 Mean cross-covariance and delay in the forearm signals across studied subjects.

	Mean (SD) cross-covariance	Mean (SD) delay (s)
BF-SO_2, n=12	0.50 (0.14)	-2.1 (1.7)
BF-oxyHb, n=10	0.52 (0.12)	-1.5 (0.98)
BF-totalHb, n=8	0.47 (0.12)	-0.51 (0.61)

At 43°C the variance of BF signal increased and the variance of OXY signals dropped significantly ruling out the cross-covariance and delay analysis. Figure 5.5 presented in Chapter 5, section 5.1.3 illustrates an increase in magnitude of BF and a decrease in magnitude of SO_2 oscillations. OXY signals exhibited significantly lower oscillations than BF and thus it was not possible to align the signals correctly. The absolute power of the signals at 33°C and 43°C was presented earlier in section 5.1.4 . Furthermore, the power of the signals acquired at 43°C showed an increased contribution from the cardiac band for all signals indicating that heartbeat became a dominant oscillation at 43°C. The loss of oscillations in OXY signals resulted in low cross-covariance values, thus it limited the accurate alignment and subsequently prevented the delay estimations at 43°C.

6.2 Discussion

The first key finding presented in this chapter was an identification of frequency coherence across the five frequency bands associated with physiological activities in order to examine how well the frequency content of BF signal agreed with the frequency content of OXY signals. The highest coherence at rest has been found between BF and SO_2 signals compared to other signal pairs. Frequency coherence was the highest for the lowest frequency band. For the warmed signals the coherence between BF and SO_2 dropped and the highest values were obtained for BF-totalHb signal. It means that, during warming totalHb signal exhibited the most similar oscillatory characteristic to BF oscillatory characteristics, when compared to SO_2, oxyHb or deoxyHb signals. These findings are important in understanding the relationship between the oscillatory processes present in BF and OXY signals.

The second key finding presented in this chapter was the development of the method for time delay assessment and the quantification of the delay between blood flux and OXY signals. The time lag at maximum cross-covariance value had been extracted and OXY signals have been found to be delayed in respect to BF signal.

6.2.1 Frequency Coherence

Chapter 4 and Chapter 5 showed that BF and OXY signals share similar PSD profiles at low frequencies (endothelial, neurogenic and myogenic bands). Similar PSD profiles suggest high frequency coherence. The results presented above indicated that highest coherence occurred at the endothelial band suggesting that BF and OXY signals exhibit the strongest modulation in frequency band associated with endothelial function. This can be considered as an indirect evidence for substantial modulation between BF and OXY signals within low frequency bands.

At a physiologically neutral temperature (33°C) the highest coherence has been found for the lowest frequency bands i.e. endothelial band (0.0095 – 0.02 Hz) for all signal pairs. The physiological process referred to as endothelial function relates to nitric oxide (NO) – the main driver of slow vasodilation of the blood vessels. It has been shown that oscillations in blood flux caused by NO-dependent vasodilation (endothelial band) are also reflected in oxy- and deoxyHb signals (Trzeciak et al., 2008; Victor et al., 2009) or vice versa. In this study the FC was estimated across five different frequency bands. The highest coherence was found in the lowest frequency band. This indicates the highest degree of concordance in spontaneous oscillations occurred across frequency band related to endothelial function compared to other (higher) frequency bands.

Previous studies by Clough et al. (2009), compared standard and high power LDF probes (no OXY probe). They measured BF in the skin (standard power probe) and in a deeper tissue (the penetration of high power probe was about 4 mm). They showed the highest coherence between BF in the skin and BF in the deeper tissue in the lowest frequency bands (endothelial and neurogenic) and lower coherence in myogenic, respiratory and cardiac bands. The results presented in this thesis agree with these findings; however they refer to different signals. The findings presented here relate to coherence between BF and OXY signals sampled with a combined probe with standard power. The highest coherence observed in endothelial and neurogenic bands in both studies (Clough et al. (2009) and this work) indicates that processes occurring at low frequencies exhibited highest similarity at different depths (study by (Clough et al.)) and between different signals (this thesis). These results extend the understanding of microcirculatory dynamics indicating that skin BF oscillations are closely related to skin OXY oscillations.

Bernjak et al. (2012b) reported a phase coherence between skin BF and SO_2 on the forearm of healthy volunteers. The phase coherence was estimated as the difference in instantaneous

phases at each frequency and each time point using a wavelet transform. The output result indicated how much the phase difference changes over time. The less change the higher the coherence. They reported significant phase coherence at low frequencies (Bernjak et al., 2012b) and also in the cardiac frequency band. They measured BF and SO_2 using the O2C device (O2C, LEA Medizintechnik, Germany) allowing for measurements at two different depths. They did not find significant phase coherence in deeper tissues (measured with fibre separation 8 mm – measurement depth was several millimetres). The results presented here agree with this study but look at the coherence from a different perspective. FC reported here was estimated as a mean measure of a 600 s long signal rather than phase coherence over time. Frequency coherence presented in this work is an overall measure of frequency content of BF and OXY signals whilst the phase coherence reported by Bernjak et al. (2012b) is based on the individual differences in phase at different time points. Both methods can be employed to study the similarities in the frequency domain. However, Bernjak et al. (2012b) performed analysis only between BF and SO_2. The study presented here investigates different signals pairs, which may be more informative than the SO_2 signal alone. It has been questioned in the literature if SO_2 is a reliable measure of tissue oxygenation. The findings presented here indicate that the component signals, i.e. oxyHb and deoxyHb, may yield additional complimentary information.

More recently, Dunaev et al. (2014) investigated the synchronisation between microvascular blood flux and oxygenation at rest and during exercise. They used a wavelet transform to identify peaks for myogenic activity for BF and SO_2 signals at rest, during stress and during exercise. They analysed BF and SO_2 signals recorded from forearm and finger (they compared sites with and without AV shunts) from eight volunteers. They analysed the synchronisation between myogenic activity in BF and SO_2 signals. They found that the oscillations of BF and SO_2 signals within the frequency band associated with the myogenic activity in the skin with AV shunts was better synchronised compared to skin without AV shunts. They have also analysed the response to adaptive changes. These analysis were performed only in two volunteers out of eight: one person was studied during exercise and one during PORH (Dunaev et al., 2014). They reported that oscillation in BF and SO_2 within the myogenic band were more synchronised during adaptive changes compared to rest. However, these results were based on measurements from two individuals therefore they should be considered as case studies and interpreted carefully. Unfortunately, the authors did not report the wavelet transform from other frequency bands therefore it is unclear whether they observed coherence at other frequencies. The frequency coherence presented in this thesis was assessed based on power

across different frequency bands rather than the location of the frequency peak. The findings published by Dunaev indicated the differences in skin with and without AV shunts, but the conclusions related to synchronicity between BF and SO_2 during adaptive changes (PORH and exercise) based on two case studies are weak and require further investigation.

There are no studies investigating the coherence between BF and SO_2 signals during thermally induced vasodilation. However, Bernjak et al. (2012a) studied the coherence between skin and muscle nerve activity at rest and during whole body warming. They also recorded skin BF but they did not conduct the coherence analysis on skin BF signals. Regarding BF, they have reported an increase in wavelet power of skin BF during heating. This study confirmed the oscillations in skin and muscle nerve activity happen across broad spectrum of frequencies and differ between subjects. Whole body warming increased skin sympathetic oscillations but did not affect muscle nerve activity. The coherence between skin and muscle nerve activity described by Bernjak et al. (2012a) regards different signals than analysed here but they estimate the oscillations across the same frequency spectrum (0.0095-2 Hz). The shape of the power spectrum of nerve activity signal indicated the stronger involvement of myogenic, respiratory and cardiac bands into the overall nerve activity signal compared to endothelial and neurogenic frequency bands. Interestingly, there were no visible peaks within the frequency range associated with neurogenic activity indicating that this activity does not occur at specific frequency but across different frequencies in neurogenic band (0.02 – 0.05 Hz) and/or these frequencies may vary in time. The measurements recorded the nerve activity in skin and muscle so it would be expected that the most power will be embedded in the neurogenic band. Nonetheless, the coherence between skin and muscle nerve activity across the frequency range of 0.0095 – 2 Hz indicated some congruent oscillations. On the other hand, the analysis of frequency coherence between BF and OXY signals resulting from the work done for this thesis led to a conclusion that BF and OXY signals exhibit highest frequency coherence for low frequency components. These observations indicate that multiple physiological processes such as skin and muscle nerve activity vs skin blood flux and oxygenation, are not directly related, and contain most signal power at different frequencies. Perhaps, there are number of other physiological signals that may oscillate in the comparable way. Future studies may investigate the coupling between oscillatory behaviour of other physiological signals to extend the current understanding of relation between various physiological processes.

The coherence analysis has been also applied to study haemoglobin oscillation in the human brain in relation to the arterial blood pressure (ABP). Cui et al. (2014) reported wavelet coherence and wavelet phase coherence between oxyHb (measured with NIRS) and ABP. Their wavelet spectrum of oxyHb resembled quite closely the PSD spectrum of oxyHb from the study presented in this thesis. The similarities relate to the higher power in the low frequency bands compared to respiratory and cardiac bands, decreasing power across endothelial, neurogenic and myogenic bands and the lowest power in the respiratory band. The main difference exists in the cardiac frequency band. Cui et al. (2014) reported a clear peak around 1 Hz whilst in the results from the study performed during the course of this PhD showed the power in cardiac frequency band was relatively low. Cui et al. (2014) reported the highest wavelet coherence between oxyHb and ABP in the cardiac frequency band. For endothelial, neurogenic and myogenic bands the wavelet coherence was about 0.30-0.35. In the light of this and other studies, the spontaneous oscillation in BF and OXY signals occur in various tissues across the human body (skin, muscle and brain). The cerebral oscillations in oxyHb are coupled with arterial blood pressure and subsequently they are associated with overall blood flow, but the results of the study conducted in this thesis indicate the strongest coupling between BF and OXY signals exist in skin microcirculation.

Most of the discussion in this work focused on the relationship between BF and SO_2 or OXY signals. However, it is also important to analyse the relationship between SO_2 and OXY signals. SO_2 signal is derived from oxyHb and deoxyHb signals – it is a ratio of oxyHb to totalHb. It is expected that SO_2 and Hb signals exhibit high FC, but it is not clear which signal: oxyHb, deoxyHb or totalHb show the highest FC with SO_2. The question remains which of these two signals (oxyHb or deoxyHb) drives the oscillations in SO_2 signal. The analysis of FC between SO_2 and Hb signals showed the highest FC is achieved in SO_2-oxyHb pair. It was exceptionally high: 0.97, 0.91 and 0.93 for endothelial, neurogenic and myogenic bands respectively. These results indicated that oscillations in oxyHb are seen much more strongly in tissue oxygenation compared to oscillations in deoxyHb. It implies that, in skin the changes in oxygenation result mostly from the variations in oxyHb rather than from the oxygen consumption (variations in deoxyHb). In healthy skin the changes in oxygen consumption reflected by the changes in deoxyHb are far smaller compared to the changes in oxyHb resulting from the changes in blood flux. Measurement of oxyHb and deoxyHb provide more specific information than the SO_2 signal and they should be analysed primarily, with the SO_2 signal as the more general assessment of the ratio between oxyHb and deoxyHb in microcirculatory blood.

The analysis of FC presented in this chapter had some limitations. The frequency coherence does not provide information about the delay and phase agreement between signals. Also the accuracy of analysis in the lowest frequency bands is limited by the signal length. For the finite length signal, there are always fewer low frequency cycles than high frequency cycles. Therefore, there may be less variation in low frequency components resulting in the artificially higher frequency coherence. Considering the above limitations, the studies performed during this work were designed to minimise the effect of signal length on frequency analysis. The signals analysed in this work were carefully acquired, assuring good quality of data. 600 s artefacts-free segments were selected, making sure the frequency analysis reflects the true frequency content of the signals. 600 s of data is generally considered sufficient to determine the lowest frequency content of interest.

6.2.2 Delay between Signals

Delay estimation is an important characteristic of the studied system and it has been widely recognised in engineering fields such as seismology and communication system but also in biomedical systems (Wang et al., 2005; Şahin et al., 2014). For example, in biomedical signals delay estimation is often applied to assess the propagation of heart electrical activity. Time delay had also been observed in blood flux and oxygenation signals in the brain (Poublanc et al., 2013; Thomas et al., 2014). The work presented in this section focuses on the delay analysis between skin BF and OXY signals. . All OXY signals were delayed in respect to BF. How do these relate to the dynamics of the underlying physiological systems? The physiological causes of delay between BF and SO_2 signals have their origin in continuous, complex interactions aiming to maintain adequate perfusion and tissue oxygenation. These include the action of multiple signalling factors, e.g. vasodilator and vasoconstrictor molecules, as well as sensory nerves and mechanical stresses within the tissue. For example, the relationship between BF and oxygenation in the brain tissue has been studied by numerous research groups. It is understood that the increased oxygen consumption causes vasodilation and subsequent increase in blood flux. The blood flux is delayed in respect to oxygen consumption. Some groups suggest this maybe of a magnitude of a few seconds (Paulson et al., 2010). In the brain, the hemodynamic response function is known as an increase in blood flow after neural activation. This response occurs with delay of 4-5 s (Uga et al., 2014). This increase in blood flow results in delivering more oxyHb and thus in the increase in the oxygenation i.e. the ratio between oxyHb and deoxyHb. However, another study in brain blood flow and oxygenation showed the increase in oxygen consumption was not always accompanied by increased blood

flow (Lu et al., 2004). They showed that the brain oxygenation signal after stimulus returns to baseline after approximately 8-10 s whilst the blood volume is increased for approximately 30 s. Another study by Cui et al. (2014) showed the haemodynamic response measured with NIRS or fMRI peaks after about 6 s after the stimulus. Considering these different findings, it is clear there is a delay between blood flow and oxygenation in the brain, however, it is not clear what the actual delay between these variables is. It can be expected that other tissues will also exhibit the delay between blood flow and oxygenation originating from oxygen consumption or other physiological processes.

The time delay varies between different tissues and different conditions. For example, exercising muscle depletes the oxygen and the subsequent tissue hypoxia triggers vasodilation and increase in BF. The increase in blood flow can be seen within 2 s after muscle contraction but the functional vasodilation happens after 5-20 s (Bangsbo et al., 2000; Clifford, 2007). However, the delay of increase in blood flow does not limit the oxygen uptake (Nyberg et al., 2010).

The study conducted by Yano et al. (2014) investigated the relationship between oscillations in skin blood flux and muscle deoxyHb at rest and during light exercise. The overall cross-correlation (at all possible time lags) between skin blood flux and deoxHb was < 0.2. At delay = 0, they have reported cross-correlation between skin BF and muscle oxyHb close to zero implying there was a time shift between signals. Unfortunately, they did not analyse this observation further. The analysis of the results presented in this chapter reporting the delay between skin BF and OXY parameters has showed all OXY parameters are delayed in respect to BF. Although, muscle oxygenation is a different variable and will exhibit different behaviour than skin oxygenation, it can also be delayed and therefore exhibit a low cross-correlation unless aligned according to the delay. The findings presented here related to delay between BF and OXY signals, can to some extend explain the lack of correlation reported by Yano.

The above findings remind that there are multiple mechanisms involved in the regulation of blood flow and oxygenation and they are not always synchronised. For example, temperature regulation achieved by varying the skin blood flux is independent of skin oxygen consumption. The opposite example can relate to increased blood flux following tissue hypoxia. Studies performed with reduced oxygen content in the air showed an increase in skin blood flow (Simmons et al., 2011) in response to the reduced oxygen content in the air. The analysis of the delay between BF and OXY signals aims to address the question, whether at the rest (non-

perturbed state) the regulation of skin oxygenation is linearly dependent on regulation of skin BF or vice versa.

The causality between changes in blood flow and oxygenation in skin is not clear. The question remains whether the changes in blood flow cause the changes in oxygenation or the changes in oxygenation induce the changes in blood flow. In other tissues such as brain or muscle, the increased oxygen demand will cause increase in blood flow. However, skin at rest is supplied with a much higher amount of oxygen than it requires. The delay analysis based on the alignment technique showed that OXY signals are delayed in respect to BF signal. Negative values of the delay, point to the corresponding changes in SO_2 and oxyHb happening after the changes in BF signal. To exclude the possibility that these observations may be caused by the methodological issues a simple experiment was conducted. BF and SO_2 signals were recorded with the probe placed on white paper with coloured strips. After 20 s the probe was rapidly moved to red colour to induce the change in BF and OXY signals. During the change both signals showed a response at the same time, confirming there was no technical delay between them. In this study the oxygenation signal was always delayed in respect to BF signal (the negative value of delays presented in results section). This is a novel observation and the scientific literature about this phenomenon is limited. Further studies are required to support and confirm the delay between BF and OXY signals. Furthermore, a delay was also observed in OXY signals in respect to BF signal in PORH peak reported in Chapter 4. Figure 6.2 shows an example of the SO_2 peak being delayed in respect to BF peak recorded from one of the volunteers in Study 1. The figure shows an overlay of BF and OXY signals recorded shortly before and after occlusion applied as a part of PORH protocol. The arrows indicate peaks of BF and SO_2 signals with the SO_2 peak occurring a few seconds after BF peak. Time to peak has not been analysed in Study 1 but it can be an interesting characteristic for future studies. The presence of the delay between BF and OXY peaks in PORH provides further evidence of time delay between BF and OXY signals.

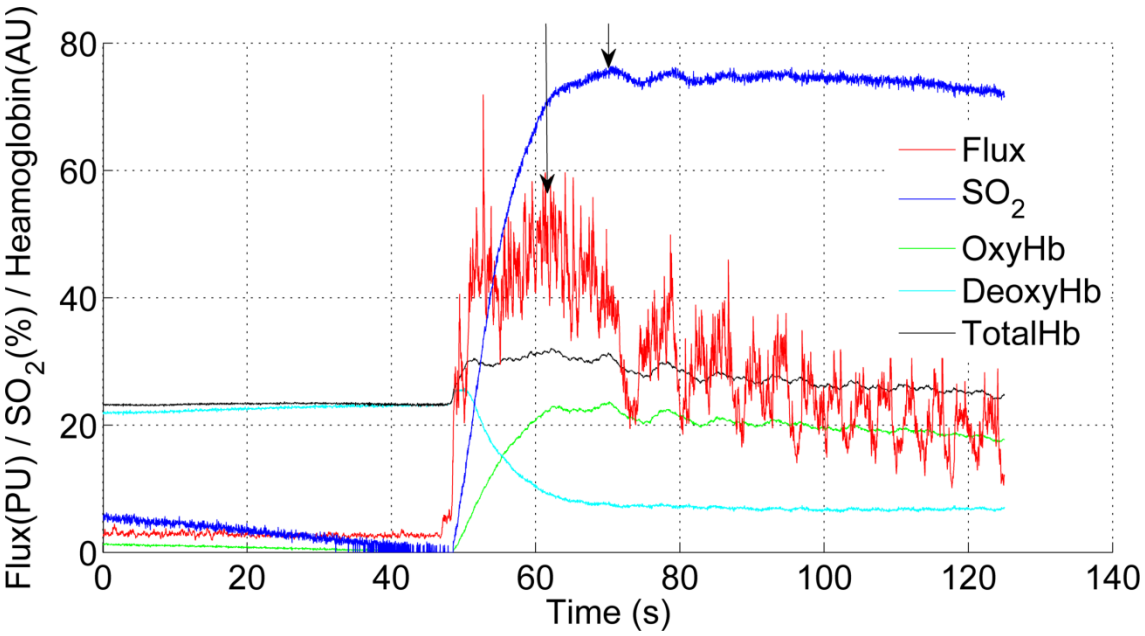

Figure 6.2 An example of a delay between BF and OXY peaks during PORH protocol recorded from one of the volunteers in Study 1.

One of the limitations of the analysis presented here is that they are indirect observations. The delay between BF and OXY signals was derived from the signals representing microvascular flux and oxygenation which were generated by the tissue, but were not measured directly in the tissue. The potential method of validating the findings would be to insert flow probes into the microvascular network to measure the changes in the flow. At the same time the other probes measuring tissue oxygenation need to be inserted in the tissue to record changes in oxygenation. This is however impossible to conduct without perturbing the tissue. Inserting the probes into the tissue would cause a number of different responses which would change normal tissue homeostasis. As a consequence, the measured blood flow and oxygenation would not represent normal condition, but the state after some perturbations. At the moment it is not possible to measure blood flow and oxygenation directly without perturbing the tissue. This however is beyond the scope of this work. Whilst the results presented here are not obtained from direct observations they give and insight into previously unexplored area. Overall, the results showed the dynamics between BF and OXY captured with the combined probe reveal time delay between these signals. Perhaps, further studies involving modelling the oxygen diffusion in the tissue in combination with the results presented here will yield a new method for quantifying the delay between skin perfusion and oxygen consumption.

It is important to identify and describe the delay corresponding to the healthy condition, in order to investigate pathological changes. For example, nicotine restricts the blood flow to the

skin and therefore the oxygen supply. It may also alter the dynamics between BF and OXY signals resulting in the mismatch between blood delivery and the demand from the tissue. Knowledge about normal physiological delay between BF and OXY signals may possibly be used as a new characteristic of relationship between BF-OXY signals. Perhaps too long or too short delay may indicate an imbalance between skin BF and skin oxygenation.

6.2.3 Other Descriptors of Time- and Frequency-Domain Characteristics

At the time of writing this work there have already been published the analysis of other time and frequency characteristics of LDF signals. Humeau et al. (2008) investigated *Hölder exponent* and *sample entropy* in healthy subjects. Buard et al. (2010) analysed *Renyi exponents* and *Legendre transform* in healthy subjects. Liao & Jan (2012) analysed nonlinear properties of LDF signals in subject at risk for pressure ulcers. They reported *Hurst exponent*, *detrended fluctuation analysis*, *sample entropy*, *correlation dimension* and *Lyapunov exponent*. Esen et al. reported *fractal complexity measure α* of *detrended fluctuation analysis* in healthy subjects (Esen et al., 2009) and subjects with essential hypertension (Esen et al., 2011). Figueiras et al. (2011) investigated whether the *sample entropy* of LDF signals can discriminate between healthy subjects, subjects with Raynaud's phenomenon and subjects with systemic sclerosis. Tankanag et al. (2014) investigated *wavelet phase coherence* of oscillations between two different skin sites in 20 healthy subjects. Humeau-Heurtier & Klonizakis (2015) analysed the *entropy of intrinsic mode function* (calculated using the empirical mode decomposition) in healthy subjects and patients with varicose veins. Tigno et al. (2011) investigated the complexity of LDF signals from nondiabetic, prediabetic and diabetic monkeys. They analysed at Lempel-Ziv complexity in baseline data (34°C) and warmed data (44°C) and they reported that with progression of diabetes the complexity of the signal decreased (Tigno et al., 2011). These findings suggest that the impact of diabetes on spontaneous oscillation is reflected in the complexity of these oscillations. However, these findings were obtained from monkeys and studies in human subjects with diabetes showed opposite trend. Hsiu et al. (2014) analysed the *approximate entropy* of beat-to-beat LDF signal in nondiabetic, prediabetic and diabetic humans. They showed and increased complexity in diabetic subjects compared to nondiabetic. However, the complexity reported by Hsiu et al. (2014) relates to complexity between consecutive heart beats rather than to low frequency oscillations. Perhaps, the adaptation of microcirculation to diabetes involves a decrease in complexity of the low frequency oscillations and an increase in the complexity of cardiac band. Further studies are required to confirm these hypotheses.

6.3 Summary and Contributions to the Body of Knowledge

In summary, this chapter has presented further analysis performed on BF and OXY signals, with the focus on frequency coherence and the delay between these signals. Frequency coherence analysis has revealed close similarities across low frequency oscillations. The delay between BF and OXY signals in skin has been identified for the first time. SO_2 and OXY signals were delayed in respect to BF signal. The values of delay identified in healthy volunteers may serve as a reference for future studies. It is important, as it will help to assess delay in groups with microvascular dysfunction and to better understand the influence of microvascular dysfunction on physiology of microcirculation.

Chapter 7

Conclusions and Future Directions

The work undertaken in this thesis aimed to apply the signal processing methods to analyse skin BF and OXY signals. The goal of performed analysis was to extract and interpret information contained in signals acquired with combined LDF and WLS probe. These signals originated from the changes occurring in skin tissue reflected in macrovascular blood flux and oxygenation. Signal processing methods such filtering, Fourier transform, frequency coherence, cross-covariance and time delay were used to identify different properties of the signals and subsequently describe the biological systems.

7.1 Summary

The time and frequency analysis of healthy BF and OXY signals were conducted in order to study the relationship between simultaneously recorded skin blood flux and oxygenation. Two studies in healthy volunteers were carried out. Study 1 investigated the relationship between BF and SO_2 in a healthy population including men and women aged between 20-65y. Study 2 was performed on a less variable group of volunteers: only men between 20-30y were included. A number of physiological perturbations of blood flux were applied in order to investigate the behaviour of microcirculatory blood flux and oxygenation under varied conditions.

The major findings were:

- the relationship between BF and SO_2 can be described with the equation: $SO_2 = -18.07 + 99.2 \times (1 - e^{-0.096 \times flux})$;
- BF and OXY signals exhibit different power spectral density contributions across endothelial, neurogenic, myogenic, respiratory and cardiac bands at the standardised resting skin temperature of 33°C and during thermally induced vasodilation achieved by local skin warming to 43°C;
- PSD contribution profiles change during warming;
- spontaneous oscillations in BF and OXY signals have highest coherence across low frequency bands;

- the maximum cross-covariance can be used to estimate the delay between BF and OXY signals;
- OXY signals were delayed with respect to BF signals with the highest delay between BF-SO_2.

The findings from this thesis prompt a re-thinking of time and frequency analysis of BF and OXY signals. The frequency analysis presented in this thesis, supported by the literature analysis led to the conclusion that the assessment of the power spectral density alone is not a clinically valid measure. The frequency analysis is a subject to large variability and it fails to provide consistent findings. Although there are a vast number of studies conducted on BF signals, they did not result in clear diagnostic application. The literature reports contradictory results and there is no clear agreement on interpretation of data.

The analysis of simultaneously recorded BF and OXY parameters offer new insights into the human skin microcirculation system. Time and frequency analysis undertaken in this thesis showed that the data extracted from BF and OXY signals is complex. The analysis presented in this work is a small part of the complex description of the microvascular function. It will be a challenge for future studies to identify other characteristics that in combination with characteristic presented here may become good descriptors of the physiological state of the tissue.

7.2 Future Directions

In summary, the priority list of studies following on research presented in this thesis should include:

- further investigation of BF-SO_2 equation in larger population including healthy older population;
- development of single analysis system incorporating multiple time and frequency descriptors;
- long-term follow-up studies to identify whether the characteristics of BF and OXY signals can inform about early changes predictive of microvascular diseases.

Better understanding of BF-SO_2 equation should be a top priority. Based on the fact that microvascular function deteriorates with age, identifying the equation describing BF-SO_2 relationship in older population will offer an insight into which and how the parameters of the equation are affected by aging. These findings will enable to further understand the relationship described by the equation and quantify the alteration resulting from aging. The

study of BF-SO_2 relationship in older population will also enable analysis of desaturation rates during arterial occlusion. The identification of this parameter for BF and OXY signals in combination with BF-SO_2 relationship will inform how the combined BF-OXY measurements can reflect the decline in microvascular function. Furthermore, extensive follow-up studies are needed to identify whether the characteristics of BF and OXY signals can inform about early changes predictive of microvascular diseases.

Future studies should also focus on combining multiple time and frequency descriptors into single model. Discussion in Chapter 6 showed some examples of versatile time- and frequency-domains analysis undertaken in recent years. They contribute small pieces of information about microvascular oscillations, but so far there are not enough consistent results to build up confidence about their importance in the assessment of the microvascular function. Perhaps, combining a number of different descriptors of BF and OXY signals may provide a more accurate assessment of the microvascular function. Incorporating a number of different analysis techniques into one model will improve the sensitivity to small changes and allow for a more comprehensive investigation. Future work should also include the standardisation of LDF and OXY signals descriptors across different analysis methods. Furthermore, multicentre collaborations will play an important role in the integration of existing knowledge into an extensive model of microvascular assessment.

It is possible that, the individuals with lower physiological blood flux maybe more susceptible in later life to ischaemia and tissue hypoxia. Low tissue perfusion may at some point in life become insufficient and lead to microvascular complications, in particular in people with higher risk of CVD and diabetes. At present, it is not known where the border between low and adequate oxygenation at rest is, and how it relates to microvascular dysfunction in later life. The hypothesis whether low physiological blood flux and oxygenation is linked to the higher risk of ischaemic events later in life is beyond the scope of this work but can be an interesting extension of the work presented here.

LDF and WLS have been shown to provide reproducible results in well controlled settings. However, in practice, it is far more difficult to obtain robust measurements in hospital settings. This does not affect scientific studies but it limits the direct, clinical usefulness of the techniques. Therefore, the future studies should also include investigation of other techniques, in particular the imaging techniques which offer an advantage of larger surface measurements and thus overcome the problem of tissue heterogeneity.

The overall aim of non-invasive, clinical measurements is to provide complimentary information to the clinical team, thus enhancing or accelerating the correct diagnosis and intervention. However, as mentioned above the microcirculation is a highly complex system with multiple time-varying components. It is therefore indispensable to develop methods integrating the BF and OXY signals across different studies into uniform format. Larger data sets and systematic analysis will help to identify more characteristic features describing the physiology of microcirculation.

Appendix 1: Participant information sheet

PARTICIPANT INFORMATION SHEET

Version 3.4 19 May 2014

Validation of non-invasive blood flow monitoring devices in healthy participants

REC Number: SOMSEC091.10 RHM MED0992

Names of Principal Investigators: Ms Katarzyna Kuliga and Prof Geraldine Clough

You are being invited to take part in a research study. Before you decide it is important for you to understand why the research is being done and what it would involve. Please take time to read the following information carefully and discuss it with friends and relatives. Ask us if there is anything that is not clear or if you would like more information. Take time to decide whether or not you wish to take part.

Thank you for reading this.

What is the purpose of the study?

This study aims to validate the use of two new devices designed to measure blood flow and tissue oxygen levels on the surface of the skin without damaging or piercing the skin; this means the devices are non-invasive. We aim to establish how repeatable these measurements are, and to test these new devices against similar devices already in use. We hope that this will provide information which can help work out what role these new imaging devices can have in helping patients. This research is funded by the Engineering and Physical Sciences Research Council (EPSRC) and by Moor Instruments UK who manufacture the two devices. The research will be submitted as part of a PhD by one of the researchers (K Kuliga).

The two new devices are:

Moor VMS-OXY™ – this device non-invasively measures blood flow and the amount of oxygen in the tissues just below the skin. It uses light shone on to the skin via a fibre optic cable and is held against the skin by a small pad.

moorFLPI™ - this camera takes pictures of blood flow in real time using a safe, low power laser The device is positioned above the body part that is being looked at and does not have contact with the skin.

We will be testing these new devices against other devices made by Moor Instruments and other devices that also monitor similar measurements.

Why have I been chosen?

You may have responded to an advertisement or personal approach.

Do I have to take part?

It is up to you to decide whether or not to take part. If you decide to take part you will be given this information sheet to keep and be asked to sign a consent form. You are free to withdraw at any time and without giving a reason.

What would happen to me if I take part?

You will be asked to attend the study centre in the Clinical Research Facilities at Southampton General Hospital, Tremona Road, Southampton, SO16 6YD.

If you are suitable and agree to take part, you will be enrolled on one or more parts of the study. The exact parts will depend on what you consent to and the time you have available.

The number and length of visits will depend on which parts of the study you choose to be involved with. The study is happening over 3 years and over that period you will be asked to help with the study up to four times. Two of the visits might be a week apart. All visits will be at times agreed by you and the researcher. All of the visits will be at our study centre, will happen at about the same time of day and will last no longer than 90 minutes.

What do I have to do?

We will ask you not to have taken strenuous exercise (for example, going to the gym, sports etc.) for 24 hours before your study visit. You are allowed to undertake your normal journey to work or to the study centre. We also will ask you not to consume any caffeine-containing drinks (such as tea, coffee, cola etc.) for 2 hours beforehand.

When you arrive at the study centre, we will bring you into the room and measure your height and weight. You will then lie down on the bed and we will ask you some questions and take your blood pressure. Depending on what you agreed to, we will position the devices at one of these sites:

- Lower arm
- Hand
- Foot

We will then record your normal skin blood flow while you rest quietly. We will then cause a brief change in your skin blood flow in one of the following ways:

1) Warming your skin
2) Cooling your skin
3) Briefly stopping the blood flow to the site we are recording using a pressure cuff. In your arm, the pressure cuff is similar to the one used to take your blood pressure. In your hand or foot, this is a small version.
4) Lowering your foot (only happens in the foot)
5) Pricking histamine into your skin to cause a small reaction a bit like a nettle sting (only when looking at your lower arm).
6) Application of a dressing that delivers oxygen to the skin

After the testing is complete, a photograph of the area we have been looking at will be taken, so we know where the measurements have been taken from. You will then be free to leave.

For the warming, cooling and pressure cuff studies, you will be invited back between five and seven days later, at a similar time of day for those tests to be repeated.

What are the alternatives for diagnosis or treatment?

This study is of no benefit to you in respect of diagnosis or treatment.

What are the possible risks of taking part?

There are no major risks of taking part. You may feel a tingling or 'pins and needles' sensation in your arm during and immediately after the inflation of the pressure cuff. You may see a small red mark at the site of local warming that may last for up to 1 hour. You may also feel a sensation of itch at the site of histamine skin prick test that may last for a few minutes after the end of the study. There is also a small risk that when you sit up after lying on the bed that you may feel faint. We shall assist you in getting off the bed to minimise the chances of this.

What are the possible benefits of taking part?

You would not receive any benefits directly. However, this study will increase our understanding of these devices and could possibly lead to improved diagnosis, management or treatment in the future.

What if something goes wrong?

This study is covered by indemnity of the University of Southampton. In the unlikely event that you come to any harm as a result of taking part in this study, the usual University complaints mechanisms are open to you. If you wish to make a complaint please contact the University Research Governance Office:

George Thomas Building 37
Room 4055
University of Southampton
Highfield
Southampton SO17 1BJ

Email: rgoinfo@soton.ac.uk

Tel: 023 8059 5058

Would my taking part in this study be kept confidential?

All data will be anonymised using an identification code that is allocated upon recruitment, which means that it cannot be traced back to you. No volunteer personal details will be stored after the end of the study. The only people who will have access to your contact details during the study will be the two investigators named here and access will be password protected. If data is published in scientific/medical journals, this will not be able to be traced back to you. If you wish to be informed of articles based on the results of the study, we will keep your details in a secure file and your details will only be used to let you know of any such articles. Your GP will not be notified of your participation in this study.

What will happen to the results of the research?

The results of the research will be evaluated and may be published in scientific papers and presented at scientific conferences. They may also be used in the information issued by the company when they market these devices. You will not be identified from these results. If you wish, we can notify you if an article based on the results of this study is published. The results of this research may indicate that there is potential for new diagnostic tests or treatments that may be further researched and developed.

Who has reviewed the study?

The University of Southampton Faculty of Medicine Ethics Committee have reviewed the study.

Contact for further information:

Ms Katarzyna Kuliga BEng

Email: kzk1m11@soton.ac.uk

Prof Geraldine Clough PhD

Tel: 023 8079 4292 Email: G.F.Clough@soton.ac.uk

If you decide to take part in the study, you will be given a copy of the information sheet and a signed consent form to keep.

Appendix 2: Consent Form

Medicine

UNIVERSITY OF Southampton

REC Number: **SOMSEC091.10**
Version no: 2.4
Date: 19.05.2014

PARTICIPANT CONSENT FORM
Version number 2.4
Validation of non-invasive blood flow monitoring devices in healthy participants
REC Number: SOMSEC091.10 RHM MED 099

Name of researchers: Ms Katarzyna Kuliga and Professor Geraldine Clough

This section relates to your consent for the current study

PLEASE **INITIAL** THE BOXES IF YOU AGREE WITH EACH SECTION:

I confirm that I have read the information sheet version 3.4 dated May 2014 for the above study and have been given a copy to keep. I have been able to ask questions about the study and I understand why the research is being done and any risks involved. ☐

I understand that my participation in this research is voluntary and that I am free to withdraw at any time without giving a reason. I understand that if I withdraw my future medical care and legal rights are not affected. ☐

I agree to participate in the following aspects of the study (please initial):

- Pressure cuff ☐
- Heating ☐
- Cooling ☐
- Limb lowering ☐
- Skin prick ☐
- Skin oxygenation ☐

I agree for any images generated during the study to be used for presentations and publication, both in academia and industry. ☐

I understand that my GP will not be informed of my participation in this study. ☐

I wish to be informed of any articles published based on the results of this study. ☐

Name of volunteer	Date	Signature
Name of person taking consent (if different from researcher)	Date	Signature
Name of researcher	Date	Signature

If you have any complaints, please contact Southampton University Research Governance Office, Geroge Thomas Building 37, Room 4055, University of Southampton, Highfield, SO17 1BJ. Email: rgoinfo@soton.ac.uk Tel: 02380 595058.

Appendix 3: Data collection Sheet

Version 1

Data Collection Sheet

Version 1

March 2011

Date:	**Time:**
Participant number:	
Date of birth (age):	M/F
Height:	Weight:
Blood Pressure:	

Consumption in last 24 hours (NB abstention for at least 2h (24h for exercise) requested on consent)

Smoking	Yes	No	(Exclude from study if yes)
Caffeine containing beverages	Yes	No	
Exercise	Yes	No	(If yes, put details in comments)

Current and recent medications (within last 1 week)

(Please include all herbal, homeopathic, other over the counter medication in addition to prescription medication)

If female

Currently using contraceptive pill/HRT (delete as appropriate) Yes No

Menstrual cycle length: day/weeks

Date of last menstruation:

Comments:

Appendix 4: Supplementary Data

Appendix Table 1 p-values of the unpaired, two-tailed t-tests for comparison between BF and OXY signals recorded without and with gel.

	p-value for measurements at resting skin temperature (31.2±1.0 °C)	p-value for measurements at 33°C	p-value for measurements at 43°C
BF (PU)	0.52	0.50	0.90
SO_2 (%)	0.42	0.54	0.59
oxyHb (AU)	0.91	0.91	0.64
deoxyHb (AU)	0.35	0.56	0.75
totalHb (AU)	0.51	0.66	0.66

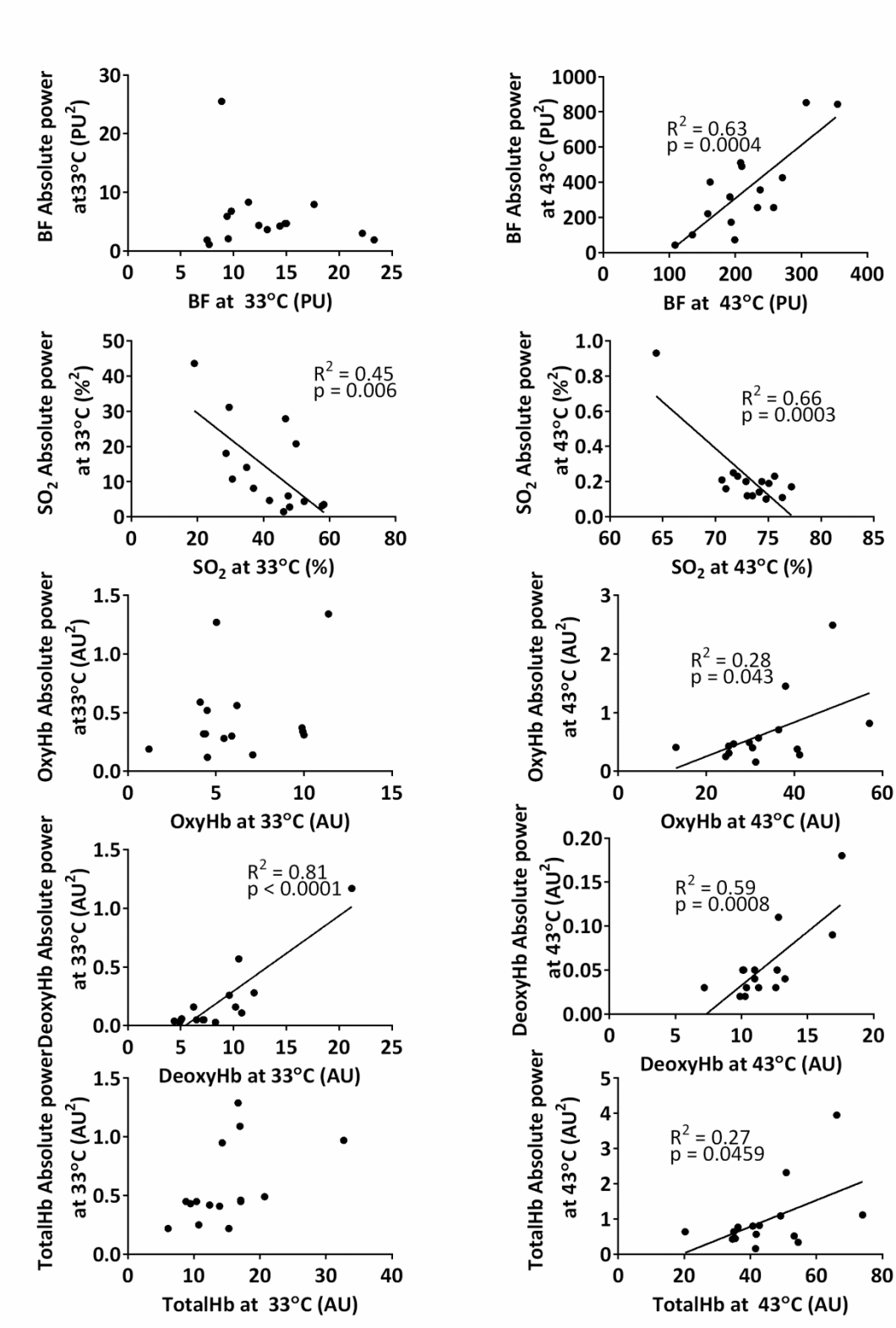

Appendix Figure 1 The relationships between absolute power of BF and OXY signals and their averege values at 33°C and 43°.

Appendix 5: An Example of Matlab Processing Code

The code below presents an example of processing scripts developed during the course of this thesis.

```
%% load data for analysis
clear all
path = 'xxxx';      % specify path here
cd(path);
load alldata_warming_n15_filt_first_smaller
%% define sampling rate
Fs = 10;
Tc = 200;
Ts = 0.1;
a=1; % choose signal for analysis, 1-5 bf,so2,oxthb,deoxyhb,totalhb

for j=1:length(alldata)
baseline_x = alldata(j).b(:,a); % select signals at baseline
at33c_x = alldata(j).at33c(:,a);% select signals at 33C
at43c_x = alldata(j).at43c(:,a);% select signals at 43C

% detrend signals
baseline = detrend(baseline_x);
at33c = detrend(at33c_x);
at43c = detrend(at43c_x);

%create Welch spectrum
Hs = spectrum.welch('Hann',pow2(11),50);
baseline_Hdsp2(j)=
psd(Hs,baseline,'Fs',Fs,'NFFT',pow2(15),'SpectrumType','onesided');
at33c_Hdsp2(j)=
psd(Hs,at33c,'Fs',Fs,'NFFT',pow2(15),'SpectrumType','onesided');
at43c_Hdsp2(j)=
psd(Hs,at43c,'Fs',Fs,'NFFT',pow2(15),'SpectrumType','onesided');

%calculate average power
baseline_Pow_endo(j) = avgpower(baseline_Hdsp2(j),[0.0095 0.02]);
baseline_Pow_neuro(j) = avgpower(baseline_Hdsp2(j),[0.02 0.06]);
baseline_Pow_myo(j) = avgpower(baseline_Hdsp2(j),[0.06 0.15]);
baseline_Pow_resp(j) = avgpower(baseline_Hdsp2(j),[0.15 0.4]);
baseline_Pow_card(j) = avgpower(baseline_Hdsp2(j),[0.4 1.6]);
baseline_Pow_total_b(j) = avgpower(baseline_Hdsp2(j),[0.0095 1.6]);
baseline_Pow_total(j) = baseline_Pow_endo(j) + baseline_Pow_neuro(j) +
baseline_Pow_myo(j) + baseline_Pow_resp(j) + baseline_Pow_card(j);


at33c_Pow_endo(j) = avgpower(at33c_Hdsp2(j),[0.0095 0.02]);
at33c_Pow_neuro(j) = avgpower(at33c_Hdsp2(j),[0.02 0.06]);
at33c_Pow_myo(j) = avgpower(at33c_Hdsp2(j),[0.06 0.15]);
at33c_Pow_resp(j) = avgpower(at33c_Hdsp2(j),[0.15 0.4]);
at33c_Pow_card(j) = avgpower(at33c_Hdsp2(j),[0.4 1.6]);
at33c_Pow_total_b(j) = avgpower(at33c_Hdsp2(j),[0.0095 1.6]);
at33c_Pow_total(j) = at33c_Pow_endo(j) + at33c_Pow_neuro(j) +
at33c_Pow_myo(j) + at33c_Pow_resp(j) + at33c_Pow_card(j);

at43c_Pow_endo(j) = avgpower(at43c_Hdsp2(j),[0.0095 0.02]);
at43c_Pow_neuro(j) = avgpower(at43c_Hdsp2(j),[0.02 0.06]);
at43c_Pow_myo(j) = avgpower(at43c_Hdsp2(j),[0.06 0.15]);
```

```
at43c_Pow_resp(j) = avgpower(at43c_Hdsp2(j),[0.15 0.4]);
at43c_Pow_card(j) = avgpower(at43c_Hdsp2(j),[0.4 1.6]);
at43c_Pow_total_b(j) = avgpower(at43c_Hdsp2(j),[0.0095 1.6]);
at43c_Pow_total(j) = at43c_Pow_endo(j) + at43c_Pow_neuro(j) +
at43c_Pow_myo(j) + at43c_Pow_resp(j) + at43c_Pow_card(j);


end

%% calculate energy contribution

for j=1:length(alldata)
baseline_contr_endo(j) = baseline_Pow_endo(j)/baseline_Pow_total(j);
baseline_contr_neuro(j) = baseline_Pow_neuro(j)/baseline_Pow_total(j);
baseline_contr_myo(j) = baseline_Pow_myo(j)/baseline_Pow_total(j);
baseline_contr_resp(j) = baseline_Pow_resp(j)/baseline_Pow_total(j);
baseline_contr_card(j) = baseline_Pow_card(j)/baseline_Pow_total(j);

at33c_contr_endo(j) = at33c_Pow_endo(j)/at33c_Pow_total(j);
at33c_contr_neuro(j) = at33c_Pow_neuro(j)/at33c_Pow_total(j);
at33c_contr_myo(j) = at33c_Pow_myo(j)/at33c_Pow_total(j);
at33c_contr_resp(j) = at33c_Pow_resp(j)/at33c_Pow_total(j);
at33c_contr_card(j) = at33c_Pow_card(j)/at33c_Pow_total(j);

at43c_contr_endo(j) = at43c_Pow_endo(j)/at43c_Pow_total(j);
at43c_contr_neuro(j) = at43c_Pow_neuro(j)/at43c_Pow_total(j);
at43c_contr_myo(j) = at43c_Pow_myo(j)/at43c_Pow_total(j);
at43c_contr_resp(j) = at43c_Pow_resp(j)/at43c_Pow_total(j);
at43c_contr_card(j) = at43c_Pow_card(j)/at43c_Pow_total(j);

end

%% create vector with frequencies

W = at33c_Hdsp2(1).Frequencies;
%%
for j=1:15
    at33c_Hdsp2_matrix(:,j) = at33c_Hdsp2(j).Data;
    at43c_Hdsp2_matrix(:,j) = at43c_Hdsp2(j).Data;
end
%%
mean_hpsd_at33 = mean(at33c_Hdsp2_matrix,2);
mean_hpsd_at43 = mean(at43c_Hdsp2_matrix,2);


%% plot frequency profiles
% frequency bands limits
fb0=0.005;
fb1=0.0095;
fb2=0.021;
fb3=0.052;
fb4=0.15;
fb5=0.6;
fb6=2;

l=ones(length(0:80),1);
figure(j)
% Change default axes fonts.
set(0,'DefaultAxesFontName', 'Calibri')
```

```
set(0,'DefaultAxesFontSize', 20)
set(0,'DefaultTextFontname', 'Calibri')
set(0,'DefaultTextFontSize', 20)
fontsize = 20;
hold on

plot(fb0*l,-40:40,'Color','black','LineWidth',2);
plot(fb1*l,-40:40,'Color','black','LineWidth',2);
plot(fb2*l,-40:40,'Color','black','LineWidth',2);
plot(fb3*l,-40:40,'Color','black','LineWidth',2);
plot(fb4*l,-40:40,'Color','black','LineWidth',2);
plot(fb5*l,-40:40,'Color','black','LineWidth',2);

for j=1:15
p5 = plot(at43c_Hdsp2(j));
p4 = plot(at33c_Hdsp2(j));
set(p5,'Color','green','LineWidth',1)
set(p4,'Color','blue','LineWidth',1);
end

p6 = plot(W,10*log10(mean_hpsd_at33));
p7 = plot(W,10*log10(mean_hpsd_at43));
set(p7,'Color','red','LineWidth',2)
set(p6,'Color','black','LineWidth',2)

set(gca);
% set(p4,'Color','black','LineStyle','--','LineWidth',1);
% set(p5,'Color','black','LineStyle',':','LineWidth',2);
% set(p6,'Color','black','LineStyle','-.','LineWidth',2);
axis([0.009 2 -40 40]);
set(gca, 'xscale','log', 'FontSize',fontsize);
%title('Average Scalogram','FontSize',12,'FontWeight','bold');
%legend(gca,'Flux1','Flux2','SO2');
h =[p4, p5, p6, p7];
legend(h,'Individual at 33{\circ}C','Individual at 43{\circ}C','Mean
at 33{\circ}C', 'Mean at 43{\circ}C');
set(legend,...
    'Position',[0.816399305555555 0.744033333333334 0.176829861111112
0.182266666666667]);

ylabel('PSD (PU^2/Hz)','FontSize',fontsize);% remember to change units
at different plots!
xlabel('Frequency (Hz)','FontSize',fontsize);
title('BF - individual and mean power spectral density at 33{\circ}C
and 43{\circ}C(n=15)', 'FontSize',18);
%title('SO_2 - individual and mean power spectral density at
33{\circ}C and 43{\circ}C(n=15)', 'FontSize',18);
%title('oxyHb - individual and mean power spectral density at
33{\circ}C and 43{\circ}C(n=15)', 'FontSize',18);

%title('SO_2 - individual and mean power spectral density at
33{\circ}C and 43{\circ}C(n=15)', 'FontSize',fontsize)

hold off
set(figure(j), 'Color', 'w');

l1 = annotation('textbox',[0.152041666666667 0.883898641588299
0.0823333333333333 0.029], 'String', 'Endothelial',
'FontSize',fontsize,'LineStyle','none');
```

```
l2 = annotation('textbox',[0.259541666666667 0.883898641588299
0.0823333333333333 0.029], 'String', 'Neurogenic',
'FontSize',fontsize,'LineStyle','none');
l3 = annotation('textbox',[0.388708333333333 0.883898641588299
0.0823333333333333 0.029], 'String', 'Myogenic',
'FontSize',fontsize,'LineStyle','none');
l4 = annotation('textbox',[0.542354166666666 0.883898641588299
0.0823333333333333 0.029], 'String', 'Respiratory',
'FontSize',fontsize,'LineStyle','none');
l5 = annotation('textbox',[0.736104166666667 0.883898641588299
0.0823333333333333 0.029], 'String', 'Cardiac',
'FontSize',fontsize,'LineStyle','none');

%% export figure
path = 'f:\My_folders\Work\matlab_all\heating\plots_PSD_5bands\';
cd(path);
set(figure(j), 'Color', 'w');
%pause;
export_fig(sprintf('Mean_PSD_33_43_sig_%d_%s_c.tiff', a, datestr(now,
1)), '-r300');
%%
```

Bibliography

Aalkjaer, C., Boedtkjer, D. & Matchkov, V. 2011. Vasomotion - what is currently thought? *Acta Physiol (Oxf),* 202**,** 253-69.

Addison, P. S., Walker, J. & Guido, R. C. 2009. Time--frequency analysis of biosignals. *Engineering in Medicine and Biology Magazine, IEEE,* 28**,** 14-29.

Agarwal, S. C., Allen, J., Murray, A. & Purcell, I. F. 2010. Comparative reproducibility of dermal microvascular blood flow changes in response to acetylcholine iontophoresis, hyperthermia and reactive hyperaemia. *Physiol Meas,* 31**,** 1-11.

Agarwal, S. C., Allen, J., Murray, A. & Purcell, I. F. 2012. Laser Doppler assessment of dermal circulatory changes in people with coronary artery disease. *Microvasc Res,* 84**,** 55-9.

Allen, J., Frame, J. R. & Murray, A. 2002. Microvascular blood flow and skin temperature changes in the fingers following a deep nspiratory gasp. *Physiol Meas,* 23**,** 365-73.

Anderson, M. E., Moore, T. L., Lunt, M. & Herrick, A. L. 2004. Digital iontophoresis of vasoactive substances as measured by laser Doppler imaging—a non-invasive technique by which to measure microvascular dysfunction in Raynaud's phenomenon. *Rheumatology,* 43**,** 986-991.

Andersson, S. E., Edvinsson, M. L., Alving, K. & Edvinsson, L. 2005. Vasodilator effect of endothelin in cutaneous microcirculation of heart failure patients. *Basic Clin Pharmacol Toxicol,* 97**,** 80-5.

Avery, M. R., Voegeli, D., Byrne, C. D., Simpson, D. M. & Clough, G. F. 2009. Age and cigarette smoking are independently associated with the cutaneous vascular response to local warming. *Microcirculation,* 16**,** 725-34.

Bangsbo, J., Krustrup, P., González-Alonso, J., Boushel, R. & Saltin, B. 2000. Muscle oxygen kinetics at onset of intense dynamic exercise in humans. *American Journal of Physiology - Regulatory, Integrative and Comparative Physiology,* 279**,** R899-R906.

Barun, V. V., Ivanov, A. P., Volotovskaya, A. V. & Ulashchik, V. S. 2007. Absorption spectra and light penetration depth of normal and pathologically altered human skin. *Journal of Applied Spectroscopy,* 74**,** 430-439.

Beckert, S., Witte, M. B., Königsrainer, A. & Coerper, S. 2004. The Impact of the Micro-Lightguide O2C for the Quantification of Tissue Ischemia in Diabetic Foot Ulcers. *Diabetes Care,* 27**,** 2863-2867.

Benedik, P. S. 2014. Monitoring Tissue Blood Flow and Oxygenation: A Brief Review of Emerging Techniques. *Crit Care Nurs Clin North Am,* 26**,** 345-356.

Bernjak, A., Cui, J., Iwase, S., Mano, T., Stefanovska, A. & Eckberg, D. L. 2012a. Human sympathetic outflows to skin and muscle target organs fluctuate concordantly over a wide range of time-varying frequencies. *J Physiol,* 590**,** 363-75.

Bernjak, A., Stefanovska, A., Mcclintock, P. V., Owen-Lynch, P. J. & Clarkson, P. B. M. 2012b. Coherence between fluctuations in bloof flow and oxygen saturation. *Fluctuation and Noise Letters,* 11**,** 1240013.

Bezemer, R., Dobbe, J., Bartels, S., Christiaan Boerma, E., Elbers, P. G., Heger, M. & Ince, C. 2011. Rapid automatic assessment of microvascular density in sidestream dark field images. *Medical & Biological Engineering & Computing,* 49**,** 1269-1278.

Binggeli, C., Spieker, L. E., Corti, R., Sudano, I., Stojanovic, V., Hayoz, D., Luscher, T. F. & Noll, G. 2003. Statins enhance postischemic hyperemia in the skin circulation of hypercholesterolemic patients: a monitoring test of endothelial dysfunction for clinical practice? *J Am Coll Cardiol,* 42**,** 71-7.

Binzoni, T., Cooper, C. E., Wittekind, A. L., Beneke, R., Elwell, C. E., Van De Ville, D. & Leung, T. S. 2010. A new method to measure local oxygen consumption in human skeletal muscle during dynamic exercise using near-infrared spectroscopy. *Physiol Meas,* 31**,** 1257-69.

Blaauw, J., Graaff, R., Van Pampus, M. G., Van Doormaal, J. J., Smit, A. J., Rakhorst, G. & Aarnoudse, J. G. 2005. Abnormal endothelium-dependent microvascular reactivity in recently preeclamptic women. *Obstet Gynecol,* 105**,** 626-32.

Blasi, R., Cope, M., Elwell, C., Safoue, F. & Ferrari, M. 1993. Noninvasive measurement of human forearm oxygen consumption by near infrared spectroscopy. *European Journal of Applied Physiology and Occupational Physiology,* 67**,** 20-25.

Boas, D. A., Elwell, C. E., Ferrari, M. & Taga, G. 2014. Twenty years of functional near-infrared spectroscopy: introduction for the special issue. *Neuroimage,* 85 Pt 1**,** 1-5.

Boas, D. A. & Franceschini, M. A. 2011. Haemoglobin oxygen saturation as a biomarker: the problem and a solution. *Philos Transact A Math Phys Eng Sci,* 369**,** 4407-24.

Boignard, A., Salvat-Melis, M., Carpentier, P., Minson, C., Grange, L., Duc, C., Sarrot-Reynauld, F. & Cracowski, J.-L. 2005. Local hyperhemia to heating is impaired in secondary Raynaud's phenomenon. *Arthritis Research & Therapy,* 7**,** 1-10.

Bonner, R. & Nossal, R. 1981. Model for laser Doppler measurements of blood flow in tissue. *Appl Opt,* 20**,** 2097-107.

Boyko, E. J., Ahroni, J. H. & Stensel, V. L. 2001. Tissue oxygenation and skin blood flow in the diabetic foot: responses to cutaneous warming. *Foot Ankle Int,* 22**,** 711-4.

Boyko, E. J., Ahroni, J. H., Stensel, V. L., Smith, D. G., Davignon, D. R. & Pecoraro, R. E. 1996. Predictors of transcutaneous oxygen tension in the lower limbs of diabetic subjects. *Diabet Med,* 13**,** 549-54.

Bracic, M., Mcclintock, P. V. E. & Stefanovska, A. 2000. Characteristic frequencies of the human blood distribution system. *Stochastic and chaotic dynamics in the lakes: STOCHAOS, Aip Conference Proceedings,* 502**,** 146-153.

Bracic, M. & Stefanovska, A. 1998. Wavelet-based analysis of human blood-flow dynamics. *Bull Math Biol,* 60**,** 919-35.

Braverman, I. M. 1997. The cutaneous microcirculation: ultrastructure and microanatomical organization. *Microcirculation,* 4**,** 329-40.

Braverman, I. M. 2000. The cutaneous microcirculation. *J Investig Dermatol Symp Proc,* 5**,** 3-9.

Buard, B., Mahé, G., Chapeau-Blondeau, F., Rousseau, D., Abraham, P. & Humeau, A. 2010. Laser Doppler flowmetry: multifractal spectra of signals recorded in hand of young healthy subjects before and after local heating. *In:* DÖSSEL, O. & SCHLEGEL, W. (eds.) *World Congress on Medical Physics and Biomedical Engineering, September 7 - 12, 2009, Munich, Germany.* Springer Berlin Heidelberg.

Buxton, R. B. & Frank, L. R. 1997. A model for the coupling between cerebral blood flow and oxygen metabolism during neural stimulation. *J Cereb Blood Flow Metab,* 17**,** 64-72.

Chang, C. H., Tsai, R. K., Wu, W. C., Kuo, S. L. & Yu, H. S. 1997. Use of dynamic capillaroscopy for studying cutaneous microcirculation in patients with diabetes mellitus. *Microvasc Res,* 53**,** 121-7.

Charkoudian, N. 2003. Skin blood flow in adult human thermoregulation: how it works, when it does not, and why. *Mayo Clin Proc,* 78**,** 603-12.

Chen, C.-L., Bojikian, K. D., Xin, C., Wen, J. C., Gupta, D., Zhang, Q., Mudumbai, R. C., Johnstone, M. A., Chen, P. P. & Wang, R. K. 2016. Repeatability and reproducibility of optic nerve head perfusion measurements using optical coherence tomography angiography. *Journal of Biomedical Optics,* 21**,** 065002-065002.

Clayton, R. H. & Murray, A. 1999. Coherence between body surface ECG leads and intracardiac signals increases during the first 10 s of ventricular fibrillation in the human heart. *Physiol Meas,* 20**,** 159-66.

Clifford, P. S. 2007. Skeletal muscle vasodilatation at the onset of exercise. *J Physiol,* 583**,** 825-33.

Clough, G., Chipperfield, A., Byrne, C., De Mul, F. & Gush, R. 2009. Evaluation of a new high power, wide separation laser Doppler probe: potential measurement of deeper tissue blood flow. *Microvasc Res,* 78**,** 155-61.

Cohen, N. D., Dunstan, D. W., Robinson, C., Vulikh, E., Zimmet, P. Z. & Shaw, J. E. 2008. Improved endothelial function following a 14-month resistance exercise training program in adults with type 2 diabetes. *Diabetes Res Clin Pract,* 79**,** 405-11.

Cosby, K., Partovi, K. S., Crawford, J. H., Patel, R. P., Reiter, C. D., Martyr, S., Yang, B. K., Waclawiw, M. A., Zalos, G., Xu, X., Huang, K. T., Shields, H., Kim-Shapiro, D. B., Schechter, A. N., Cannon, R. O. & Gladwin, M. T. 2003. Nitrite reduction to nitric oxide by deoxyhemoglobin vasodilates the human circulation. *Nature Medicine,* 9**,** 1498-1505.

Coulon, P., Constans, J. & Gosse, P. 2012. Impairment of skin blood flow during post-occlusive reactive hyperhemy assessed by laser Doppler flowmetry correlates with renal resistive index. *J.Hum.Hypertens.,* 26**,** 56-63.

Cracowski, J. L., Minson, C. T., Salvat-Melis, M. & Halliwill, J. R. 2006. Methodological issues in the assessment of skin microvascular endothelial function in humans. *Trends Pharmacol Sci,* 27**,** 503-8.

Cracowski, J. L. & Roustit, M. 2012. Reproducibility of LDF blood flow measurements: dynamical characterization versus averaging. A response to the letter from Stefanovska. *Microvasc Res,* 83**,** 97.

Cracowski, J. L. & Roustit, M. 2015. Current methods to assess human cutaneous blood flow. An updated focus on laser based-techniques. *Microcirculation*.

Cui, R., Zhang, M., Li, Z., Xin, Q., Lu, L., Zhou, W., Han, Q. & Gao, Y. 2014. Wavelet coherence analysis of spontaneous oscillations in cerebral tissue oxyhemoglobin concentrations and arterial blood pressure in elderly subjects. *Microvasc Res,* 93**,** 14-20.

Cutolo, M. & Smith, V. 2013. State of the art on nailfold capillaroscopy: a reliable diagnostic tool and putative biomarker in rheumatology? *Rheumatology (Oxford),* 52**,** 1933-40.

Czernichow, S., Greenfield, J. R., Galan, P., Jellouli, F., Safar, M. E., Blacher, J., Hercberg, S. & Levy, B. I. 2010. Macrovascular and microvascular dysfunction in the metabolic syndrome. *Hypertens Res,* 33**,** 293-7.

De Backer, D., Donadello, K. & Cortes, D. O. 2012. Monitoring the microcirculation. *J Clin Monit Comput,* 26**,** 361-6.

De Backer, D., Donadello, K., Taccone, F. S., Ospina-Tascon, G., Salgado, D. & Vincent, J. L. 2011. Microcirculatory alterations: potential mechanisms and implications for therapy. *Ann Intensive Care,* 1**,** 27.

De Backer, D., Ospina-Tascon, G., Salgado, D., Favory, R., Creteur, J. & Vincent, J. L. 2010. Monitoring the microcirculation in the critically ill patient: current methods and future approaches. *Intensive Care Med,* 36**,** 1813-25.

De Boer, M. P., Meijer, R. I., Wijnstok, N. J., Jonk, A. M., Houben, A. J., Stehouwer, C. D., Smulders, Y. M., Eringa, E. C. & Serné, E. H. 2012. Microvascular Dysfunction: A Potential Mechanism in the Pathogenesis of Obesity-associated Insulin Resistance and Hypertension. *Microcirculation,* 19**,** 5-18.

De Jongh, R. T., Serne, E. H., Rg, I. J., Jorstad, H. T. & Stehouwer, C. D. 2008. Impaired local microvascular vasodilatory effects of insulin and reduced skin microvascular vasomotion in obese women. *Microvasc Res,* 75**,** 256-62.

De Mul, F. F., Blaauw, J., Smit, R. J., Rakhorst, G. & Aarnoudse, J. G. 2009. Time development models for perfusion provocations studied with laser-Doppler flowmetry, applied to iontophoresis and PORH. *Microcirculation,* 16**,** 559-71.

Debbabi, H., Bonnin, P., Ducluzeau, P. H., Leftheriotis, G. & Levy, B. I. 2010. Noninvasive assessment of endothelial function in the skin microcirculation. *Am J Hypertens,* 23**,** 541-6.

Del Pozzi, A. T. & Hodges, G. J. 2014. To reheat, or to not reheat: that is the question: The efficacy of a local reheating protocol on mechanisms of cutaneous vasodilatation. *Microvasc Res,* 97C**,** 47-54.

Del Pozzi, A. T., Miller, J. T. & Hodges, G. J. 2016. The effect of heating rate on the cutaneous vasomotion responses of forearm and leg skin in humans. *Microvasc Res,* 105**,** 77-84.

Dunaev, A. V., Sidorov, V. V., Krupatkin, A. I., Rafailov, I. E., Palmer, S. G., Stewart, N. A., Sokolovski, S. G. & Rafailov, E. U. 2014. Investigating tissue respiration and skin microhaemocirculation under adaptive changes and the synchronization of blood flow and oxygen saturation rhythms. *Physiol Meas,* 35**,** 607-21.

Durand, S., Tartas, M., Bouye, P., Koitka, A., Saumet, J. L. & Abraham, P. 2004. Prostaglandins participate in the late phase of the vascular response to acetylcholine iontophoresis in humans. *J Physiol,* 561**,** 811-9.

Durduran, T., Choe, R., Baker, W. B. & Yodh, A. G. 2010. Diffuse optics for tissue monitoring and tomography. *Reports on Progress in Physics,* 73**,** 076701.

Eberl, N., Piehlmeier, W., Dachauer, S., Konig, A., Land, W. & Landgraf, R. 2005. Blood flow in the skin of type 1 diabetic patients before and after combined pancreas/kidney transptantation. *Diabetes-Metabolism Research and Reviews,* 21**,** 525-532.

Ekbal, N. J., Dyson, A., Black, C. & Singer, M. 2013. MOnitoring tissue perfusion, oxygenation, and metabolism in critically ill patients. *CHEST Journal,* 143**,** 1799-1808.

Elliott, M., Tate, R. & Page, K. 2006. Do clinicians know how to use pulse oximetry? A literature review and clinical implications. *Australian Critical Care,* 19**,** 139-144.

Esen, F., Aydin, G. S. & Esen, H. 2009. Detrended fluctuation analysis of laser Doppler flowmetry time series. *Microvasc Res,* 78**,** 314-8.

Esen, F., Caglar, S., Ata, N., Ulus, T., Birdane, A. & Esen, H. 2011. Fractal scaling of laser Doppler flowmetry time series in patients with essential hypertension. *Microvasc Res,* 82**,** 291-5.

Esen, H., Ata, N. & Esen, F. 2014. Transitions in skin blood flow fractal scaling: The importance of fluctuation amplitude in microcirculation. *Microvasc Res,* 97C**,** 6-12.

Fedorovich, A. A. 2012. Non-invasive evaluation of vasomotor and metabolic functions of microvascular endothelium in human skin. *Microvasc Res,* 84**,** 86-93.

Feger, J. & Braune, S. 2005. Measurement of skin vasoconstrictor response in healthy subjects. *Auton Neurosci,* 120**,** 88-96.

Feihl, F., Liaudet, L. & Waeber, B. 2009. The macrocirculation and microcirculation of hypertension. *Curr Hypertens Rep,* 11**,** 182-9.

Ferrari, M., Muthalib, M. & Quaresima, V. 2011. The use of near-infrared spectroscopy in understanding skeletal muscle physiology: recent developments. *Philos Transact A Math Phys Eng Sci,* 369**,** 4577-90.

Figoni, S. F., Scremin, O. U., Kunkel, C. F., Opava-Rutter, D., Johnson, J., Schmitter, E. D. & Scremin, A. M. 2006. Preamputation evaluation of limb perfusion with laser Doppler imaging and transcutaneous gases. *J Rehabil Res Dev,* 43**,** 891-904.

Figueiras, E., Roustit, M., Semedo, S., Ferreira, L. F., Crascowski, J. L. & Humeau, A. 2011. Sample entropy of laser Doppler flowmetry signals increases in patients with systemic sclerosis. *Microvasc Res,* 82**,** 152-5.

Forst, T., Hohberg, C., Tarakci, E., Forst, S., Kann, P. & Pfutzner, A. 2008. Reliability of lightguide spectrophotometry (O2C) for the investigation of skin tissue microvascular blood flow and tissue oxygen supply in diabetic and nondiabetic subjects. *J Diabetes Sci Technol,* 2**,** 1151-6.

Fredriksson, I., Fors, C. & Johansson, J. 2007. *Laser Doppler Flowmetry - a Theoretical Framework.* Linköping University.

Fredriksson, I., Larsson, M. & Stromberg, T. 2008. Optical microcirculatory skin model: assessed by Monte Carlo simulations paired with in vivo laser Doppler flowmetry. *J Biomed Opt,* 13**,** 014015.

Fromy, B., Abraham, P., Bouvet, C., Bouhanick, B., Fressinaud, P. & Saumet, J. L. 2002. Early Decrease of Skin Blood Flow in Response to Locally Applied Pressure in Diabetic Subjects. *Diabetes,* 51**,** 1214-1217.

Fukuda, M. 2012. Near-infrared spectroscopy in psychiatry. *Brain Nerve,* 64**,** 175-83.

Gambichler, T., Pljakic, A. & Schmitz, L. 2015. Recent advances in clinical application of optical coherence tomography of human skin. *Clin Cosmet Investig Dermatol,* 8**,** 345-54.

Gélis, A., Fattal, C., Dupeyron, A., Pérez-Martin, A., Colin, D. & Pelissier, J. 2009. Reproducibility of Transcutaneous Oxygen Pressure Measurements in Persons With Spinal Cord Injury. *Archives of Physical Medicine and Rehabilitation,* 90**,** 507-511.

Geyer, M. J., Jan, Y. K., Brienza, D. M. & Boninger, M. L. 2004. Using wavelet analysis to characterize the thermoregulatory mechanisms of sacral skin blood flow. *J Rehabil Res Dev,* 41**,** 797-806.

Gooding, K. M., Hannemann, M. M., Tooke, J. E., Clough, G. F. & Shore, A. C. 2006. Maximum skin hyperaemia induced by local heating: possible mechanisms. *J Vasc Res,* 43**,** 270-7.

Grattagliano, V., Iannone, F., Praino, E., De Zio, A., Riccardi, M. T., Carrozzo, N., Covelli, M., Maggi, P. & Lapadula, G. 2010. Digital laser doppler flowmetry may discriminate "limited" from "diffuse" systemic sclerosis. *Microvasc Res,* 80**,** 221-6.

Green, D. J., Maiorana, A. J., Siong, J. H. J., Burke, V., Erickson, M., Minson, C. T., Bilsborough, W. & O'driscoll, G. 2006. Impaired skin blood flow response to environmental heating in chronic heart failure. *European Heart Journal,* 27**,** 338-343.

Gregson, W., Black, M. A., Jones, H., Milson, J., Morton, J., Dawson, B., Atkinson, G. & Green, D. J. 2011. Influence of cold water immersion on limb and cutaneous blood flow at rest. *Am J Sports Med,* 39**,** 1316-23.

Gunawardena, H., Harris, N. D., Carmichael, C. & Mchugh, N. J. 2007. Maximum blood flow and microvascular regulatory responses in systemic sclerosis. *Rheumatology,* 46**,** 1079-1082.

Gurley, K., Shang, Y. & Yu, G. 2012. Noninvasive optical quantification of absolute blood flow, blood oxygenation, and oxygen consumption rate in exercising skeletal muscle. *J Biomed Opt,* 17**,** 075010.

Gush, R. J., King, T. A. & Jayson, M. I. V. 1984. Aspects of laser light scattering from skin tissue with application to laser Doppler blood flow measurement. *Physics in Medicine and Biology,* 29**,** 1463-1476.

Han, Q., Zhang, M., Li, W., Gao, Y., Xin, Q., Wang, Y. & Li, Z. 2014. Wavelet coherence analysis of prefrontal tissue oxyhaemoglobin signals as measured using near-infrared spectroscopy in elderly subjects with cerebral infarction. *Microvasc Res,* 95C**,** 108-115.

Hannemann, M. M., Liddell, W. G., Shore, A. C., Clark, P. M. & Tooke, J. E. 2002. Vascular function in women with previous gestational diabetes mellitus. *J Vasc Res,* 39**,** 311-9.

Hansell, J., Henareh, L., Agewall, S. & Norman, M. 2004. Non-invasive assessment of endothelial function - relation between vasodilatory responses in skin microcirculation and brachial artery. *Clin Physiol Funct Imaging,* 24**,** 317-22.

Henton, J. M., Simmons, J. M., Hettiaratchy, S. & Jain, A. 2015. Perfusion dynamics in lower limb reconstruction: Investigating postoperative recovery and training using combined white light photospectroscopy and laser Doppler (O2C((R))). *J Plast Reconstr Aesthet Surg,* 68**,** 1286-92.

Hodges, G. J. & Del Pozzi, A. T. 2014. Noninvasive examination of endothelial, sympathetic, and myogenic contributions to regional differences in the human cutaneous microcirculation. *Microvasc Res,* 93**,** 87-91.

Hodges, G. J., Zhao, K., Kosiba, W. A. & Johnson, J. M. 2006. The involvement of nitric oxide in the cutaneous vasoconstrictor response to local cooling in humans. *J Physiol,* 574**,** 849-57.

Holowatz, L. A., Thompson-Torgerson, C. S. & Kenney, W. L. 2008. The human cutaneous circulation as a model of generalized microvascular function. *Journal of Applied Physiology,* 105**,** 370-372.

Hsiu, H., Hsu, C. L., Hu, H.-F., Hsiao, F.-C. & Yang, S.-H. 2014. Complexity analysis of beat-to-beat skin-surface laser-Doppler signals in diabetic subjects. *Microvascular Research,* 93**,** 9-13.

Huang, H. W., Jou, I. M., Wang, C. K., Chen, P. Y., Wang, W. C. & Lin, C. C. 2011. Power spectral analyses of index finger skin blood perfusion in carpal tunnel syndrome and diabetic polyneuropathy. *Exp Diabetes Res,* 2011**,** 465910.

Humeau-Heurtier, A., Guerreschi, E., Abraham, P. & Mahe, G. 2013. Relevance of laser Doppler and laser speckle techniques for assessing vascular function: state of the art and future trends. *IEEE Trans Biomed Eng,* 60**,** 659-66.

Humeau-Heurtier, A. & Klonizakis, M. 2015. Processing of laser Doppler flowmetry signals from healthy subjects and patients with varicose veins: Information categorisation approach based on intrinsic mode functions and entropy computation. *Med Eng Phys,* 37**,** 553-9.

Humeau, A., Buard, B., Mahe, G., Rousseau, D., Chapeau-Blondeau, F. & Abraham, P. 2010. Multiscale entropy of laser Doppler flowmetry signals in healthy human subjects. *Med.Phys.,* 37**,** 6142-6146.

Humeau, A., Chapeau-Blondeau, F., Rousseau, D., Rousseau, P., Trzepizur, W. & Abraham, P. 2008. Multifractality, sample entropy, and wavelet analyses for age-related changes in the peripheral cardiovascular system: preliminary results. *Med.Phys.,* 35**,** 717-723.

Humeau, A., Saumet, J. L. & L'huillier, J. P. 2000. Use of Wavelets to Accurately Determine Parameters of Laser Doppler Reactive Hyperemia. *Microvasc Res,* 60**,** 141-148.

Humeau, A., Steenbergen, W., Nilsson, H. & Stromberg, T. 2007. Laser Doppler perfusion monitoring and imaging: novel approaches. *Med Biol Eng Comput,* 45**,** 421-35.

Iabichella, M. L., Melillo, E. & Mosti, G. 2006. A review of microvascular measurements in wound healing. *Int J Low Extrem Wounds,* 5**,** 181-99.

Ikawa, M. & Karita, K. 2015. Relation between blood flow and tissue blood oxygenation in human fingertip skin. *Microvasc Res,* 101**,** 135-42.

Ingegnoli, F., Gualtierotti, R., Lubatti, C., Zahalkova, L., Meani, L., Boracchi, P., Zeni, S. & Fantini, F. 2009. Feasibility of different capillaroscopic measures for identifying nailfold microvascular alterations. *Semin Arthritis Rheum,* 38**,** 289-95.

Ioannidis, J. P. 2005. Why most published research findings are false. *PLoS Med,* 2**,** e124.

Jaffer, U., Aslam, M. & Standfield, N. 2008. Impaired Hyperaemic and Rhythmic Vasomotor Response in Type 1 Diabetes Mellitus Patients: A Predictor of Early Peripheral Vascular Disease. *European Journal of Vascular and Endovascular Surgery,* 35**,** 603-606.

Jakobsson, A. & Nilsson, G. E. 1993. Prediction of sampling depth and photon pathlength in laser Doppler flowmetry. *Medical and Biological Engineering and Computing,* 31**,** 301-307.

Jan, Y.-K., Shen, S., Foreman, R. D. & Ennis, W. J. 2013. Skin blood flow response to locally applied mechanical and thermal stresses in the diabetic foot. *Microvascular Research,* 89**,** 40-46.

Jan, Y.-K., Struck, B. D., Foreman, R. D. & Robinson, C. 2009. Wavelet analysis of sacral skin blood flow oscillations to assess soft tissue viability in older adults. *Microvascular Research,* 78**,** 162-168.

Johnson, J. M. & Kellogg, D. L. 2010. Local thermal control of the human cutaneous circulation. *Journal of Applied Physiology,* 109**,** 1229-1238.

Jorneskog, G., Djavani, K. & Brismar, K. 2001. Day-to-day variability of transcutaneous oxygen tension in patients with diabetes mellitus and peripheral arterial occlusive disease. *J Vasc Surg,* 34**,** 277-82.

Joshi, D., Shiwalkar, A., Cross, M. R., Sharma, S. K., Vachhani, A. & Dutt, C. 2010. Continuous, non-invasive measurement of the haemodynamic response to submaximal exercise in

patients with diabetes mellitus: evidence of impaired cardiac reserve and peripheral vascular response. *Heart,* 96**,** 36-41.

Jue, T. & Masuda, K. 2013. *Application of Near Infrared Spectroscopy in Biomedicine*, Springer US.

Kelechi, T. J. & Michel, Y. 2007. A descriptive study of skin temperature, tissue perfusion, and tissue oxygen in patients with chronic venous disease. *Biol Res Nurs,* 9**,** 70-80.

Kellogg, D. L., Jr. 2006. In vivo mechanisms of cutaneous vasodilation and vasoconstriction in humans during thermoregulatory challenges. *J Appl Physiol (1985),* 100**,** 1709-18.

Kernick, P. D., Tooke, E. J. & Shore, C. A. 1999. The biological zero signal in laser doppler fluximetry – origins and practical implications. *Pflügers Archiv* 437**,** 624-631.

Khan, F. & Belch, J. J. 1999. Skin blood flow in patients with systemic sclerosis and Raynaud's phenomenon: effects of oral L-arginine supplementation. *J Rheumatol,* 26**,** 2389-94.

Kim, M. N., Durduran, T., Frangos, S., Edlow, B. L., Buckley, E. M., Moss, H. E., Zhou, C., Yu, G., Choe, R., Maloney-Wilensky, E., Wolf, R. L., Grady, M. S., Greenberg, J. H., Levine, J. M., Yodh, A. G., Detre, J. A. & Kofke, W. A. 2010. Noninvasive measurement of cerebral blood flow and blood oxygenation using near-infrared and diffuse correlation spectroscopies in critically brain-injured adults. *Neurocrit Care,* 12**,** 173-80.

Klonizakis, M., Manning, G. & Donnelly, R. 2011. Assessment of lower limb microcirculation: exploring the reproducibility and clinical application of laser Doppler techniques. *Skin Pharmacol Physiol,* 24**,** 136-43.

Kolarsick, P. a. J., Kolarsick, M. A. & Goodwin, C. 2009. Anatomy and Physiology of the Skin (Chapter 1). *In:* MUELHBAUER, P. & MCGOWAN, C. (eds.) *Site-Specific Cancer Series: Skin Cancer.* Oncology Nursing Society.

Kooijman, M., Poelkens, F., Rongen, G., Smits, P. & Hopman, M. E. 2007. Leg blood flow measurements using venous occlusion plethysmography during head-up tilt. *Clinical Autonomic Research,* 17**,** 106-111.

Korthuis, R. J. 2011. *Skeletal Muscle Circulation*, Morgan & Claypool Life Sciences.

Kragelj, R., Jarm, T. & Miklavčič, D. 2000. Reproducibility of Parameters of Postocclusive Reactive Hyperemia Measured by Near Infrared Spectroscopy and Transcutaneous Oximetry. *Annals of Biomedical Engineering,* 28**,** 168-173.

Kruger, A., Stewart, J., Sahityani, R., O'riordan, E., Thompson, C., Adler, S., Garrick, R., Vallance, P. & Goligorsky, M. S. 2006. Laser Doppler flowmetry detection of endothelial dysfunction in end-stage renal disease patients: Correlation with cardiovascular risk. *Kidney Int,* 70**,** 157-164.

Kuck, M., Strese, H., Alawi, S. A., Meinke, M. C., Fluhr, J. W., Burbach, G. J., Krah, M., Sterry, W. & Lademann, J. 2014. Evaluation of optical coherence tomography as a non-invasive diagnostic tool in cutaneous wound healing. *Skin Res Technol,* 20**,** 1-7.

Kuliga, K. Z., Mcdonald, E. F., Gush, R., Michel, C. C., Chipperfield, A. J. & Clough, G. F. 2014. Dynamics of microvascular blood flow and oxygenation measured simultaneously in human skin. *Microcirculation,* 21**,** 562-573.

Kume, D., Akahoshi, S., Song, J., Yamagata, T., Wakimoto, T., Nagao, M., Matsueda, S. & Nagao, N. 2013. Intermittent breath holding during moderate bicycle exercise provokes consistent changes in muscle oxygenation and greater blood lactate response. *J Sports Med Phys Fitness,* 53**,** 327-35.

Kvandal, P., Landsverk, S. A., Bernjak, A., Stefanovska, A., Kvernmo, H. D. & Kirkebøen, K. A. 2006. Low-frequency oscillations of the laser Doppler perfusion signal in human skin. *Microvascular Research,* 72**,** 120-127.

Kvandal, P., Stefanovska, A., Veber, M., Désirée Kvermmo, H. & Arvid Kirkebøen, K. 2003. Regulation of human cutaneous circulation evaluated by laser Doppler flowmetry, iontophoresis, and spectral analysis: importance of nitric oxide and prostaglandines. *Microvascular Research,* 65**,** 160-171.

Kvernmo, H., Stefanovska, A. & Kirkebøen, K. 2003. Enhanced endothelial activity reflected in cutaneous blood flow oscillations of athletes. *European Journal of Applied Physiology,* 90**,** 16-22.

L'esperance, V. S., Cox, S. E., Simpson, D., Gill, C., Makani, J., Soka, D., Mgaya, J., Kirkham, F. J. & Clough, G. F. 2013. Peripheral vascular response to inspiratory breath hold in paediatric homozygous sickle cell disease. *Exp Physiol,* 98**,** 49-56.

Larsson, M., Steenbergen, W. & Stromberg, T. 2002. Influence of optical properties and fiber separation on laser doppler flowmetry. *J Biomed Opt,* 7**,** 236-43.

Lenasi, H. 2011. Assessment of Human Skin Microcirculation and Its Endothelial Function Using Laser Doppler Flowmetry. *In:* ERONDU, O. F. (ed.) *Medical Imaging.* InTech.

Li, Z., Wang, Y., Li, Y., Wang, Y., Li, J. & Zhang, L. 2010. Wavelet analysis of cerebral oxygenation signal measured by near infrared spectroscopy in subjects with cerebral infarction. *Microvasc Res,* 80**,** 142-7.

Li, Z., Zhang, M., Xin, Q., Luo, S., Zhou, W., Cui, R. & Lu, L. 2013. Assessment of cerebral oxygenation oscillations in subjects with hypertension. *Microvasc Res,* 88**,** 32-41.

Liao, F. & Jan, Y.-K. 2011. Using multifractal detrended fluctuation analysis to assess sacral skin blood flow oscillations in people with spinal cord injury. *Journal of Rehabilitation Research & Development,* 48**,** 787-800.

Liao, F. & Jan, Y.-K. 2012. Enhanced phase synchronization of blood flow oscillations between heated and adjacent non-heated sacral skin. *Med Biol Eng Comput,* 50**,** 1059-70.

Lin, Y., He, L., Shang, Y. & Yu, G. 2012. Noncontact diffuse correlation spectroscopy for noninvasive deep tissue blood flow measurement. *Journal of Biomedical Optics,* 17**,** 010502-1.

Liu, F. W. H., Levinson, C. J., Murphy, A. L., Benaron, D. A., Parachikov, I. H., Cheong, W.-F., Friedland, S., Rubinsky, B. E., Otten, D. M., Price, J. W., Talmi, Y., Weersing, J. P., Duckworth, J. L., Hörchner, U. B. & Kermit, E. L. 2005. Design of a visible-light spectroscopy clinical tissue oximeter. *Journal of Biomedical Optics,* 10**,** 044005-044005-9.

Liu, H. L., Huang, J., Wu, C. T. & Hsu, Y. Y. 2002. Detectability of blood oxygenation level-dependent signal changes during short breath hold duration. *Magn Reson Imaging,* 20**,** 643-8.

Lotrič Bračič, M. & Stefanovska, A. 2000. Synchronization and modulation in the human cardiorespiratory system. *Physica A: Statistical Mechanics and its Applications,* 283**,** 451-461.

Lu, H., Golay, X., Pekar, J. J. & Van Zijl, P. C. 2004. Sustained poststimulus elevation in cerebral oxygen utilization after vascular recovery. *J Cereb Blood Flow Metab,* 24**,** 764-70.

Mahé, G., Humeau-Heurtier, A., Durand, S., Leftheriotis, G. & Abraham, P. 2012. Assessment of Skin Microvascular Function and Dysfunction With Laser Speckle Contrast Imaging. *Circulation: Cardiovascular Imaging,* 5**,** 155-163.

Mars, M., Mckune, A. & Robbs, J. V. 1998. A comparison of laser Doppler fluxmetry and transcutaneous oxygen pressure measurement in the dysvascular patient requiring amputation. *European Journal of Vascular and Endovascular Surgery,* 16**,** 53-58.

Martin, D. S., Goedhart, P., Vercueil, A., Ince, C., Levett, D. Z., Grocott, M. P. & Caudwell Xtreme Everest Research, G. 2010. Changes in sublingual microcirculatory flow index and vessel density on ascent to altitude. *Exp Physiol,* 95**,** 880-91.

Mathieu, D. & Mani, R. 2007. A review of the clinical significance of tissue hypoxia measurements in lower extremity wound management. *Int J Low Extrem Wounds,* 6**,** 273-83.

Melik, Z., Kobal, J., Cankar, K. & Strucl, M. 2012. Microcirculation response to local cooling in patients with Huntington's disease. *Journal of Neurology,* 259**,** 921-928.

Mesquita, R. C., Durduran, T., Yu, G., Buckley, E. M., Kim, M. N., Zhou, C., Choe, R., Sunar, U. & Yodh, A. G. 2011. Direct measurement of tissue blood flow and metabolism with diffuse optics. *Philos Transact A Math Phys Eng Sci,* 369**,** 4390-406.

Messere, A. & Roatta, S. 2013. Influence of cutaneous and muscular circulation on spatially resolved versus standard Beer-Lambert near-infrared spectroscopy. *Physiol Rep,* 1**,** e00179.

Minson, C. T. 2010. Thermal provocation to evaluate microvascular reactivity in human skin. *J Appl Physiol,* 109**,** 1239-46.

Mintun, M. A., Lundstrom, B. N., Snyder, A. Z., Vlassenko, A. G., Shulman, G. L. & Raichle, M. E. 2001. Blood flow and oxygen delivery to human brain during functional activity: theoretical modeling and experimental data. *Proc Natl Acad Sci USA,* 98**,** 6859-64.

Miranda De Sá, A. M. F. L., Infantosi, A. F. C. & Simpson, D. M. 2002. Coherence between one random and one periodic signal for measuring the strength of responses in the electro-encephalogram during sensory stimulation. *Medical and Biological Engineering and Computing,* 40**,** 99-104.

Mirzabeigi, M. N., Wang, T., Kovach, S. J., Taylor, J. A., Serletti, J. M. & Wu, L. C. 2012. Free flap take-back following postoperative microvascular compromise: predicting salvage versus failure. *Plast Reconstr Surg,* 130**,** 579-89.

Monostori, P., Baráth, Á., Fazekas, I., Hódi, E., Máté, A., Farkas, I., Hracskó, Z., Varga, I., Sümegi, V., Gellén, B., Bereczki, C. & Túri, S. 2010. Microvascular reactivity in lean, overweight, and obese hypertensive adolescents. *European Journal of Pediatrics,* 169**,** 1369-1374.

Morales, F., Graaff, R., Smit, A. J., Bertuglia, S., Petoukhova, A. L., Steenbergen, W., Leger, P. & Rakhorst, G. 2005. How to assess post-occlusive reactive hyperaemia by means of laser Doppler perfusion monitoring: Application of a standardised protocol to patients with peripheral arterial obstructive disease. *Microvascular Research,* 69**,** 17-23.

Morales, F., Graaff, R., Smit, A. J., Gush, R. & Rakhorst, G. 2003. The influence of probe fiber distance on laser Doppler perfusion monitoring measurements. *Microcirculation,* 10**,** 433-441.

Morlet, J., Arens, G., Fourgeau, E. & Glard, D. 1983. Wave propagation and sampling theory. Part I: Complex signal and scattering in multilayered media. *Geophysics,* 47**,** 203-221.

Morris, S. J. & Shore, A. C. 1996. Skin blood flow responses to the iontophoresis of acetylcholine and sodium nitroprusside in man: possible mechanisms. *J Physiol,* 496 (Pt 2)**,** 531-42.

Mucke, T., Rau, A., Merezas, A., Kanatas, A., Mitchell, D. A., Wagenpfeil, S., Wolff, K. D. & Steiner, T. 2014. Changes of perfusion of microvascular free flaps in the head and neck: a prospective clinical study. *Br J Oral Maxillofac Surg,* 52**,** 810-5.

Murkin, J. M. & Arango, M. 2009. Near-infrared spectroscopy as an index of brain and tissue oxygenation. *British Journal of Anaesthesia,* 103**,** i3-i13.

Nhs. 2012. *Cardiovascular disease* [Online]. The Department of Health. Available: http://www.nhs.uk/Conditions/cardiovascular-disease/Pages/Introduction.aspx.

Nilsson, G. E., Tenland, T. & Oberg, P. A. 1980. A New Instrument for Continuous Measurement of Tissue Blood Flow by Light Beating Spectroscopy. *Biomedical Engineering, IEEE Transactions on,* BME-27**,** 12-19.

Nyberg, M., Mortensen, S. P., Saltin, B., Hellsten, Y. & Bangsbo, J. 2010. Low blood flow at onset of moderate-intensity exercise does not limit muscle oxygen uptake. *Am J Physiol Regul Integr Comp Physiol,* 298**,** R843-8.

Pachauri, N. & Mishra, D. K. 2012. Phase Synchronization and Coherence Analysis between ECG & Arterial Blood Pressure. *International Journal of Computer Applications,* 44**,** 27-80.

Paulson, O. B., Hasselbalch, S. G., Rostrup, E., Knudsen, G. M. & Pelligrino, D. 2010. Cerebral blood flow response to functional activation. *J Cereb Blood Flow Metab,* 30**,** 2-14.

Pellicer, A. & Bravo, M. D. C. 2011. Near-infrared spectroscopy: A methodology-focused review. *Seminars in Fetal and Neonatal Medicine,* 16**,** 42-49.

Pereda, E., Quiroga, R. Q. & Bhattacharya, J. 2005. Nonlinear multivariate analysis of neurophysiological signals. *Progress in Neurobiology,* 77**,** 1-37.

Petrie, J. R., Ueda, S., Morris, A. D., Murray, L. S., Elliott, H. L. & Connell, J. M. 1998. How reproducible is bilateral forearm plethysmography? *Br J Clin Pharmacol,* 45**,** 131-9.

Piotrowski, L., Urbaniak, M., Jedrzejczak, B., Marcinek, A. & Gebicki, J. 2016. Note: Flow mediated skin fluorescence-A novel technique for evaluation of cutaneous microcirculation. *Rev Sci Instrum,* 87**,** 036111.

Pittman, R. N. 2005. Oxygen transport and exchange in the microcirculation. *Microcirculation,* 12**,** 59-70.

Pittman, R. N. 2012. Oxygen transport in the microcirculation and its regulation. *Microcirculation*.

Poredos, P., Rakovec, S. & Guzic-Salobir, B. 2005. Determination of amputation level in ischaemic limbs using tcPO2 measurement. *Vasa,* 34**,** 108-12.

Poublanc, J., Han, J. S., Mandell, D. M., Conklin, J., Stainsby, J. A., Fisher, J. A., Mikulis, D. J. & Crawley, A. P. 2013. Vascular steal explains early paradoxical blood oxygen level-dependent cerebrovascular response in brain regions with delayed arterial transit times. *Cerebrovasc Dis Extra,* 3**,** 55-64.

Prazny, M., Kasalova, Z., Mazoch, J., Kvasnicka, J. & Skrha, J. 2009. Microvascular Reactivity and Endothelial Function in Type 2 Diabetic Patients with Hyperlipidemia Treated with Simvastatin: 3-year Follow-up. *Prague Med Rep,* 110**,** 290-300.

Qi, W. 2011. *Fourier and wavelet analysis of skin laser Doppler flowmetry signals.* Thesis (M.Phil.), University of Southampton.

Quattrini, C., Harris, N. D., Malik, R. A. & Tesfaye, S. 2007. Impaired skin microvascular reactivity in painful diabetic neuropathy. *Diabetes Care,* 30**,** 655-9.

Rajan, V., Varghese, B., Van Leeuwen, T. G. & Steenbergen, W. 2009. Review of methodological developments in laser Doppler flowmetry. *Lasers Med Sci,* 24**,** 269-83.

Rich, K. 2001. Transcutaneous oxygen measurements: Implications for nursing. *Journal of Vascular Nursing,* 19**,** 55-61.

Ropella, K. M., Sahakian, A. V., Baerman, J. M. & Swiryn, S. 1989. The coherence spectrum. A quantitative discriminator of fibrillatory and nonfibrillatory cardiac rhythms. *Circulation,* 80**,** 112-119.

Rossi, M., Bertuglia, S., Varanini, M., Giusti, A., Santoro, G. & Carpi, A. 2005a. Generalised wavelet analysis of cutaneous flowmotion during post-occlusive reactive hyperaemia in patients with peripheral arterial obstructive disease. *Biomed Pharmacother,* 59**,** 233-9.

Rossi, M., Bradbury, A., Magagna, A., Pesce, M., Taddei, S. & Stefanovska, A. 2011. Investigation of skin vasoreactivity and blood flow oscillations in hypertensive patients: effect of short-term antihypertensive treatment. *J Hypertens,* 29**,** 1569-76.

Rossi, M. & Carpi, A. 2004. Skin microcirculation in peripheral arterial obliterative disease. *Biomed Pharmacother,* 58**,** 427-31.

Rossi, M., Maurizio, S. & Carpi, A. 2005b. Skin blood flowmotion response to insulin iontophoresis in normal subjects. *Microvasc Res,* 70**,** 17-22.

Roustit, M., Blaise, S., Millet, C. & Cracowski, J. L. 2010a. Reproducibility and methodological issues of skin post-occlusive and thermal hyperemia assessed by single-point laser Doppler flowmetry. *Microvasc.Res.,* 79**,** 102-108.

Roustit, M., Blaise, S., Millet, C. & Cracowski, J. L. 2011. Impaired transient vasodilation and increased vasoconstriction to digital local cooling in primary Raynaud's phenomenon. *Am J Physiol Heart Circ Physiol,* 301**,** H324-30.

Roustit, M. & Cracowski, J.-L. 2012. Non-invasive Assessment of Skin Microvascular Function in Humans: An Insight Into Methods. *Microcirculation,* 19**,** 47-64.

Roustit, M. & Cracowski, J.-L. 2013. Assessment of endothelial and neurovascular function in human skin microcirculation. *Trends in Pharmacological Sciences,* 34**,** 373-384.

Roustit, M., Maggi, F., Isnard, S., Hellmann, M., Bakken, B. & Cracowski, J. L. 2010b. Reproducibility of a local cooling test to assess microvascular function in human skin. *Microvasc Res,* 79**,** 34-39.

Roustit, M., Simmons, G. H., Carpentier, P. & Cracowski, J. L. 2008. Abnormal digital neurovascular response to local heating in systemic sclerosis. *Rheumatology,* 47**,** 860-864.

Şahin, İ., Simaan, M. A. & Kearsley, A. J. 2014. Successive frequency domain minimization for time delay estimation. *Signal Processing,* 98**,** 96-101.

Sakr, Y. 2010. Techniques to assess tissue oxygenation in the clinical setting. *Transfus Apher Sci,* 43**,** 79-94.

Sakr, Y., Dubois, M. J., De Backer, D., Creteur, J. & Vincent, J. L. 2004. Persistent microcirculatory alterations are associated with organ failure and death in patients with septic shock. *Crit Care Med,* 32**,** 1825-31.

Sampoalesi, J. R. 2012. *Laser Scanning: Update 1: First Official Publication of the International Society of Laser Scanning: INSOLAS*, Springer Netherlands.

Sax, F. L., Cannon, R. O., 3rd, Hanson, C. & Epstein, S. E. 1987. Impaired forearm vasodilator reserve in patients with microvascular angina. Evidence of a generalized disorder of vascular function? *N Engl J Med,* 317**,** 1366-70.

Scheeren, T. W., Schober, P. & Schwarte, L. A. 2012. Monitoring tissue oxygenation by near infrared spectroscopy (NIRS): background and current applications. *J Clin Monit Comput,* 26**,** 279-87.

Schroeter, M. L., Schmiedel, O. & Von Cramon, D. Y. 2004. Spontaneous Low-Frequency Oscillations Decline in the Aging Brain. *J Cereb Blood Flow Metab,* 24**,** 1183-1191.

Secomb, T. W. & Pries, A. R. 2011. The microcirculation: physiology at the mesoscale. *The Journal of Physiology,* 589**,** 1047-1052.

Sekiyama, J. Y., Camargo, C. Z., Andrade, L. E. C. & Kayser, C. 2013. Reliability of Widefield Nailfold Capillaroscopy and Videocapillaroscopy in the Assessment of Patients With Raynaud's Phenomenon. *Arthritis Care & Research,* 65**,** 1853-1861.

Selber, J. C., Angel Soto-Miranda, M., Liu, J. & Robb, G. 2012. The survival curve: factors impacting the outcome of free flap take-backs. *Plast Reconstr Surg,* 130**,** 105-13.

Shang, Y., Gurley, K., Symons, B., Long, D., Srikuea, R., Crofford, L., Peterson, C. & Yu, G. 2012. Noninvasive optical characterization of muscle blood flow, oxygenation, and metabolism in women with fibromyalgia. *Arthritis Research & Therapy,* 14**,** 1-12.

Shang, Y., Zhao, Y., Cheng, R., Dong, L., Irwin, D. & Yu, G. 2009. Portable optical tissue flow oximeter based on diffuse correlation spectroscopy. *Opt Lett,* 34**,** 3556-8.

Sheppard, L. W., Vuksanovic, V., Mcclintock, P. V. & Stefanovska, A. 2011. Oscillatory dynamics of vasoconstriction and vasodilation identified by time-localized phase coherence. *Phys Med Biol,* 56**,** 3583-601.

Simmons, G. H., Barrett-O'keefe, Z., Minson, C. T. & Halliwill, J. R. 2011. Cutaneous vascular and core temperature responses to sustained cold exposure in hypoxia. *Experimental Physiology,* 96**,** 1062-1071.

Simpson, D. M., Rosas, D. a. B. & Infantosi, A. F. C. 2005. Estimation of coherence between blood flow and spontaneous EEG activity in neonates. *Biomedical Engineering, IEEE Transactions on,* 52**,** 852-858.

Skobe, M. & Detmar, M. 2000. Structure, Function, and Molecular Control of the Skin Lymphatic System. *J Investig Dermatol Symp Proc,* 5**,** 14-19.

Soderstrom, T., Stefanovska, A., Veber, M. & Svensson, H. 2003. Involvement of sympathetic nerve activity in skin blood flow oscillations in humans. *Am J Physiol Heart Circ Physiol,* 284**,** H1638-46.

Stanhewicz, A. E., Greaney, J. L., Larry Kenney, W. & Alexander, L. M. 2014. Sex- and limb-specific differences in the nitric oxide-dependent cutaneous vasodilation in response to local heating. *Am J Physiol Regul Integr Comp Physiol,* 307**,** R914-9.

Stefanovska, A., Bracic, M. & Kvernmo, H. D. 1999. Wavelet analysis of oscillations in the peripheral blood circulation measured by laser Doppler technique. *IEEE transactions on bio-medical engineering,* 46**,** 1230-9.

Stern, M. D. 1975. In Vivo Evaluation of Microcirculation by Coherent Light Scattering. *Nature,* 254.

Stiefel, P., Moreno-Luna, R., Vallejo-Vaz, A. J., Beltran, L. M., Costa, A., Gomez, L., Ordonez, A. & Villar, J. 2012. Which parameter is better to define endothelial dysfunction in a test of postocclusive hyperemia measured by laser-Doppler flowmetry? *Coron Artery Dis,* 23**,** 57-61.

Strain, W., Hughes, A., Mayet, J., Wright, A., Kooner, J., Chaturvedi, N. & Shore, A. 2010. Attenuation of microvascular function in those with cardiovascular disease is similar in patients of Indian Asian and European descent. *BMC Cardiovascular Disorders,* 10**,** 1-6.

Strain, W. D., Adingupu, D. D. & Shore, A. C. 2012. Microcirculation on a large scale: techniques, tactics and relevance of studying the microcirculation in larger population samples. *Microcirculation,* 19**,** 37-46.

Sun, P.-C., Chen, C.-S., Kuo, C.-D., Lin, H.-D., Chan, R.-C., Kao, M.-J. & Wei, S.-H. 2012. Impaired microvascular flow motion in subclinical diabetic feet with sudomotor dysfunction. *Microvascular Research,* 83**,** 243-248.

Sun, P. C., Kuo, C. D., Chi, L. Y., Lin, H. D., Wei, S. H. & Chen, C. S. 2013. Microcirculatory vasomotor changes are associated with severity of peripheral neuropathy in patients with type 2 diabetes. *Diab Vasc Dis Res,* 10**,** 270-6.

Svalestad, J., Hellem, S., Vaagbo, G., Irgens, A. & Thorsen, E. 2010. Reproducibility of transcutaneous oximetry and laser Doppler flowmetry in facial skin and gingival tissue. *Microvasc Res,* 79**,** 29-33.

Tan, Q., Zhang, M., Wang, Y., Zhang, M., Wang, B., Xin, Q. & Li, Z. 2016. Age-related alterations in phase synchronization of oxyhemoglobin concentration changes in prefrontal tissues as measured by near-infrared spectroscopy signals. *Microvasc Res,* 103**,** 19-25.

Tankanag, A. V., Grinevich, A. A., Kirilina, T. V., Krasnikov, G. V., Piskunova, G. M. & Chemeris, N. K. 2014. Wavelet phase coherence analysis of the skin blood flow oscillations in human. *Microvasc Res,* 95C**,** 53-59.

Tansey, E. A. & Johnson, C. D. 2015. Recent advances in thermoregulation. *Adv Physiol Educ,* 39**,** 139-48.

Tew, G. A., Klonizakis, M., Moss, J., Ruddock, A. D., Saxton, J. M. & Hodges, G. J. 2011. Reproducibility of cutaneous thermal hyperaemia assessed by laser Doppler flowmetry in young and older adults. *Microvasc.Res.,* 81**,** 177-182.

Thijssen, D. H., Bleeker, M. W., Smits, P. & Hopman, M. T. 2005. Reproducibility of blood flow and post-occlusive reactive hyperaemia as measured by venous occlusion plethysmography. *Clin Sci (Lond),* 108**,** 151-7.

Thomas, B. P., Liu, P., Park, D. C., Van Osch, M. J. & Lu, H. 2014. Cerebrovascular reactivity in the brain white matter: magnitude, temporal characteristics, and age effects. *J Cereb Blood Flow Metab,* 34**,** 242-7.

Thorn, C. E., Kyte, H., Slaff, D. W. & Shore, A. C. 2011. An association between vasomotion and oxygen extraction. *Am J Physiol Heart Circ Physiol,* 301**,** H442-9.

Thorn, C. E., Matcher, S. J., Meglinski, I. V. & Shore, A. C. 2009. Is mean blood saturation a useful marker of tissue oxygenation? *American Journal of Physiology - Heart and Circulatory Physiology,* 296**,** H1289-H1295.

Tigno, X. T., Hansen, B. C., Nawang, S., Shamekh, R. & Albano, A. M. 2011. Vasomotion becomes less random as diabetes progresses in monkeys. *Microcirculation,* 18**,** 429-39.

Tikhonova, I. V., Tankanag, A. V. & Chemeris, N. K. 2010. Time-amplitude analysis of skin blood flow oscillations during the post-occlusive reactive hyperemia in human. *Microvasc Res,* 80**,** 58-64.

Trzeciak, S., Cinel, I., Phillip Dellinger, R., Shapiro, N. I., Arnold, R. C., Parrillo, J. E. & Hollenberg, S. M. 2008. Resuscitating the Microcirculation in Sepsis: The Central Role of Nitric Oxide, Emerging Concepts for Novel Therapies, and Challenges for Clinical Trials. *Academic Emergency Medicine,* 15**,** 399-413.

Trzeciak, S., Dellinger, R. P., Parrillo, J. E., Guglielmi, M., Bajaj, J., Abate, N. L., Arnold, R. C., Colilla, S., Zanotti, S. & Hollenberg, S. M. 2007. Early microcirculatory perfusion derangements in patients with severe sepsis and septic shock: relationship to hemodynamics, oxygen transport, and survival. *Ann Emerg Med,* 49**,** 88-98, 98.e1-2.

Turner, J., Belch, J. J. & Khan, F. 2008. Current concepts in assessment of microvascular endothelial function using laser Doppler imaging and iontophoresis. *Trends Cardiovasc Med,* 18**,** 109-16.

Tyle, P. 1986. Iontophoretic Devices for Drug Delivery. *Pharm Res,* 3**,** 318-26.

Uga, M., Dan, I., Sano, T., Dan, H. & Watanabe, E. 2014. Optimizing the general linear model for functional near-infrared spectroscopy: an adaptive hemodynamic response function approach. *Neurophotonics,* 1**,** 015004.

Van Beekvelt, M. C., Colier, W. N., Wevers, R. A. & Van Engelen, B. G. 2001. Performance of near-infrared spectroscopy in measuring local O(2) consumption and blood flow in skeletal muscle. *J Appl Physiol,* 90**,** 511-9.

Vasdev, V., Bhakuni, D. S., Bhayana, A. & Kamboj, P. 2011. Nailfold capillaroscopy: A cost effective practical technique using digital microscope. *Indian Journal of Rheumatology,* 6**,** 185-191.

Victor, V. M., Nunez, C., D'ocon, P., Taylor, C. T., Esplugues, J. V. & Moncada, S. 2009. Regulation of Oxygen Distribution in Tissues by Endothelial Nitric Oxide. *Circulation Research,* 104**,** 1178-1183.

Vinet, A., Obert, P., Dutheil, F., Diagne, L., Chapier, R., Lesourd, B., Courteix, D. & Walther, G. 2015. Impact of a lifestyle program on vascular insulin resistance in metabolic syndrome subjects: the RESOLVE study. *J Clin Endocrinol Metab,* 100**,** 442-50.

Vionnet, J., Calero-Romero, I., Heim, A., Rotaru, C., Engelberger, R. P., Dischl, B., Noël, B., Liaudet, L., Waeber, B. & Feihl, F. 2014. No Major Impact of Skin Aging on the Response of Skin Blood Flow to a Submaximal Local Thermal Stimulus. *Microcirculation,* 21**,** 730-737.

Vuksanovi, V., Sheppard, L. W. & Stefanovska, A. 2008. Nonlinear Relationship between Level of Blood Flow and Skin Temperature for Different Dynamics of Temperature Change. *Biophysical journal,* 94**,** L78-L80.

Walker, H. A., Jackson, G., Ritter, J. M. & Chowienczyk, P. J. 2001. Assessment of forearm vasodilator responses to acetylcholine and albuterol by strain gauge plethysmography: reproducibility and influence of strain gauge placement. *Br J Clin Pharmacol,* 51**,** 225-9.

Waltz, X., Pichon, A., Lemonne, N., Mougenel, D., Lalanne-Mistrih, M. L., Lamarre, Y., Tarer, V., Tressieres, B., Etienne-Julan, M., Hardy-Dessources, M. D., Hue, O. & Connes, P. 2012. Normal muscle oxygen consumption and fatigability in sickle cell patients despite reduced microvascular oxygenation and hemorheological abnormalities. *PLoS One,* 7**,** e52471.

Wang, Z., He, Z. & Chen, J. D. 2005. Robust time delay estimation of bioelectric signals using least absolute deviation neural network. *IEEE Trans Biomed Eng,* 52**,** 454-62.

Wiernsperger, N., Nivoit, P., De Aguiar, L. G. K. & Bouskela, E. 2007. Microcirculation and the Metabolic Syndrome. *Microcirculation,* 14**,** 403-438.

Wilkinson, I. B. & Webb, D. J. 2001. Venous occlusion plethysmography in cardiovascular research: methodology and clinical applications. *British journal of clinical pharmacology,* 52**,** 631-646.

Wolff, C. B. 2013. Oxygen delivery: the principal role of the circulation. *Adv Exp Med Biol,* 789**,** 37-42.

Wollina, U., Heinig, B., Naumann, G., Scheibe, A., Schmidt, W. D. & Neugebauer, R. 2011. Effects of low-frequency ultrasound on microcirculation in venous leg ulcers. *Indian J Dermatol,* 56**,** 174-9.

Yamamoto-Suganuma, R. & Aso, Y. 2009. Relationship between post-occlusive forearm skin reactive hyperaemia and vascular disease in patients with Type 2 diabetes—a novel index for detecting micro- and macrovascular dysfunction using laser Doppler flowmetry. *Diabetic Medicine,* 26**,** 83-88.

Yang, Q., Ren, Z. H., Chickooree, D., Wu, H. J., Tan, H. Y., Wang, K., He, Z. J., Gong, C. J., Ram, V. & Zhang, S. 2014. The effect of early detection of anterolateral thigh free flap crisis on the salvage success rate, based on 10 years of experience and 1072 flaps. *Int J Oral Maxillofac Surg,* 43**,** 1059-63.

Yano, T., Afroundeh, R., Yamanaka, R., Arimitsu, T., Lian, C. S., Shirakawa, K. & Yunoki, T. 2014. Oscillation in O_2 uptake in impulse exercise. *Acta Physiologica Hungarica,* 101**,** 143-149.

Yano, T., Lian, C. S., Arimitsu, T., Yamanaka, R., Afroundeh, R., Shirakawa, K. & Yunoki, T. 2013. Oscillation of oxygenation in skeletal muscle at rest and in light exercise. *Acta Physiol Hung***,** 1-9.

Young, T. M., Asahina, M., Nicotra, A. & Mathias, C. J. 2006. Skin vasomotor reflex responses in two contrasting groups of autonomic failure. *Journal of Neurology,* 253**,** 846-850.

Yu, G., Durduran, T., Lech, G., Zhou, C., Chance, B., Mohler, E. R., 3rd & Yodh, A. G. 2005. Time-dependent blood flow and oxygenation in human skeletal muscles measured with noninvasive near-infrared diffuse optical spectroscopies. *J Biomed Opt,* 10**,** 024027.

Yu, G., Floyd, T. F., Durduran, T., Zhou, C., Wang, J., Detre, J. A. & Yodh, A. G. 2007. Validation of diffuse correlation spectroscopy for muscle blood flow with concurrent arterial spin labeled perfusion MRI. *Opt Express,* 15**,** 1064-75.

Yvonne-Tee, G. B., Rasool, A. H., Halim, A. S. & Rahman, A. R. 2005. Reproducibility of different laser Doppler fluximetry parameters of postocclusive reactive hyperemia in human forearm skin. *J Pharmacol Toxicol Methods,* 52**,** 286-92.